Universität Hamburg
DER FORSCHUNG | DER LEHRE | DER BILDUNG

Dissertation

Walking in Virtual Reality:

Perceptually-inspired Interaction Techniques for Locomotion in Immersive Environments

Dissertation with the aim of achieving a doctoral degree at the Faculty of Mathematics, Informatics and Natural Sciences

Eike Langbehn

Human-Computer Interaction
Department of Informatics
Universität Hamburg

2019

Supervisor & Reviewer:	Prof. Dr. Frank Steinicke
Reviewer:	Prof. Dr. Bernd Fröhlich
Reviewer:	Prof. Mary C. Whitton
Head of Examination Commission:	Prof. Dr. Simone Frintrop
Deputy Head of Examination Commission:	Prof. Dr.-Ing. Timo Gerkmann
Date of Thesis Defense:	17.10.2019

ABSTRACT

Natural walking is often considered one of the most advantageous locomotion techniques for virtual reality (VR). In comparison to other techniques, it reduces VR sickness, provides enhanced spatial knowledge, supports wayfinding, and increases the user's sense of presence. However, natural walking in VR is limited by the available tracking space in the real world, which is only up to a few square meters in common room-scale setups.

Locomotion techniques such as walking-in-place or redirected walking aim to combine the advantages of natural walking with the unconstrained exploration of large-scale virtual environments (VEs). These techniques leverage human movements and exploit perceptual limitations to support the sensation of infinite walking. Because of this, we consider this kind of locomotion techniques as *perceptually-inspired* in the scope of this work. For instance, it is possible to slightly rotate the user's view in one direction while she walks on a straight path in the virtual world. Most likely, she will subconsciously compensate for the rotation by walking on a circular arc to the opposite direction in the real world. So far, a circle with a radius of 10m - 25m is necessary in the physical world for undetectable infinite straight walking in the virtual world. For most situations, this physical space is not available for tracking.

The main goal of this dissertation is to achieve natural unconstrained locomotion in VEs. This includes a detailed understanding of perceptual aspects of locomotion and the design of novel perceptually-inspired locomotion techniques. Contributions of this work are (i) a deeper knowledge about spatial perception and its effects on locomotion, (ii) a better understanding of perceptual detection thresholds for redirected walking, and (iii) evaluation of novel locomotion techniques, ranging from seated and standing to room-scale VR experiences.

For part (i), the effects of artificial visual blur particularly on distance and speed estimation were evaluated, to understand how much of the perceptual discrepancies between real and virtual worlds might be explained by visual blur, and to find out if this can be leveraged for locomotion. Other aspects, such as the effects of the type of environment, existence of visual body feedback, and presence of other avatars on dominant scale estimation were investigated.

For part (ii), perceptual detection thresholds for redirected walking in different situations were estimated that go beyond previous experiments. It was found that there only is a small difference in detection thresholds when redirection is performed with and without a visual self-representation. The type of environment still has a larger impact on thresholds. In the next step, it was shown that sensitivity to bending of already curved paths is lower than for bending of straight paths. This result was extended in another experiment in which transcranial direct-current stimulation was applied to participants who were walking on curved paths. Additionally, it was shown that subtle repositioning and reorientation during eye blinks is a very effective method to further improve redirected walking on curved paths.

For part (iii), novel locomotion techniques that are based on findings of the previous parts were built and evaluated regarding criteria such as usability, VR sickness, sense of presence, spatial knowledge, and effectiveness. A turning technique based on dynamic rotation gains, a novel approach to walking-in-place, a scale-based walking technique, and a redirected walking technique based on curved paths were introduced. Additionally, this redirected walking technique was compared to virtual travel techniques and support for multiple users was designed. Finally, the combination of several subtle redirection techniques and their integration with gameplay and narration of a VR experience was demonstrated.

ZUSAMMENFASSUNG

Natürliches Gehen wird oft als die vorteilhafteste Fortbewegungstechnik für Virtual Reality (VR) betrachtet. Im Vergleich zu anderen Techniken reduziert es die VR Krankheit, stellt erweitertes räumliches Wissen bereit, unterstützt die Wegfindung und erhöht das Präsenzgefühl der Benutzer*in. Natürliches Gehen in VR ist jedoch limitiert durch den zur Verfügung stehenden Trackingbereich in der realen Welt, welcher in üblichen VR Setups für Zimmergröße nur bis zu einige Quadratmeter groß ist.

Fortbewegungstechniken wie Walking-in-Place oder Redirected Walking zielen darauf ab die Vorteile von Natürlichem Gehen mit unbeschränktem Erkunden von sehr großen virtuellen Umgebungen (VEs) zu kombinieren. Diese Techniken verwenden menschliche Bewegungen und nutzen Limitationen der menschlichen Wahrnehmung aus um den Eindruck von unendlichem Gehen zu vermitteln. Deswegen betrachten wir im Rahmen dieser Arbeit diese Art von Fortbewegungstechniken als *wahrnehmungs-inspiriert*. Zum Beispiel ist es möglich, das Sichtfeld der Benutzer*in leicht in eine Richtung zu drehen, während sie auf einem geraden Pfad in der virtuellen Welt läuft. Daraufhin wird sie sehr wahrscheinlich unterbewusst die Rotation kompensieren, indem sie in der realen Welt auf einem kreisförmigen Bogen in die entgegengesetzte Richtung läuft. Bisher ist ein Kreis mit einem Radius von 10m - 25m in der physischen Welt erforderlich, damit die Benutzer*in in der virtuellen Welt unendlich geradeaus läuft und die Manipulation nicht bemerkt. In den meisten Situationen ist ein so großer physischer Raum nicht verfügbar.

Das Hauptziel dieser Dissertation ist es, natürliche unbeschränkte Fortbewegung in virtuellen Umgebungen zu erreichen. Dies beinhaltet ein detailliertes Verständnis der Wahrnehmungsaspekte von Fortbewegung und das Design von neuartigen wahrnehmungs-inspirierten Fortbewegungstechniken. Beiträge dieser Arbeit sind (i) ein tieferes Verständnis von räumlicher Wahrnehmung und ihrer Effekte auf Fortbewegung, (ii) ein besseres Verständnis von Wahrnehmungsschwellen für Redirected Walking und (iii) die Evaluation von neuartigen Fortbewegungstechniken für VR Erfahrungen im Sitzen, Stehen und auf Zimmergröße.

Für Teil (i) wurden die Effekte von visuellem Weichzeichnen auf Distanz- und Geschwindigkeitseinschätzung evaluiert, um zu verstehen wieviel der Wahrnehmungsunterschiede zwischen realer und virtueller Welt durch visuelle Unschärfe erklärt werden können, und um heraus zu finden ob dies für Fortbewegung genutzt werden kann. Andere Aspekte, wie die Effekte des Umgebungstyps, der Existenz von visuellem Körperfeedback und der Präsenz von anderen Avataren auf die Einschätzung des dominanten Maßstabs, wurden ebenfalls untersucht.

Für Teil (ii) wurden Wahrnehmungsschwellen für Redirected Walking in verschiedenen Situationen ermittelt, die über frühere Experiment hinaus gehen. Es stellte sich heraus, dass es nur einen geringen Unterschied bei den Wahrnehmungsschwellen gibt in Abhängigkeit davon, ob eine visuelle Selbstrepräsentation vorhanden ist oder nicht. Der Umgebungstyp hat noch einen größeren Einfluss auf die Grenzwerte. Im nächsten Schritt wurde gezeigt, dass die Sensitivität für das Biegen von bereits gekrümmten Pfaden geringer ist als für das Biegen von geraden Pfaden. Dieses Ergebnis wurde in einem anderen Experiment erweitert, in welchem transkranielle Stimulation auf Versuchsteilnehmer*innen angewandt wurde, die auf gekrümmten Pfaden liefen. Zusätzlich wurde gezeigt, dass subtile Repositionierung und Reorientierung während des Blinzelns eine sehr effektive Methode ist um Redirected Walking auf gekrümmten Pfaden weiter zu verbessern.

Für Teil (iii) wurden neuartige Fortbewegungstechniken, die auf den Ergebnissen der vorhergehenden Teile basieren, entwickelt und bezüglich Kriterien wie Usability, VR Krankheit, Präsenzgefühl, räumliches Wissen und Effektivität evaluiert. Eine Drehtechnik, die auf dynamischen Rotationsverstärkungen basiert, ein neuartiger Ansatz für Walking-in-Place, eine skalierungs-

basierte Fortbewegungstechnik und eine Redirected Walking Technik, die auf gekrümmten Pfaden basiert, wurden eingeführt. Zusätzlich wurde diese Redirected Walking Technik mit virtuellen Fortbewegungstechniken verglichen und Mehrbenutzer*innen-Unterstützung wurde entworfen. Schließlich wurde eine Kombination von verschiedenen subtilen Redirection Techniken und deren Integration mit Gameplay und Narration einer VR Erfahrung demonstriert.

CONTENTS

APPENDIX

1. INTRODUCTION

"With appropriate programming such a display
could literally be the Wonderland
into which Alice ***walked****".*

Ivan Sutherland, 1965

1.1 Motivation

Virtual reality (VR) has received enormous attention since its vision was first characterized in 1965 by Ivan Sutherland. In his essay *The Ultimate Display*, Sutherland described VR as "*a room within which the computer can control the existence of matter. A chair displayed in such a room would be good enough to sit in. Handcuffs displayed in such a room would be confining, and a bullet displayed in such a room would be fatal.*" [Sut65]. In a more formal way, VR can be defined as a computer-generated digital environment that can be experienced and interacted with as if it were real [Jer15], most often by using several displays for different senses, 3D tracking technology, and interaction devices. Frederick Brooks, another pioneer of VR, named three requirements for VR: (i) real-time rendering according to head-tracking data, (ii) real space, i. e., a concrete or abstract virtual environment, and (iii) real interactions [Bro10]. To distinguish VR from similar technologies such as augmented reality (AR), Milgram introduced the *Reality-Virtuality Continuum* [MK94] that orders these realities on a continuous scale (see Figure 1.1). According to this, all worlds between the purely real world and a purely virtual world can be called *Mixed Reality*.

Three years after Sutherland published his essay, he built the first version of a mixed reality head-mounted display (HMD) [Sut68] (see Figure 1.2 a and b). Later, other approaches to VR followed, for example, projection-based setups [Cru95] (see Figure 1.2 c). Those setups make use of displays or projection walls all around the user instead of mounting a display directly to the head of the user. Until a few years ago, only very few people had access to VR devices, mainly in research labs. In recent years, VR technology made great advancements. Especially, novel HMDs, based on smartphone technology, were introduced [Ols+11]. These consumer devices set a new level of quality [Che+19; KCS17; NLL17] and price, and they quickly became successful.

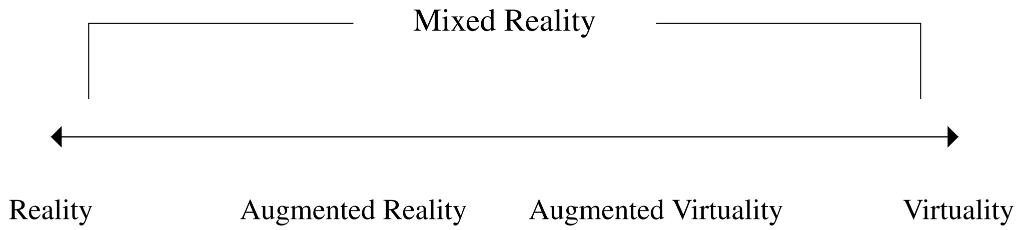

Figure 1.1: The reality-virtuality continuum covers the space between purely real environments and purely virtual environments (adapted from [MK94]).

Nowadays, VR technology has a very high availability and a large number of software developers started to build VR experiences. Many different application domains are interested in using this technology, e. g., in the areas of architecture, health and medicine, psychiatry and psychology, simulation and training, engineering and construction, archaeology and history, tourism, entertainment and games, education, data visualization, or art and culture.

According to Brooks, a key aspect of VR is interactiveness [Bro10]. The user of a VR system is not just a passive observer like, e. g., in a movie, but she can manipulate and control the system directly in real-time. Hence, a VR system usually does not only consist of output devices, i. e., displays, but also contains 3D input devices. The combination of such output as well as input devices, then form a 3D user interface (3D UI) [LaV+17]. 3D UIs enable the user to complete her tasks directly in a real or virtual 3D space. This space is usually created with an interactive 3D graphics engine and denoted *virtual environment* (VE). The interaction tasks that have to be solved with a 3D UI might be application-specific, but some tasks are universal to almost every VR experience [Min95]. Those generic interaction tasks include object selection and manipulation, system control, and, especially, locomotion [LaV+17].

Locomotion is constantly carried out in our daily lives and might appear in various forms like driving, riding, or flying. However, bipedal human walking is the most natural and common locomotion technique in the physical world [Ste+13]. Of course, locomotion is an important activity in immersive virtual environments (IVEs) since it allows users to explore the virtual world. While purely virtual locomotion techniques like teleportation exist, it is beneficial to leverage real walking since it is supposed to be the most presence-enhancing form of locomotion [Uso+99a]. Basic implementations of real walking can be realized by using modern tracking systems to map position and orientation of a user's head one-to-one to the virtual camera. Then, a one meter forward movement in the physical world is mapped to a one meter forward movement in the VE. This provides the user with near-natural sensory feedback similar to the physical world but restricts the accessible VE to the size of the physical tracking space. The confined physical tracking space of typical VR setups, e. g., the HTC Vive with Lighthouse tracking, is nowadays often denoted as *room-scale VR*, i. e., up to approximately 5m $\times$ 5m.

Therefore, the challenge is to create interaction techniques for locomotion in IVEs that fit into the available space and are based on real walking. One possibility are hardware solutions such as omnidirection treadmills [Sou+11], motion platforms [BS02], or motion robot tiles [Iwa+05] which are not in the focus of this work. Instead, this work focuses on software solutions that do not require expensive or bulky hardware devices. So far, there are already a few approaches, e. g., *walking-in-place* techniques [NSN16], which exploit walk-like gestures that give the user the impression of walking while she stands in one spot. Another interesting technique is *redirected walking* [RKW01] which is inspired by findings from the field of perceptive psychology. It guides the user on a different path in the real world than she is traveling in the virtual world without being consciously perceived by the user. Redirection techniques might be applied in many different fields

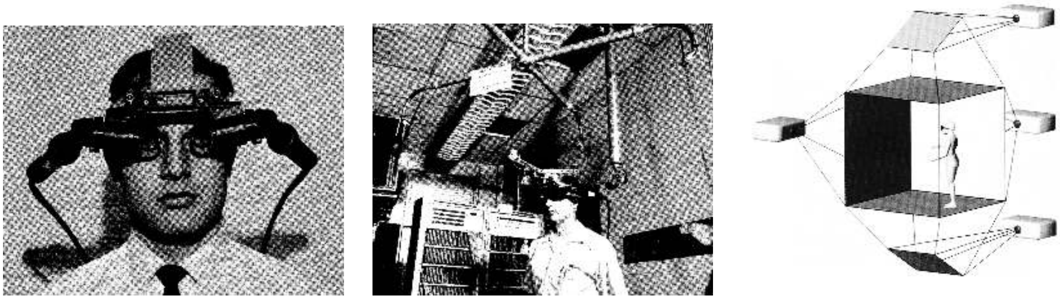

(a) (b) (c)

Figure 1.2: Sutherland's first HMD (a and b) (images from [Sut68]), and the CAVE (c) (image from [Cru95]).

such as to control a remote tele-robot by walking [Gro+05], in tourism [Ste+08b], for architectural visualizations [BSH09], or in video games [Ste+09b]. However, there are still some limitations when using this technique. For example, an area of approximately 45 m $\times$ 45 m in the physical world can be necessary to walk on an infinite straight path in the VE [Ste+10b]. If the physical tracking space is smaller or if the user does not want to walk only straight, *resetting* techniques [Wil+07] have to be used. That means, in case the user hits a boundary of the tracking space, she must be turned to face to the center of the tracking space again. These techniques are overt in most cases and interrupt the VR experience.

Hence, novel techniques are needed to bring unnoticeable redirected walking to room-scale VR. These techniques might be based on peculiarities of the human perceptual system, which has an important role for interactions in VR, and they have to be developed, investigated, and evaluated.

1.2 Research Goals

The main goal of this dissertation is to achieve natural unconstrained locomotion in virtual worlds. Therefore, this work will explore perceptual aspects of locomotion in IVEs, which in turn might be used to enhance perceptually-inspired locomotion techniques such as walking-in-place and redirected walking. Contributions towards this goal will be discussed in three parts.

First, perception in VR, especially spatial perception, will be investigated. Accurate estimations of spatio-temporal circumstances like distances, sizes, and self-motion speed are essential for many activities, especially for locomotion and way-finding, e. g., to avoid collisions, reach high navigation performance, or build up an accurate mental map of the environment. Previous research shows that spatial perception in VR differs significantly from the real world, though we are lacking a good understanding of where and how such differences originate as well as if they can be eliminated. It is fundamental to have knowledge in space perception in VR to be able to exploit such differences for locomotion and, in particular, redirected walking. This dissertation details work exploring how visual blur can be used to alter perception of (i) distances and (ii) self-motion speed. Simulated visual blur may compensate for missing accommodation cues in real-time rendered virtual environments and, therefore, increase the perceived naturalness and improve spatial estimations. Varying the degree of blur, in turn, might be used to support the viewpoint manipulation that is introduced during redirected walking. Furthermore, spatial perception in (iii) multi-scale VEs will be investigated. Multi-scale VEs enable users to change their size and explore a virtual world from multiple scale levels. This approach raises several questions, e.g., which cues or landmarks are used to estimate spatial relations such as distances and sizes. Moreover, changing the scale might also be leveraged for the development of locomotion techniques as introduced later on.

Second, detection thresholds for unnoticeable redirected walking will be estimated. Researchers put much effort on identifying such thresholds for translation, rotation, and curvature gains in psychophysical experiments. However, the previously estimated thresholds mark conservative lower bounds. To further improve redirected walking, the need for a better understanding of perceptual detection thresholds that go beyond previous experiments was identified. In this dissertation, detection thresholds will be estimated for situations in which (i) users are able to see their own feet in the VE, (ii) users are already walking on curves in the VE, and (iii) users are exposed to transcranial direct-current stimulation. While users are expected to be more sensitive to redirected walking manipulations when seeing their feet, the other two situations might lead to wider thresholds and, therefore, reduced space requirements for redirected walking. Furthermore, (iv) thresholds for position and orientation redirection during eye blinks will be estimated. This is an orthogonal approach in addition to previously introduced redirection techniques and can increase the effectiveness of redirected walking significantly since it exploits situations in which visual input of the user is suppressed.

Third, locomotion techniques for a variety of situations will be developed and, for this, the results of the two previous parts will be leveraged. Locomotion can be carried out by purely virtual travel techniques. However, to approximate real walking and exploit its benefits, there is a need for novel perceptually-inspired locomotion techniques. Therefore, techniques for seated, standing, and, finally, room-scale VR experiences are covered. These techniques will be evaluated regarding criteria like usability, VR sickness, sense of presence, spatial knowledge, and effectiveness. In this dissertation, (i) a turning technique based on dynamic rotation gains, (ii) a novel approach to walking-in-place, (iii) a scale-based walking technique, (iv) a novel technique to lay out curved walking paths for redirected walking, (v) a technique that shows how support for multiple users in the same tracking space could be added to redirected walking, and finally, (vi) an approach of combining several subtle redirection techniques and integrating them with gameplay and narration of the VR experience will be investigated.

To summarize, the contributions of this dissertation are

- a deeper knowledge about spatial perception and its effects on locomotion,
- a better understanding of perceptual detection thresholds for redirected walking,
- and, novel locomotion techniques, ranging from seated and standing VR to room-scale experiences.

1.3 Outline

The remainder of this dissertation is structured as follows. Part I focusses on fundamental background information. Chapter 2 presents related work in the field of perception and Chapter 3 summarizes previous work on locomotion in VR [E L16; E L19; ES18].

Part II reports several experiments that consider important aspects of spatio-temporal judgments in VR, i. e., on distance, speed, and size perception. Chapter 4 evaluates the influence of depth of field blur on distance estimation [E L+16]. Chapter 5 evaluates the influence of motion blur on speed estimation [E L+16]. And Chapter 6 analyzes dominant scale estimation in multi-scale VEs [EBS15; EBS16a].

Part III presents several experiments that reveal sensitivities to redirection under different conditions. Chapter 7 reports if the virtual self-representation of the user's feet changes the detection thresholds for translation gains [KEF18]. Chapter 8 introduces bending gains that define discrepancies between physical and virtual paths in situations where both are bent and reports the user's sensitivity to these gains [E L+17b]. Chapter 9 investigates the influence of transcranial direct-current stimulation on bending gains [E L+19a]. Chapter 10 analyzes the amount of redirection that can be induced during eye blinks and discusses how this can be used to improve traditional redirection approaches [BE17; EBS16b; E L+18].

Part IV presents perceptually-inspired locomotion techniques for VR experiences that are based on the findings of the previous experiments, and evaluates and compares them. Chapter 11 reports of several rotation techniques that help the user in cases when the possibilities of physical turning are limited [E L+19b]. Chapter 12 introduces a novel walking-in-place technique with omnidirectional tracking whose speed control is based on leaning [E L+15]. Chapter 13 presents a technique that scales the size of the user while walking to cover larger distances [Boy+18]. Chapter 14 introduces a novel redirected walking approach that exploits bending gains to guide the user on paths which will never hit the boundaries of the tracking space [E L+17a; E L+17b]. Chapter 15 compares this redirected walking approach to teleportation and joystick locomotion [ELS18a]. Chapter 16 explores the challenge of collision avoidance for this redirected walking approach when multiple users are walking in the same physical space at the same time [EHS18; HES17]. Chapter 17 presents VR experiences that combine this redirected walking approach with several other approaches such as impossible spaces and align them with gameplay and narration [ELS18b; ES19].

Finally, Part V summarizes the results of this work and concludes the dissertation.

1.4 Publications

The main contributions of this dissertation have been published in peer-reviewed national and international venues.

Main Authorship

The following publications were mainly created by myself while co-authors contributed parts of the implementation, writing of paper sections, or supervision. These include 2 journal articles, 2 book chapters, 9 conference papers, 2 posters, 3 research demonstrations and a doctoral consortium extended abstract.

Journal Articles

[E L+17b] **E. Langbehn**, P. Lubos, G. Bruder, and F. Steinicke. “Bending the Curve: Sensitivity to Bending of Curved Paths and Application in Room-Scale VR”. In: *IEEE Transactions on Visualization and Computer Graphics (TVCG)* 23.4 (2017), pages 1389–1398.

[E L+18] **E. Langbehn**, F. Steinicke, M. Lappe, G. F. Welch, and G. Bruder. “In the Blink of an Eye - Leveraging Blink-Induced Suppression for Imperceptible Position and Orientation Redirection in Virtual Reality”. In: *ACM Transactions on Graphics (TOG), Special Issue on ACM SIGGRAPH* 37.4 (2018), 66 (11 pages).

Book Chapters

[E L19] **E. Langbehn**. “Fortbewegung im virtuellen Raum”. In: *Mit weit geschlossenen Augen. Virtuelle Realitäten entwerfen*. Edited by P. Reinfeld and C. Höfler. (Architektur der Medien - Medien der Architektur, ed. by K. Nakas and Ph. Reinfeld, Vol. 1.) Wilhelm Fink Verlag, 2019.

[ES18] **E. Langbehn** and F. Steinicke. “Redirected Walking in Virtual Reality”. In: *Encyclopedia of Computer Graphics and Games*. Edited by N. C. Nilsson. Springer International Publishing, 2018.

Conference Papers

[Boy+18] Y. Boysen, M. Husung, T. Mantei, L. Müller, J. Schimmelpfennig, L. Uzolas, and **E. Langbehn**[1]. "Scale & Walk: Evaluation von skalierungsbasierten Interaktionstechniken zur natürlichen Fortbewegung in VR". In: *Mensch und Computer*. 2018, (12 pages).

[E L+16] **E. Langbehn**, B. Bolte, T. Raupp, G. Bruder, M. Lappe, and F. Steinicke. "Visual Blur in Immersive Virtual Environments: Does Depth of Field or Motion Blur Affect Distance and Speed Estimation?" In: *ACM Symposium on Virtual Reality Software and Technology (VRST)*. 2016, pages 241–250.

[EBS16a] **E. Langbehn**, G. Bruder, and F. Steinicke. "Scale Matters! Analysis of Dominant Scale Estimation in the Presence of Conflicting Cues in Multi-Scale Collaborative Virtual Environments". In: *IEEE Symposium on 3D User Interfaces (3DUI)*. 2016, pages 211–220.

[E L+15] **E. Langbehn**, T. Eichler, S. Ghose, K. von Luck, G. Bruder, and F. Steinicke. "Evaluation of an Omnidirectional Walking-in-Place User Interface with Virtual Locomotion Speed Scaled by Forward Leaning Angle". In: *GI Workshop on Virtual and Augmented Reality (GI VR/AR)*. 2015, pages 149–160.

[EHS18] **E. Langbehn**, E. Harting, and F. Steinicke. "Shadow-Avatars: A Visualization Method to Avoid Collisions of Physically Co-Located Users in Room-Scale VR". In: *IEEE Virtual Reality (VR) Workshop on Everyday Virtual Reality (WEVR)*. 2018, (4 pages).

[ELS18a] **E. Langbehn**, P. Lubos, and F. Steinicke. "Evaluation of Locomotion Techniques for Room-Scale VR: Joystick, Teleportation, and Redirected Walking". In: *ACM Virtual Reality International Conference (VRIC)*. 2018, (9 pages).

[E L+19a] **E. Langbehn**, F. Steinicke, P. Koo-Poeggel, L. Marshall, and G. Bruder. "Stimulating the Brain in VR: Effects of Transcranial Direct-Current Stimulation on Redirected Walking". In: *ACM Symposium on Applied Perception (SAP) (under review)*. 2019, (8 pages).

[E L+19b] **E. Langbehn**, J. Wittig, N. Katzakis, and F. Steinicke. "Turn Your Head Half Round: VR Rotation Techniques for Situations With Physically Limited Turning Angle". In: *Mensch und Computer (accepted)*. 2019, (9 pages).

[KEF18] L. Kruse, **E. Langbehn**, and F. Steinicke[2]. "I Can See on my Feet While Walking: Sensitivity to Translation Gains with Visible Feet". In: *IEEE Virtual Reality (VR)*. 2018, pages 305–312.

Other

[E L16] **E. Langbehn**. "Development and Evaluation of Interactive Locomotion User Interfaces". In: *IEEE Virtual Reality (VR) (Doctoral Consortium)*. 2016.

[EBS15] **E. Langbehn**, G. Bruder, and F. Steinicke. "Moving Towards Natural Interaction Between Multiscale Avatars in Multi-User Virtual Environments[3]". In: *International Conference on Artificial Reality and Telexistence, Eurographics Symposium on Virtual Environments (ICAT-EGVE) (Poster)*. 2015.

[1] This publication is based on a bachelor project. The students implemented and ran the experiment under my supervision. I designed the experiment and wrote the paper.

[2] This publication is based on a Bachelor thesis. The student implemented and ran the experiment under my supervision. I designed the experiment and wrote the paper.

[3] This publication received the *Best Poster Award* and the *Best Poster Audience Award*.

[EBS16b] **E. Langbehn**, G. Bruder, and F. Steinicke. “Subliminal Reorientation and Repositioning in Virtual Reality During Eye Blinks[4]”. In: *ACM Symposium on Spatial User Interaction (SUI) (Poster)*. 2016, pages 213–213.

[E L+17a] **E. Langbehn**, P. Lubos, G. Bruder, and F. Steinicke. “Application of Redirected Walking in Room-Scale VR”. In: *IEEE Virtual Reality (VR) (Demo)*. 2017.

[ELS18b] **E. Langbehn**, P. Lubos, and F. Steinicke. “Redirected Spaces: Going Beyond Borders”. In: *IEEE Virtual Reality (VR) (Demo)*. 2018.

[ES19] **E. Langbehn** and F. Steinicke. “Space Walk: A Combination of Subtle Redirected Walking Techniques Integrated with Gameplay and Narration”. In: *ACM SIGGRAPH Emerging Technologies*. 2019.

Co-Authorship

The following publications were mainly created by someone else and are not part of this dissertation. However, I contributed critical parts of the implementation, experiment design, or paper writing. These include 2 journal articles, 2 conference papers, 3 posters, and an abstract for an oral presentation.

Journal Articles

[Jan+17b] O. Janeh, **E. Langbehn**, F. Steinicke, G. Bruder, A. Gulberti, and M. Poetter-Nerger. “Walking in Virtual Reality: Effects of Manipulated Visual Self-Motion on Walking Biomechanics”. In: *ACM Transactions on Applied Perception (TAP)* 14.2 (2017), 12 (15 pages).

[Zha+18b] J. Zhang, **E. Langbehn**, D. Krupke, N. Katzakis, and F. Steinicke. “Detection Thresholds for Rotation and Translation Gains in 360 Video-based Telepresence System”. In: *IEEE Transactions on Visualization and Computer Graphics (TVCG)* 24.4 (2018), pages 1671–1680.

Conference Papers

[Rie+18] M. Rietzler, J. Gugenheimer, T. Hirzle, M. Deubzer, **E. Langbehn**, and E. Rukzio. “Rethinking Redirected Walking: On the Use of Curvature Gains Beyond Perceptual Limitations and Revisiting Bending Gains”. In: *IEEE International Symposium on Mixed and Augmented Reality (ISMAR)*. 2018, (8 pages).

[Zha+18a] J. Zhang, **E. Langbehn**, D. Krupke, N. Katzakis, and F. Steinicke. “A 360 Video-based Robot Platform for Telepresent Redirected Walking”. In: *ACM Human-Robot Interaction (HRI) Workshop on Virtual, Augmented and Mixed Reality for Human-Robot Interaction*. 2018, (5 pages).

Other

[BE17] G. Bruder and **E. Langbehn**. “Subliminal Rotations During Eye Blinks for Redirected Walking”. In: *Journal of Vision (Talk)* 17.10 (2017), pages 1266–1266.

[HES17] P. Heidicker, **E. Langbehn**, and F. Steinicke. “Influence of Avatar Appearance on Presence in Social VR”. In: *IEEE Symposium on 3D User Interfaces (3DUI) (Poster)*. 2017, pages 233–234.

[Jan+17a] O. Janeh, **E. Langbehn**, F. Steinicke, G. Bruder, A. Gulberti, and M. Poetter-Nerger. “Biomechanical Analysis of (Non-)Isometric Virtual Walking of Older Adults”. In: *IEEE Virtual Reality (VR) (Poster)*. 2017, pages 217–218.

[4]This publication received the *Honorable Mention for Best Poster*.

[Kru+16] D. Krupke, L. Einig, **E. Langbehn**, J. Zhang, and F. Steinicke. "Immersive Remote Grasping: Realtime Gripper Control by a Heterogenous Robot Control System". In: *ACM Symposium on Virtual Reality Software and Technology (VRST) (Poster)*. Nov. 2016, pages 337–338.

I FUNDAMENTALS

2. PERCEPTION

2.1 The Human Perceptual System

According to the model human processor, which is a simplification especially designed for human-computer interaction, human information processing can be divided into three parts: (i) perception, (ii) cognition, and (iii) action [CMN83]. This process is inspired by the way how a computer processes information (see Figure 2.1). First, a computer gets input from the user, e. g., by using a keyboard or mouse. Then, its internal state is updated according to the input. In the end, some output is delivered to the user, e. g., via the display screen or sound speakers.

In return, the user perceives the output of the computer, e. g., a text on the screen. Then, she processes the information cognitively and makes decisions which may result in actions, e. g., a mouse click, which is again handled as an input by the computer.

In VR, this cycle is repeated several times per second. A short example would be: The user perceives the current images displayed on the HMD, processes this information and decides to turn her head to face into a different direction. This turn is recognized as input by the VR system and a new image is rendered according to the new direction of the user's head. Since a framerate of at least 90 frames per second is recommended [Int18; Ocu18], the VR system needs to be able to perform this cycle 90 times per second.

The human perceptual system is not limited to the visual sense, but uses different sensory channels. Indeed, the visual channel is the one through which most information is processed [McC13]. In a nutshell, light is falling into the human eyes and mirrored on the retina. There, it is captured by two kinds of photoreceptors (i.e. rods and cones) and converted into electrical signals, which send the information to the primary visual cortex of the brain [Gol09]. Vision is able to perceive colors and shapes best in the center of the retina, whereas it becomes worse towards the periphery. Instead, peripheral vision is superior in perceiving motions [LaV+17].

The ears are the organs of the auditory channel and divided into three parts: outer, middle, and inner ear. Sound waves are forwarded by the outer ear to the eardrum and make it vibrate, which in turn moves the small bones in the middle ear (malleus, incus, stapes) [Jer15]. Because of this, the fluid in the inner ear starts to move and stimulates the receptors (hair cells) in the inner ear (cochlea) [LaV+17]. These receptors send electrical signals to the auditory cortex of the brain.

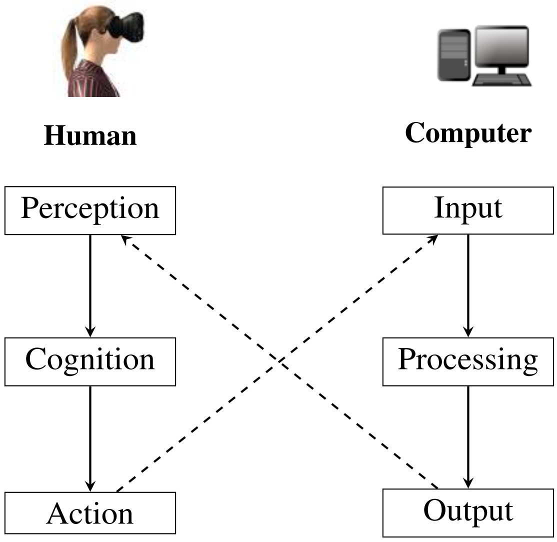

Figure 2.1: Simplified illustration of human information processing in combination with a real-time computer system.

Another use of the ear is the vestibular sense. This channel is able to perceive linear and rotational accelerations [Iva+97]. It is located in the inner ear and consists of the two otolith organs (utricle and saccule) and the semicircular canals [LaV+17]. Both contain hair cells similar to the auditory channel, which are stimulated by movement of fluid. The otolith organs deliver information about gravity and linear acceleration, i. e., linear movements. Interestingly, they can not distinguish between a head tilt and linear movement since they perceive only the overall sum of gravity and inertial acceleration (GIA vector) [BS16]. The semicircular canals provide information about angular accelerations, i. e., rotational movements. Over time, the sensory output adapts to the constant stimulation and after some seconds of constant angular or linear velocity they are not able to disambiguate between no velocity and some constant velocity [Gol09].

Another important channel for VR is the sense of touch which can be divided into haptic and tactile perception as well as proprioception. Tactile perception is based on receptors under the skin, which can feel pressure, pain, and temperature [LaV+17]. Haptic perception is based on receptors of muscles and joints. Both can be active or passive depending on whether a person actively explores an object or is being touched or moved by an external force [Jer15]. Proprioception describes the perception of self-movements (kinesthetics) and position of the body and limbs.

Other channels which are neglected in the fields of human-computer interaction and VR are smell and taste [Che06]. This is also due to the circumstance that it is more difficult to build stimulation devices for these senses. However, these senses are not in the focus of this dissertation.

Sutherland's vision of *The Ultimate Display* included the statement that such a display *„... should serve as many senses as possible“* [Sut65]. Actually, it would be a display of smell, taste, vision, audio, and touch. Hence, this first vision of VR already emphasized the importance of multimodal human perception.

2.1.1 Multisensory Integration

Information from different sensory channels might be related to characteristics of the same object. For example, self-motion during head turns can be perceived by the visual as well as by the vestibular sense, neck proprioception and an efference copy of the motor command to turn the head [Cro+98] (see Figure 2.2). The human perceptual system combines and integrates those redundant information [EB04; EB05]. A successful integration is necessary for receiving a coherent

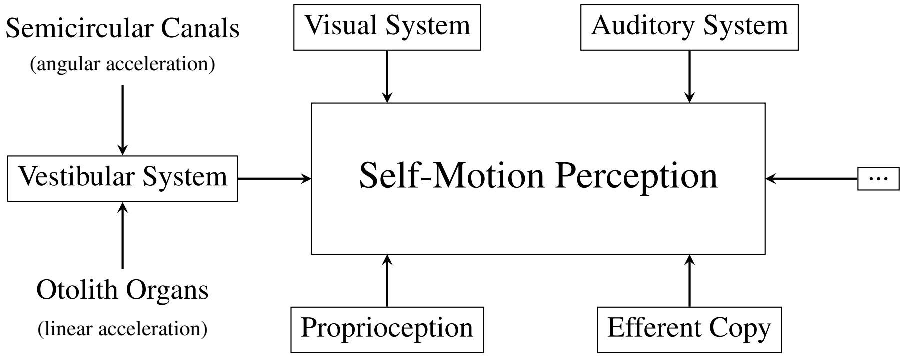

Figure 2.2: Self-motion perception is based on information from multiple sensory channels like vision, audio, vestibular system, proprioception, and the efferent copy signal, which is the copy of motor commands and contains information about executed actions (adapted from [BS16]).

overall perception during interactions with the environment [RDE16].

For this integration, each modality contributes with a certain amount defined by the reliability assigned by the human. In general, there are two often considered models to describe the integration. A (i) *maximum-likelihood estimation* delivers the most reasonable possible combination of the involved sensory channels in a statistically optimal manner [RDE16]. According to this, the quality of the sensory information determines its weight in the calculation [EB05]. This can be described as follows:

$$I = \sum_{i=1}^{N} w_i I_i \text{ with } \textstyle\sum_{i=1}^{N} w_i = 1, \tag{2.1}$$

with I denoting the finally perceived information, I_i the individual information from one sensory channel, and w_i normalized weights. These weights depend on the quality of the information. For instance, a sensory channel might be *noisy* and, therefore, the quality of the information is worse. It was shown in experiments that sensory channels get a greater weight when they offer better quality [EB02]. For instance, if an object can be seen clearly, the visual sense is dominating, but when visual quality decreases, e. g., by adding artificial blur to an image, the other channels become more important [EB02]. Indeed, in general, vision tends to dominate the other sensory channels in many situations [PNK76].

However, human perception is not only based on the different sensory channels. The information from the channels are integrated with prior knowledge about the world [EB05]. This prior knowledge is gained by experiences and interactions with the environment but might also be inherited via our genes [AGE04]. (ii) *Bayes' rule* describes the combination of information from sensory channels and prior knowledge:

$$p(S|O) = \frac{p(O|S) \times p(S)}{p(O)} \tag{2.2}$$

In equation 2.2, $p(S)$ is the so-called *a priori probability* given S which describes prior knowledge. $p(O|S)$ is the likelihood for the observation O given S and $p(O)$ is the probability for the observation itself. This results in $p(S|O)$, which is the probability of S, given the observation O [BK11].

Figure 2.3 illustrates the bayesian integration. In addition to the likelihood and the a priori probability, a goal or target is needed to trigger an action or decision, which again influences perception.

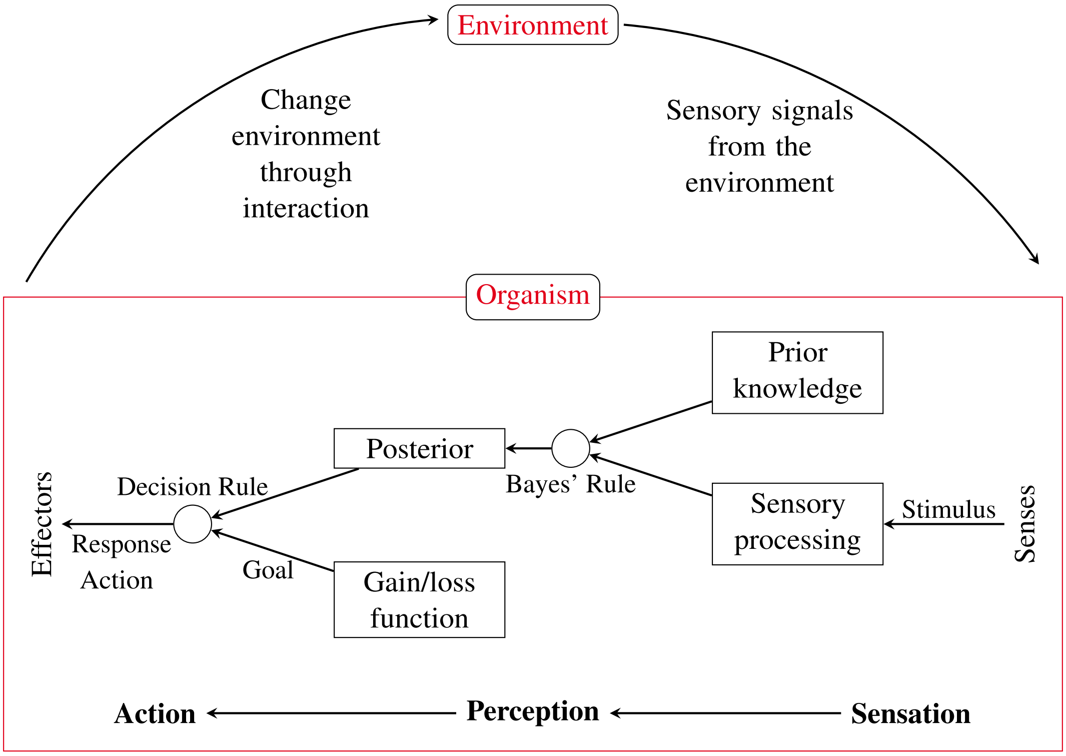

Figure 2.3: Multisensory integration according to Ernst and Buelthoff: The maximum-likelihood estimation and the a priori probability are integrated and a target is added to make a decision (adapted from [EB04]).

2.1.2 VR Sickness

A very dominant problem in VR is *cybersickness* [LaV00]. It is also called *simulator sickness* out of historical reasons, i. e., because an influential systematic investigation of sickness symptoms by Kennedy et al. goes back to flight simulators by the US Air Force [Ken+93]. However, it turned out that there are differences between both kinds of sickness [SKD97]. Cybersickness often denotes the discomfort that may be involved when using a computer in general. To emphasize the sickness that occurs especially in VR, a more modern term for cybersickness is *VR sickness* [FF16; LaV+17], which is the term that is used throughout this dissertation. VR sickness, cybersickness, and simulator sickness are related to *motion sickness* which in turn is related to the visual-vestibular conflict [Aki+03] and occurs during passive self-motion (e. g., car, bus, train) or self-motion illusions (e. g., games, movies, VR) [BS16]. All these phenomena share similar symptoms. Those symptoms can be, for instance, dizziness, nausea, stomach awareness, sweating, headache, fatigue, and so on [BS16; LaV00].

The most accepted explanation for VR sickness is the sensory-conflict theory [LaV00]. Different sensory channels typical deliver slightly different information. For instance, a sensory conflict may arise when the visual system indicates a self-movement but the vestibular system indicates that no movement is occurring. When this mismatch of sensory information is too large, no integration is performed. This is thought to be the source of VR sickness since the human perceptual system does not expect conflicting cues.

The most accepted evaluation method for VR sickness is the Kennedy-Lane Simulator Sickness Questionnaire (SSQ) [Ken+93; SK97].

2.1.3 Psychophysics

Psychophysics describes the relationship of physically measurable stimuli and the subjective perception of those stimuli [Fec60]. The basic question of psychophysical experiments is how well a person can consciously detect the presence of a given stimulus [Raz05], e. g., a 200 Hz tone or a 500 THz color. The stimulus can be of any sensory channel, e. g., visual, auditive, or proprioceptive.

According to Weber's law [Web17], the relation k between the perceivable change of a stimulus intensity ΔS and the prior stimulus intensity S remains constant:

$$k = \frac{\Delta S}{S} \tag{2.3}$$

This is the so-called *just noticeable difference* (JND). It means that the intensity change needs to be greater for a stimulus that already has a very high intensity. For instance, if a candle is put in a dark room, we perceive a change of the intensity of the light. However, if there are already 100 candles in the room, putting in another one might not lead to a perceivable difference of the intensity anymore. Instead, one might need 100 additional candles to achieve a noticeable change.

Regarding the JND, the Weber-Fechner law states that the subjectively perceived sensory sensation is proprotional to the logarithm of the objectively measured intensity of the physical stimulus [Web17]. Therefore, it describes the relation between stimulus intensity S and perceived intensity E:

$$E = c \cdot \ln \frac{S}{S_0} \tag{2.4}$$

In equation 2.4, S_0 is the threshold at which the intensity can just be perceived, while c is a constant used for specific stimuli.

The absolute minimal intensity of a stimulus at which a person can detect it is called *detection threshold* (DT) [Raz05]. For example, when a person hears a 200 Hz tone, the DT would be the loudness at which she can detect it. In an ideal world, all intensities below this threshold would be undetectable and all intensities above this threshold would be detectable. And this would be true every time the person would be exposed to this stimulus.

However, human perception is more complicated. Intensities at values close to thresholds will often be detectable. Therefore, thresholds are considered to be the intensities at which the stimulus is detected only some proportion of the time. For instance, a person might detect a stimulus of a certain intensity only 25% of the time. It is assumed that the probability of detecting the stimulus increases with the intensity of the stimulus [Raz05]. Therefore, the DT is usually considered to be the intensity at which the person correctly detects the stimulus 75% of the time [SLH85].

Optimally, the factors that are involved when measuring DTs are the intensity of the stimulus and the *sensitivity* of the person. However, in most situations there might be background noise, which has to be minimized for best experimental results. Additionally, the participants of a psychophysical experiment can be biased by a lot of different aspects, ranging from their prior knowledge to the experiment design. For example, if a participant is forced to choose between answers like "I do not perceive the stimulus" and "I do perceive the stimulus", the answer can depend in part on her bias and prior experience [Raz05]. Some participants might tend to answer that they did not perceive the stimulus in situations when they are unsure while others might answer that they perceived the stimulus.

There are several different methods for measuring detection thresholds through psychophysical experiments, e. g., the method of constant stimulus [Spe08], the staircase method [Cor62], or the method of adjustment [Ste58]. In this work, we focused on the *two-alternative forced-choice task* method [Bog+06] in all of the conducted psychophysical experiments to determine detection thresholds.

Two-Alternative Forced-Choice Task

In order to determine detection thresholds a standard psychophysical procedure called *two-alternative forced-choice (2AFC)* task is used in the course of this work. Using this method, the participants of a psychphysical experiment are exposed to different intensities of a stimulus. Each time, they have to choose between one of two answer possibilities, for example, if the intensity was smaller or greater than a predetermined reference intensity. Answers like "I don't know" are not allowed. Instead, the participants have to guess and will be correct in 50% of the cases on average.

Applied to redirected walking gains as done in this work (see Part III), e. g. to curvature gains (see Chapter 3.4), this means participants walk a straight path in the VE, which is bent by a curvature gain either to the left or to the right in the real world. Then, they have to judge if the physical path was bent either to the *"left"* or *"right"*. The gain at which the participants respond *"left"* in 50% of the trials is taken as the point of subjective equality (PSE), at which the participants estimate virtual and real movements as identical. As the gain decreases or increases from this value the ability of the participant to detect the difference between physical and virtual movement increases, resulting in measuring points, through which a psychometric curve will be fitted for the discrimination performance. When the participant's answers converge to 100% respectively the 0% chance level, it is more likely that they can detect the redirection reliably. As described above, the DT is the point of intensity at which participants can just detect a discrepancy between physical and virtual motion.

Since the detection rate is often a smooth and gradually increasing function, in psychophysical experiments, usually the point at which the curve reaches the middle between the chance level and 100% is taken as a threshold [Ste+10b]. Therefore, the DT for gains smaller than the PSE is the gain at which the participant has 75% probability of choosing the "left" response correctly and the detection threshold for gains greater than the PSE is the gain at which the participant chooses the "left" response in only 25% of the trials (since the correct response "right" was then chosen in 75% of the trails).

2.2 Immersion and Presence

Immersion is defined as the degree to which a user's senses can experience a VR system [SW97]. The immersive nature of VR directly couples the human sensory channels to the supported technology. Immersion is limited by the objective capabilities of the VR technology, which are technical factors like, for instance, vision, tracking, field of view, resolution, or graphics quality. This means, a VR system that provides stereoscopic vision is more immersive than a VR system that provides only monoscopic vision. A VR system that provides position and orientation tracking is more immersive than a VR system that provides only orientation tracking. A VR system that renders real-time shadows is more immersive than a system that does not support any shadows. Current head-mounted displays (like the Oculus Rift or HTC Vive) usually support stereoscopic vision, position and orientation tracking, high resolution (i. e., more than Full HD), low latency (below 20ms), high frequency (90 Hz), and a wide field of view (circa $110°$). This already delivers a relatively high degree of immersion, but it does not address all capabilities of the human perceptual system. The human field of view is about $220°$ and the human eyes would need a resolution of approximately $116,000,000$ pixels to guarantee that no distinction can be made between individual pixels while Rift and Vive offer only $2,592,000$ pixels [Kod15].

Immersion is an objective metric, whereas *presence* is defined as the subjective estimation of *being there* in an environment while actually being located in a different place [SUS94]. This is also called *place illusion* (PI) [Sla09]. Users who experience a high sense of presence in a VR system tend to perceive the VE more like a place that they visited rather than images that they saw.

In addition to PI, plausibility illusion (Psi) is defined as the illusion that the scenario in the VE is actually occurring [Sla09]. To get users to respond realistically to a certain situation in VR, PI and Psi have to be induced. Since presence is a subjective perception, it depends on immersion and takes into account the psychological state of the user as well [Jer15]. Although, immersion can be a limiting factor. A standard method for measuring presence is the use of questionnaires like the Slater-Usoh-Steed Presence Questionnaire (SUS) [SU93; SUS94] or the Igroup Presence Questionnaire (IPQ) [SFR01].

Visual Self-Representation

In a VE, using a visual self-representation like a fully articulated avatar generally increases the degree of presence since additional modalities are provided to the user. The concept of having a virtual body is an approach to decrease the contradiction between sensory data and proprioception [MS96; SU94], and, therefore, induce a sense of agency. A contradiction is caused when proprioception informs the user that her body is in one place, but the VE provides the user with visual evidence of the absence of her body in that space.

Usoh et al. propose that association with the virtual body also increases the feeling of presence and that, therefore, the avatar should be as realistic as possible [Uso+99a]. Implementing an avatar with incorrect behaviour can dissociate the user from the virtual environment. Heeter et al. point out that having an avatar increases the user's sense of presence [Hee92] but only if that avatar is similar to the real user. When implementing a VE, it is important to note that the virtual limb should have similar physical appearence and anatomical orientation as the real one [Llo07]. When a fake hand is seen in place of a real hand, cells in the premotor cortex fire, but they decrease their firing rate when similarity decreases [EHP05; ESP04; Gra99].

2.3 Spatial Perception

During walking in the real world, accurate estimations of distances, sizes, and self-motion speed are essential, e. g., to avoid collisions, reach high navigation performance, or build up an accurate mental map of an environment [Kla+98]. Spatial perception describes the ability of being aware of such spatial characteristics and involves the integration of different cues that are extracted from multiple senses [CV95]. Important visual cues are binocular disparity, convergence, accommodative focus, linear perspective, aerial perspective, occlusion, shading, and motion parallax [Bow+04; How02; Loy18; RVH13].

Accurate judgements of spatial circumstances are important in the real world, and are often needed in VEs as well. In particular, when walking in VR, one should achieve a similar performance as in the real world. Unfortunately, many studies report that there is a significant spatial misperception in VR [LK03; WK98]. We will discuss reasons and possible improvements for distance, speed, and scale perception in the following sections.

2.3.1 Distance Perception

A lot of empirical evidence has been collected over the last decade, which indicates that distance perception in VEs significantly differs from the real world, with very close distances often being overestimated while distances in vista space tend to be underestimated [Bru+15; BYB18; Cre+05; Cre+15; Li+15; RGA95; Rou+15; Wil+08]. Renner et al. [RVH13] reviewed the extensive literature on distance perception in VEs.

Several theories and approaches to improve spatial perception in VEs have been presented. For instance, some researchers suggest that feedback during interaction might be sufficient for the highly adaptable human perceptual system to reduce spatial misperception given sufficient time [RW07]. Other researchers suggest that the sense of presence in VEs has a direct effect on the

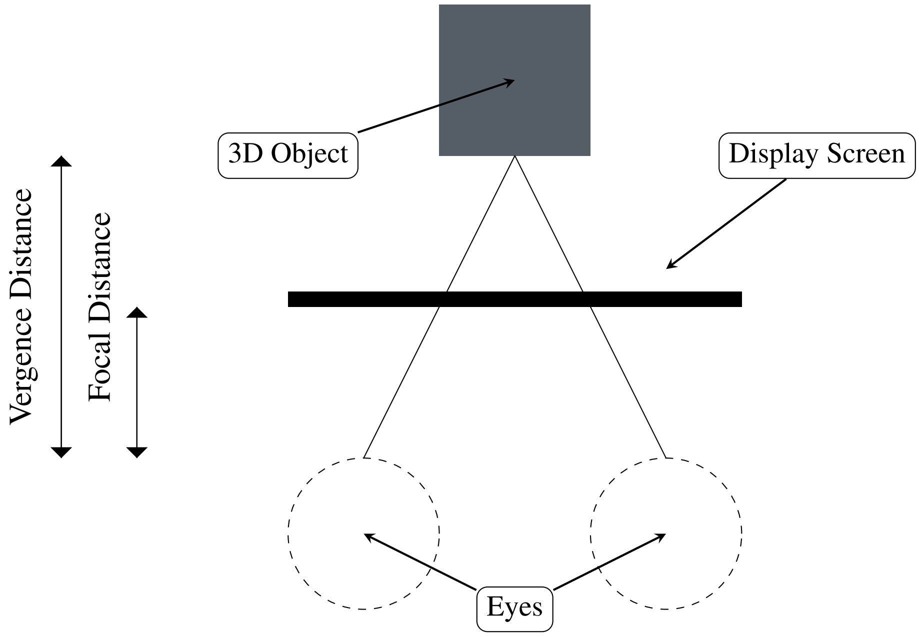

Figure 2.4: Accommodation-convergence conflict: Accommodative focus is fixed on the distance to the display screen while the eyes converge to the actual position of the fixated object.

quality of spatial judgments [Int+07], such that low fidelity virtual worlds might indirectly impair spatial judgments [Ahm+10; Phi+12; Tho+04]. In contrast, presenting a richer and more realistic virtual world using high quality graphics might improve distance estimation in VEs [RVH13]. Moreover, distance perception benefits from a user's visual self-representation [Moh+10; VMH16]. Psychophysical experiments revealed significant differences when estimating distances in non-photorealistic versus high-fidelity VEs [NCH11; Phi+09]. Furthermore, this is supported by the finding that image resolution influences perception of distances as well [RHS05].

So far, current head-mounted displays have not been able to match the human visual system in terms of resolution, field of view, or temporal fidelity (see Section 2.2 and Section 2.1), which likely constitutes a cause of distortions in human perception. Probably, spatial judgements in VR will be more accurate when display quality gets better [Che+19; KCS17].

Another potential explanation for the described misinterpretation might originate from incorrect depth cues provided to the human eye when looking through an HMD, such as the accommodation-convergence conflict [Hof+08]. Convergence and vergence is the ability of the eyes to rotate inwards and outwards to fixate a certain object. By triangulation, this ability can help estimating a distance to this object. When focusing on an object in the real world, the human eye adjusts the ciliary muscles to bring the object into sharp focus on the retina, while the shape of the lens causes objects at different distances behind or in front of it to appear blurred (see Figure 4.1). This is called accommodation and supports distance estimation as well [CV95]. In the real world, both distance cues usually match, however, in VR, they do not necessarily match (see Figure 2.4). With current HMDs, independently of where and on which the eyes of the observer are focused, every object in the visual field appears sharply since the accommodative focus is fixed to the distance of the screen. Hence, to provide a similar viewing experience as in the real world, researchers and engineers work on light-field displays which consist of several layers [LL13]. These layers enable the observer to focus to different distances. Multiple layers require much more computing power and, so far, only displays with low resolutions are available [HLW15].

In order to provide additional depth cues on conventional displays, some researchers propose to add artificial blur to the rendered imagery [CR15; Cid+16; Hil+07]. In particular, Held et al. [Hel+10] found that visual blur plays a significant role in perceiving size and distance, at least in non-stereoscopic images. They presented a probabilistic model based on Bayes' Law to explain how blur in combination with perspective cues can provide correct estimations of absolute egocentric distances to objects in static images viewed on a CRT monitor. Blur effects like depth-of-field (DOF) are also known to mitigate the accommodation-convergence conflict in HMDs and therefore help to reduce visual discomfort like eye fatigue, headaches and nausea [CR15]. Moehring et al. [MGD09] state that DOF blur in HMD environments might additionally improve spatial perception.

2.3.2 Speed Perception

Research on speed perception in HMD environments indicate a general tendency to underestimate self-motion speed as well [NSN15]. Banton et al. [Ban+05] hypothesized that speed misperception might originate from the small field of view (FOV) of HMDs, which does not reach into the far periphery of the eyes [JSB13]. In particular, they assume that visual flow is necessary for a correct speed perception and that this cue is cut off by a limited FOV because the user can not see the ground while looking straight ahead. They found a significant effect showing that the display's FOV was inversely proportional to the underestimation of walking speed in a VE, while speed estimation was more accurate when participants perceived visual flow [Moh+07b; NSN14]. Furthermore, motion blur has been suggested to improve speed estimation. Several studies have shown that humans are generally able to gain information about the direction and speed of moving from motion blur [BR02; FK01; Ros04]. Furthermore, Kim and Francis [KF98] showed that motion lines have the potential to change motion perception as well. In general, research on speed estimation in VEs as compared to the extensive literature on distance estimation is still underrepresented in this field of research.

2.3.3 Scale Perception

By adding several scale levels to an IVE, users have the chance to explore the VE from different perspectives resulting in a more comprehensive viewing experience [Kop+06]. For example, they might benefit from overviews, which could be perceived from a high scale level of the VE, or they might look at every detail at a low scale level. VR setups in general, and multi-scale VEs in particular, have great potential to study different perceptual illusions. For instance, previous work has shown that body scale illusions can be induced [Ehr+05]. Linkenauger et al. and Jung et al. presented studies to investigate body-based scaling [Jun+18; Lin+13]. In their experiments, they focussed on the hand, which acts as a metric which individuals use to scale the apparent sizes of objects in the environment [Jun+18; Lin+13]. Gibson introduced the notion that individuals do not perceive the environment, but rather perceive relationships between their body and the environment [Gib79]. Moreover, perceptual distortions of scale such as micropsia or macropsia are even known to occur in persons in the real world in a rare disorienting neurological condition known as the Alice in Wonderland Syndrome or Todd's Syndrome [Tod55].

Large differences in spatial perception between users reduce the ability to see the same artifacts in the scene and perceive the same affordances [Pol+12]. Furthermore, one needs to understand that egocentric distances in VEs are often underestimated [Bru+15; RVH13] (see Section 2.3.1). In this context, Interrante et al. compared distance estimation between the real environment and a scaled VE that is a replica of the real environment [Int+07].

Scale perception is also an important factor for (social) presence and interaction between multiple users in multi-scale VEs. Hall [Hal66] introduced *proxemics*, which describe spatial distances between humans and their social impact. He differentiates between the *intimate*, *personal*, *social* and *public* distance. As described in [BM98], the proximity to other avatars (i. e., within the inter-personal distance) is highly relevant in VEs as well. However, when it comes to multi-scale VEs there are some challenges with proxemics [ZF02]: Since the user can scale herself, a situation might occur in which there are “giant” and “mini” representations of collaborating users. In such a situation, the giant avatar might perceive the mini avatar (who is very small in the giant’s field of vision) as not being in her intimate or personal distance. However, the mini avatar might perceive the situation the other way around. Zhang and Furness have considered such effects for static, but not fully articulated avatars [ZF02]. In a similar way, interpretations of the scale of the VE or oneself has also the potential to affect the perceived affordances in the VE [Nor99]. For instance, the perceived affordance of objects might change during a scale change of the VE in such a way that an object, which was interpreted as moveable in a shrunk visualization, might be interpreted as unmovable in an enlarged level since the user might assume more weight to the object. Such changes in the perceived affordances might also apply to other affordances such as grabbing, pressing, lifting etc.

3. LOCOMOTION

3.1 Overview

According to Bowman et al. [BKH97] VR navigation tasks can be divided into cognitive and physical components: (i) wayfinding and (ii) (active or passive) travel. Wayfinding is defined as the building and maintaining of a spatio-cognitive map and is essential for identifying how to get from one place to another [DAA98]. Wayfinding aids, such as maps or compasses, can be used to support this task [DC99; FWK17; FWK18; SCP95]. Travel rely on the informations gained by the wayfinding task, but in return, the travel technique might support wayfinding up to a certain degree. At its core, travel involves the movement of the viewpoint within the VE from one location to another, which could also be induced by the system, i. e., passive travel. On the other hand, active travel is controlled by the user. In the scope of this work, active travel is also denoted *locomotion* [Bol17]. Active travel, i. e. locomotion, can be carried out physically (e.g. walking-in-place) or purely virtual (e.g. self-triggered teleportation).

Locomotion is one of the most frequently used types of interaction in VR [Bow+04]. However, its realistic implementation is also one of the most challenging tasks in VR development [Ste+13]. A locomotion technique has to fit the specific task that the user wants to carry out and the context in which she acts. For instance, exploration tasks might require a different technique than search tasks. Furthermore, the travel distance, spatial orientation, or the target visibility should be considered [Bow+04].

In general, real human walking is the most natural way of locomotion in VR [Ste+13]. It is based on multi-sensory cues like vestibular, proprioceptive, as well as visual information that create an inherent perception of self-motion acceleration, velocity and direction. Furthermore, real walking has been shown to increase a user's sense of feeling presence [SUS95; Uso+99a], improve spatial knowledge [PFW11; RVB10; RL09], and reduce VR sickness symptoms [LaV00]. Basic implementations of real walking can be realized by mapping position and orientation of a user one-to-one to the virtual camera. Then, a one meter forward movement in the real world is mapped to a one meter forward movement in the virtual world. This provides the user with near-natural sensory feedback similar to the real world. When using real walking, however, the size of the VE is limited to the size of the tracking space in the physical world. Systems like *Oasis* [SGM17;

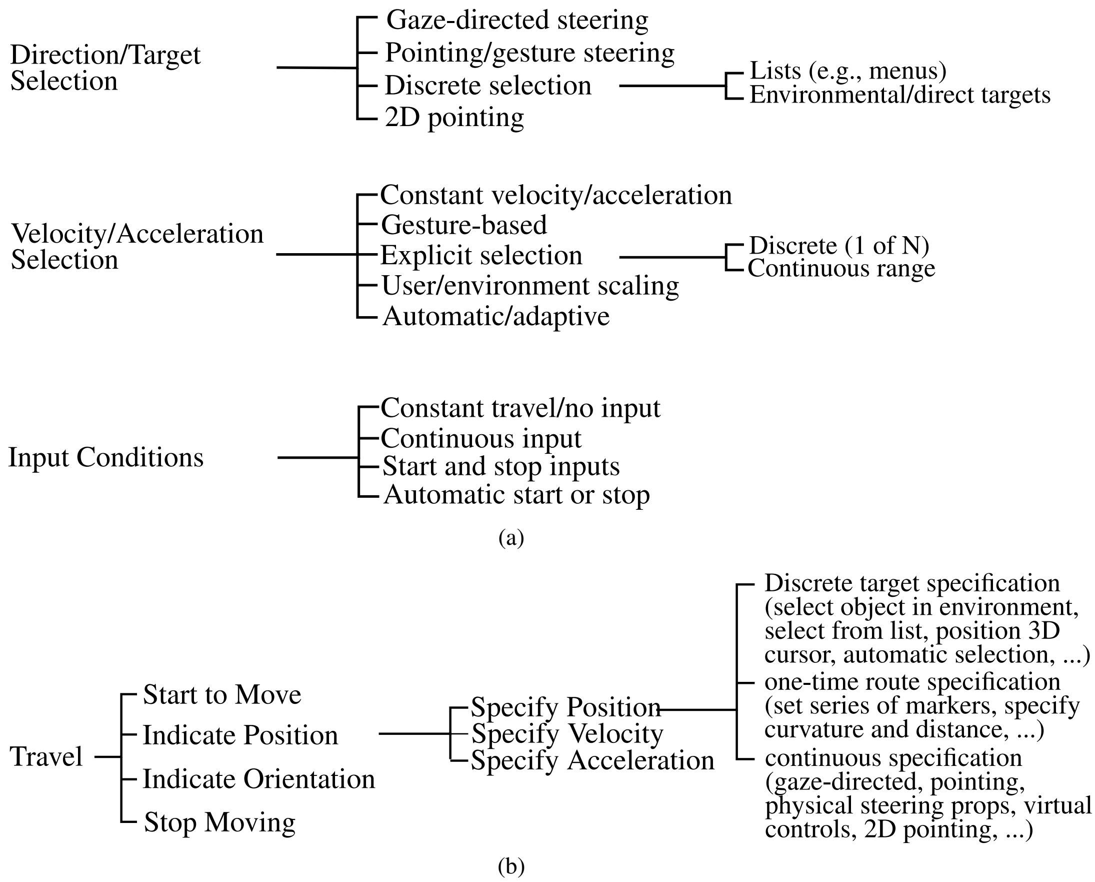

Figure 3.1: Taxonomies of virtual travel techniques: Either ordered by subtasks of travel (a) or by level of user control (b) (adapted from [BKH97] and [Bow+99]).

Sra+16], *VirtualSpace* [Mar+18], and *Scenograph* [MB18] try to match the real and virtual space to enable as much walking as possible. For instance, *Oasis* scans the real world room beforehand and generates a virtual world automatically according to the available walkable space. *Scenograph* extends this approach by flexibilizing the narrative structure of an experience depending on the size and shape of the tracking space. But still, the VR experience is limited to the size of the walkable physical space.

To address this limitation, a lot of alternative locomotion techniques have been developed, e. g., virtual travel techniques such as teleportation [BSB11; Boz+16] or flying [Uso+99a], hardware devices like omnidirectional treadmills [Sou+11], motion platforms [BS02; Bou+02], motion robot tiles [Iwa99; IHT06; Iwa+05] or motion carpets [STU07], and walking-in-place [NSN16]. Another interesting collection of techniques are *Redirection Techniques* because they aim to combine the advantages of real walking with the exploration of unlimited VEs. A similar approach is called motion compression which is used for teleoperation and based on path prediction [NHS04]. Furthermore, it is possible to map virtual and physical reality in such a way that the virtual view is distorted [Don+17; SWK16].

This chapter provides an overview of different locomotion techniques, including virtual travel techniques, walking-in-place, and redirected walking.

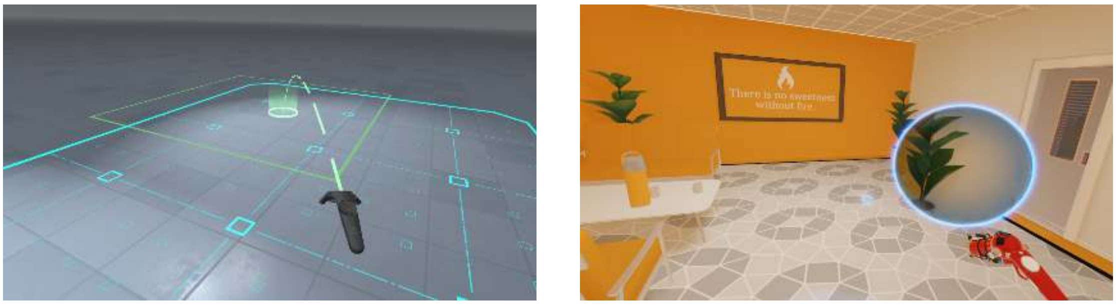

(a) (b)

Figure 3.2: Teleportation techniques in *The Lab* [Val16] (a) and *Budget Cuts* [Cor17] (b). The first one uses a pointing technique to specify the target and teleports the user instantaneous to this location. The second one provides a preview of the target before the actual teleportation is initiated.

3.2 Virtual Travel Techniques

Bowman introduced different taxonomies of travel techniques (see Figure 3.1): Techniques can either be ordered by subtasks of travel [BKH97], like target selection and velocity selecetion [FWK16a], or by the level of user control [Bow+99]. LaViola et al. provide a comprehensive overview of travel techniques [LaV+17] by classifying them into steering, selection-based travel, manipulation-based travel, and walking [NB16].

An example for steering techniques is gaze-directed steering where the user is moving in her gaze direction or optionally in the lateral directions [CH02]. Selection-based travel requires the user to perform a selection task, which, for instance, can teleport users to a target location and back to the start, allowing them to explore certain (predefined) spots in the VE [Zel+02]. Other selection-based techniques allow users to point at a location on a map to get transported there along the shortest path [Bow+98]. Similarly to world-in-miniature solutions, manipulation-based techniques might show a miniaturized version of the VE within the user's interaction range and allow her to move their avatar within this miniature representation [WHB06]. Another manipulation-based technique, which was also implemented by Google Earth VR, lets users pull the world towards themselves [WO90].

The VR games published in the last years use several approaches to address the challenge of unlimited locomotion and providing a joyful overall user experience [FSW17]. Some games avoid locomotion beyond small evasive movements, e. g. "Job Simulator" [Lab16] and "Space Pirate Trainer" [Ill16]. However, for most current games, it is essential that players can move around the VE up to a certain degree. The game "Robinson: The Journey" [Cry16] uses a modified version of traditional gamepad controls for navigation. It sets a comparatively low walking speed and enables fixed changes of direction. An alternative solution is to avoid active locomotion of the player, but to move a vehicle which in turn moves the player. This is often done on pre-defined paths like rails [Gam16].

However, when using virtual travel techniques such as flying by joystick controllers, users may get conflicting movement cues from proprioception, the vestibular sense and from vision. Though the eyes perceive the motion, the hair cells in the inner ear, which are sensitive to acceleration and orientation, do not perceive the same information, which is the major cause for VR sickness according to the sensory-conflict theory [LaV00]. Furthermore, this discrepancy can also affect the sense of presence in the VE [Uso+99a].

The most prominent examples of instantaneous selection-based travel are *point & teleport* techniques allowing users to point to a destination in the virtual world to which they can virtually teleport their viewpoint [Boz+16; KCO10]. Examples include Valve's "The Lab" [Val16] (see

Figure 3.2 (a)) and "SportsBar VR" [CP16]. However, there are a lot of variations of these technique. "Budget Cuts", for instance, provides a preview of the target position and orientation before the actual teleportation is initiated [Cor17] (see Figure 3.2 (b)). The jumper metaphor [BSB11] leverages the head direction to select the destination and a physical jump of the user to trigger the teleportation. And "Smash Hit Plunder" combines a continuous motion to the chosen target location with interrupting blinks [Pix17], which is supposed to decrease motion sickness.

Travel in Multi-Scale Virtual Environments

Multi-scale VEs (see Section 2.3.3) offer the chance to explore a VE from different perspectives resulting in a more comprehensive viewing experience [Kop+06]. These multi-scale VEs enable and require different locomotion techniques than VEs at a single scale. Perlin and Fox introduced multi-scale interfaces for 2D interaction [PF93], which are the basis of various interfaces, like the Pad++ [BH94]. These multi-scale interfaces were extended to 3D interaction by Zhang to "augment our limited cognitive capabilities" in VEs [ZF05]. According to his results changing the scale supports users in better understanding the structure of large objects [Zha08]. However, the introduction of multi-scale VEs required new interaction techniques for navigation purposes. In multi-scale VEs, 3D navigation in space can be implemented in the same way as in VEs displayed at a single scale, but it is necessary to navigate in scale as well [GK11], for instance, by using techniques such as zooming-in and zooming-out [Kop+06]. LaViola et al. suggest hands-free navigation methods, in particular with a foot-gesture controlled *step WIM* and a leaning technique [LaV+01]. It should be noted that space and scale in multi-scale VEs are usually coupled tightly together. To travel in multi-scale VEs users can manipulate the scale of the virtual space and the relative size of space as two different actions, or combine them into a single action [Zha09]. However, it can be challenging for users to traverse the space-scale [FB95; Zha09].

3.3 Walking-in-Place

Walking-in-place (WIP) denotes a class of locomotion techniques that enable users to walk through infinitely large VEs by mimicking walking movements with their body in the real world [SUS95]. In comparison to real walking, WIP techniques can be used even in very small physical workspaces and the requirements on tracking hardware accuracy and precision are comparably lower [Ste+13]. However, in the past, providing a WIP technique, in which a user can orient the body in any direction in the real world and start walking, presented a challenge to WIP tracking technologies, which often did not allow users to turn in the real world or suffered from limited tracking performance in such cases [Ste+13]. Different approaches have been proposed as workarounds in case of such tracking limitations by simulating turning in the VE, such as redirected walking-in-place [Raz+02].

Many different WIP locomotion techniques have been presented, which differ in inputs, outputs, control of virtual displacements and feedback of virtual locomotion [Ste+13]. Different segments of the user's body can be analyzed to initiate virtual self-motion, such as the feet, shins, knees, fingers, or head [BPJ13; FWW08; Raz+02; Sar+17; SUS95; TDS99; Ter+10]. While early WIP techniques triggered discrete virtual steps [SUS95], state-of-the-art systems use the physical body movements as input for algorithms to maintain continuous virtual self-motion, e. g., using sinusoidal velocity profiles [WWB10]. Inspired by real walking gaits, algorithms analyzing the movements of these body parts based on neural networks and signal processing [FWW08], state machines [WWB10], or pattern recognition [TDS99] have helped to reduce starting and stopping latency and improved the smoothness of virtual locomotion.

For these algorithms it is important that the user's body parts are tracked with high precision and accuracy, as well as low latency. Different tracking technologies have been evaluated for WIP techniques, including magnetic [FWW08; SUS95] and optical [Uso+99a] tracking systems, as well

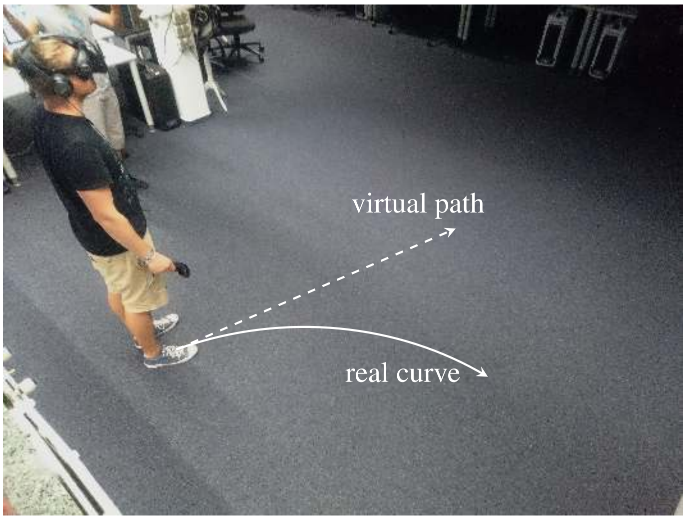

Figure 3.3: A user walking virtually straight while being redirected using a curvature gain.

as Wii Balance Boards [Wil+11] and Wiimotes [SH08]. However, these solutions usually do not support full-body tracking or do not provide omnidirectional full-body tracking at low cost. One solution for this is to use multiple Kinects and fuse their detected skeletons [WQL14].

3.4 Redirected Walking

Redirected Walking (RDW) is a collection of VR locomotion techniques that enables humans to walk on paths in the real world, which may vary from the paths they perceive in the VE [Bru+13; Nil+18; VK17a]. RDW can be implemented by manipulations applied to the virtual camera, usually by using *redirection gains*, which require the user to compensate by repositioning and/or reorienting themselves in order to maintain their intended walking direction in the VE. Within certain detection thresholds such manipulations are subtle for the user.

The traditional approach of *Redirected Walking* that was introduced by Razzaque et al. [RKW01] and extended by others [Eng+08; FV04; Gol12; Ste+10b] is based on slightly rotating the user's view to one direction while she walks on a straight path in the VE. Then, she will unconsciously compensate the rotation by walking on a curved path in the opposite direction. As a result, she will walk on a circular arc in the real world (see Figure 3.3). About a decade later, Steinicke et al. revisited this technique and described such manipulations by means of gains. For example, curvature gains can be defined as follows: $g_C := \frac{1}{r_{real}}$, where r_{real} describes the radius of the circle on which the users are guided in the real world [Ste+10b]. When redirecting a user, her visual feedback is consistent with movements in the VE, but proprioceptive and vestibular feedback systems are coupled to the physical world. It is known from perceptual and cognitive psychology that vision often dominates proprioception and vestibular sensation when the information from these senses is in conflict [Ber00; DB78]. However, if the visual-proprioceptive conflicts are small enough, humans will not even be able to notice that they are manipulated. In perceptual experiments where human participants can use only vision to judge their motion through a virtual scene, they can successfully estimate their momentary direction of locomotion, but are worse in perceiving their paths of travel [BIL00; LBv99]. Since humans tend to compensate for slight visual-proprioceptive inconsistencies during locomotor control while walking, it becomes possible to guide users along real-world paths, which differ from the paths they perceive in the virtual world.

There are several other redirection techniques in addition to curvature gains. While the traditional RDW approach is based on curvature gains, the terms *Redirected Walking* and *Redirection*

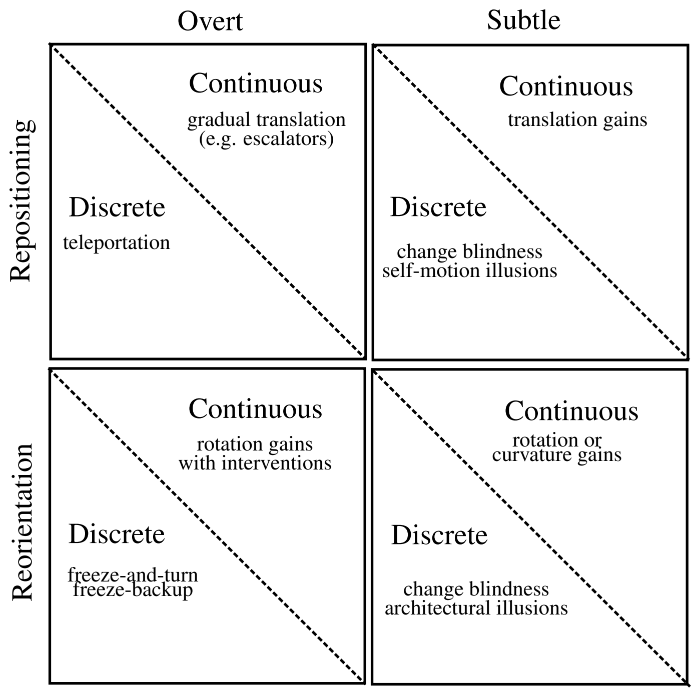

Figure 3.4: Taxonomy of redirection techniques (adapted from [Sum+12a]).

Techniques are often used almost interchangeably. Suma et al. introduced a taxonomy of *Redirection Techniques* (see Figure 3.4) that classifies these techniques into the categories *Repositioning* or *Reorientation*, *Subtle* or *Overt*, and *Discrete* or *Continuous* [Sum+12a]. Repositioning techniques manipulate the position of the virtual viewpoint of the user, whereas reorientation techniques manipulate their orientation, which are usually focused on the yaw rotation. Subtle techniques are intended to be not noticed by the user, i. e., manipulations are below the user's detection thresholds. Discrete techniques redirect the user in discrete steps. For example, instant teleportation [Boz+16] is a discrete overt repositioning technique, and impossible spaces [Sum+12b] are a discrete subtle redirection technique based on scene layouts, which would be impossible in the real world. For instance, such impossible spaces are composed of scenes whose architecture is self-overlapping or changing when the user does not pay attention. Continuous techniques, on the other hand, make use of a continuous motion. One set of techniques in this category are *gains* for translation, rotation, and also curvature. A gain describes differences between real and virtual motions, i. e., ratios between a user's movements in the real world and in the VE. A translation gain $g_T := \frac{T_{virtual}}{T_{real}}$ manipulates the virtual velocity of the user, making her walk slower or faster in the VE compared to the velocity in the real world [IRA07]. A rotation gain $g_R := \frac{R_{virtual}}{R_{real}}$ increases or decreases the virtual rotation of the viewpoint relative to the rotation in the real world. When a rotation gain g_R is applied to a real-world head rotation with angle α, the virtual camera is rotated by $\alpha \cdot g_R$ instead of α. Furthermore, Steinicke et al. defined displacement gains for mapping physical rotations to virtual translations and time-dependent gains for manipulations that are independent of physical movements but introduce changes over time [Ste+09a]. Later, gains for redirected jumping [Hay+19] and for scaling the user's size [Abt+19] were added. Moreover, electrical muscle stimulation was leveraged to imrove RDW [APS19].

However, no matter which technique is used, when the user hits a boundary of the tracking space, she has to be stopped and reset in a suitable way. For this *resetting phase*, several discrete and continuous approaches exist, e. g., freeze-and-turn [Wil+07] or visual distractors [PFW08].

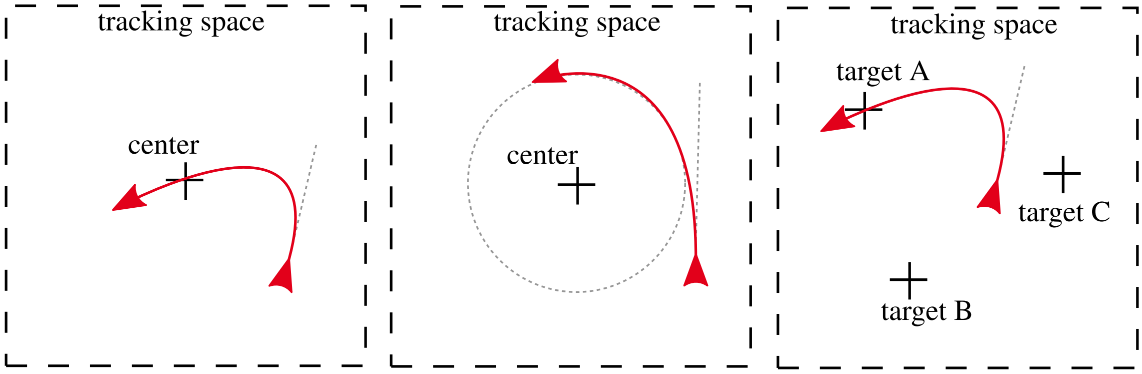

Figure 3.5: Steering algorithms: Steer-to-center, steer-to-orbit, and steer-to-multiple-targets (adapted from [Raz05]).

3.4.1 Steering Algortihms

When implementing RDW with curvature gains, two things have to be provided or assumed: (i) the target or direction of the user in the VE, and (ii) the target of the redirection in the real world. Then, the amount of redirection, i. e., the gain, can be calculated and a corresponding rotation can be applied to the user's view.

A heuristic approach to predict the target of the user leverages the current gaze direction, which is available through rotational head tracking [Ste+08c] or eye tracking [ZK16], the past walking direction [ZK15], or the direction of the user's torso. A combination of these methods or the usage of probabilistic models is also possible [SAH07].

In small tracking spaces, it is required to steer the user away from the boundaries. Therefore, Razzaque proposed three algorithms: (i) steer-to-center, (ii) steer-to-orbit and (iii) steer-to-multiple-targets [Raz05]. These techniques are based on the idea to redirect the user always to a certain point, on a certain orbit, or to multiple certain points (see Figure 3.5), i. e., these are the targets of the redirection in the real world. In these scenarios, the user's walking direction is constantly changing while she is walking freely in the virtual world. Hence, the required amount of redirection is constantly recalculated so that the user is always steered towards these certain points or orbits. Hodgson et al. [HB13] added the (iv) steer-to-multiple-centers algorithm, which is an extension of the steer-to-multiple-targets algorithm, and compared them regarding metrics like number of wall contacts and maximum distances from the tracking area center. In these experiments, steer-to-center showed the best performance. In another experiment, where the VE was constrained by virtual walls and the walking directions were therefore limited, steer-to-orbit performed better [HBT14]. In general, larger tracking spaces offer improved performance starting with a minimum viable size of approximately 6m$\times$6m [Azm+15]. Instead of using the center or random targets it might be beneficial to use physical proxy objects inside the tracking space as steering targets [Ste+08c]. These objects can provide the user with passive haptic feedback for unlimited virtual objects [Koh+05]. Hodgson et al. [HBW11] introduced a generalized RDW algorithm for gymnasium-sized spaces while others implemented their algorithms for spaces with a size of approximatly 6m$\times$6m [Sum+15].

In order to guide users always in an optimal way, a planning method can be used to select the most suitable redirection technique for a given situation [Zmu+13]. Therefore, a manually defined graph of weighted walking paths based on the known VE is used to predict the user's travel path. This technique revealed a significant improvement compared to the steer-to-center algorithm [NHK14]. Furthermore, it has been shown that the graphs can be generated automatically based on navigation meshes [Azm+16b; ZK17]. Recently, novel methods for steering based on deep learning [Don19] and artificial potential fields [Bac+19; Jus19; TR19] were introduced.

There were also approaches, which combined RDW algorithms with other travel techniques such as portals [BSH09; FRK14; Ste+09b], teleportation [Liu+18], or redirection-free zones [LBS14].

3.4.2 Resetting

No matter which redirection technique or steering algorithm is used, it can still happen that the user hits a boundary of the tracking space. In this case, she needs to be stopped and reset, i. e., the user must be turned to face to the center of the tracking space again. For instance, most redirection solutions, e. g., the RDW toolkit [Azm+16a], make use of a *stop-and-go* approach. Using these approaches, the user walks until the boundary of the tracking space is reached, for example, while a curvature gain is applied. Then, she will be rotated until there are no obstacles in front of her new walking direction. Afterwards, the user can continue walking in the desired direction.

For this *resetting phase* or *reorientation phase*, several techniques exist. Williams et al. introduced the three methods (i) Freeze-Backup, (ii) Freeze-Turn, and (iii) 2:1-Turn [Wil+07]. In the Freeze-Backup method, the position of the user in the VE is frozen and she can walk backward until she has enough empty physical space in front of her. In the Freeze-Turn method, the orientation of the user in the VE is frozen and she can turn around until she has enough empty physical space in front of her. In the 2:1-Turn method, the user turns around 180 degrees physically (so that she has enough empty physical space in front of her), while she turns 360 degrees virtually (and looks in the same direction in the VE as before the turn). Such a manipulated turn is implemented using a rotation gain g_R=2. In this case, visual distractors can be used to make these manipulated turns less obvious and to appear more natural [PFW11; PFW08]. The resetting phase can also be integrated into the domain or the narration of the VR application [Sra+18; Yu+18] by using suitable metaphors, e. g., a turning bookshelf [Yu+17].

To reduce the number of resetting phases in this stop-and-go approach, Zhang et al. [ZK13; ZWK15] developed heuristics to dynamically adjust RDW gains for guiding the user in the best direction. It turned out that the users walked a significantly longer distance between two resetting phases when using this method.

3.4.3 Detection Thresholds

Redirection techniques may be subtle under certain conditions. Therefore, detection thresholds for different manipulations have been analyzed using a 2AFC task (see Section 2.1.3). We collected several estimated detection thresholds for different gains and conditions in Table 3.1[1].

Steinicke et al. conducted several experiments to reveal detection thresholds for translation, rotation, and curvature gains [Ste+10b][2]. The detection thresholds indicate just-noticeable differences between vision and vestibular system. According to their results, a straight path in the VE can be turned into a circular arc in the real world with a radius of at least 22m, for which users are not able to consciously detect manipulations. This means, that a physical space of at least 45m×45m would be necessary to enable infinite virtually straight walking. Furthermore, rotations can be scaled by gains between 0.67 and 1.24 and translations can be scaled by gains between 0.78 and 1.22 without that users are able to detect the manipulations. These experiments have been replicated with different settings and extended several times [Bru+09; Bru+12; FWK16b; KSB11; Ste+08b; Ste+09b]. For example, Grechkin et al. found that a radius of only 12m can be sufficient for unlimited straight walking in a VE [Gre+16]. The differences in the results between those experiments could be explained by the different hardware that was used in the experiments as well as methodological and population differences. In general, current hardware appears to improve RDW techniques.

[1] In this table, we already added the results that we present in Part III.
[2] While there most likely was a bias in the question of their first experiments [Ste+08a], they repeated them [Ste+10b].

Gain	Comment	Thresholds[1]	$°/m$ Notation[2]	Source
Translation	Question Bias	0.78 - 1.22	-	[Ste+08a]
Translation	-	0.78 - 1.22	-	[Ste+10b]
Translation	-	0.87 - 1.29	-	[Bru+12]
Translation	Driving	0.94 - 1.36	-	[Bru+12]
Translation	-	0.86 - 1.26	-	Chapter 7
Translation	Virtual Feet	0.88 - 1.15	-	Chapter 7
Translation	Low-cue VE	0.73 - 1.25	-	Chapter 7
Translation	Saccades	-50 - 50	-	[BL15]
Translation	Eye Blinks	-9.75 - 7.71	-	Chapter 10
Rotation	Question Bias	0.59 - 1.1	-	[Ste+08a]
Rotation	-	0.67 - 1.24	-	[Ste+10b]
Rotation	-	0.68 - 1.26	-	[Bru+12]
Rotation	Driving	0.77 - 1.26	-	[Bru+12]
Rotation	-	0.93 - 1.27	-	[Pal+16]
Rotation	16 objects	0.82 - 1.20	-	[Pal+16]
Rotation	Saccades	-5 - 5	-	[BL15]
Rotation	Eye Blinks	-4.76 - 5.78	-	Chapter 10
Curvature	Original: $1°/s$	$r > 57.3$m	$1°/m$	[Raz05]
Curvature	Question Bias	$r > 16$m	$3.5°/m$	[Ste+08a]
Curvature	Question Bias & 2m start-up	$r > 24$m	$2.35°/m$	[Ste+08a]
Curvature	-	$r > 22.03$m	$2.6°/m$	[Ste+10b]
Curvature	-	$r > 14.92$m	$3.84°/m$	[Bru+12]
Curvature	Driving	$r > 8.97$m	$6.39°/m$	[Bru+12]
Curvature	$v = 0.75m/s$	$r > 10.57$m	$5.42°/m$	[Net+12]
Curvature	$v = 1.00m/s$	$r > 23.75$m	$2.41°/m$	[Net+12]
Curvature	$v = 1.25m/s$	$r > 26.99$m	$2.12°/m$	[Net+12]
Curvature	-	$r > 11.61$m	$4.9°/m$	[Gre+16]
Curvature	Audio	$r > 27.5$m	$2.08°/m$	[Ser+13]
Curvature	Audio & Vision	$r > 6.0$m	$9.55°/m$	[MNF16]
Bending	$r_{real} = 1.25m$	3.25	$31.7°/m$	Chapter 8
Bending	$r_{real} = 2.5m$	4.35	$17.6°/m$	Chapter 8
Bending	$r_{virtual} = 3m$	1.63	$7.41°/m$	Chapter 9
Bending	tDCS, $r_{virtual} = 3m$	1.61	$7.31°/m$	Chapter 9

Table 3.1: Detection Thresholds of Redirection Techniques

[1] For translation and rotation gains, the range of undetectable gains is stated. For bending gains, the maximal gain is stated. For curvature gains, the radius of the resulting arc in the real world is stated. And for blinks and saccades, the maximal offset in cm or ° is stated.

[2] For comparing curvature and bending gains, this notation is more suitable since it does not rely on the radius of the curves. It can be calculated if real and virtual radii are given.

After being blindfolded and exposed to the rubber hand illusion for only 30 seconds, participants from the study by Ehrsson et al. had to point to their right index finger with their left hand, which resulted in a pointing error of 3 cm [EHP05]. Without visual feedback, perceived limb position even drifts over time [Bro02; WI92]. In general, strongest ratings for realness and presence were given when the physical limb position and the virtual limb position are closest. Lloyd et al. claimed that ratings decayed significantly after a distance of 30cm from the virtual to the physical position [Llo07]. Burns et al. found a mean detection threshold of 0.4 in a study where they changed the user's hand position with a drift of 5mm/s for a movement faster than 5cm/s [Bur+05].

Furthermore, it was found that an isometric mapping is not always the most natural one. Geometrically correct optic flow appears to be too slow and users estimate a virtual walking velocity as more natural when it is slightly increased compared to the user's physical body movement [Ban+05; Jan+17b; NSN14]. Steinicke et al. found that virtual translation has to be increased by 7% to appear natural [Ste+08a; Ste+10b]. It was shown that rotation manipulations are less obvious to detect if the VE moves against head rotation compared to situations where the VE moves with head rotation [Jer+08]. It was found that sensitivity to curvature gains depends on walking velocity: a slower walking speed allows higher redirection gains [Net+11; Net+12]. Redirection can also be applied for driving simulations, for example, when applying curvature gains to a user sitting in an electric wheelchair, this resulted in greater possible redirection [Bru+12], which might be related to the proprioceptive feedback users receive by walking, whereas this feedback is mostly missing while driving in a wheelchair. When combining curvature gains and translation gains, curvature detection thresholds are not affected [Gre+16]. So far, curvature detection thresholds were estimated when the users walk straight ahead in the VE. An effect of the visual density of the VE, i. e., the number of visual objects that were present in the VE, on the detection thresholds could not be shown [Pal+16]. Subtle redirection techniques may not only be based on visual manipulations of the VE, but also on audio [MNF16; Nil+16; NF16; Rew+19] or haptics [Mat+16b]. When using passive haptic cues during RDW even more redirection is possible [Mat+16a]. Detection thresholds may be different for individual users [Hut+18; Ngo+16] and increase during exposure time [Böl+19].

Although, ideally RDW is a subconscious process, Bruder et al. have shown that cognitive resources are required to compensate even subtle manipulations [BLS15]. In secondary verbal and spatial memory tasks, they have shown that performance decreased in the secondary task when the redirection gain increased. More precisely, correct answers decreased and answer time increased as well.

3.4.4 Impossible Spaces

An alternative approach to implement RDW is to use impossible or flexible spaces [Vas+13], which can be based on self-overlapping or changing architectural layouts. In these spaces, the VE itself is manipulated (in contrast to the user's viewpoint) with the same goal of enlarging the virtual space, which can be explored by real walking. Such manipulations can be realized, for example, by moving walls or doors outside the user's view [Sum+10], to exploit the same real-world space for different virtual rooms. The phenomenon that users are unable to detect such changes is known as *change blindness* [SL97]. It was shown that virtual rooms may overlap by more than 50% before users detect the manipulation [Sum+12b]. Moreover, curved corridors between the overlapping rooms are more beneficial than right-angled corridors in terms of manipulation detection [VK17b], and a corridor with additional turns is more efficient than a longer corridor [VK15].

A similar approach of exploiting the available tracking space for real walking is used by the VR game Unseen Diplomacy [Pix16]. It arranges the (self-overlapping) rooms in such a way that the player does not recognize that she is only walking back and forth in a 3m$\times$4m large area.

3.5 Comparison of Techniques

In previous work, several of the above mentioned navigation techniques have been compared regarding different aspects. In general, these studies suggest that natural techniques are slightly advantageous to semi- or non-natural techniques when it comes to sense of presence [Uso+99a] or user preferences [Boz+16].

For example, Usoh et al. compared real walking to walking-in-place and a joystick-like locomotion technique and found that the sense of presence benefits from proprioceptive and vestibular feedback [Uso+99a]. Real walking, walking-in-place, and joystick were also compared regarding task behaviour and task performance and the results suggest an ordering of locomotion techniques by "naturalness" [Whi+05]. Real walking, the Virtusphere device, and a gamepad were compared regarding user task performance and it was found that the Virtusphere technique was significantly slower and less accurate [Nab+15]. Teleportation was compared to walking-in-place and joystick regarding usability [Boz+16]. The results show that teleportation was subjectively preferred as a user friendly locomotion technique. However, an extended version of this teleportation technique for which it was possible to set a certain target direction into which the user should face after the teleportation, showed a decrease of the user experience. Bolte et al. compared teleportation to real walking and to the jumper metapher [BSB11]. The result shows that teleportation and jumper metapher are more effective techniques than real walking. Furthermore, in a CAVE, teleportation was compared to joystick and real walking with portals that were used to reorient the user in the tracking space [FRK14]. Teleportation was faster than real walking, but led to an increased loss of orientation compared to joystick. They could not find any differences between teleportation and real walking concerning motion sickness.

Peck et al. compared RDW to walking-in-place and joystick regarding navigational ability (i.e., the performance during a search task) and reported that participants ‘traveled shorter distances, made fewer wrong turns, pointed to hidden targets more accurately and more quickly, and were able to place and label targets on maps more accurately‘ when using RDW [PFW11]. It was also found that body-based informations like proprioception improved navigational performance as well as the user’s cognitive maps [RVB10; RL09]. Though it is a very popular and easy solution for travel, after teleporting, it takes some time for the user to understand her new surroundings, potentially leading to disorientation, which in turn can break the feeling of presence [FRK14; RVB10; Uso+99a]. Bowman et al. found that instant teleportation is correlated with decreased spatial orientation [Bow+99]. Similar results regarding spatial orientation and teleportation were found by Bakker et al. [BPW03] and Cliburn et al. [Cli+09]. Nevertheless, teleportation is a comfortable and easy technique, which is suitable for a lot of situations or application domains [FSW17].

II EGOCENTRIC SPATIAL PERCEPTION

4. EFFECTS OF DOF BLUR ON DISTANCE ESTIMATION

4.1 Motivation

While humans are quite accurate when estimating distances in the real world [Rie+90], in VEs such spatial judgments tend to significantly differ from the real world, i. e., often they are less precise and accurate with a large bias to underestimation in vista space [LK03; WK98].

The perception of distances involves the integration of different cues that are extracted from the visual sense and body senses. While previous research has focused on analyzing different factors for their effect on spatial judgments in VEs [RVH13], one factor has received less attention in the published literature: *visual blur* [Hel+10; Pal99].

There are several situations where visual blur is involved when using head-mounted displays (HMDs):

- When humans focus on an object in the real world, the eyes verge towards it to bring it into the fovea, while they also accommodate to the distance of the object to bring it into sharp focus on the retina. Assuming that a user has 20/20 visual acuity in the real world, this is usually reduced in HMDs due to the lower pixel resolution or caused by only partial accommodation responses in the scope of the accommodation-convergence conflict [Pal99]. Or, in other words, the entire virtual world appears slightly blurred compared to what one would see in a similar situation in the real world.
- When fixating on an object in the real world, the power of the lenses in the eyes is changed such that objects at the same or similar distances within a region around the horopter [Pal99] appear sharply throughout the visual field, whereas objects that have a smaller or larger distance from the eyes appear increasingly blurred (see Figure 4.1). Most current-state HMDs are not able to naturally replicate this effect in VEs, with a few exceptions based on light-field technologies [LL13]. However, assuming that the fixation point of the user's eyes is known or tracked, it is possible to induce similar visual blur in the computer-graphically generated visual imagery that is shown on the HMD by using depth-of-field effects [CR15]. Since most HMDs do not come with an integrated eye tracker, VEs are usually not presented with (perceptually accurate) depth-of-field effects.

Hence, there are multiple differences between the real world and HMDs in terms of the amount

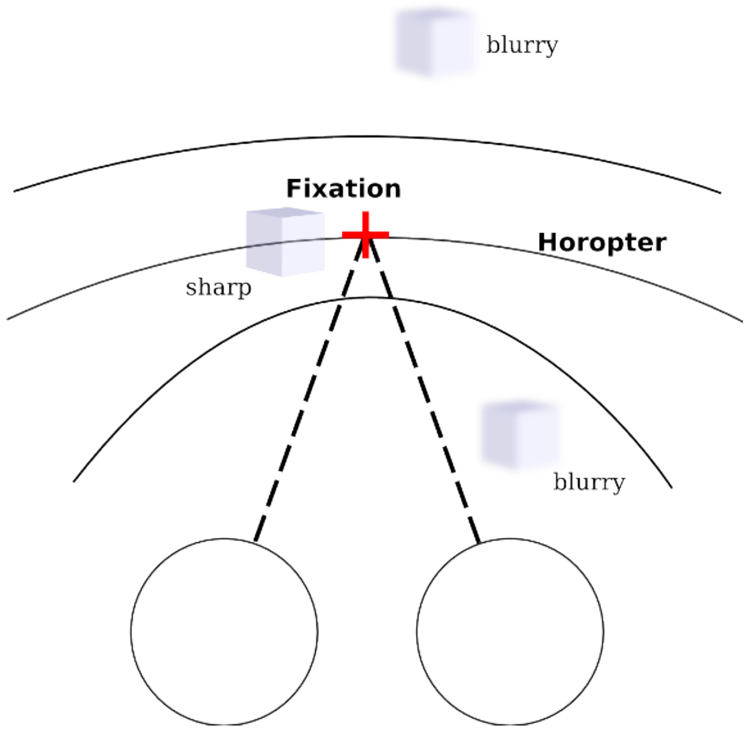

Figure 4.1: Objects can be fused and appear sharply only if their distance matches panum's fusional area around the horopter defined by the fixation point of the observer's eyes.

of blur present which either increase or reduce blur compared to natural viewing.

In this chapter, we present an experiment, in which we investigate whether visual blur has a noticeable effect on distance estimation, and also to understand how much of the perceptual discrepancies between real and virtual worlds might be explained by visual blur. Although, with the current state of HMD hardware technologies it is not possible to test perceptual effects without any of the above outlined blur differences, we analyzed depth-of-field (DOF) with different levels of magnitude and measured its impact on distance estimation.

The chapter is structured as follows: Sections 4.2, 4.3, and 4.4 describe the experimental setup. Section 4.5 presents the results and Section 4.6 discusses their impact. Section 4.7 concludes the chapter.

4.2 Participants

20 participants (2 female and 18 male, ages $19-36$, $M=27.2$) completed the experiment. The participants were students or members of the local department of informatics, who obtained class credit for their participation. All of our participants had normal or corrected-to-normal vision. Eight participants wore glasses and two participants wore contact lenses during the experiment. None of our participants reported a disorder of equilibrium. One of our participants reported an artificial lens in his left eye. No other vision disorders have been reported by our participants. 11 participants had participated in an experiment involving HMDs before. The experience of the participants with 3D stereoscopic displays (cinema, games etc.) in a range of 1 (no experience) to 5 (lots of experience) was $M=3.5$ ($SD=1.27$). Most of them had experiences with 3D computer games ($M=3.45$, $SD=1.6$, in a range of 1 = no experience to 5 = lots of experience) and they usually played 6.65 hours per week on average ($SD=8.84$). We measured the interpupillary distances (IPDs) of our participants before the experiment using the built-in measurement process of the Oculus

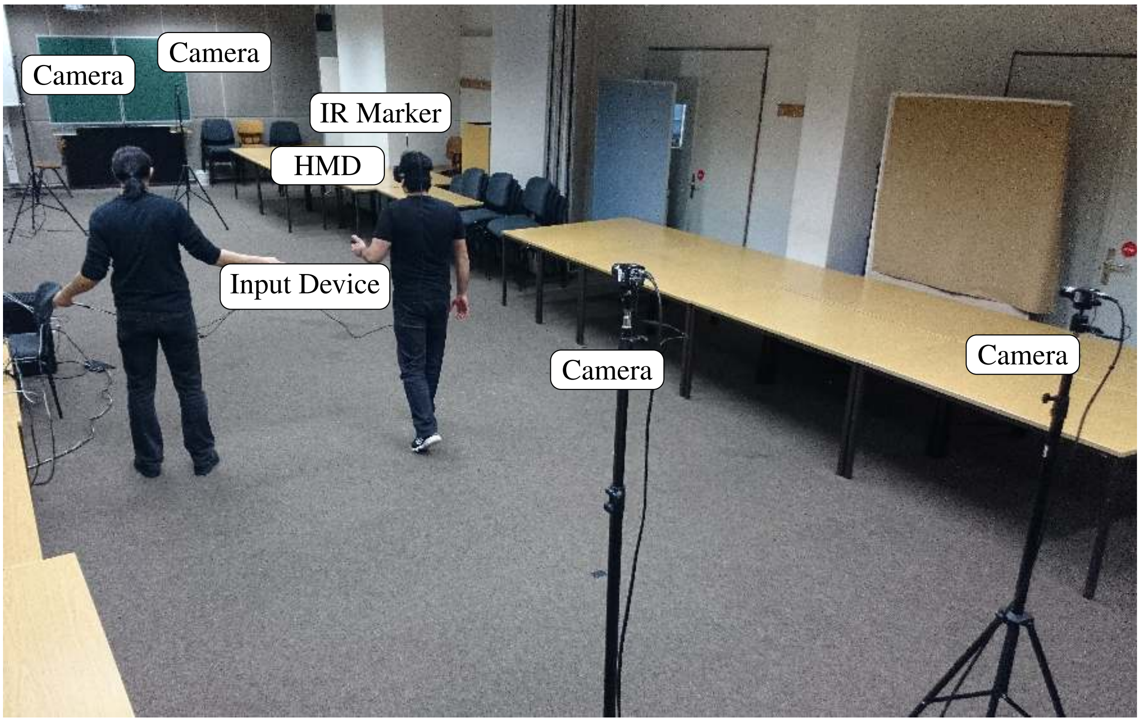

Figure 4.2: A participant and an experimenter walking in the laboratory space.

Rift configuration utility. The IPDs of our participants ranged between $6.2-6.9$cm ($M = 6.5$cm, $SD = .2$cm). We used the IPD of each participant to provide a correct perspective and stereoscopic rendering on the HMD. The body height of the participants varied between $1.60-1.90$m ($M = 1.79$m, $SD = .07$m). The total time per participant, including pre-questionnaires, instructions, experiment, breaks, post-questionnaires, and debriefing, was 30 minutes. Participants wore the HMD for approximately $20-25$ minutes. They were allowed to take breaks at any time between trials.

4.3 Materials

The experiment took place in a sealed-off empty seminar room (see Figure 4.2). We instructed the participants to wear an Oculus Rift DK2 HMD, which provides a resolution of 960×1080 pixels per eye with an approximately 110° diagonal field of view. Positional tracking was done with a WorldViz PPT tracking system that consisted of four cameras, one in each corner of the room, and an infrared LED marker at the participant's head. The tracking system sent the position data via VRPN and a local network to the rendering computer. During the experiment the room was darkened in order to reduce the participant's perception of the real world. The participants received instructions on slides presented on the HMD. A Gyration Air Mouse GO Plus served as an input device via which the participants provided responses during the experiment. For rendering, system control and logging we used an Intel computer with 3.5GHz Core i7 processor, 32GB of main memory and an Nvidia Geforce GTX 980 graphics card.

The virtual environment was rendered using the Unreal Engine 4 and showed a natural forest scene and a straight path in front of the participant (see Figure 4.3). We chose this environment because blur effects are much more visible in a high fidelity visually rich scene than in an abstract reduced-cue scene. As commonly done when using the blind walking method to assess distance perception in HMD environments we displayed a red target on the path at a computer-controlled

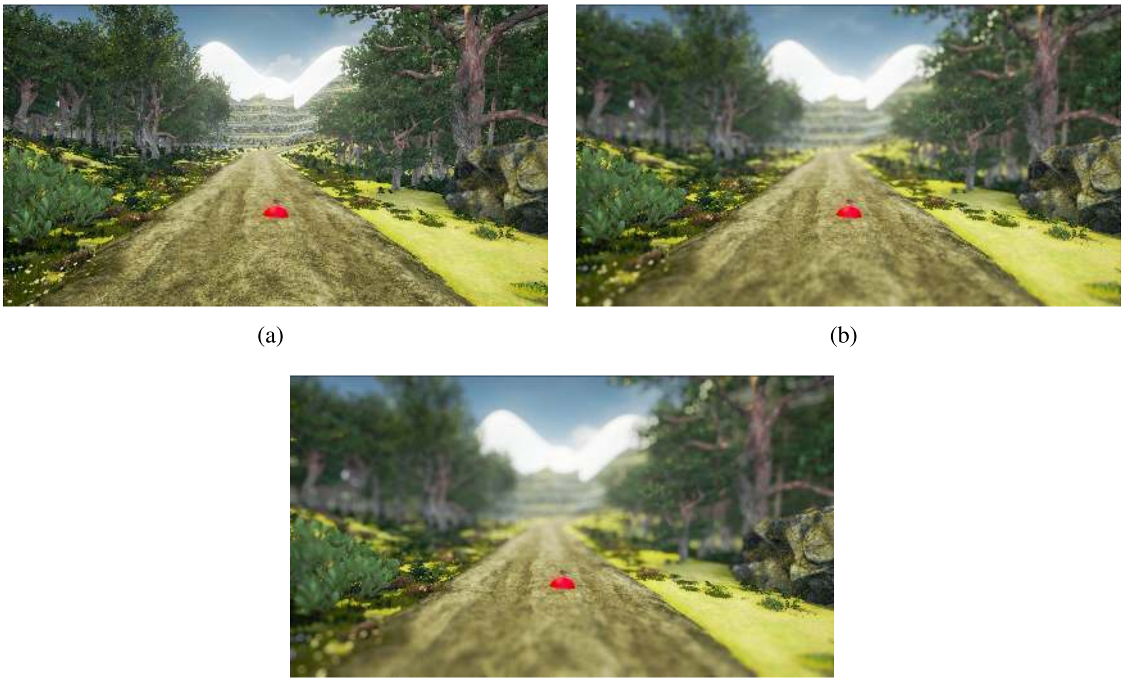

(a) (b) (c)

Figure 4.3: The focus point in this condition is 5m in front of the participant: the environment without blur (a), with low blur (b) and high blur (c).

distance. In some of the experimental conditions, we applied a perceptually-inspired depth-of-field post-processing shader in the Unreal Engine that showed everything at the focused distance sharply, but blurred the rest of the scene. For this, we used the built-in BokehDOF effect (MaxBokehSize = 1.5, NearTransitionRegion = 200, FarTransitionRegion = 200, FocalRegion = 200) with a scale of 0.5 or 1.0, respectively (low blur and high blur). The focused distance of the shader matched the distance to the red target. The participants were instructed to maintain a focus on this target, which we found worked well to control the focused distance without the need for an eye tracking device to observe the participant's eyes and adjust the focus.

4.4 Methods

We used a 4×3 full-factorial within-subjects experimental design. We tested 4 blur conditions (real environment, virtual environment without blur, with low blur and with high blur) and 3 distance conditions (3m, 5m and 7m in front of the participant). The low blur condition was chosen to closely approximate a "real" blur when focusing on an object. This was configured by a subjective estimation of the experimenters according to a similar real-world situation. Figure 4.3 illustrates the conditions.

The baseline conditions in the real environment were tested in a block at the beginning of the experiment, followed by the conditions in the virtual environment. The conditions were randomized but uniformly distributed within the blocks. The positions at which the participant was located in the virtual world were randomized between trials. In order to assess the perceived distance to the red target we used the active response method of blind walking [WS98]. Using this method, the participants had to look at the red target marker or a laser pointer mark at the given distance in the virtual or real environment, respectively. After a few seconds, the participants clicked on the input device and the scene turned black. Now, without vision, they had to walk the distance to the target

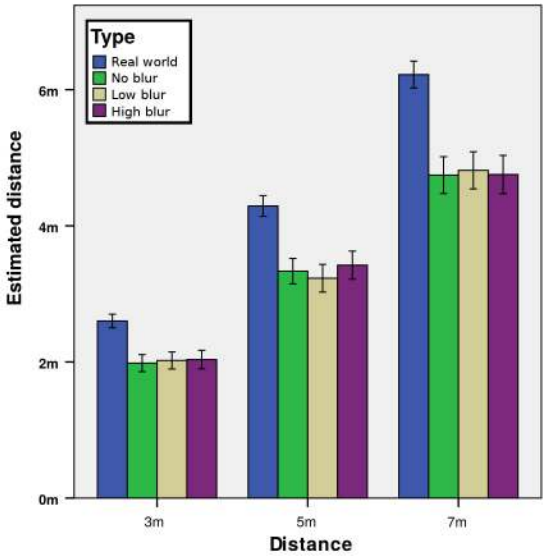

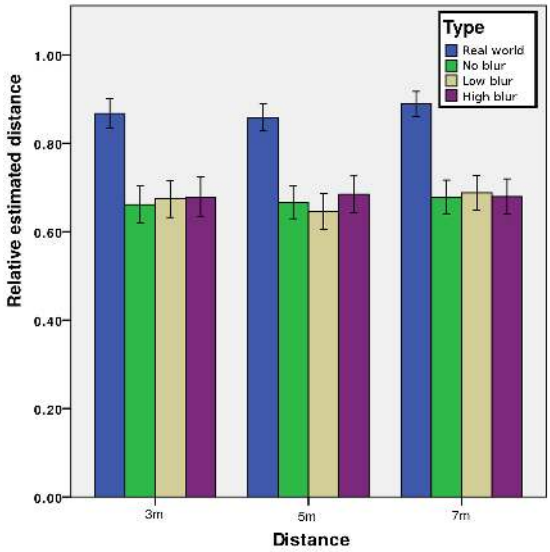

Figure 4.4: Pooled results of the distance estimation experiment for the different visual blur conditions: (left) absolute and (right) relative. The vertical bars indicate the standard error.

they had previously seen. In the conditions in the real world, we used a sleep mask to blindfold them. When the participants thought that they had reached the distance, they clicked again and we saved the walked distance by computing the Euclidean distance between the end point and the start point on the floor in two dimensions (see [RVH13]). Then, still blindfolded, the participants were guided back to the start position with the help of the experimenter, and the next trial started.

4.5 Results

We analyzed the results with a repeated-measures ANOVA and TukeyHSD multiple comparisons at the 5% significance level. A Shapiro-Wilk test did not indicate that the assumption of normality had been violated. When Mauchly's test of sphericity indicated that the assumption of sphericity had been violated we used Greenhouse-Geisser estimates of sphericity to correct the degrees of freedom. We report statistics for both absolute and relative judgments in the following to achieve comparability for the two mainly used types of analyses in the distance estimation literature.

Figure 4.4 (left) shows the absolute values of the estimated distances and Figure 4.4 (right) the relative values. We found a significant main effect of the blur type on distance estimation for absolute values, $F(1.5,28.4) = 39.67$, $p < .001$, $\eta_p^2 = .676$, and relative values, $F(1.4,28.3) = 40.74$, $p < .001$, $\eta_p^2 = .682$. Post-hoc tests showed that the estimated distances between the real world condition and each of the conditions in the virtual world were significantly different ($p < .001$). We could not find any significant effect between the different blur types in the VE. The bayes factor for this was .061.

Furthermore, we found a significant main effect of the target distance on distance estimation for absolute values, $F(1.2,22) = 330.13$, $p < .001$, $\eta_p^2 = .946$, but not for relative values, $F(1.25,23.6) = .68$, $p = .45$, $\eta_p^2 = .034$. For relative values, we found a bayes factor of .062. Post-hoc tests showed that the estimated distances between each two target distances were significantly different ($p < .001$).

Moreover, we found a significant interaction effect between blur type and target distance on distance estimation for absolute values, $F(3.2,61.5) = 7.35$, $p < .001$, $\eta_p^2 = .279$, but not for relative values, $F(6,114) = .52$, $p = .8$, $\eta_p^2 = .026$. For relative values, we found a bayes factor of .003.

Questionnaires

We measured a mean SSQ-score [Ken+93] of 11.8 (SD = 16.7) before the experiment, and a mean SSQ-score of 31.8 (SD = 30.9) after the experiment. The mean SUS-score [Uso+99b] for the sense of feeling present in the VE was 4.46 (SD = 1.1).

4.6 Discussion

It is an interesting result that our experiment did not reveal a significant effect on distance estimation of the even quite large amount of blur that we added with DOF to the visual stimulus. It is reasonable to assume that the statistical effect size of such blur effects is relatively low. Additionally, the relatively small value of the bayes factor even suggests that there is an overwhelming support for the null hypothesis. In fact, the different blur conditions could only explain a very small part of the variance in the responses.

We believe that there are three potential explanations why we observed such small effect sizes and observed power in the blur conditions in the VE:

a) The tested distances were still in the range where convergence and motion parallax offer good distance cues, which might have dominated any effect from even large amounts of DOF blur. This might explain why related studies using monoscopic imagery have found an effect of blur on distance and size estimation [Hel+10].
b) Despite our perceptual calibration, the types and strengths of blur that we tested in this experiment based on DOF visual effects might not have been interpreted as a depth cue by the human perceptual system due to slight differences in magnitude or distribution (see Bayesian cue integration [Ern06]).
c) The resolution of the Oculus Rift DK2 HMD, which supports only 960×1080 pixels per eye, limited the visual acuity. A potential explanation might be that the additional amount of blur had no noticeable additional effect on distance estimation, but that less blur might have had an effect. However, we should note that this explanation would conflict with results of related studies, which found that higher resolution did not improve distance estimation (e. g., [Bru+15]).

However, from the point of view of a practitioner in the field of VR, we believe that it is warranted to provide the guideline that for practical purposes the effect of blur on distance misperception in the visual imagery can be neglected.

This also can be applied to the current questions how much resolution of visual displays is required by indicating that unless the resolution is largely improved to approximate the visual acuity of the human eyes, blur due to lower resolutions is likely not an important cause of spatial misperception.

Furthermore, it is to take note of the fact, that we found a much higher underestimation in VE conditions than others who used similar hardware (e. g., [Cre+15; Li+15]). This might be explained by slightly different tested distances, different VEs (indoor vs. outdoor) and different calibration. We measured and set the IPD of each participant individually while Creem-Regehr et al. set the IPD to $6.25cm$ for all participants. Additionally, we also set the height of the camera according to the height of the participants.

We also found a slight underestimation in the real world condition. Since we do not know what is the reason for this, we guess it is related to the construction of the room which had the form of a tube.

4.7 Conclusion

In this chapter, we reported a psychophysical experiment that was conducted to investigate the influence of DOF blur on distance estimation. Because we found no significant effect and only very low effect sizes, we draw the conclusion that there is–if at all–only a negligibly small effect. Even if this result is, technically, a null result we believe that it is an important finding that will provide new insights to the research direction because there are important reasons why researchers might assume an influence of blur, which, so far, has not been proven or disproven in the published literature.

However, we have to consider that our findings are based on a snapshot of currently available HMD technology. Once available in the (distant) future, we will have to revisit effects of blur using an HMD with a field of view and resolution that match those of the human eyes. However, even then, blur might not prove to have much influence on distance estimation due to the availability of stronger cues such as motion parallax and convergence.

5. EFFECTS OF MOTION BLUR ON SPEED ESTIMATION

5.1 Motivation

In Chapter 4, we already anaylzed the effect of visual blur on distance estimation. However, visual blur does not only occur while standing still but also during motions. Due to the limited refresh rate of current HMDs, the natural amount of optic flow present during movements in the real world is reduced, which is often counteracted by using a visual effects technique called motion blur [PC83].

In this chapter, we present a psychophysical experiment in which we analyzed the effect of different levels of motion blur on speed estimation with an HMD.

The chapter is structured as follows: Sections 5.2, 5.3, and 5.4 describe the experimental setup. Section 5.5 presents the results and Section 5.6 discusses their impact. Section 5.7 concludes the chapter.

5.2 Participants

20 participants (2 female and 18 male, ages $19-36$, $M = 27.2$) completed the experiment. The participants were students or members of the local department of informatics, who obtained class credit for their participation. All of our participants had normal or corrected-to-normal vision. Eight participants wore glasses and two participants wore contact lenses during the experiment. None of our participants reported a disorder of equilibrium. One of our participants reported an artificial lens in his left eye. No other vision disorders have been reported by our participants. 11 participants had participated in an experiment involving HMDs before. The experience of the participants with 3D stereoscopic displays (cinema, games etc.) in a range of 1 (no experience) to 5 (lots of experience) was $M = 3.5$ ($SD = 1.27$). Most of them had experiences with 3D computer games ($M = 3.45$, $SD = 1.6$, in a range of 1 = no experience to 5 = lots of experience) and they usually played 6.65 hours per week on average ($SD = 8.84$). We measured the IPDs of our participants before the experiment using the built-in measurement process of the Oculus Rift configuration utility. The IPDs of our participants ranged between $6.2-6.9$cm ($M = 6.5$cm, $SD = .2$cm). We used the IPD of each participant to provide a correct perspective and stereoscopic rendering on the HMD. The body height of the participants varied between $1.60-1.90$m ($M = 1.79$m, $SD = .07$m). The total time

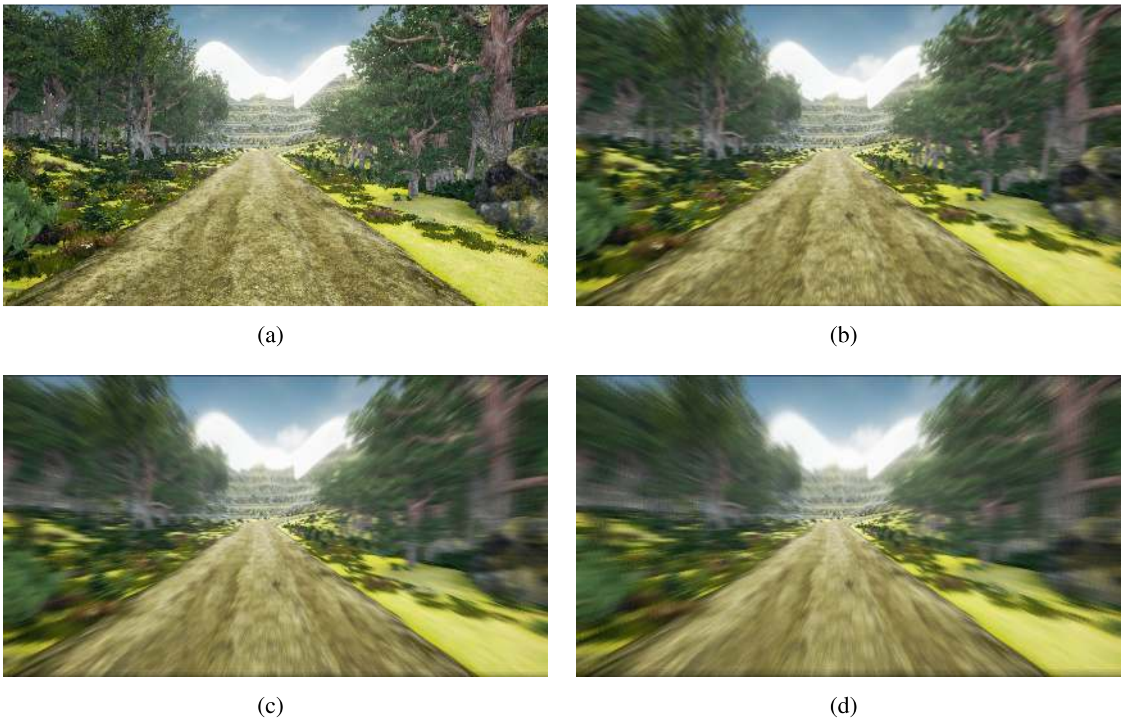

Figure 5.1: Camera flight through the VE with no blur (a), low blur (b), medium blur (c) and high blur (d).

per participant, including pre-questionnaires, instructions, experiment, breaks, post-questionnaires, and debriefing, was 30 minutes. Participants wore the HMD for approximately $20-25$ minutes. They were allowed to take breaks at any time between trials.

These were exactly the same participants as described in Section 4.2.

5.3 Materials

The experiment took place in a sealed-off empty seminar room (see Figure 4.2). We instructed the participants to wear an Oculus Rift DK2 HMD, which provides a resolution of 960×1080 pixels per eye with an approximately 110° diagonal field of view. Positional tracking was done with a WorldViz PPT tracking system that consisted of four cameras, one in each corner of the room, and an infrared LED marker at the participant's head. The tracking system sent the position data via VRPN and a local network to the rendering computer. During the experiment the room was darkened in order to reduce the participant's perception of the real world. The participants received instructions on slides presented on the HMD. A Gyration Air Mouse GO Plus served as an input device via which the participants provided responses during the experiment. For rendering, system control and logging we used an Intel computer with 3.5GHz Core i7 processor, 32GB of main memory and an Nvidia Geforce GTX 980 graphics card.

The virtual environment was rendered using the Unreal Engine 4 and showed a natural forest scene and a straight path in front of the participant (see Figure 5.1). We chose this environment because blur effects are much more visible in a high fidelity visually rich scene than in an abstract reduced-cue scene. These were exactly the same materials as described in Section 4.3.

We tested the effects of motion blur post-processing by using a shader (see [Tom16]) that showed the focused point in the scene sharply and everything else blurry, similar to the (fast) motion of a movie camera. For this, we used following settings: RadiusExponent = 2, BlurRadius = 0.1,

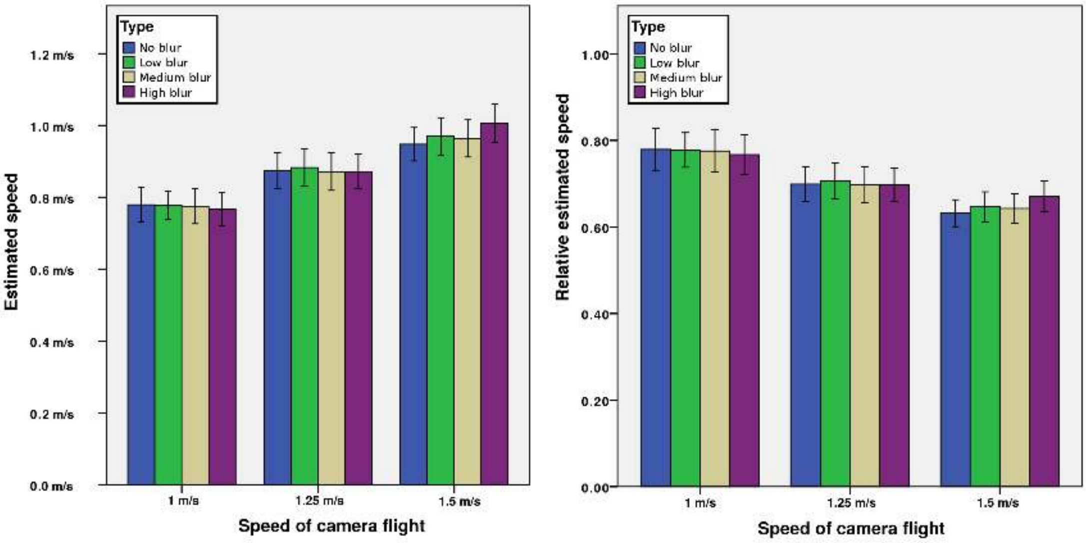

Figure 5.2: Pooled results of the speed estimation experiment for the different motion blur conditions: (left) absolute and (right) relative. The vertical bars indicate the standard error.

BlurAmount = 0.25, 0.5 or 0.75, respectively. In this experiment, we decided against including a baseline condition in which we would usually test speed estimation in a real-world environment due to the fact that we are mainly interested in the relative differences between the different amounts of motion blur.

5.4 Methods

We used a 4×3 full-factorial within-subjects experimental design. We tested 4 blur conditions (without blur, with low blur, with medium blur and with high blur) and 3 velocity conditions (1m/s, 1.25m/s and 1.5m/s). Figure 5.1 illustrates the conditions. The conditions were presented randomly but uniformly distributed.

In order to assess the perceived walking speed we used a visual-proprioceptive perceptual matching method. Using this method, the participants had to stand on the start point in the real world and look forward while a camera flight through the VE with different levels of motion blur was shown. After the flight ended, the scene turned black. Now, without vision, they had to walk forward at the speed they had seen before. After the participants walked five meters, we saved the time they needed to walk this distance and calculated the mean speed. Then, still blindfolded, they had to walk back to the start position with the help of the experimenter, and the next trial started. The positions at which the participant was located in the VE were randomized between trials, so that participants could not use their position as a reference point.

5.5 Results

We analyzed the results with a repeated-measures ANOVA and TukeyHSD multiple comparisons at the 5% significance level. A Shapiro-Wilk test did not indicate that the assumption of normality had been violated. When Mauchly's test of sphericity indicate that the assumption of sphericity had been violated we used Greenhouse-Geisser estimates of sphericity to correct the degrees of freedom. Again, we report statistics for both absolute and relative judgments.

Figure 5.2 (left) shows the absolute values of the estimated speeds and Figure 5.2 (right) the relative values. We found no significant effect of the blur type on speed estimation for absolute values, $F(3,57) = .39$, $p = .76$, $\eta_p^2 = .02$, and relative values, $F(3,57) = .2$, $p = .89$, $\eta_p^2 = .01$.

We found a significant main effect of the target speed on speed estimation for absolute values, $F(2,38) = 70.05$, $p < .001$, $\eta_p^2 = .787$, and relative values, $F(1.53,29) = 34.89$, $p < .001$, $\eta_p^2 = .647$. Post-hoc tests showed that the estimated speeds between each two target speeds were significantly different ($p \leq .001$).

Moreover, we found no significant interaction effect between blur type and target speed on speed estimation for absolute values, $F(6,114) = .91$, $p = .49$, $\eta_p^2 = .046$, and relative values, $F(6,114) = .67$, $p = .67$, $\eta_p^2 = .034$.

5.6 Discussion

As in the experiment regarding distance estimation using DOF blur (see Chapter 4), our results in this experiment showed no significant effect of the different motion blur conditions on speed estimation. Again, the effect sizes indicate that motion blur can only explain a very small part of the variance in the responses.

As for potential explanations of this effect, we believe that those discussed in Section 4.6 might also apply to motion blur. These are: (i) convergence and motion parallax might offer sufficient distance cues, (ii) types and strengths of blur that we tested might not have been interpreted as a depth cue, and (iii) the resolution of the HMD limited the visual acuity and the additional amount of blur had no noticeable additional effect on speed estimation. Moreover, most of the motion blur was visible in the periphery of the HMD, which, although it has a large field of view of 110° diagonally, might not be entirely the same as during real-world viewing, considering the human visual field spanning over about 200° horizontally into the far periphery of the eyes. Since the periphery of the eyes is highly sensitive to motion, an additional explanation might be that an even larger field of view of HMDs is required for this stimulation with blur to take effect [NSN14].

5.7 Conclusion

In this chapter, we reported a psychophysical experiment that was conducted to investigate the influence of motion blur on speed estimation. Because we found no significant effect and only very low effect sizes, we draw the conclusion that there is–if at all–only a negligibly small effect. Even if this result is, technically, a null result we believe that it is an important finding that will provide new insights to the research direction because there are important reasons why researchers might assume an influence of blur, which, so far, has not been proven or disproven in the published literature.

However, we have to consider that our findings are based on a snapshot of currently available HMD technology. Once available in the (distant) future, we will have to revisit effects of blur using an HMD with a field of view and resolution that match those of the human eyes. However, even then, blur might not prove to have much influence on speed estimation due to the availability of stronger cues such as motion parallax and convergence.

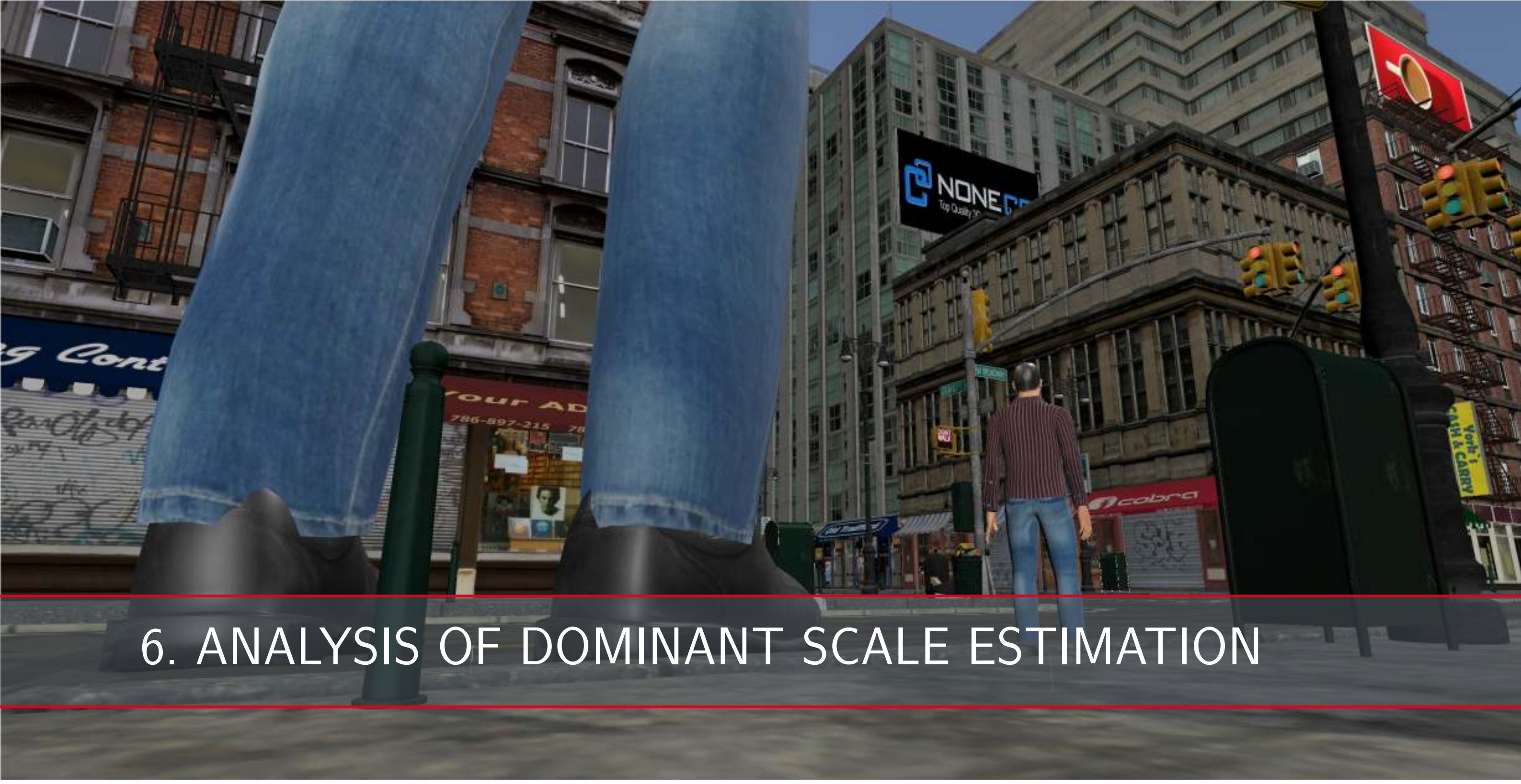

6. ANALYSIS OF DOMINANT SCALE ESTIMATION

6.1 Motivation

For more than half a century the effects and characteristics of being able to explore an environment at different scale levels have been addressed in fiction literature and movies such as *Alice's Adventures in Wonderland*, *The Incredible Shrinking Man*, and *Gulliver's Travels*. In these fictional works, interactions of the main characters with their surroundings were described after they intentionally or accidentally changed their scale by shrinking or growing in size, which opened up entirely different perspectives onto the same environment. VR technologies and, in particular, multi-scale collaborative virtual environments (MCVEs) [ZF05] have addressed these unnatural and magical possibilities by implementing shared VEs in which multiple users can be present and interact in a 3D virtual world at several different scale levels at the same time. For instance, a common feature of MCVEs is that the scale of the environment can be changed with zooming in or out gestures, e. g., by using multi-touch on interactive tabletops or 3D gestures in immersive VEs [Kop+06].

For many application domains, such as architecture, simulation, decision support systems, education [Joh+99], industrial training [OSG00], research [Son+01], and community building [LHM97], MCVEs have proven to be very useful and versatile, with the caveat that it becomes very important that users acquire a consistent understanding and sense of scale of the VE as well as other users [Kop+06; LaV+01; MLY01]. For an effective collaboration during spatial tasks, it is not sufficient just to know the location of each other, but also to understand at which scale others perceive and act in the VE.

In this context, we often see the problem that users perceive and communicate based on deictic references using different scale systems. For example, one user might try to indicate a point of interest by stating "I mean the building two meter in front of you", whereas the addressed user perceives the building at two hundred meters distance in such an MCVE (see Figure 6.1). Conversely, we sometimes observe that users change their perspective to other users, when they indicate the distance or size of points of interest, which–if not made clear during the conversation––again could lead to communication problems. In order to remedy such problems, it is essential to understand how *dominant scale*, i. e., the scale level relative to which a user interprets spatial relations, changes due to the VE and due to interaction with other users.

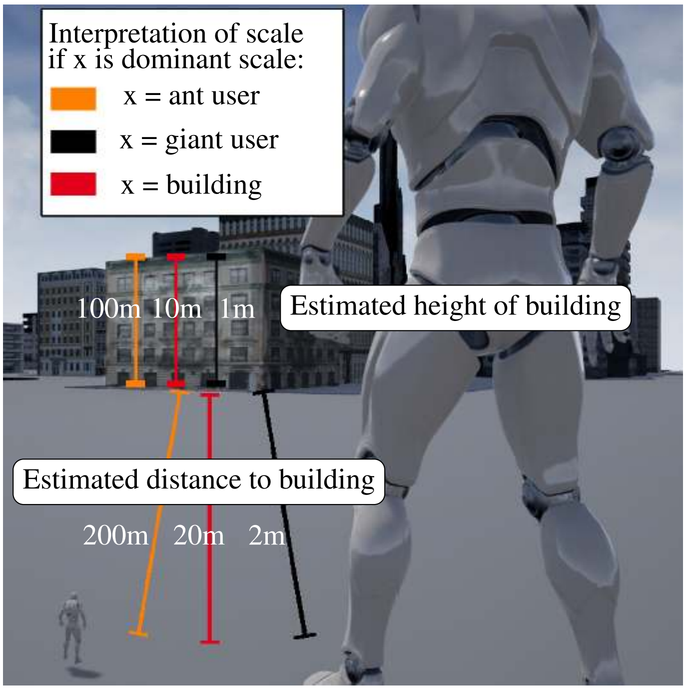

Figure 6.1: Without a common scale level the participants' notion of distances and sizes in the pilot study differed largely and hindered a meaningful collaboration in spatial tasks.

A user, who sees the VE from a high scale level, can interpret it in two ways: (i) either she is of normal size and the buildings are just a miniature model (like miniature building blocks) or (ii) she is a giant in a normal-sized city. Conversely, a user, who sees the VE from a small scale level, can interpret it in two ways: (iii) either she is of normal size and the buildings are gigantic or (iv) she is an ant in a normal-sized city. From a technical or mathematical viewpoint in each case the two interpretations are exactly the same; there is no difference in the images presented to the user's eyes. Differences can only occur in the cognitive interpretation of the stimuli, which makes this a difficult, challenging, but interesting problem. For these reasons, it is important to analyze if and how important aspects of the VE such as virtual body feedback, the presence of others or the type of VE, affect a user's interpretation of the scale of the VE.

In this chapter, a pilot study is described and based on the results two psychophysical experiments are presented focused on analyzing factors that affect dominant scale estimation in MCVEs. The results of this work contribute to understanding the effects of the

- type of the environment (artificial vs. urban),
- visual body feedback, i. e., ability to see one's body in the MCVE, and
- presence of other avatars, i. e., group effects.

Knowledge about these aspects is an important step towards the development and design of novel MCVEs [Kop+06; LaV+01; MLY01].

The chapter is structured as follows. Section 6.2 describes a pilot study, in which the problem is analyzed with a focus group. Based on the results, two psychophysical experiments using an improved protocol were designed, which are described in Sections 6.3 and 6.4. Section 6.5 provides a general discussion of the results and implications for MCVEs. Section 6.6 states rules for the design of MCVEs. Section 6.7 concludes the chapter.

6.2 Pilot User Study

We performed a pilot user evaluation with a focus group of six participants (2 female and 4 male, ages $22-29$, $M = 24.8$) in an urban MCVE inspired by a local city planning project. The participants were students or professionals of informatics or architecture.

In groups of two, participants were placed in the MCVE and asked to collaborate in certain tasks by building a consistent spatial impression of sizes and distances in the urban scene, while we collected their informal comments using a think aloud protocol [Lew82]. Both participants were displayed using a different scale level. We observed that all pairs of participants had serious difficulties when trying to communicate absolute distances and sizes. For example, when we asked each group of participants to indicate the distance and size of a building in the urban environment their answers usually diverged largely. In particular this was the case, when they could not see the other user, i. e., the visibility of themselves affected their estimation. Two participants stated “I am bigger than a skyscraper" when they were at a high scale level. These responses indicate that they might interpret the city as an invariant and not as a miniature model. When they changed to a smaller scale level, they responded to feel “in accordance with the environment".

Hence, the ability to change perspective and correctly estimate size, scale, and proportion is crucial for effective interaction and communication in MCVEs. During the focus group discussion, we figured out if and how this is influenced by different factors like the type of the environment, the visibility of an avatar or other avatars. Overall, we observed that participants only chose between two alternatives: an embodied interpretation with their own body indicating the dominant scale level, or a world-scale interpretation in which they estimated the urban environment to be at dominant scale. The alternatives had a direct effect on their estimation of distances and sizes in the environment. Since we only experienced these two alternatives in the pilot study, we feel that the so-called Two-Alternative Forced-Choice method [Fer08] is a useful paradigm for evaluation such conflicting interpretations, and hence we decided to exploit this approach in the following experiments (see Section 6.3.3).

To our knowledge, perception and cognition of dominant scale in MCVEs has not been evaluated in-depth, and fully-articulated tracked 3D body representations have been ignored in this context so far. The ability to support basic interaction techniques such as gestural interaction, e. g., pointing and waving, has enormous potential to effect 3D perception, cognition, and collaboration in MCVEs.

6.3 Experiment E1: Virtual Body and Environment

In this section, we describe the psychophysical experiment in which we analyzed the estimation of dominant scale in an artificial and an urban environment while participants were either provided with fully-articulated visual tracked body feedback or without a visual self-representation. Moreover, we analyzed interpersonal differences between the participants in the experiment.

6.3.1 Participants

18 participants (4 female and 14 male, ages $20-38$, $M = 26.6$) completed the experiment. The participants were students or members of the local department of informatics, who obtained class credit for their participation. All of our participants had normal or corrected-to-normal vision. Five participants wore glasses and three participants wore contact lenses during the experiment. None of our participants reported a disorder of equilibrium. One of our participants reported a color blindness and one a strong eye dominance. No other vision disorders have been reported by our participants. 16 participants had participated in an experiment involving HMDs before. We measured the IPDs of our participants before the experiment using the built-in measurement process of the Oculus Rift configuration utility. The IPDs of our participants ranged between $5.7-7.0$cm ($M = 6.5$cm, $SD = 0.3$cm). We used the IPD of each participant to provide a

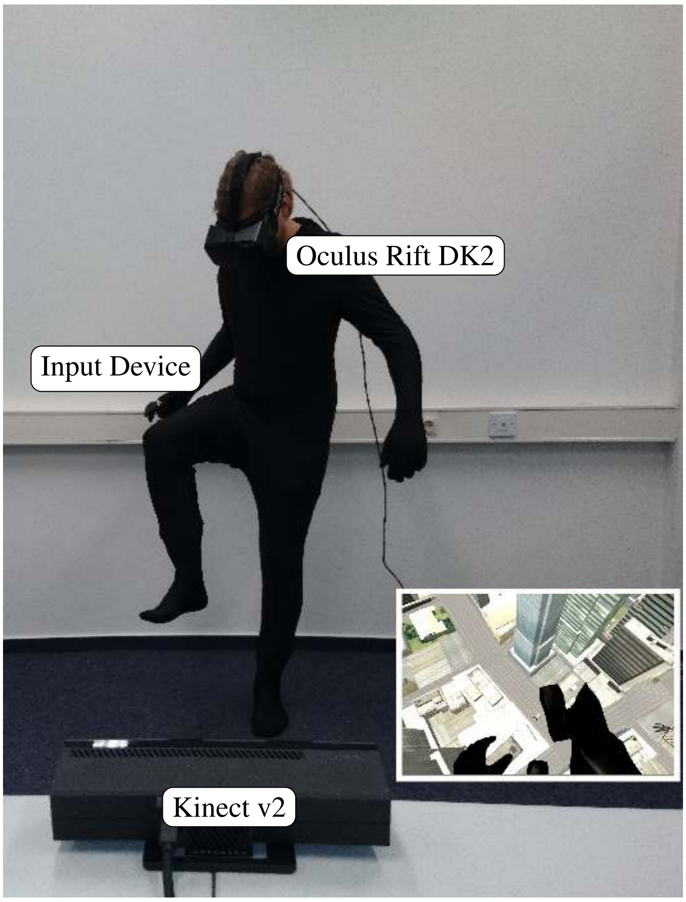

Figure 6.2: Experimental setup: User standing in front of a Kinect v2, equipped with an Oculus Rift DK2, while interacting with the VE using a hand-held device, and (inset) screenshot showing the VE with the user's virtual body from the user's egocentric point of view.

correct perspective and stereoscopic rendering on the HMD. The body height of the participants varied between $1.60 - 1.90$m ($M = 1.76$m, $SD = 0.08$m). The total time per participant, including pre-questionnaires, instructions, experiment, breaks, post-questionnaires, and debriefing, was 30 minutes. Participants wore the HMD for approximately $20 - 25$ minutes. They were allowed to take breaks at any time between trials.

6.3.2 Materials

We performed the experiment in a sealed-off VR laboratory room. As shown in Figure 6.2, we instructed the participants to wear an Oculus Rift DK2 HMD, which provides a resolution of 960×1080 pixels per eye with an approximately 110° diagonal field of view. During the experiment the room was darkened in order to reduce the participant's perception of the real world. The participants received instructions on slides presented on the HMD. A Gyration Air Mouse GO Plus served as an input device via which the participants provided responses during the experiment. For rendering, system control and logging we used an Intel computer with 3.5GHz Core i5 processor, 8GB of main memory and a Nvidia GeForce GTX 970 graphics card.

The virtual scene was rendered using the Unity3D 5 engine and our own software with which the system maintained a frame rate of 60 frames per second. The visual stimulus consisted of two different scenes: (i) an artificial environment, which is showing abstract cone-like geometry (see Figure 6.3(top row)), and (ii) a realistically rendered urban environment based on a city model (see

Figure 6.3(bottom row)). We chose the urban environment since in city models there is usually one scale level that matches its dominant scale in the real world, whereas the artificial environment has no real-world counterpart and thus provides no obvious notion of dominant scale.

In this experiment, it was important to provide participants with visual body feedback in the VE that matched the size and look of their body in the real world in order to support a high illusion of embodiment. There are generally two possibilities to achieve this goal. Unfortunately, it is still not possible to fully scan a participant's body and clothes in the real world and present them in the VE without significant cost of time. Hence, we decided to apply the alternative approach in which we altered the look of the participant's body in the real world to mimic the participant's visual body representation in the VE. To realize this approach, we instructed participants to put on a dark full-body suit in the real world at the beginning of the experiment (see Figure 6.2). After approximately five minutes of getting comfortable and familiar with their real-world body appearance in the suit, participants were instructed to don the HMD. We tracked the participant's body with a Microsoft Kinect v2 sensor and mapped the movements to a virtual replica in the VE (using the 'Kinect v2 with MS-SDK' Unity3D plugin from RF Solutions), which we scaled uniformly according to the height as well as body proportions of the real body. In the conditions in which the virtual body was visible, it approximated the look of the participant's body in the real world from the participant's egocentric point of view (see Figure 6.2(inset)). During the experiment, participants were allowed to look around freely, but we instructed them to remain in the tracking range of the Kinect sensor. The main forward direction at which instructions were shown between trials was oriented towards the Kinect sensor such that participants would always orient themselves towards the sensor after each trial, which optimized body tracking performance.

In order to test different scale levels of the participant relative to the environment, we scaled the participant's virtual *self*-representation with a scale gain $s_s \in \mathbb{R}^+$, which describes the ratio between the virtual body height relative to the participant's real-world body height with $s_s = \frac{\textit{virtual height}}{\textit{real height}}$. Therefore, we applied the scale gain as a uniform scale factor onto the participant's virtual self-representation, including the tracked Kinect data as well as the stereoscopic rendering for the Oculus Rift HMD. As a result, the virtual eye height, as well as the geometric IPD [KTC08] of the participant, changed consistently with the scale of her virtual body (see Figure 6.3). Hence, from the participant's point of view applying a scale gain $s_s = 2$ can either be interpreted as the participant being twice as big as naturally in the VE or it can be interpreted as the environment being scaled down by a factor of $\frac{1}{2}$. These two interpretations are both valid and depend on the participant's spatial impression.

6.3.3 Methods

We used a $2 \times 2 \times 5$ full-factorial within-subjects experimental design. We tested 2 environmental conditions (artificial vs. urban) and 2 virtual body conditions (visible vs. invisible) at 5 scale levels of the participant's virtual body ($s_s \in \{10^{-2}, 10^{-1}, 10^0, 10^1, 10^2\}$). Figure 6.3 illustrates the conditions with visible body feedback. We included 5 training trials to familiarize the participants with the controls. These trials were excluded from the analysis.

For the experiment, we used the method of constant stimuli. In the method of constant stimuli, the applied scale levels are not related from one trial to the next but presented randomly and uniformly distributed. The conditions in the artificial and natural environment were tested in blocks since this was deemed as most ecologically valid; scale level and position of a user in an MCVE usually change more rapidly than the environment itself. The order between and within the blocks was randomized. The positions at which the participant was located in the VE were randomized between trials. The participants were asked to look around in the VE and get a feeling for their environment. When they have looked enough, they pressed a button and got to the question mentioned in the next subsection. After answering the question, the next condition was started.

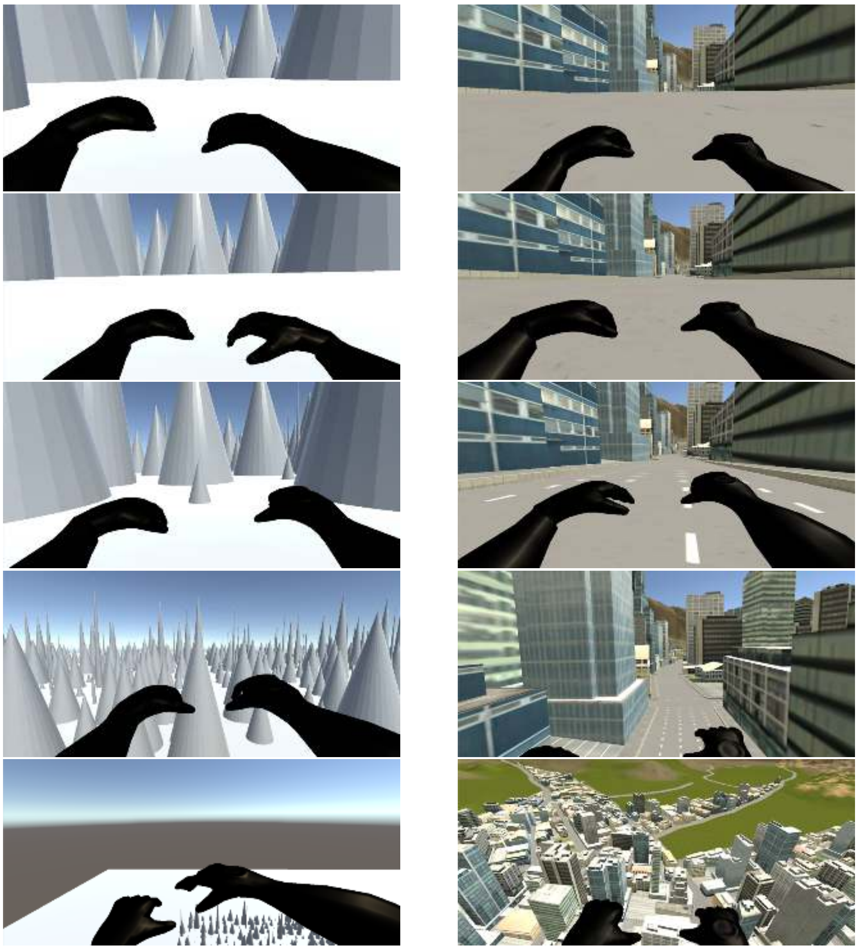

Figure 6.3: Illustration of the conditions in experiment E1 with virtual body: artificial environment (left) and urban environment (right) with virtual body at scale levels of $s_s \in \{10^{-2}, 10^{-1}, 10^{0}, 10^{1}, 10^{2}\}$ from top to bottom, respectively. The conditions without virtual body feedback in the experiment differed only in terms of the participant's body being invisible.

Two-Alternative Forced-Choice Task

As mentioned above, we used a two-alternative forced-choice (2AFC) task for the experiment, which forces participants to decide and concentrate on trying to provide an answer, thus generally provides more accurate results in situations with high uncertainty [Fer08]. Participants had to judge their impression of dominant scale based on either the interpretation that (i) they themselves seemed to be up- or downscaled with the environment at dominant scale, or the interpretation that (ii) they themselves seemed to be at dominant scale with a down- or upscaled environment. However, instead of asking users to decide on one of these two alternatives, discussions during the focus group as well as pilot tests showed that particular users naïve to MCVEs found it less cognitively demanding to answer a revised question during the experiment in which the alternatives were negated. In this revised question the participant chooses between one of two possible responses (roughly translated from German):

Q "I had the impression that: (left) I *myself* seemed to be of *unnatural* scale or (right) the *environment* seemed to be of *unnatural* scale."

The notion of *unnatural scale* means that this is not the dominant scale.[1] Participants responded

[1] This may sound unfamiliar in English, but we ensured that all of our participants understood the wording in German.

by pressing either the left or right button on the input device; responds like "I can't tell." were not allowed. In this version, when the participant cannot detect the dominant scale (e. g., when environment and avatar are at the same scale), she must guess, resulting in 50% probability of responses towards either answer on average over all trials. As the percentage of responses decreases or increases from this value, the participant indicates a preference for one of the two cognitive interpretations.

Before the experiment, all participants filled out an informed consent form and received instructions on how to perform the task. Furthermore, they filled out the Kennedy-Lane SSQ [Ken+93] immediately before and after the experiment, further the SUS presence questionnaire [Uso+99b], and a demographic questionnaire. We further observed the behavior of the participants during the experiment and asked them open questions about their spatial interpretations during the debriefing.

Hypotheses

In this experiment we tested the following hypotheses:

- H_1 Participants judge the urban environment to be at dominant scale, particularly when their own virtual body is not visible.
- H_2 Participants judge themselves to be at dominant scale in the artificial environment, particularly when they are able to see their own virtual body.
- H_3 Individual differences exist with some participants always estimating their own body to be at dominant scale, and others always estimating the environment to be at dominant scale, but most participants are affected by external stimuli.

6.3.4 Results

We analyzed the results with repeated-measure ANOVAs and TukeyHSD multiple comparisons at the 5% significance level. We confirmed the assumptions of the ANOVA for the experiment data. In particular, Mauchly's test did not indicate that the assumption of sphericity had been violated, and a Shapiro-Wilk test did not indicate that the assumption of normality had been violated.

Figure 6.4 shows the pooled responses plotted as probabilities for participants to judge that the environment was represented at dominant scale. Note that values close to "1" indicate that they judged the environment to be at dominant scale, whereas values close to "0" indicate that they judged themselves to be at dominant scale. Figure 6.4(a) shows the main differences between the environment and virtual body feedback conditions with bar charts. Figure 6.4(b) shows the results for the five tested scale levels. The vertical bars show the standard error of the mean. The stippled horizontal lines indicate the chance level at the 50% mark for deciding towards either alternative in the 2AFCT trials.

Our results show that the virtual body feedback had a significant effect on whether participants judged the environment or themselves to be at dominant scale. We found a significant main effect ($F(1,17) = 4.971$, $p = .040$, $\eta_p^2 = .226$) between the conditions with virtual body feedback ($M = .456$, $SD = .293$) and without virtual body feedback ($M = .600$, $SD = .244$) on responses. With virtual body feedback participants estimated with a significantly higher probability that they themselves were presented at dominant scale, whereas the environment was upscaled or downscaled.

Moreover, our results show a trend that the type of the environment has an effect on dominant scale estimates. We found a trend for a main effect ($F(1,17) = 2.833$, $p = .111$, $\eta_p^2 = .143$) between the conditions in the artificial environment ($M = .478$, $SD = .254$) and in the urban environment ($M = .578$, $SD = .294$) on responses. In comparison to the artificial environment, there is a trend of higher probability in the urban environment that participants estimated that the environment was at dominant scale and not themselves.

We found no effect of the tested scale levels on the results ($F(4,68) = .319$, $p = .864$, $\eta_p^2 = .018$). Our results indicated neither two-way interaction effects nor a three-way interaction effect between the factors environment, virtual body feedback and scale level on the results. However, our results

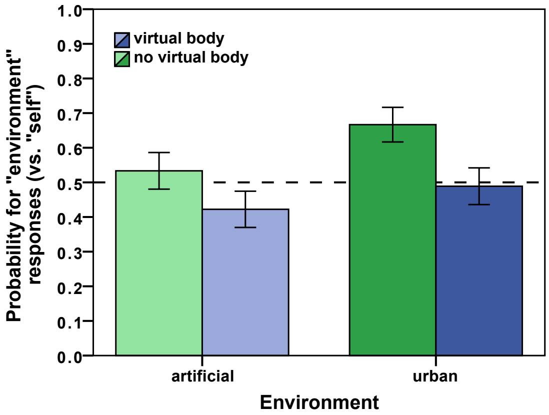

(a)

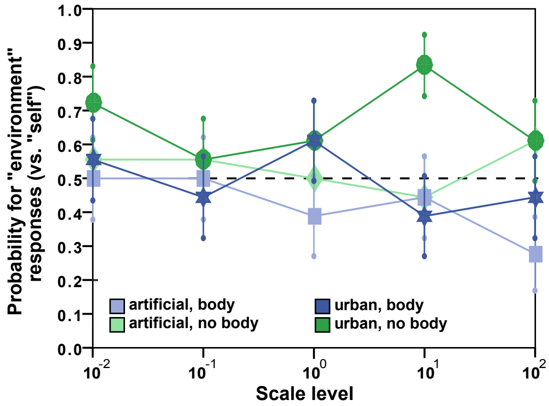

(b)

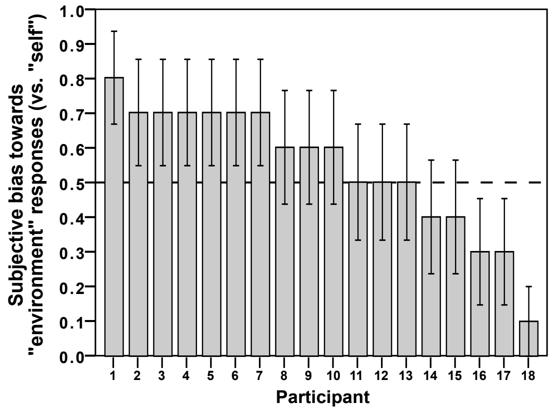

(c)

Figure 6.4: Results of experiment E1: Bar charts showing the pooled differences in probability for participants judging that the environment was presented at dominant scale on the *y*-axis for the two environment conditions and two body feedback conditions (a), and pooled results for all scale levels on the *x*-axis with probability for participants judging that the environment was presented at dominant scale on the *y*-axis (b). Response biases indicating interpersonal differences in estimating the environment or themselves to match dominant scale (c).

indicate that responses in two conditions approximated the chance level, i. e., in the artificial environment without virtual body ($M = .533$, $SD = .228$) as well as in the urban environment with virtual body ($M = .489$, $SD = .316$), which suggests indecisiveness towards one of the 2AFCT alternatives. Conversely, the results in the condition with artificial environment with virtual body ($M = .422$, $SD = .273$) suggest a tendency towards estimating the participant to be at dominant scale. Moreover, the results in the urban environment without virtual body ($M = .667$, $SD = .247$) suggest a tendency towards estimating the environment to be at dominant scale.

Interpersonal Differences

Figure 6.4(c) shows the mean probability for each participant for responding that their own scale deviates from what they estimate as dominant scale in the VE during the experiment. The 18 participants in this plot are ordered from left to right according to their response biases. These individual differences indicate that ten participants had a tendency towards judging the environment to be at dominant scale during the experiment. Conversely, five participants showed a tendency towards judging themselves to be at dominant scale during the experiment. Overall, ten participants showed a noticeable deviation from a chance level of approximately 20% on average towards one of the alternative interpretations, and two of these participants even showed a strong deviation of 30% or 40% from chance level.

The individual response biases indicate that some participants were inherently inclined to estimate the environment to be at dominant scale or to estimate themselves to be at dominant scale. However, most participants' interpretations were not inherently biased and changed depending on the external stimuli of body and environment.

Questionnaires

We measured a mean SSQ-score of 1.66 ($SD = 3.4$) before the experiment, and a mean SSQ-score of 12.46 ($SD = 17.4$) after the experiment. The mean SUS-score [Uso+99b] for the sense of feeling present in the VE was 4.7 ($SD = 1.1$).

6.3.5 Discussion

In line with hypothesis H_1, the experiment indicates that for natural urban environments the participants were inclined to judge the environment to be at dominant scale if they were not seeing their own visual avatar representation. In contrast, virtual body feedback at a scale different from that of the environment resulted in a higher probability that participants judge themselves to be at dominant scale in an artificial environment, which confirms hypothesis H_2. One potential interpretation of the results is that the virtual body feedback reinforces the estimation of oneself being at dominant scale in environments that one has not experienced in real-world knowledge before. In contrast, it appears that the absence of virtual body feedback reinforces the probability of estimating the environment to be at dominant scale in environments that are supported by prior experience in urban regions in the real world.

The individual differences that we observed in the experiment might be interpreted by different mental models that the participants built during the experiment. For instance, while most people only experience urban environments at dominant scale in the real world, other users, for instance, those with an architectural background, bring different prior experience, which stems from routinely evaluating urban development regions with physical or digital models at different scale levels. Although none of the participants mentioned such a background in architecture, we cannot rule out potential prior experience in related fields, e. g., virtual city simulations or video games. However, the results might also be explained by some users just being inclined to rather perceive the environment as invariant, while others might perceive themselves as invariant, which supports hypothesis H_3.

During debriefing in the experiment, we collected informal responses from the participants. Several participants reported that they were influenced in their estimation by the visibility of the body. Others said they trusted their intuition or "feelings". One participant stated representatively:

> "In the artificial world I had no sense of scale at all, but in the city, I had the impression that I was scaled relative to the environment."

Another participant mentioned the following:

> "[..] I did not know if I was very big or just flying when I had no virtual body."

Surprisingly, one participant reported to have suffered in the past from the so-called "Alice in Wonderland syndrome" [Tod55], which describes a non-veridical perception of one's size relative to the environment in the real world. However, since the responses of this participant did not show a significant difference to those from the other participants, we decided to further consider the dataset in the analyses; the participant's data corresponds to index #17 in Figure 6.4(c).

6.4 Experiment E2: Group Effects

In this section, we describe the second experiment in which we further analyzed the estimation of dominant scale in MCVEs with a focus on the questions whether and how the visibility of other avatars at a consistent scale level in an MCVE may affect a user's dominant scale estimation. These questions are particularly interesting considering that MCVEs are subject to group effects, which are known to shape collaborative interaction [Pol+12] and may also affect dominant scale estimation similar to that of the urban environment in experiment E1. A group of avatars at a consistent scale level may thus help to provide a common dominant scale and thus ground collaboration and interaction in MCVEs.

6.4.1 Participants

20 participants (4 female and 16 male, ages $20-38$, $M=26.9$) participated in the experiment. 18 of them also participated in experiment E1. The participants were students or members of the local department of computer science, who obtained class credit for their participation. All of our participants had normal or corrected-to-normal vision. Six participants wore glasses and three participants wore contact lenses during the experiment. None of our participants reported a disorder of equilibrium. One of our participants reported a color blindness and one a strong eye dominance. No other vision disorders have been reported by our participants. We measured the IPDs of our participants before the experiment as in the first experiment. The IPDs of our participants ranged between $5.7-7.0$cm ($M=6.4$cm, $SD=0.3$cm). The total time per participant, including pre-questionnaires, instructions, experiment, breaks, post-questionnaires, and debriefing, was 30 minutes. Participants wore the HMD for approximately $20-25$ minutes. They were allowed to take breaks at any time between trials.

6.4.2 Materials

In this experiment, we used the same experimental setup as in experiment E1. Since the urban environment provides an inherent concept of dominant scale, and since the results of the first experiment indicated no persistent bias in the urban environment with virtual body feedback, we have chosen to focus on this condition in the experiment. Additionally, to simulate other avatars, we have included six virtual agents in the virtual scene, which were displayed at randomized positions in the visible range around the participant's virtual location (see Figure 6.5). We applied an idle animation to the six avatars.

The scale level of these avatars was set independently from the scale level of the participant in the trials. However, all of these avatars were always presented at the same scale level in order to test for group dominance effects. We scaled the participant's virtual *self*-representation relative to their real-world body height with a scale gain $s_s = \frac{virtual\ height}{real\ height}$ as in experiment E1. Additionally, in each trial in the experiment the *other* avatars were all scaled with the same scale gain $s_o = \frac{virtual\ height}{reference\ height}$. The reference height of the six avatars in the urban environment at dominant scale was 1.70m (see Figure 6.5).

Hence, for instance, scaling both the participant and avatars with the scale gains $s_s = s_o = 2$ resulted in the participant seeing the avatars at the same scale as herself. In this case, the participant might still interpret herself and the avatars as being twice as big as naturally in the VE or it can be interpreted as the environment being scaled down by a factor of $\frac{1}{2}$. Moreover, for different scale gains between the participant and the avatars she might either interpret herself, the avatars or the environment to be at dominant scale. All three alternatives have to be considered valid spatial interpretations.

(a) (b) (c) (d)

Figure 6.5: Illustration of different conditions of experiment E2: participant's virtual body and avatars at scale level $s_s = s_o = 1$ (a), participant's virtual body and avatars at scale level $s_s = s_o = 100$ (b), participant's virtual body at scale level $s_s = 1$ and avatars at scale level $s_o = 10$ (c), participant's virtual body at scale level $s_s = 100$ and avatars at scale level $s_o = 10$ (d).

6.4.3 Methods

We used a 5×5 full-factorial within-subjects experimental design. We tested 5 scale levels of the participant with $s_s \in \{10^{-2}, 10^{-1}, 10^0, 10^1, 10^2\}$ as well as 5 scale levels of the other avatars with $s_o \in \{10^{-2}, 10^{-1}, 10^0, 10^1, 10^2\}$. The applied combinations of scale levels were presented randomly and uniformly distributed using again the method of constant stimuli. We included 5 training trials to familiarize the participants with the controls. These trials were excluded from the analysis.

The participants were asked to look around in the VE and get a feeling for their environment. When they have looked enough, they pressed a button and got to the question mentioned in the next subsection. After answering the question the next condition was started.

Two-Alternative Forced-Choice Tasks

Participants had to judge their impression of dominant scale based on the interpretation that (i) they themselves (*self*) seemed to be at dominant scale, (ii) the *environment* seemed to be at dominant scale, or (iii) the *other* avatars seemed to be at dominant scale. For the experiment, we decided to use two 2AFC tasks as in experiment E1. While it would have been possible to use a 3AFC task to indicate the preference for one of the three alternatives [Fer08], we decided against it, since it does not provide sufficient clarity about the order in which the three stimuli relate to the interpretation of dominant scale. As in experiment E1, we decided to use negated questions in the experiment. Participants had to choose between one of two possible responses for each of the following questions:

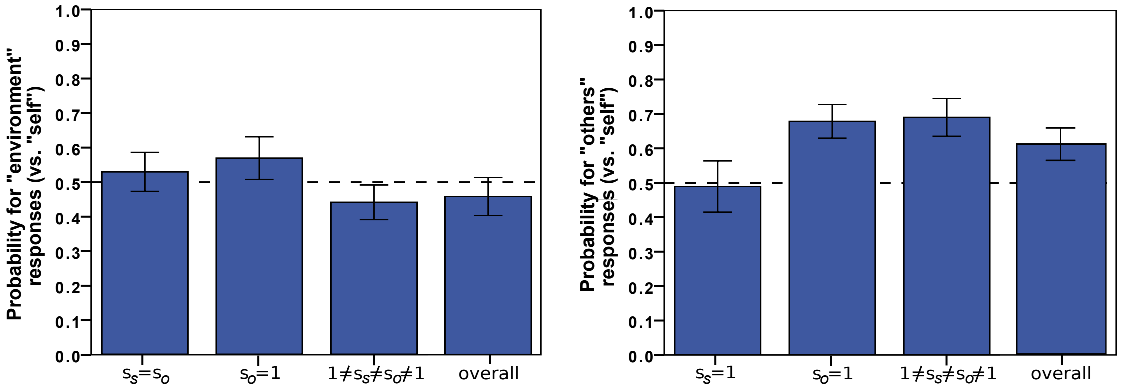

(a) (b)

Figure 6.6: Results of experiment E2 for the conditions with matching scale levels ($s_s = s_o$, $s_s = 1$ or $s_o = 1$) non-matching scale levels ($1 \neq s_s \neq s_o \neq 1$) and overall for the two 2AFCT questions in the experiment: Probability for estimating that the environment was at dominant scale compared to onself (a), and probability for estimating that the other avaters were at dominant scale compared to onself (b).

Q1 "I had the impression that: (left) I myself seemed to be of unnatural scale or (right) the environment seemed to be of unnatural scale."

Q2 "I had the impression that: (left) I myself seemed to be of unnatural scale or (right) the other avatars seemed to be of unnatural scale."

Again, the notion of *unnatural scale* means that this is not the dominant scale. As in the first experiment, for each question participants responded by pressing either the left or right button on the input device. We logged the responses and identified preferences for one of the alternatives in each of the three questions when mean responses deviated from a chance level of 50% probability of responses towards either answer on average over all trials.

Before the experiment, all participants filled out an informed consent form and received instructions on how to perform the task. Furthermore, they filled out the Kennedy-Lane SSQ [Ken+93] immediately before and after the experiment, further the SUS presence questionnaire [Uso+99b], and a demographic questionnaire.

Hypotheses

In this experiment we evaluated the following hypotheses:

H_4 Participants rather estimate the common scale level of the group of avatars as dominant scale in the MCVE than their own scale level.

H_5 When two scale levels coincide between the three factors environment, self-representation, and other avatars, participants rather estimate the matching factors as dominant scale than the remaining factor.

6.4.4 Results

We analyzed the results with repeated-measure ANOVAs and TukeyHSD multiple comparisons at the 5% significance level. A Shapiro-Wilk test did not indicate that the assumption of normality had been violated. We corrected the results with Greenhouse-Geisser estimates of sphericity when Mauchly's test indicated that the assumption of sphericity had been violated.

Effects of the Presence of the Avatars

Figure 6.6 shows the pooled overall responses plotted as probabilities for participants to answer the 2AFCT questions. The stippled line indicates the chance level at the 50% mark for deciding towards either alternative in the 2AFCT trials.

Our results show that the presence of the other avatars had a significant effect on responses. Overall, participants estimated the other avatars to be at dominant scale rather than themselves with a probability of 61.60% ($SD = 21.38\%$) in the experiment. This deviation from chance level was significant in the experiment ($p = .02$).

Similar to the results of the first experiment, we found that participants overall estimated the environment to be at dominant scale compared to themselves with a probability of 45.80% ($SD = 19.40\%$) in the experiment, i. e., close to chance level. This deviation from chance level was not significant in the experiment ($p = .34$).

Effects of the Different Scale Levels

Figure 6.7 shows all responses for the different scale levels of the other avatars and the participant in the experiment plotted as probabilities for participants to answer the 2AFCT questions. The vertical bars show the standard error of the mean. The stippled horizontal lines indicate the chance level at the 50% mark for deciding towards either alternative in the 2AFCT trials.

We found a significant interaction effect between the other avatars' scale level and the participant's scale level for the first 2AFCT question ($F(16,304) = 2.155$, $p = .007$, $\eta_p^2 = .102$) and for the second 2AFCT question ($F(16,304) = 3.590$, $p < .001$, $\eta_p^2 = .159$).

Moreover, we found a significant main effect of the participant's scale level on the responses for the first 2AFCT question ($F(2.774,52.714) = 5.239$, $p = .004$, $\eta_p^2 = .216$), but not for the second 2AFCT question ($F(2.713,51.541) = 2.129$, $p = .114$, $\eta_p^2 = .101$).

Furthermore, we found a significant main effect of the other avatars' scale level on the responses for the first 2AFCT question ($F(4,76) = 8.778$, $p < .001$, $\eta_p^2 = .316$) as well as for the second 2AFCT question ($F(4,76) = 4.650$, $p = .002$, $\eta_p^2 = .197$).

Effects of Consistency Among Factors

Figure 6.6 shows the pooled responses in the conditions with varying consistency among different factors plotted as probabilities for participants to answer the 2AFCT questions. The vertical bars show the standard error of the mean. The stippled horizontal lines indicate the chance level at the 50% mark for deciding towards either alternative in the 2AFCT trials.

For the first 2AFCT question we found no significant main effect but a trend ($F(1.524,28.960) = 2.090$, $p = .138$, $\eta_p^2 = .099$) between the three conditions in which the scale level of the other avatars matched the scale level of the participant ($s_o = s_s$) or the scale level of the environment ($s_o = 1$), and in the trials in which none of the scale levels matched ($1 \neq s_s \neq s_o \neq 1$).

For the second 2AFCT question we found a significant main effect ($F(1.550,29.445) = 6.533$, $p = .004$, $\eta_p^2 = .256$) between the three conditions in which the participant's scale level matched the scale level of the environment ($s_s = 1$), and when the scale level of the other avatars matched the scale level of the environment ($s_o = 1$), as well as in the trials in which none of the scale levels matched ($1 \neq s_s \neq s_o \neq 1$). Post-hoc tests showed that participants were significantly ($p < .02$) more likely to estimate the other avatars to be at dominant scale than oneself for ($s_o = 1$) compared to ($s_s = 1$) as well as for ($1 \neq s_s \neq s_o \neq 1$) compared to ($s_s = 1$). Post-hoc tests showed no significant difference ($p = .807$) between ($1 \neq s_s \neq s_o \neq 1$) and ($s_o = 1$).

Questionnaires

We measured a mean SSQ-score of 11.8 ($SD = 16.7$) before the experiment, and a mean SSQ-score of 31.8 ($SD = 30.9$) after the experiment. The results indicate a typical increase in simulator

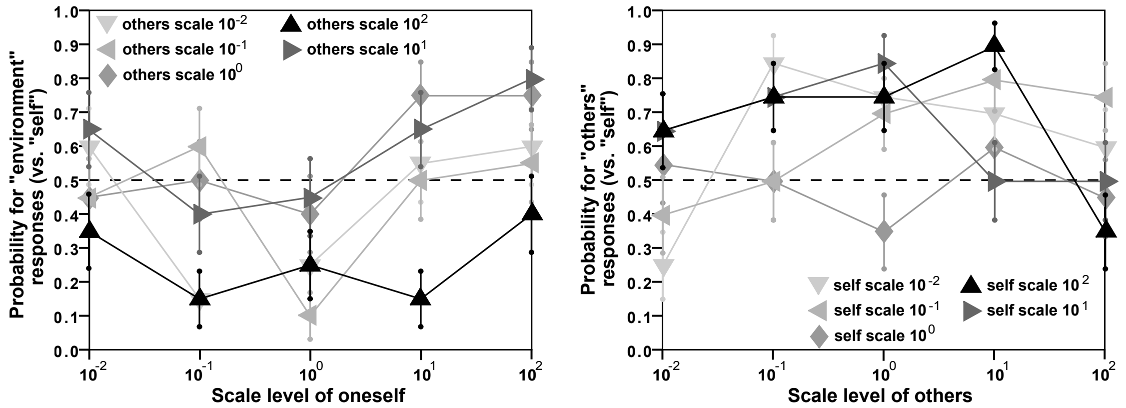

(a) (b)

Figure 6.7: All results of the second experiment for the different scale levels of the participant and other avatars for the two 2AFCT questions: Comparison between environment and self (a), and comparison between other avatars and self (b).

sickness with an HMD over the time of the experiment. The mean SUS-score for the sense of feeling present in the VE was 4.46 ($SD = 1.1$), which indicates a high sense of presence [Uso+99b].

6.4.5 Discussion

The results show that, indeed, group effects can affect how participants interpret scale in MCVEs. First of all, we observed that when the group of avatars was presented at the same scale level as the environment, this resulted in a higher probability for the participants to consider the environment (and the other avatars) as the dominant scale rather than themselves. Since this probability is higher than that for separately the environment and the group of users, it appears to be generally a good idea to combine both scale indicators by populating virtual scenes in MCVEs with avatars at the environment's scale level, i. e., thus improving the notion of a common scale. The matching scale levels of the urban environment and the group of avatars seemed to provide a reasonably dominant scale for users when they collaborate in such environments even when they are at different scale levels themselves. It seems likely that the addition of a group of avatars (even if they are only moving by idle animations as we used in this experiment) to artificial scenes as tested in experiment E1 would also help to provide a common scale level that would be estimated as dominant by users independently of their own scale level.

Further, we observed that when compared to themselves, participants rather estimated the group of avatars as the dominant scale in most cases. This confirms our hypothesis H_4. Moreover, the group of avatars was not primarily estimated as the dominant scale by participants when they were at the same scale level as the environment. The results imply that in this case the two matching scale factors dominate the remaining factor, i. e., two against one, which confirms our hypothesis H_5. Participants still had a balanced estimation of dominant scale when comparing the environment to themselves, which is equivalent to what we observed in experiment E1 and to what is stated in our hypothesis H_3.

One possible explanation of these results is that the visibility of the greater number of other avatars in our experiment (six) outweighed the influence of the participant's own body, and, therefore, they dominated the estimation of scale. Another explanation is that the idle virtual humans dominated the estimation of scale more than the static urban environment, which might explain why we observed a balanced estimation of dominant scale when comparing the environment to themselves in experiment E1 (urban with a virtual body).

6.5 General Discussion

The results of our experiments provide valuable insights into scale estimation in MCVEs. We found interesting individual differences and overall a balanced estimation of dominant scale between oneself and the environment, when the environment is of a type that is known from real-world experience and when the virtual body is visible, potentially since both provide familiar artifacts and thus legitimate alternatives. However, when no visual body feedback was available, participants showed a tendency towards estimating that the environment was at dominant scale. This result was independent of the scale level and the presence of other avatars in the scene in our experiment.

The experiments revealed that artificial environments hinder scale estimation, especially when a user's virtual body is not visible. Participants found it difficult to estimate whether themselves or the environment was at dominant scale when there were few familiar points of reference that could help them estimate scale. We observed a slight trend for them to estimate that themselves were at dominant scale when the virtual body was visible, potentially since this is then the only visual artifact with a known size that they were familiar with from the real world.

Furthermore, we found a higher probability that the other avatars were estimated to be at dominant scale when users were asked to estimate dominant scale between themselves and the other avatars. This may be explained by the greater number of other avatars in our experiment, which might dominate the user's impression of her own scale. It would be interesting to evaluate in future work if the estimation of scale changes with a fewer number of avatars or might even be increased with more avatars.

When the scale of the participants was the same as that of the environment, the estimation of scale between themselves and the other avatars was again balanced. We observed a majority effect: The results suggest that the other avatars would appear more consistent (i. e., resulting when oneself is not at the same scale level as the environment), but it appears that two matching scale levels seem to dominate that of the third factor.

While the focus of our studies was on the influence of the type of the environment, the visibility of an avatar and the presence of other avatars, we found no significant effect of the different scale levels of the participants or other avatars on scale estimation in our experiments. Hence, several question remains for future work. Moreover, our experiments were focused on scale estimation from an egocentric point of view, in which we compared scale estimation between oneself and another element of the environment. In future work, it would be interesting to investigate how these scale estimations change when considered from an allocentric point of view, e. g., comparing scales between two visual artifacts, such as the other avatars and the environment.

6.6 Design Guidelines

The results of our experiments provide some important insights into perception, cognition, and action in MCVEs. In particular, the findings of the experiments lead to the following design rules and guidelines for implementing MCVEs:

1. Communicate dominant scale of the MCVE to all users. *This is the motivation from the pilot study: participants had serious difficulties when trying to communicate absolute distances and sizes without having a common dominant scale.*
2. If unnatural artificial MCVEs are displayed, use additional scale cues for all users, such as a group of avatars at a consistent scale level. *That is, because in artificial MCVEs the participants could not detect a clear dominant scale (see figure 6.4a) and additional cues can help (see hypotheses H_2 as well as hypotheses H_4 and H_5).*
3. Even natural urban MCVEs benefit from such additional scale cues at a consistent scale with the environment by reinforcing its dominant scale. *That is, because in urban MCVEs with virtual body the participants could not detect a clear dominant scale (see figure 6.4a) and*

additional cues can help (see hypotheses H_4 and H_5).

4. Visibility of one's virtual avatar increases the probability that users use it as dominant scale *(see hypotheses H_1)*, which can be beneficial if collaborating users are at the same scale level, but leads to misunderstandings otherwise *(see hypotheses H_5)*.

Indeed, the guidelines provide a first step towards the development and design of novel MCVEs, in particular, in the area of application domains such as urban planning, interactive city visualization, or architectural exploration.

6.7 Conclusion

In this chapter, we analyzed the estimation of dominant scale in the presence of conflicting cues in MCVEs. Therefore, we presented a pilot study and two experiments in which we analyzed different factors and their effects on the participants' estimation of dominant scale in an MCVE.

Our results suggest an interaction effect between the visibility of the participant's virtual body, the type of the VE as well as the presence of a group of avatars and their relative scale levels. We summarized the results as guidelines for the design of MCVEs.

The scope of this work may seem limited, relative to the general problem of effective collaboration in an MCVE. It is unclear at all, how many applications for MCVEs there are or will be. But the results provide insights into MCVEs, which have enormous potential to stimulate further research directions.

III BEYOND DETECTION THRESHOLDS

7. SENSITIVITY TO REDIRECTION WITH VISIBLE FEET

7.1 Motivation

As far as we know, all experiments for identifying detection thresholds of movement manipulations (see Section 3.4.3) were carried out without a virtual representation of the user's body [Ste+08a; Ste+10b]. In contrast, previous work has focused on shifting the camera position while ignoring the tracked limb positions of the user. Indeed, Nagao et al. showed virtual shoes for vertical redirected walking techniques [Nag+17] but they did not report detection thresholds. A full-body visual representation is known to increase the sense of presence (see Chapter 2.2). Hence, it will become an important challenge to integrate full-body tracking in redirected walking.

When full body tracking is available, the problem occurs that when the user is redirected the virtual body movements have to be manipulated in the same way as the virtual camera. This, in turn, might have an impact on the detectability of such manipulations since it could potentially make the manipulation more obvious. In addition, the part of the visual stimulus that is not manipulated, i. e., the VE and its objects, might also have an influence on the detectability in such situations. When the virtual camera or virtual body is manipulated in VEs in which several objects are close to the user, by means of redirected walking techniques, such manipulations might get more noticeable compared to VEs that do not provide many self-motion cues.

In this chapter, we address the research question if the virtual self-representation of the user's feet changes the detection thresholds for translation gains. Therefore, we add a visual representation of the user's feet to the VE and examine the limits of tracking the user's feet and unobtrusively changing their position by applying translation gains to make the user feel like walking faster or slower. The aim of this experiment is to find the detection thresholds for translation gains without a visual representation of the user's feet and compare them to the thresholds with a feet representation. Furthermore, a visually rich environment is compared to a low cue VE to evaluate also the influence of the part of the visual stimulus that is not manipulated. In particular, we assumed the following hypotheses and evaluated them in a psychophysical experiment:

- H1: The range of translation gains, which can be applied unnoticeable for the user, is smaller when the user is able to see a visual representation of her feet.

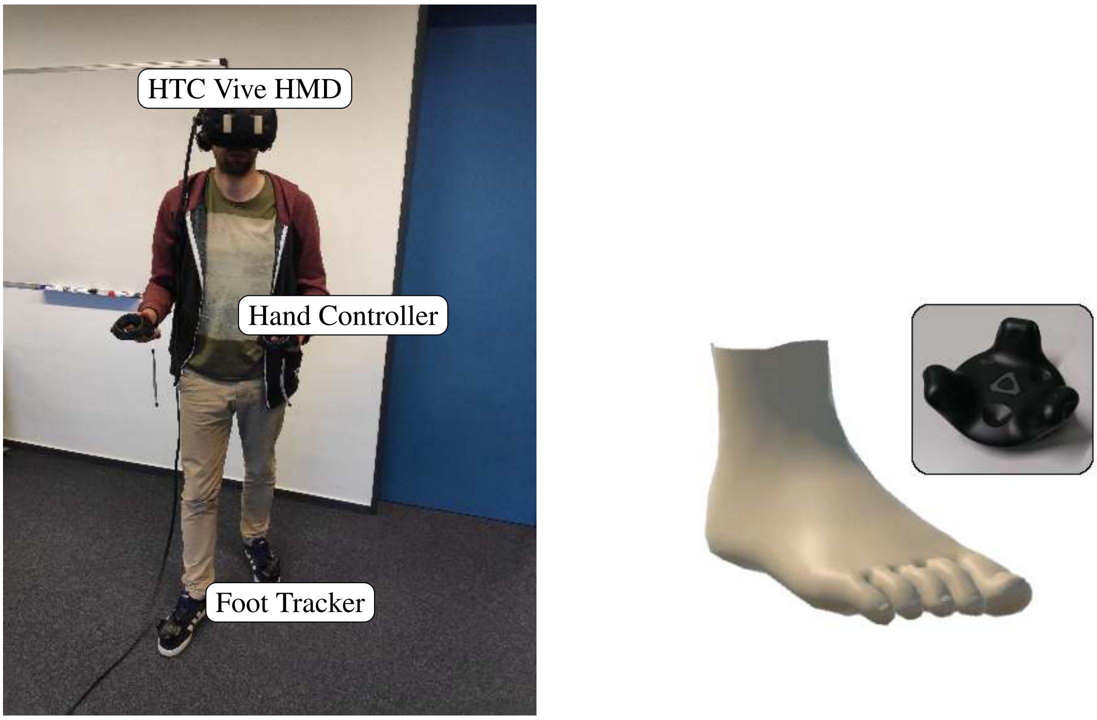

(a) (b)

Figure 7.1: A participant during the experiment, wearing the HTC Vive HMD, two hand controllers and two trackers for the feet (a). The virtual foot model that was placed in the VE (b) according to the tracker (inset) that was mounted right above the ankle at the physical foot of the participant.

- H2: The range of translation gains, which can be applied unnoticeable for the user, is smaller when the VE provides more motion visual cues.
- H3: The sense of presence will be lowest in the VE, which provides less motion visual cues.

The remainder of this chapter is structured as follows. Section 7.2, Section 7.3 and Section 7.4 describe the psychophysical experiment, which we conducted to identify detection thresholds for the different conditions. Section 7.5 presents the results, which are discussed in Section 7.6. Section 7.7 concludes the chapter.

7.2 Participants

20 participants completed the experiment. All of them were students of the local university, while 14 of them were students of a computer science related subject who obtained class credit for their participation. 13 participants were male and 7 were female, with an average age of 25.75 years (21-45 years) and an average height of approximately 178cm. All except for one participant with Amblyopia had normal or corrected-to-normal sight. No other vision disorders have been reported by our participants. None of our participants reported a disorder of equilibrium. 14 participants played 3d computer games on a regular basis. The participants spent an average of approximately 6 hours per week playing. 18 participants had used an HMD before. The total time per participant, including pre-questionnaires, instructions, experiment, breaks, post-questionnaires, and debriefing, was about 75 minutes, out of which around 40 minutes were spent in VR. During the experiment, the participants were allowed to take breaks at any time.

(a) (b)

Figure 7.2: The VEs, which were used in Condition 1 and Condition 2 (a) and in Condition 3 (b). While the first one offered a lot of different visual cues to judge the manipulations, the second one consisted only of a white plane and a horizon. The black cross marked the place where the participants should stop walking.

7.3 Materials

The experiment took place in a 12m $\times$ 6m laboratory room. We instructed the participants to wear an HTC Vive HMD (see Figure 7.1 (a)), which provides a resolution of 1080×1200 pixels per eye with an approximately 110° diagonal field of view and a refresh rate of 90 hz. Positional tracking was done by a lighthouse tracking system that is delivered with the HTC Vive. The lighthouse system was calibrated so that there was an available walking space of 6m $\times$ 4m. During the experiment the room was darkened in order to reduce the participant's perception of the real world. The participants received instructions on slides presented on the HMD. A HTC Vive controller served as an input device via which the participants provided responses during the experiment. The HTC Vive trackers were used to track the user's feet and mounted right above the ankles (see Figure 7.1 (b)). The model of the virtual foot had a size of 25.5 cm. For rendering, system control and logging we used an Intel computer with 3.2GHz Core i7 processor, 32GB of main memory and a Nvidia Geforce GTX 1080 graphics card. The virtual environment was rendered using the Unity3D engine 5.6

7.4 Methods

We used a 3×9 within-subjects experimental design. 3 different combinations of environment and feet tracking were tested (see Figure 7.2). These were

1. Condition 1: No visible virtual feet in a high-fidelity visually rich VE,
2. Condition 2: Visible virtual feet in a high-fidelity visually rich VE,
3. Condition 3: Visible virtual feet in a low cue VE.

For each of these conditions, we tested 9 different translation gains $g_T \in \{0.6, 0.7, 0.8, 0.9, 1, 1.1, 1.2, 1.3, 1.4\}$. Each gain was repeated 3 times. The experiment was separated in 3 blocks, one for each environment/feet condition. The order of the blocks was counter-balanced. In a block, all trials were randomized. In total, the participants completed $3 \times 9 \times 3 = 81$ trials.

7.4.1 Blocks

In Condition 1, the VE consisted of a natural surrounding with trees, grass, and sand. The foot trackers were attached to the feet of the participant, but were not used in this condition. This means that the participant could not see a representation of their own feet, though the biomechanics of walking were affected in the same as in the other conditions. This condition served as baseline condition for redirected walking, since it was already tested in previous experiments [Jan+17b; Ste+10b].

For Condition 2, we used the same VE as in Condition 1 described above. The difference between Condition 1 and Condition 2 is that the mounted foot trackers were used to display a virtual representation of each foot. This condition provided the participants with an additional source of information to detect their velocity, i. e., movements of their feet.

In Condition 3, we used the same setup as described in Condition 2, i. e., with visual feet feedback, but displayed a VE with reduced motion cues. The participants were placed in an empty VE and the only thing they could see was a representation of their feet on a white floor and a horizon. This condition was used in order to prevent visual cues from helping them when estimating their pace length and velocity in VR, while their feet were manipulated. If Condition 1 and Condition 2 would provide significantly different results, the results of Condition 3 could help to determine whether the difference is due to the fact that the participants' feet are visible, or due to the fact that the two sources of information, namely the feet and the visually rich environment, are used in conjunction. Additionally, this condition determines the impact that showing the participants' feet can have on their ability to detect translation manipulations when they have no other source of information available. The fourth possible combination, i. e., no representation of virtual feet in a low cue VE, was not tested, since the participants would not have any information sources at all to judge their forward motions and/or if they were manipulated.

7.4.2 Procedure

Upon arrival, participants were informed about the procedure of the experiment and signed a consent form. Then, all participants filled out a pre-questionnaire and the SSQ [Ken+93]. The foot trackers were mounted on their ankles and they donned on the HMD and grabbed the hand controllers. Then, they started in an introductory scene where their individual foot position was adjusted and they received instructions about how to use the touchpad of the controller. Before the actual experiment started, three training trials were presented to the participants: the slowest gain used in the experiment (0.6), the gain without manipulation (1.0) and the fastest gain of the experiment (1.4). During these training trials, participants were allowed to ask questions.

Once the training was finished, participants received headphones to remove all sound from the physical environment and the actual experiment started. Depending on the current condition, the participant was placed in a visually rich or reduced cue environment with a representation of their feet visible, or, as in Condition 1, no visible representation of their feet. The participants had to walk following a green dot on the ground 0.4m in front of them. The participants were not instructed to keep their virtual feet on sight. But they were told to look at this dot while walking. This way, we assured that the participant's feet were visible in their field of view without paying too much attention to them. While they were walking, a translation gain was applied to their feet and the virtual camera, making them walk slower with smaller steps, or faster with larger steps.

The participants walked forwards until the green dot turned red. This happened when they reached a physical distance of 5m. Then, an information sign appeared in front of them on eye height level, asking them to judge whether their virtual movement was slower or faster than their physical movement. The participants answered by using the left side of the controller's touchpad to indicate a slower movement and the right side of the touchpad to indicate a faster movement. Participants had to answer the question in a 2AFC task (see Section 3.4.3) that only allows the answers "slower" or "faster". Whenever the participants were not sure about the manipulation, they had to guess, with a chance of 50% to guess the correct answer. Answers like "equal" were not allowed in order to avoid a bias caused by uncertainty towards the answer "equal".

After they answered the 2AFC question, the participants had to turn around and walk back to their starting point, again, indicated by a green dot. On the way back, their virtual feet were hidden,

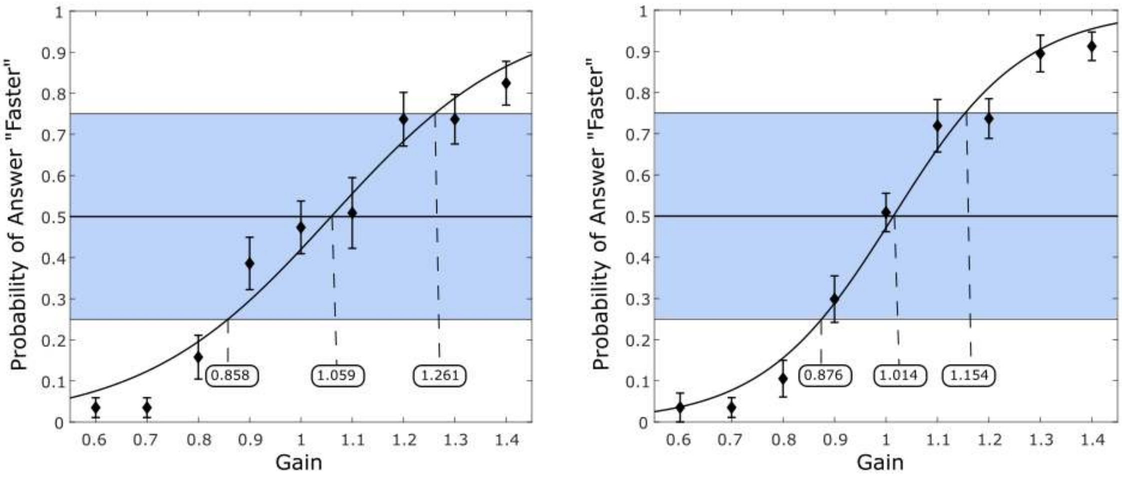

(a) (b)

Figure 7.3: Plotted results of the experiment for Condition 1 (a) and Condition 2 (b). The x-axis shows the applied translation gains and the y-axis shows the probability of the participants' statement that they walked faster than in the real world. The psychometric function shows PSE as well as lower and upper detection thresholds.

so, on the next trial, a comparison between the last and the current gain would not be possible. When the participants reached their starting point and pressed a button on their controller, the next gain was applied. In block 2 and 3, the feet were shown again. In the visually rich conditions, the users were placed in a different part of the scene in order to prevent visual comparison of the last and the current distance walked during the 5 physical meters. After 27 trials, each block was over. The participants saw an information sign thanking them and they took off their HMD and the trackers. Then, they filled out the SUS presence questionnaire [Uso+99b]. When they felt ready, the next round was started with a different block. At the end of the experiment, the participants filled out the second SSQ and a questionnaire to collect their demographical data. Then, they were informed about the goal of the experiment.

7.5 Results

In this section, we summarize the results of the experiment with respect to the identified detection thresholds, required times, presence, and VR sickness.

7.5.1 Detection Thresholds

Figure 7.3 shows the pooled results over all participants for Condition 1 (see Figure 7.3(a)), Condition 2 (see Figure 7.3(b)), and Condition 3 (see Figure 7.4).

The x-axes of the plots in Figure 7.3 show the applied translation gains $g_T \in \{0.6, 0.7, 0.8, 0.9, 1, 1.1, 1.2, 1.3, 1.4\}$. The y-axes show the probability of the participants' statements that they walked faster than in the real world. For each gain, the mean and standard error bars are displayed in the plot. The intersection of the graph with the 25% line was marked as the lower threshold, the 50% intersection is the PSE and the 75% mark represents the upper threshold. Each plot was fitted with a sigmoidal psychometric function, which determines the PSE and DTs.

The results are also summarized in Table 7.1 showing the exact numbers. The content of the table cells means that the physical movement has to be scaled by the corresponding number from the cell in order to calculate the corresponding virtual movement speed.

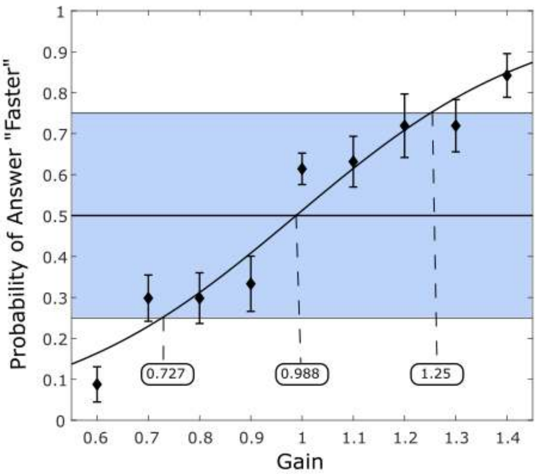

Figure 7.4: Plotted results of the experiment for Condition 3. The x-axis shows the applied translation gains and the y-axis shows the probability of the participants' statement that they walked faster than in the real world. The psychometric function shows PSE as well as lower and upper detection thresholds.

We calculated individual DTs and PSEs for each participant to run significance tests. A Kolmogorov-Smirnov test reveals that the data is not normally distributed. Hence, we analyzed the results with a Friedman test at the 5% significance level. The results show a significant effect of the condition on the lower DT ($p = .03$) and the PSE ($p = .004$). We found no significant effect of the condition on the upper DT. A post-hoc test using Wilcoxon signed-rank test returned significant effects for both, PSE and lower DTs, between Condition 1 and Condition 3 and between Condition 2 and Condition 3 ($p_{lower13} = .049$, $p_{PSE13} = .0025$, $p_{lower23} = .0043$, $p_{PSE23} = .04$), which partly confirms Hypothesis H2. No significant difference could be found between Condition 1 and Condition 2 ($p_{lower12} = .469$, $p_{PSE12} = .147$) and for the upper thresholds ($p_{upper12} = .295$, $p_{upper13} = .653$, $p_{upper23} = .528$). Hence, Hypothesis H1 could not be confirmed.

Table 7.1: Lower and upper detection thresholds (DTs) as well as the points of subjective equality (PSE) for all three conditions. Lower DT and PSE of Condition 3 is significantly different from Condition 1 and Condition 2.

Condition	**Lower DT**	**PSE**	**Upper DT**
Condition 1	0.85823	1.05895	1.26054
Condition 2	0.87583	1.01437	1.15388
Condition 3	*0.72745	*0.9884	1.25038

7.5.2 Presence

The results of the SUS presence questionnaire are shown in Table 7.2. The questionnaire consisted of six questions with 7 point Likert scales. Condition 2 receives the highest mean with 4.52 ($SD = 0.32$), followed by Condition 1 with a mean of 4.45 ($SD = 0.32$). Condition 3 has the lowest rating with a mean of 3.74 ($SD = 0.37$).

A Kolmogorov-Smirnov test reveals that the data is not normally distributed. We analyzed the results with a Friedman test at the 5% significance level. According to this test, at least one

Table 7.2: Mean, standard deviation, and Count of the SUS presence questionnaire for all conditions. The SUS count is the number of answers of 6 or 7 points.

Condition	SUS Mean	SUS Count
Condition 1	4.45 (SD = 0.32)	1.6 (SD = 1.76)
Condition 2	4.5167 (SD = 0.32)	1.8 (SD = 1.79)
Condition 3	3.7417 (SD = 0.37)	1.1 (SD = 1.02)

condition differs significantly from the others ($p = .0196$). A post-hoc Wilcoxon signed-rank test found out that Condition 3 differs significantly from Condition 1 ($p = .0221$) and from Condition 2 ($p = .0104$). Hence, the participant's sense of presence was lowest in Condition 3, which confirms Hypothesis 3. There is no significant difference between Condition 1 and Condition 2 ($p = .4736$). The SUS Count is the number of answers of 6 or 7 points, and it gives a similar result as the mean. Condition 2 has the highest count with a mean count of 1.8, followed by Condition 1 with a mean count of 1.6. Condition 3 has the lowest count with a mean count of 1.1. A Kolmogorov-Smirnov test reveals that the data is not normally distributed. We analyzed the results with a Friedman test at the 5% significance level. No significant differences between the three conditions were found ($p = 0.4036$).

7.5.3 VR Sickness

We measured a mean SSQ-score of 19.26 ($SD = 20.35$) before the experiment, and a mean SSQ-score of 31.23 ($SD = 31.3$) after the experiment. A Kolmogorov-Smirnov test showed that the data was not normally distributed. We analyzed the results with a Wilcoxon signed-rank test at the 5% significance level. We found that the SSQ-score was significantly higher after the experiment ($p = .01$).

7.6 Discussion

The results show that in a visually rich environment where the user's feet are not shown (Condition 1), a downward scaling of 14% and an upward scaling of 26% was possible without user being able to notice. This finding is inline with previous findings [Ste+10b]. A manipulation of about 12% downward and 15% upward was unnoticeable for user in a visually rich environment where the user's feet are shown (Condition 2). This means that it was easier to detect the manipulation when participants could see their feet, which would be inline with Hypothesis H1, though, this finding could not be confirmed by the statistical test. Hence, we can not confirm H1, although there might be an effect whose size is just very small. For a low cue environment (Condition 3), a downward scaling of 27% is applicable and an upward scaling of 25%. In this case, the results of the psychometric function as well as the significance tests lead to the assumption that participants were generally better at estimating their walking velocity if a visually rich environment was presented as opposed to a reduced-cue environment. This means that the participants still heavily relied on their visual information, e. g., optic flow or motion parallax, to estimate their walking speed. Regarding the found DTs and the results of the significance tests, Hypothesis H2 can be mostly accepted, although we did not find significant differences for the upper thresholds. Although, a visual self-representation of the participant's feet might have an influence on the detection thresholds for translation gains, the nature of the VE is still the more important factor for estimating those thresholds. This might be due to the fact that the VE is the part of the visual stimulus that takes up more space of the field of view of the user than the feet. The feet are comparatively small. But still, these findings are interesting, and they might get even more impact when a full avatar is used as a visual self-representation and when the field of view of HMDs will increase in the future.

Furthermore, the results show that the movement has to be upscaled by 6% in Condition 1, in order to appear natural to the participants, which is similar to the findings of Steinicke et al. that movements have to be upscaled by 7% to appear natural [Ste+10b]. The results for Condition 2 and Condition 3 suggest that the participants were able to estimate their speed quite well with only 1% upscaling in Condition 2 and 1% downscaling in Condition 3. This might be interpreted as a trend for the statement that virtual feet did help the participants to judge their natural walking speed similar to previous finding in which a virtual avatar helped to judge virtual distances [Moh+10].

Although, the environment where the user's feet were shown (Condition 2) received higher means for the user's subjective sense of presence than the visually rich environment without feet (Condition 1), these differences were not significant. This is an indicator that having a visual self-representation of the feet did not have a significant impact on the sense of presence of the participants in the VE or that the effect was too small to be revealed with the considered number of participants. Another limiting factor might be the appearance of the virtual feet. They were presented barefoot in the VE while the participants wore shoes. A reduced-cue environment leads to an even lower presence score compared to the visually rich environment without feet. This also supports the finding that the VE is much more important for the whole visual perception than the self-representation.

The significant increase of VR sickness during the experiment might be related to the stronger gains that were obviously perceivable by the participants. Nevertheless, since we did not collect data about VR sickness for each single gain, we can not confirm this assumption.

7.7 Conclusion

In this chapter, we evaluated the influence of a visual self-representation of the feet on translation gains. Therefore, we conducted a psychophysical experiment with three different conditions and 9 different gains from the interval of 0.6 to 1.4 These three conditions were: presenting the gains in a visually rich environment without tracking the user's feet (Condition 1), showing the user's feet in a high fidelity visually rich environment (Condition 2) and showing the user's feet in a reduced-cue environment (Condition 3). The participants performed a 2AFC task to determine if their virtual movement was slower or faster than their physical movement. The results revealed detection thresholds for translations gains, which cannot be detected by the user when the virtual feet were visible. Nevertheless, the difference between visible and invisible feet was smaller than expected and the nature of the VE had still a bigger impact on the DTs.

8. SENSITIVITY TO BENDING OF CURVED PATHS

8.1 Motivation

When walking through VEs, users do not always follow an exactly straight path. So far, it has not been investigated how much the bending of a physical path can vary from the bending of a virtual path in situations in which users already walk on such a curved virtual path. While straight paths are considered the most difficult situation for RDW manipulations, in practical situations, users tend to walk on curved paths more often than on straight paths, while the curvature radius can vary from slight to strong and from left to right [Ste+13]. During straightforward walking, any rotation that users perceive in their physical walking path indicates that they are being manipulated. In contrast, when walking on a curved virtual path, the magnitude of the change in heading has to be compared between the real and virtual environment while walking. Razzaque already mentioned that there is a kind of training effect when users are walking on a curve that becomes tighter during walking [Raz05], which might be explained by the podokinetic afterrotation (PKAR) [Web+98]. We hypothesize that users will be much less aware of the redirection in such situations, so that it might be possible to leverage such undetectable manipulations even for room-scale VR setups.

In this chapter, we introduce a new kind of redirection method which is based on *bending gains* that define discrepancies between physical and virtual paths in situations where both are bent. Furthermore, we present an experiment in which we analyze the user's sensitivity to these gains. Therefore, users walk on a curved path in the VE, while they are guided on a physical path with a different curvature. Using a psychophysical measure, we determine the largest amount of discrepancy between the real and virtual path that is still undetectable by users for different levels of curvature.

This chapter is structured as follows: Section 8.2 introduces bending gains for altering the curvature of virtual and real paths. Section 8.3, Section 8.4, and Section 8.5 describe the experiment in which we evaluate the sensitivity to different physical curvatures while walking curved virtual paths. Section 8.6 presents the results. Section 8.7 concludes the chapter.

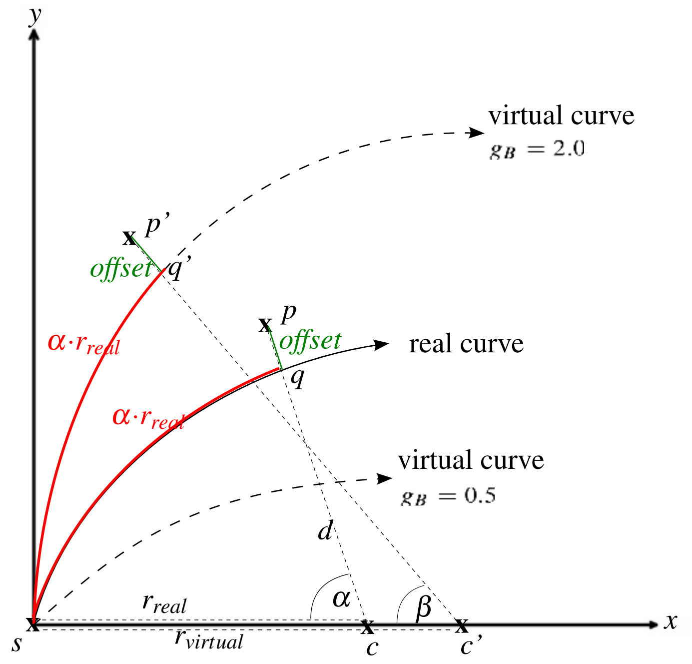

Figure 8.1: Illustration of bending gains applied to a curved path: A gain smaller than one means that the virtual curvature has a smaller radius than the real curved path whereas a gain greater than one means that the virtual curvature has a greater radius. The position and orientation of the user in the VE (*p'*) is calculated according to the user's position and orientation on the real world path (*p*). In this case, the x axis corresponds to the strafe direction of the user and the y axis corresponds to the look direction. $\alpha \cdot r_{real}$ denotes the length of the walked path.

8.2 Bending Gains

According to translation, rotation, and curvature gains, which were introduced in previous work [Ste+10b], we add *bending gains* $g_B \in \mathbb{R}$. Bending gains are similar to curvature gains, as they combine walking and rotations, but are applied to curved paths instead of straight paths. In a similar way, this kind of redirection can be achieved by combining curvature and rotation gains. However, the definition of bending gains is useful in cases where the curvature of the virtual path is known as in the locomotion technique that we introduce in Chapter 14. Furthermore, we can simply use this virtual radius to calculate the camera manipulations, which is more efficient for the implementation.

For curvature gains, Steinicke et al. defined $g_C := \frac{1}{r_{real}}$, where r_{real} denotes the radius of the curvature in the real world. Since, this gain was defined for straightforward paths only, bending gains need to incorporate the bending of the virtual curve as well. Let this curve in the VE be part of a circle with the radius $r_{virtual}$. Furthermore, during walking on this virtual path the user is redirected on a different circular path in the real world with the radius r_{real}.

Hence, we can specify bending gains by multiplying the curvature gain with $r_{virtual}$, i. e., $g_B := r_{virtual} \cdot g_C = \frac{r_{virtual}}{r_{real}}$. Assuming, this gain is applied to a curve to the right and $r_{virtual} > r_{real}$, then $g_B > 1$, then the user's real-world path is bent to the right, i. e., the user walks physically right of the virtual path (or on a smaller circle). If $r_{virtual} < r_{real}$ then $g_B < 1$, the user is walking physically left of the virtual path (or on a larger circle). Figure 8.1 illustrates this situation. For paths, which are bent to the left, the situation is the other way around. For cases in which $r_{virtual} = r_{real}$, then $g_B = 1$ no redirection is applied. Furthermore, for situations the real walking path of a user is bent in such a way that it gets a straight path, i. e., $r_{real} = \infty$, for the bending gain it is $g_B = 0$.

Implementation

Redirection by means of a bending gain is implemented by calculating position and orientation of the user in the VE according to the user's position and orientation in the real world (see Figure 8.1). Let the radii r_{real} and $r_{virtual}$ as well as the start position s be given as illustrated. That means, we have to know how much the virtual path is bent and how much discrepancy between virtual and real path is possible. The first part requires knowledge about the VE and the second part is evaluated in the experiment. The current position p (as well as the orientation o) of the user in the real world is provided by the tracking system.

With these data (s, p, o, r_{real} and $r_{virtual}$), it is possible to apply a bending gain and compute the position p' (as well as the orientation o') of the user in the virtual world. First, we calculate the center points c (of the real world circle) and c' (of the virtual world circle) by extending the orthogonal vector of the user's view direction from start position s by r_{real} and $r_{virtual}$, respectively. We calculate also the distance d from c to p. Then, we can determine the *offset*, i. e., the deviation of the user's position from the real world circle, by $offset = d - r_{real}$. If the user would stand exactly on a point of the real world circle q (which means the distance from c to p is $d = r_{real}$), it would be $offset = d - r_{real} = 0$.

The angle α can be calculated by using the dot product:

$$\cos(\alpha) = \frac{(c-s)\cdot(c-p)}{|c-s|\cdot|c-p|} \tag{8.1}$$

The actual walked distance on the path is $\alpha \cdot r_{real}$ according to the definition of radian. This can be used to calculate the angle β of the virtual curvature (again according to the definition of radian):

$$\beta = \alpha \cdot \frac{r_{real}}{r_{virtual}} \tag{8.2}$$

Now, the position on the virtual circle q' can be determined by using sine and cosine:

$$q'_x = (c'_x + r_{virtual} \cdot \cos(\beta)), q'_y = (c'_y + r_{virtual} \cdot \sin(\beta)) \tag{8.3}$$

In the end, to get the exact position p', we have to add the calculated *offset* to q'.

The virtual orientation of the user o' is computed accordingly. It is composed by the tracked orientation in the real world o and a corresponding shift of $\alpha - \beta$.

8.3 Participants

15 participants (2 female and 13 male, ages $24 - 39$, $M = 30.5$) completed the experiment. The participants were students or members of the local department of informatics, who obtained class credit for their participation. All of our participants had normal or corrected-to-normal vision. Six participants wore glasses during the experiment. None of our participants reported a disorder of equilibrium. One of our participants reported a strong eye dominance. No other vision disorders have been reported by our participants. 14 participants had participated in an experiment involving HMDs before. The experience of the participants with 3D stereoscopic displays (cinema, games etc.) in a range of 1 (no experience) to 5 (much experience) was $M = 4.3$ ($SD = 1.03$). Most of them had experiences with 3D computer games ($M = 4.3$, $SD = 1.25$, in a range of 1 = no experience to 5 = much experience) and they usually played 5.3 hours per week on average ($SD = 6.54$). The body height of the participants varied between $1.60 - 1.87$m ($M = 1.77$m, $SD = .07$m). The total time

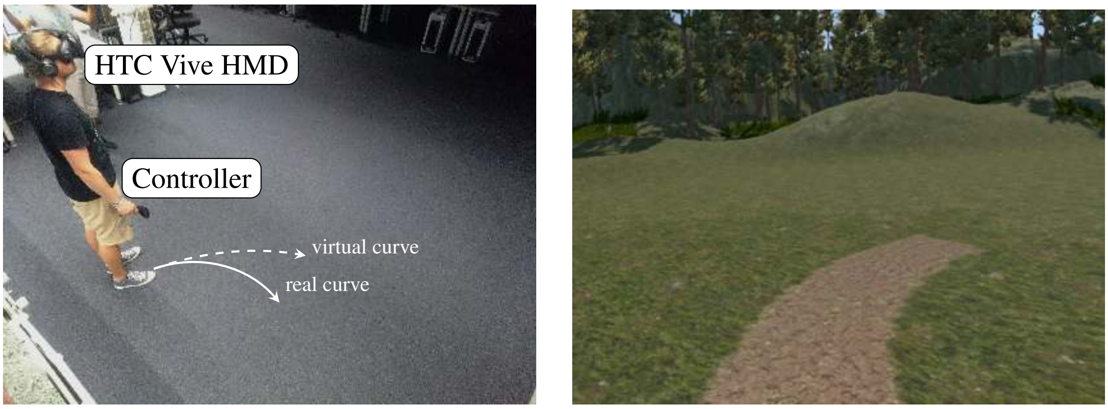

(a) (b)

Figure 8.2: The experimental setup: a user is walking on a curved path in the VE which has a different radius than the curved path in the real world he is redirected on (a), and user's view to the VE with a curved virtual path (b).

per participant, including pre-questionnaires, instructions, experiment, breaks, post-questionnaires, and debriefing, was 60 minutes. Participants wore the HMD for approximately 45 minutes. They were allowed to take breaks at any time between trials.

8.4 Materials

The experiment took place in a 12m $\times$ 6m laboratory room. We instructed the participants to wear an HTC Vive HMD, which provides a resolution of 1080×1200 pixels per eye with an approximately 110° diagonal field of view and a refresh rate of 90 hz. Positional tracking was done by a lighthouse tracking system that is delivered with the HTC Vive. The lighthouse system was calibrated so that there was an available walking space of 4m $\times$ 4m (see Figure 8.2 (a)). During the experiment the room was darkened in order to reduce the participant's perception of the real world. The participants received instructions on slides presented on the HMD. A HTC Vive controller served as an input device via which the participants provided responses during the experiment. For rendering, system control and logging we used an Intel computer with 3.5GHz Core i7 processor, 32GB of main memory and two Nvidia Geforce GTX 980 graphics card.

The virtual environment was rendered using the Unity3D engine 5.4 and showed a natural forest scene and a curved path in front of the participant (see Figure 8.2 (b)). The path was computed by first calculating a circle with a specific radius and then drawing only that part of the circle that started at the virtual camera position and ended after 4m. Dependent on the current condition, the path was curved to the right or to the left. Hence, the center point of the circle was to the left or to the right of the virtual camera position.

8.5 Methods

We used a 4×5 full-factorial within-subjects experimental design. We tested 4 different curves in the real world (with a radius of 1.25m, 2.5m, 6.25m and 12.5m) and 5 gains for the virtual curves: $g_B \in \{1,2,3,4,5\}$ for the real world curves of 1.25m and 2.5m and $g_B \in \{1, \frac{1}{2}, \frac{1}{3}, \frac{1}{4}, \frac{1}{5}\}$ for the real world curves of 6.25m and 12.5m. We tested both directions (left and right) and repeated each condition 2 times. Hence, each gain was tested 4 times in total. All conditions were randomized. In total, the participants completed $4 \times 5 \times 2 \times 2 = 80$ trials.

8.5.1 Conditions

We decided to use these conditions because the curved paths with radii of 1.25m and 2.5m would fit into a room-scale VR setup. The considered curves provide two radii (one is twice as large as the other one), which both could be used in the room-scale locomotion technique as introduced in Chapter 14. Obviously, we are particularly interested in detection thresholds for bending a curved virtual path towards a curved real-world path that fits into the room-scale VR setup. The other case, i. e., how strong a curved virtual path can be straightened in the real-world before users notice, is of less interest because one of the major goals of our approach is to decrease the space requirements and to remain in a confined tracking space.

According to the results of several pre-tests, we identified that bending the real-world path with a gain of $g_B = 5$ could be reliably detected in most cases. Hence, we applied gains $g_B \in \{1,2,3,4,5\}$ to the real curves (with radii 1.25m, 2.5m), which resulted in virtual curves with radii of $r_{virtual} \in \{1.25, 2.5, 3.75, 5, 6.25\}$ meters and $r_{virtual} \in \{2.5, 5, 7.5, 10, 12.5\}$ meters, respectively.

While bending these virtual radii towards the real-world target radii of 1.25m and 2.5m makes sense, a bending towards smaller radii does not make sense, since users could not follow the paths if the radii are too small. However, in order to provide an equal number of increased and decreased bending conditions, we added real-world curves with radii of 6.25m and 12.5m and applied the corresponding smaller gains $g_B \in \{1, \frac{1}{2}, \frac{1}{3}, \frac{1}{4}, \frac{1}{5}\}$ to them. Using these conditions provide virtual radii of $r_{virtual} \in \{1.25, 2.5, 3.75, 5, 6.25\}$ meters and $r_{virtual} \in \{2.5, 5, 7.5, 10, 12.5\}$ meters, respectively. As a result, participants would experience the same number of increased and decreased bending conditions.

8.5.2 Procedure

Before the experiment, all participants filled out an informed consent form and received detailed instructions on how to perform the experimental task. Furthermore, they filled out a demographic questionnaire after the experiment. Participants completed 5 training trials before the experiment.

For each trial, participants were instructed to walk along the virtual path, which had a total distance of 4m. While participants were walking along the virtual path, we applied the different bending gains as explained in Section 8.5. After the participant reached the end of the path, they pressed a button on the controller and the following 2AFC task question was displayed: *"At which side from the virtual path did you walk physically in the real world?"*. They had the two answer options *"left"* and *"right"* that could be chosen by using the touchpad of the controller. Afterwards, participants were guided to the next start position in the laboratory by displaying a 2D compass and distance metrics on the HMD. By using this method, the participants were kept unaware of their position and orientation in the real world. So, they could not use this information to identify the amount of redirection that was applied. The next trial started once participants reached the new initial position and indicated that they were ready to start by pressing a button on the controller.

In pre-tests of the experiment, we found that participants had serious problems in identifying on which side of the virtual path they physically walked. During the pre-test, several participants mentioned that they noticed a redirection in terms of “something strange happened”. However, they could not detect reliably at which side of the path they walked. The main reason was that participants adapted to the redirection and walked on the virtual path, which made it hard for them to estimate on which side of the path they are located in the real world. Therefore, we explained to them that they needed to focus on the direction in which the VE turned, which was easier to identify, and provided us with more conservative detection thresholds.

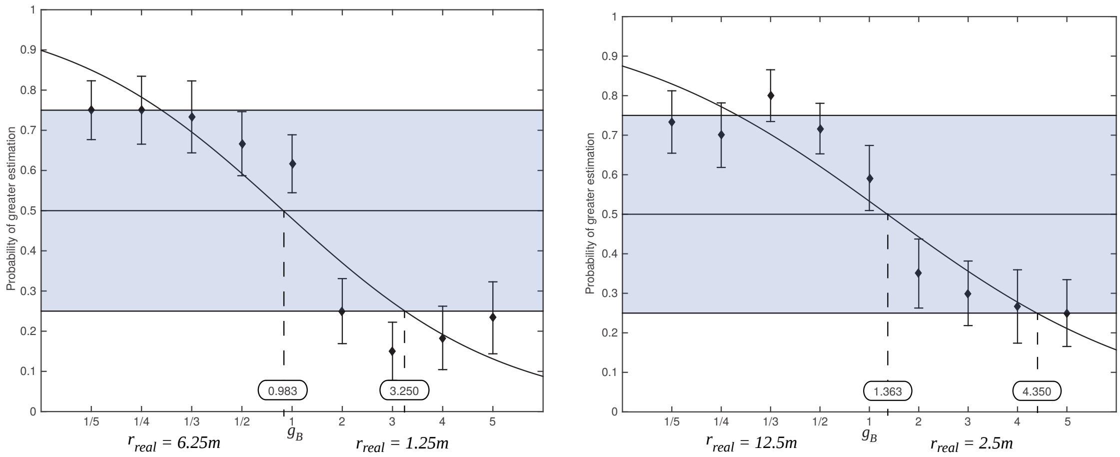

(a) (b)

Figure 8.3: Plotted results of the psychophysical experiment: The x-axis shows the applied bending gains and the y-axis shows the probability of the participants' statement that they walked on a greater circle in the real world. The psychometric function shows PSE and lower detection threshold for bending gains that are applied to $r_{real} = 1.25$m (a) and $r_{real} = 2.5$m (b). Results for $g_B \leq 1$ are applied to $r_{real} = 6.25$m (a) and $r_{real} = 12.5$m (b) and are also plotted but of less interest in this experiment, in which we mainly focus on the potential to reduce the circular path radius in the real world.

8.6 Results

Figure 8.3 shows the pooled results over all participants for the real radii of 1.25m and 6.25m (see Figure 8.3 (a)) and 2.5m and 12.5m (see Figure 8.3 (b)). In Figure 8.3 (a), the gains $g_B \geq 1$ were applied to $r_{real} = 1.25$m and the gains $g_B \leq 1$ were applied to $r_{real} = 6.25$m. In Figure 8.3 (b), the gains $g_B \geq 1$ were applied to $r_{real} = 2.5$m and the gains $g_B \leq 1$ were applied to $r_{real} = 12.5$m. As described in Section 8.2 we are mainly interested in the lower detection thresholds because we focus on gains that enlarge the virtual space, i. e., gains $g_B \geq 1$. As stated in Section 8.5, these gains $g_B < 1$ were exclusively set up for the experiment so that participants would experience the same number of increased and decreased bending conditions.

The x-axes of the plots in Figure 8.3 show the applied bending gains $g_B \in \{\frac{1}{5}, \frac{1}{4}, \frac{1}{3}, \frac{1}{2}, 1, 2, 3, 4, 5\}$. The y-axes show the probability of the participants' statements that they walked on a curve with a larger radius in the real world. For each gain, the mean and standard error bars are displayed in the plot. Each plot was fitted with a Weibull logistic psychometric function [Kle01], which determines the PSE and detection threshold.

The PSE in Figure 8.3 (a) is 0.983 and the lower bound threshold is determined at 3.25. In Figure 8.3 (b), the PSE is 1.363 and the lower bound threshold is determined at 4.35.

The results of the experiment show that it is possible to apply bending gains of approximately 3.5 without users being able to reliably identify discrepancies between the bending of the curve in the real world and virtual environment. In particular, the detection thresholds suggest that a virtual curvature can be bent up to 4.35 times its radius in the real world. This means, a curvature in the real world with a radius of r_{real}= 2.5m can be mapped to a virtual curvature with the radius $r_{virtual}$=2.5m $\cdot$4.35 = 10.875. And a curvature with a radius of r_{real}=1.25m can be mapped to a virtual curvature with the radius $r_{virtual}$=1.25m$\cdot$3.25=4.0625. In contrast to previous findings described in [Net+12; Pal+16; Ste+10b], these range of gains provide much greater unnoticeable redirection possibilties than achievable by other subtle and continuous redirection methods. Moreover, the results suggest that the greater r_{real} is the greater gains can be applied without users being aware of the redirection.

8.7 Conclusion

In this chapter, we defined bending gains and presented a psychophysical experiment in which we analyzed the human sensitivity to discrepancies between the bending of curved paths in the real world and a curved path in the virtual environment. We found that users are less aware of redirection manipulations while walking on curved paths in contrast to traditional redirected walking with curvature gains, when users walk straight in the VE.

9. SENSITIVITY TO REDIRECTION WITH TDCS

9.1 Motivation

It has been a long-term vision to create more realistic experiences by connecting VR directly to the brain. This way, thoughts of the user could be read without detours and leveraged to control the VR system or manipulate the virtual world. Through so-called Brain-Computer Interfaces (BCI), VR could become a more natural experience for users, with the potential to significantly impact a variety of fields ranging from video games to medicine. Recent advances in machine learning and BCI combined with the development of inexpensive wearable sensors has made practical the interaction of users with computers and mobile devices through brain electroencephalography (EEG) signals [TN10; Wol+02]. This is already moving quickly to become widely available as the sensor technology is becoming more economical. Also there exists some first steps of using BCI for VR [BB00; Léc+08]. The intersection of these two technologies, VR and BCI, is the topic of this chapter. But while EEG denotes the ability to *read* electrical activity of the brain, we present a method to *write* to the human brain, i. e., to use electrical signals to stimulate the activity of the brain.

In this context, transcranial direct current stimulation (tDCS) is meanwhile a widely employed technique to modify cortical excitability and activity. The underlying concept of applying such a relatively weak current to the scalp is that it can facilitate or suppress ongoing neuronal activity without affecting non-active neuronal networks [SAN18]. To the best of our knowledge, tDCS has not been applied to RDW so far. Since it was shown that the cognitive activity underlying RDW can interact with cognitive abilities required for working memory [BLS15] and both, egocentric as well as allocentric, reference systems of spatial navigation are presumably involved in RDW, we aimed to apply tDCS in such a way as affect these brain functions. The goal was to achieve positive effects on RDW performance, i. e., to enlarge the walkable VE and improve the overall VR experience. Our hypothesis is that tDCS can lower the abilities of spatial cognition and, therefore, higher redirection gains might be applied without being consciously perceived by the user. This would lead to wider detection thresholds and a reduction of the space requirements for unlimited walking in VR. Moreover, this stimulation might also have an effect on cyber sickness and the sense of presence in VR.

The remainder of this chapter is structured as follows. Section 9.2 discusses background information on RDW and tDCS. Section 9.3 presents the experimental procedure and methods on tDCS application during RDW in VR. Section 9.4 discusses our findings. Section 9.5 concludes the chapter and gives an outlook on future work.

9.2 Background

Using electrical stimulations for RDW is a promising approach. For example, galvanic vestibular stimulation is a technology that uses electrical stimulation via electrodes placed on the mastoid bones behind each ear to stimulate the vestibular system. Sra et al. implemented a VR game based on galvanic vestibular stimulation for redirection of the players [SXM17].

TDCS is a non-invasive stimulation technique and its application to the respective cortical area has been shown to modulate spontaneous brain excitability and activity, for example, anodal stimulation typically increases whereas cathodal stimulation decreases excitability [NP00]. Recent studies have established that tDCS can affect not only the stimulated region but also functional network [Ant+12; Kee+11; Web+14]. The use of tDCS together with VR has been receiving increased attention, primarily due to its potential therapeutic use in neurological disoders [Mas+17]. However, the effect of tDCS on RDW is scarcely known. Previous studies have shown that a widespread parietal-prefrontocortical network underlies spatial navigation, whereby the prefrontal cortex is particularly relevant for information processing relative to the target of navigation [Bla+16; BBB07; Eps08; Ito+15; Spi08; SM06]. More specifically, spatial navigation can involve, to different extents, egocentric and allocentric reference system components as well as higher cognitive limbic and cortical processes [BBB07; TVY13]. Thus, there is a wide range of brain regions, of which stimulation may affect redirected walking. While a proper exploration of all regions is beyond the scope of this investigation, here we placed the cathode over the right prefrontal cortex (AF4) and the anode over the parietal cortex (Pz). Stimulation at these regions has been shown to affect spatial navigation, and modulate effective connectivity during spatial navigation [HBH14]. Cathodal stimulation over the occipital region was not targeted here as this region is relevant for the processing of large field motion, a function definitely required for movement within the VE [Dup+97].

9.3 Experiment

In this experiment, we evaluated the effect of tDCS on RDW as well as on other important parameters like cyber sickness and presence. In particular, we analyzed bending gains for this experiment as presented in Chapter 8.

Due to the interdisciplinary nature of our approach combining neurostimulation and VR, the experiment was approved by two ethics commissions: The ethics commission of Universität zu Lübeck, which evaluated the use of tDCS and the ethics commission of Department of Informatics, Universität Hamburg, which evaluated the use of immersive technology.

9.3.1 Participants

Eligible for participation in the experiment were non-smoking and healthy subjects between 18 and 40 years who were free of medication (except oral contraceptives). Females were only permitted to participate if they took oral contraceptives since it is reported that hormonal fluctuation could impact the effect of tDCS [Tom+14]. Furthermore, pregnant women, subjects with a pacemaker, any history of epileptic seizures, childhood absence epilepsy or migraine, and people with brain injuries or any known disorder of the central nervous or cardiovascular system were not permitted to take part in the experiment. Participants were instructed not to take caffeine, alcohol, drugs, or medicine (except oral contraceptives) on the days of the experiment.

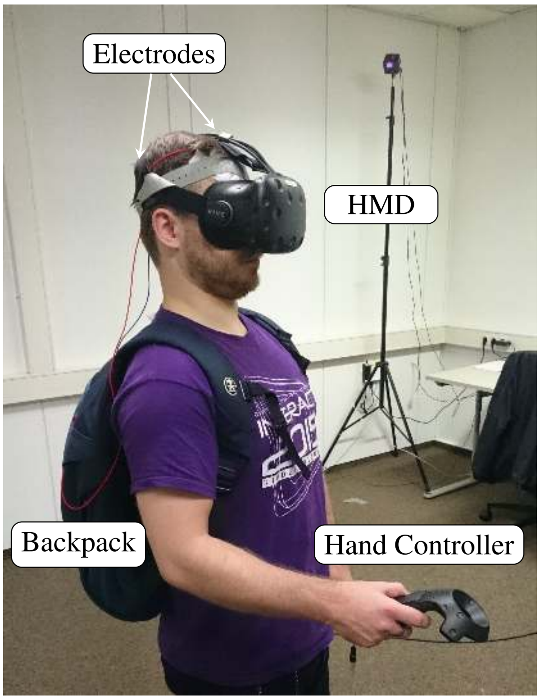

(a)

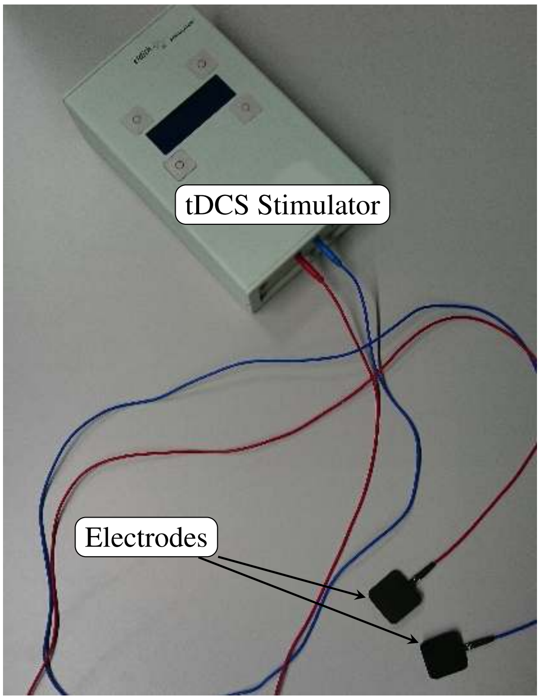

(b)

Figure 9.1: The experimental setup: a user is wearing the HTC Vive HMD, a hand controller for input, two electrodes at the head, and a backpack for the tDCS stimulator (a). The tDCS stimulator and the electrodes in detail (b).

The experiment was completed by 34 subjects (3 female and 31 male, ages 19–36 years, $M = 24$). One participant of the initial 35 had dropped out due to non-experiment related sickness. For the analysis, we had to exclude four additional participants due to sickness or because they took medicine. Thus 30 participants entered the analyses. This number of participants is sufficient for our estimated effect size of $d = .8$ ($p = .05$). The participants were students, who obtained class credits, or professionals at the local Department of Informatics. The body height of the participants varied between 1.68–1.97 m ($M = 1.82$ m, $SD = 0.07$ m).

All of our participants had normal or corrected-to-normal vision. Ten participants wore glasses during the experiment and one wore contact lenses. None of our participants reported having any disorder of equilibrium. One participant reported having a dyschromatopsia, one a strong eye dominance, one a deuteranomaly, and one an amblyopia. None of these disorders were considered sufficient to exclude any subject from the analysis. No other vision disorders were reported by our participants. To determine the eye dominance, the thumb test was conducted. Participants had to extend one arm out and holding the thumb of that hand in an upright position while keeping both eyes open and focused on a distant object. Then, they superimposed their thumb on that object and alternately closed one eye at a time. According to this test, 18 participants had a right eye dominance and 12 had a left eye dominance. All participants were right handed.

All participants had used HMDs before. Their average experience with HMDs was $M = 3.25$ ($SD = 1.06$, in a range of 1 = no experience to 5 = much experience). The experience of the participants with 3D stereoscopic displays (cinema, games etc.) in a range of 1 (no experience) to 5 (much experience) was $M = 3.15$ ($SD = 1.18$). Most of them had some experience with 3D computer games ($M = 3.71$, $SD = 1.60$, in a range of 1 = no experience to 5 = much experience) and they usually played 8.31 hours per week on average ($SD = 6.88$).

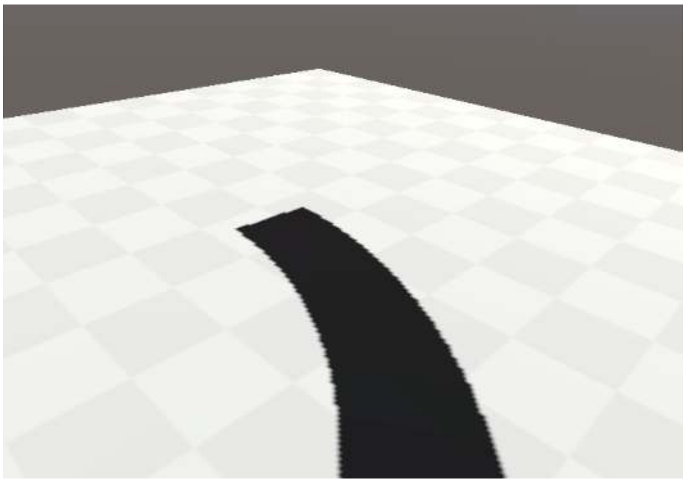

Figure 9.2: Illustration of the virtual environment shown to the participant. The curved path was part of a circle with the radius of 3m and had a length of 4m.

9.3.2 Materials

The experiment took place in a 5m $\times$ 7m laboratory room. We instructed the participants to wear an HTC Vive HMD (see Figure 9.1a), which provides a resolution of 1080 $\times$ 1200 pixels per eye with an approximately 110° diagonal field of view and a refresh rate of 90 Hz. Positional tracking was done by a Lighthouse tracking system that is delivered with the HTC Vive. The Lighthouse system was calibrated so that there was an available walking space of 4m $\times$ 4m. The participants received instructions on slides presented on the HMD. An HTC Vive controller served as an input device via which the participants provided responses during the experiment. The participants wore a backpack during the experiment which contained the tDCS stimulator. For rendering, system control, and logging we used an Intel computer with 3.5 GHz Core i7 processor, 32 GB of main memory and two Nvidia Geforce GTX 980 graphics cards. The VE was rendered using the Unity3D engine 2017.1 and showed a curved path in front of the participant (see Figure 9.2). The path was computed by first calculating a circle with a radius of 3m and then drawing only that part of the circle that started at the virtual camera position and ended after 4m. Dependent on the current condition, the path was curved to the right or to the left. Hence, the center point of the circle was to the left or to the right of the virtual camera position.

TDCS was delivered using a commercial stimulator (Eldith DC Stimulator, Neuroconn GmbH, Ilmenau, Germany) via a pair of square rubber electrodes (3 x 3 cm; see Figure 9.1 b). The cathode electrode was placed over AF4 while the anode was placed over Pz (according to the international 10-20 system for EEG electrode placement). Following disinfection the stimulation sites were prepared using an abrasive gel. Thereafter a conductive adhesive paste (EC2, Natus, Middleton, USA) was spread evenly across the electrodes and attached to the AF4 and Pz scalp locations (international 10:20 system). A current strength of 1.25 mA was applied. Further details are given in 3.3.1. Procedure.

9.3.3 Methods

We used a 5 $\times$ 8 $\times$ 2 full-factorial within-subjects experimental design. We tested 5 different gains $g_B \in \{\frac{3}{2.59}, \frac{3}{2.28}, \frac{3}{2.04}, \frac{3}{1.84}, \frac{3}{1.68}\}$ (the real radius varied while the virtual radius always stayed 3m) which correspond to actual rotations of $3°/m$, $6°/m$, $9°/m$, $12°/m$, and $15°/m$. Each gain was repeated 8 times: 4 times with a left curve and 4 times with a right curve. Participants had to complete 2 sessions: one session with tDCS and one without (Sham). In total, the participants completed $5 \times 8 = 40$ trials per session. All trials in one session were randomized.

These gains were chosen based on previous work as described in Rietzler et al. who reported detection thresholds around $5.5^\circ/m$ for bending gains and recommended to use gains that scale in a linear way with the perceived manipulation [Rie+18].

Procedure

The two sessions were carried out on different days separated by at least one week. On both days subjects participated at the identical time of day. The procedure of both sessions was the same so that participants were blinded as to which session stimulation was conducted. The order of conditions was counterbalanced across subjects, i. e., half of the participants started with the tDCS condition, the other half with sham.

Before the experiment, all participants filled out informed consent forms and received detailed instructions about the experiment and on how to perform the experimental task. Furthermore, they filled out a questionnaire about their experiences with VR, stereoscopic displays, and games, a handedness questionnaire, a questionnaire about vision impairments, and a general questionnaire about diseases, medication, and sleeping habits.

Before each session, participants filled out the Simulator Sickness Questionnaire (SSQ) [Ken+93]. Subsequently, in the tDCS as well as sham condition electrodes were applied using the gel and paste.

Participants completed four training trials before the actual experimental trials. After the training trials and the subject had returned to the start position, the stimulation was turned on for 1200s (20 minutes) in the tDCS condition, which included a 30 seconds ramp up and down period at the beginning and end of the stimulation, respectively. In the sham condition, currents were only ramped up and down for 30 seconds at the beginning of the session. After these 30 seconds no stimulation was applied.

For each trial, participants were instructed to walk along the virtual path shown in the VE. When they reached the end of the path, they had to press a button on the controller, turn around, and walk back to the beginning of the path. In one of these walking directions a bending gain was applied as explained in Section 9.3.3. After the participants reached the beginning of the path again, they pressed a button on the controller and had to answer the displayed question using the touchpad of the controller (see Section 9.3.3). Afterwards, participants were guided to the next start position in the laboratory by displaying a 2D compass and distance metrics in the HMD. By using this method, the participants were kept unaware of their position and orientation in the real world. This, they could not use this information to identify the amount of redirection that was applied. The next trial started once participants reached the new initial position and indicated that they were ready to start by pressing a button on the controller.

After the session, participants filled out the SSQ again, the Slater-Usoh-Steed (SUS) presence questionnaire [Uso+99b], and a demographic questionnaire, and the electrodes were removed.

The total time per participant for each session, including pre-questionnaires, application of tDCS electrodes, instructions, experiment, breaks, post-questionnaires, and debriefing, was about 120-150 minutes, out of which around 25 minutes were spent in VR.

Two-Alternative Forced-Choice Task

To measure the amount of deviation that is unnoticeable, we used a 2AFC task (see Chapter 2.1.3). In our case, using bending gains, previous experiments showed that participants had serious problems in identifying on which side of the virtual path they physically walked. For instance, participants mentioned that they noticed a redirection in terms of “something strange happened” but could not detect reliably at which side of the path they walked (see Chapter 8). This is because participants adapted to the redirection and walked on the virtual path, which made it hard for them to estimate on which side of the path they are located in the real world. Another method

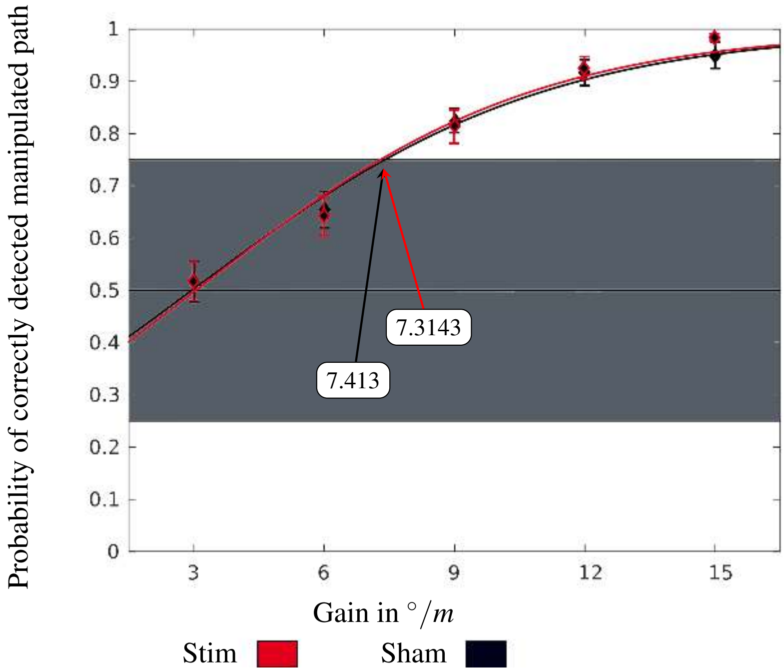

Figure 9.3: The pooled results of the 2AFC task over all participants. The x-axis shows the applied gain in degrees per meter. The y-axis shows the probability of correctly detecting the manipulated path. Results of the sham condition are plotted in black and results of the tDCS condition are plotted in red. For each gain, the mean and standard error bars are displayed.

was introduced to the RDW community, which seems to produce more stable results for bending gains [Rie+18].

According to this method, participants walk two times the same path while only one of the paths is manipulated. Then, the following question is displayed: *"Which path was manipulated?"*. They have two answer options *"First (There)"* or *"Second (Back)"*. Answers like "I don't know" are not allowed. Instead, the participants have to choose one option randomly and will be correct in 50% of the cases on average.

9.3.4 Results

In this section, we describe the results for the 2AFC task, subjective estimates of cyber sickness and presence, and the additional questionnaires responses.

Where appropriate, we analyzed the results with a t-test at the 5% significance level. In cases in which a Shapiro-Wilk test revealed that the data is not normally distributed, we analyzed the results with a Wilcoxon test at the 5% significance level.

Detection Thresholds

Figure 9.3 shows the pooled results of the 2AFC task over all participants. The x-axis shows the applied gain in degrees per meter. The y-axis shows the probability of correctly detecting the manipulated path. Results of the sham condition are plotted in black and results of the tDCS condition are plotted in red. For each gain, the mean and standard error bars are displayed. Each curve was fitted with a sigmoidal psychometric function which determines the DT. In the tDCS condition, the DT is at $7.3143°/m$. In the sham condition, the DT is at $7.413°/m$.

Additionally to these pooled results over all participants, we calculated individual plots and DTs for each participant (see table 9.1). These DTs were used to perform a significance test in order to compare the thresholds between sham and tDCS condition. We did not find any significant differences ($p = .514$).

Furthermore, we compared the mean probability for each gain between sham and tDCS condition. We did not find any significant differences for the $3°/m$ gain ($p = .927$), the $6°/m$ gain ($p = .848$), the $9°/m$ gain ($p = .812$), or for the $12°/m$ gain ($p = .608$). We found a significant difference for the $15°/m$ gain ($p = .018$), indicating that the mean probability of correctly detecting the manipulated path was higher in the tDCS condition.

Cyber Sickness

In the sham condition, we measured a mean SSQ-score of 11.47 ($SD = 11.98$) before the experiment, and a mean SSQ-score of 17.83 ($SD = 18.5$) after the experiment. In the tDCS condition, we measured a mean SSQ-score of 19.2 ($SD = 12.98$) before the experiment, and a mean SSQ-score of 17.7 ($SD = 19.44$) after the experiment.

We did not find any significant differences between total SSQ-scores before and after the experiment for the sham condition ($p = .162$) and the tDCS condition ($p = .291$). However, we also calculated the scores for the three subsections of the SSQ: oculomotor, nausea, and disorientation. Results are shown in Figure 9.4 (a) and (b). We observed a significant increase of disorientation in the sham condition ($p = .008$) but not in the tDCS condition ($p = .308$). We found a significant decrease of oculomotor sickness symptoms in the tDCS condition ($p = .016$) but not in the sham condition ($p = 1.0$). We did not find any significant differences for nausea in the sham ($p = .142$) or tDCS conditions ($p = .06$).

Presence

The mean SUS-score for the sense of feeling present in the VE was 2.16 ($SD = 1.84$) on a five-point Likert scale in the sham condition and 2.26 ($SD = 1.6$) in the tDCS condition. We did not find any significant differences of SUS-scores between sham and tDCS conditions ($p = .729$).

Additional Questionnaires

When the participants were asked *"Did you feel a stimulation during this session?"* at the end of each session, two participants answered yes after sham condition and three participants after the tDCS condition. Other than on these few sessions, subjects did not report on having felt the stimulation.

When the participants were asked *"Do you think that this session was the session with stimulation or without?"* after the sham condition, 14 participants said *"Sham"* and 6 *"Stimulation"* (the rest did not know). After the tDCS condition, 9 participants said *"Sham"* and 8 *"Stimulation."*

On average participants spent 24.3 minutes ($SD = 4.4$) for all experiment trials. In the tDCS condition, it was 23.7 minutes ($SD = 4.3$), and, in the sham condition, it was 24.9 minutes ($SD = 4.5$).

We did not find any significant difference between the duration of sham and tDCS conditions ($p = .295$).

9.4 Discussion

The working hypothesis of the present experiment was that cathodal tDCS over the prefrontal cortex would have a significant effect on RDW performance. Based on our power analysis, we designed the experiment and 2AFC task accordingly. Unfortunately, this hypothesis was not supported by our results: Overall, the detection thresholds for the sham and tDCS conditions did not reveal any significant differences. As discussed below one reason may be that our tDCS protocol did not sufficiently target the involved brain regions. Although, it cannot be excluded that tDCS is inadequate to affect RDW performance, it would be premature at this stage to draw such a conclusion.

In fact, we did find an effect of tDCS for the highest redirection gain, i. e., when redirection was the strongest. This effect indicates it was easier for the participants to detect the redirection in the tDCS condition. Thus the effect was opposite to that of our working hypotheses. There are at least two conclusions to be drawn from the experimental results. Firstly, the distribution of cortical activity specifically involved in our RDW task, which involved in conflicted proprioceptve, vestibular and visual sensation [BLS15], is scarcely known. Thus, although we intended to suppress excitability in the prefrontocortical network relative to the parietal network, and thereby subdue perceived deviation between real and virtual pathways, this may have not been the optimal strategy. Based on our results, a better strategy may have been to relatively suppress the parietal network, as the direction of effects was contrary to our hypotheses. Interestingly, since a facilitated detection of deviance between virtual and real paths occurred with an anodal return current over Pz, and anodal tDCS is typically associated with enhancing excitability, our findings might carefully be taken to suggest a relevance of parietal networks in detecting RDW. Nonetheless, further investigations along these lines are needed. Egocentric navigation has been associated with egocentric representations

Participant ID	**DT (Sham)**	**DT (tDCS)**
0	10.63	9.44
1	6.50	7.66
2	8.77	7.27
3	6.66	6.66
4	8.94	9.00
5	7.78	10.05
6	9.24	5.48
7	5.44	7.81
8	10.07	9.10
9	3.12	4.55
10	7.72	8.77
11	7.10	7.68
12	6.14	6.23
13	3.11	3.03
14	3.66	3.02
16	5.07	4.27
17	7.08	5.39
20	7.20	7.07
22	6.47	9.39
23	4.41	12.58
24	3.19	5.48
25	6.29	7.41
26	10.31	14.78
28	6.95	8.34
29	8.51	3.79
30	5.29	6.29
31	3.11	3.03
32	8.17	15.26
34	6.84	6.52

Table 9.1: Individual detection thresholds for each participant in the sham and tDCS conditions in $^{\circ}/m$. No significant differences between sham and tDCS were found.

in the parietal cortex (precuneus and cuneus, inferior parietal lobe [Col+17; NBG17]), yet these structures lie deeper than the presumed primary cortical target area of stimulation. Thus a direct effect of Pz stimulation cannot be simply concluded.

Secondly, the finding that tDCS was efficient only when redirection was strongest suggests that efficacy of tDCS requires a comparatively high cognitive, in which a high cognitive load has been shown for such high redirection gains [BLS15]. It could be speculated that only conditions of high cognitive load would enable endogenous cortical activity to emerge to a sufficient level as to be modified by the subtle effects of tDCS. A higher current density was not used in the present study in order to blind subjects as to the tDCS and sham sessions, which employed only two stimulation sites. This problem may in the future be circumvented by the use of multiple stimulation electrodes. Further experiments will reveal whether stimulation of the opposite polarity may thus indeed suppress detection of path deviation.

Furthermore, we found very interesting results for the influence of tDCS on features of cyber sickness. Oculomotor sickness symptoms, which includes fatigue, headache, eye strain, and difficulty concentrating, decreased during the tDCS session as compared to baseline. In contrast, disorientation, which includes symptoms like fullness of head, blurred vision, vertigo, and dizzy, increased during the sham, but not during the tDCS session. These findings show that our tDCS protocol counteracted cyber sickness symptoms in VR, and support results of another study, in which anodal tDCS applied at the temporoparietal junction ameliorated subjective disorientation symptoms possibly by affecting the visual-vestibular system function [Tak+18].

To our best knowledge, these are the first results indicating potential effects of tDCS on locomotion and interaction in VR, which we believe are highly interesting for this field to be studied in more detail in future work.

9.5 Conclusion

In this chapter, we presented a sychophysical experiment using tDCS to change the sensitivity to RDW manipulations. In the stimulation conditon 1.25 mA cathodal tDCS were applid over the prefrontal cortex (AF4 with Pz for the return current) for 20 minutes. Although, our results do not show a strong effect of tDCS on detection thresholds for low and medium redirection gains, the experiment revealed an interesting effect for strong gains, which might suggest an interaction between tDCS and cognitive load in VR. Moreover, our results showed interesting insights into the general use of tDCS in VR. For instance, it might be possible to reduce cyber sickness symptoms during VR exposure with tDCS.

While this chapter presents the first results on the use of tDCS in the scope of locomotion and interaction in VR, we see much potential in extending this line of research in the area of neurostimulation in VR.

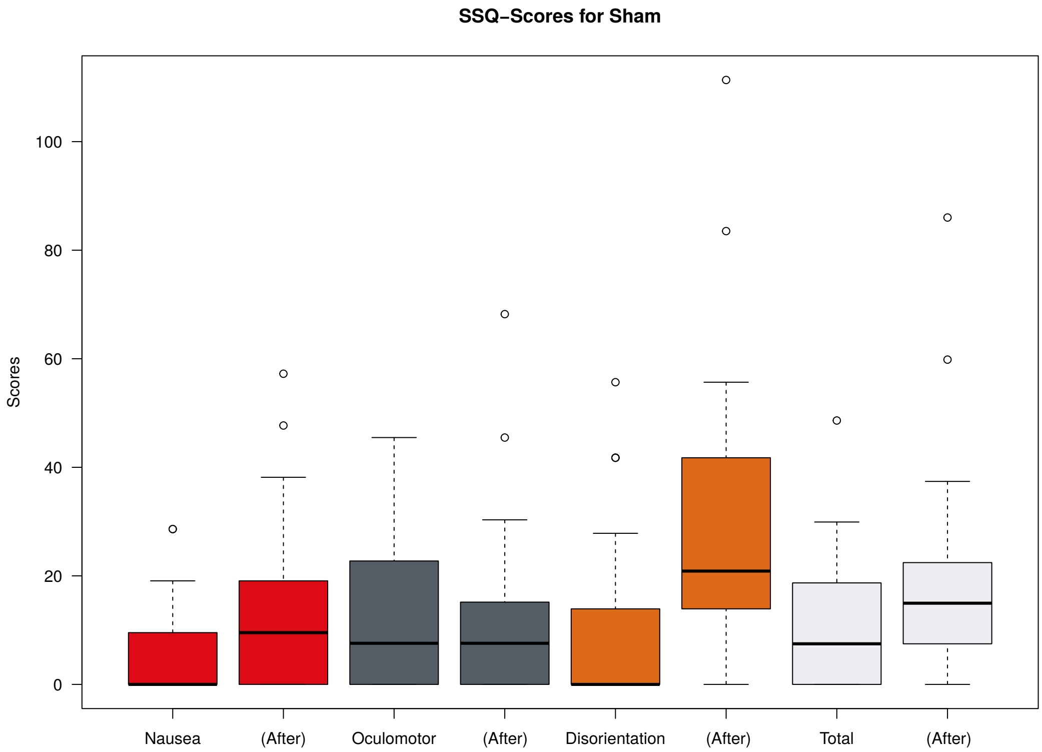

(a)

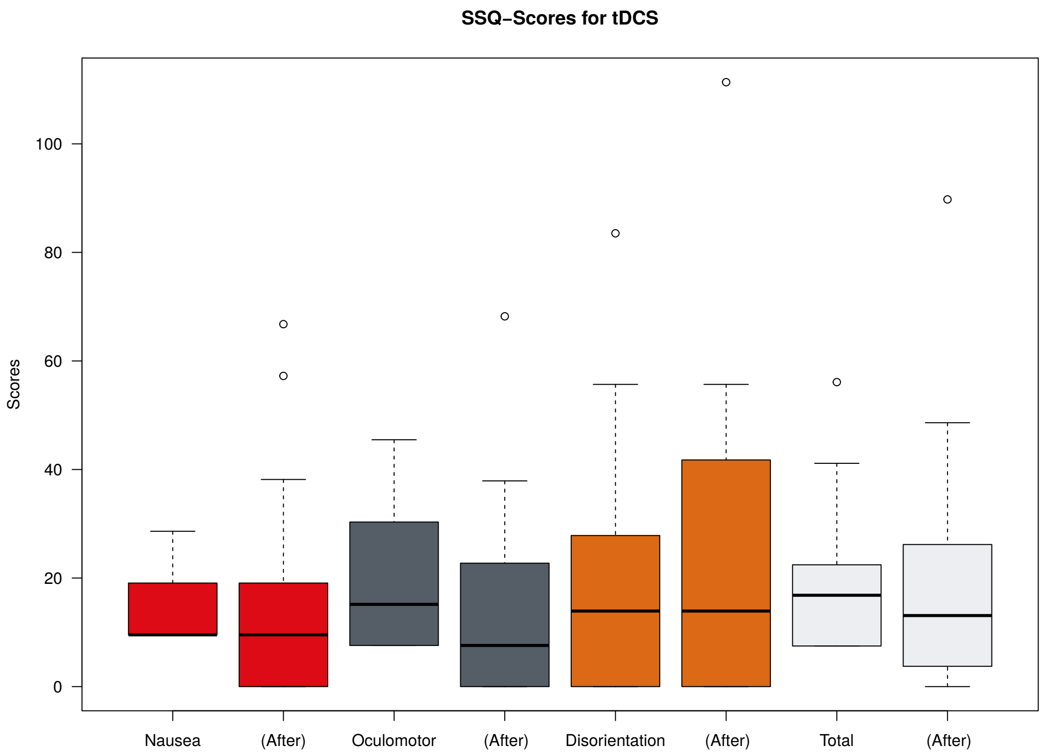

(b)

Figure 9.4: SSQ scores before and after the experiment for oculomotor, nausea, and disorientation in the sham condition (a) and in the tDCS condition (b).

10. SENSITIVITY TO REDIRECTION DURING EYE BLINKS

10.1 Motivation

Psychophysical experiments have shown that RDW is undetectable and thus basically equivalent to real walking in terms of vestibular, proprioceptive, and visual feedback if a tracked physical 45 m $\times$ 45 m walking area is available [Ste+10b]. We have already shown that these thresholds may vary under different conditions (see Chapter 7 and Chapter 8).

While advances to reduce these spatial requirements have also been made by other researchers [Azm+16b; HBT14; NHK14; Sum+15], they are dwarfed by the demands in the gaming and entertainment fields. For instance, HTC and Valve follow the design paradigm *Room-Scale VR*, postulating that all VR experiences should be possible within the circa 4 m $\times$ 4 m walking area of a typical living room. Hence, there is a strong need for orthogonal concepts that can be integrated into RDW systems without tapping into the same perceptual processes.

Traditional RDW works by introducing slight continuous rotations and/or translations each rendering frame, which ideally are unnoticeable for the user. In contrast, in this chapter we focus on an approach that is *orthogonal* to this main line of RDW research. Instead of inducing slight manipulations in each frame, our concept is based on the approach to induce large manipulations in those frames when visual input is suppressed. Due to the orthogonal nature, both approaches could potentially be combined.

Human vision is suppressed during natural motor processes such as eye blinks and saccades, which occur infrequently, but accumulate to humans being functionally blind for about 10% of the time during waking hours [Joh+09]. These visual interruptions are responsible for a cognitive phenomenon called *change blindness*, which describes the inability to notice even large changes during brief moments of missing visual input [SL97]. We believe that this constitutes potential, since the combination of an eye tracker and a VR system allow for undetectable changes, which could be used, e. g., to significantly improve RDW. While traditional RDW is only unnoticeable for rotations of 1-3 degrees per second when users are walking at their preferred speed [Raz05; Ste+10b], the results of our approach show that we can induce additional 5 degrees during *eye blinks* that happen every 4–19 seconds (see Figure 10.1).

In this chapter, we show that visual change during eye blinks is (i) a useful and versatile

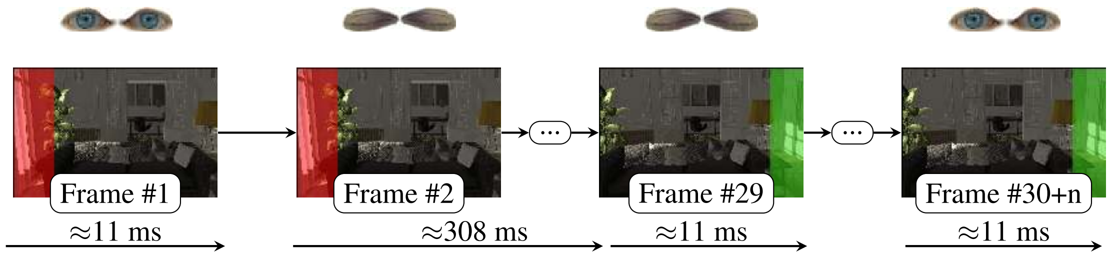

Figure 10.1: Illustration of synchronizing the human visual processes with the computer graphics rendering system: On the top, a blink of the user is represented, and below, the frames that are displayed on the HMD are presented. In this illustration, we assume a framerate of 90 frames per second, i. e., one frame lasts approximately 11 ms. When the eyes are closed for at least 300 ms (28 frames $\approx$ 308 ms), the blink is detected and the virtual viewpoint is rotated around the up-axis. The user might keep the eyes closed a few frames longer. The green areas mark the region that is newly visible after the rotation. The red areas mark the region that is not visible anymore.

concept for perceptually-inspired locomotion in VR and (ii) easy to integrate in current-state HMDs and rendering systems, (iii) we empirically evaluate the amount of visual change, which can be induced during eye blinks, in two psychophysical experiments, and (iv) discuss the implications for practitioners in different fields.

The remainder of this chapter is structured as follows. Section 10.2 introduces background information about eye blinks and change blindness. Section 10.3 describes the both psychophysical experiments, which we conducted to identify detection thresholds for visual changes during eye blinks. Section 10.4 discusses application scenarios for movements during eye blinks and Section 10.5 reports the confirmatory study. Section 10.6 discusses our results and Section 10.7 concludes the chapter.

10.2 Background

In this section we first provide background information on human eye blinks, followed by an explanation of change blindness illusions and how they relate to eye blinks, and finally we discuss how our approach extends the work on RDW.

10.2.1 Eye Blinks and Visual Suppression

Eye blinks are characterized by a rapid closing and opening of the eyelid with durations of 100–400 ms, depending on the situation and cause of the eye blink [Mos81; Ram08; Rel06]. Apart from the motor process of eyelid movements that prevents light from reaching the retina, visual perception is additionally actively suppressed during eye blinks [VRM80]. This suppression of visual input begins before the onset of the blink and lasts until after the blink [Vol86]. Visual awareness is extrapolated across such periods of suppressed visual input such that they are usually not consciously perceived [Bri+05].

Eye blinks can be classified as *voluntary* blinks, which occur, for instance, as a means for communication and social interaction, and *involuntary* blinks, which occur in semi-regular intervals without conscious control [Fit15]. Causes for the latter include corneal lubrication, reflexes for the protection of the eyes, e. g., due to sudden or rapid visual motions or proximity [Col+89], processing of certain visual stimuli, e. g., bright light [ETP04], vestibulo-palpebral reflexes [Fon61], blink reflexes during gaze movement [Evi+94], and can be learned via eyeblink conditioning [TKK03].

Human eye blinks occur approximately 10–20 times per minute, about every 4–19 seconds [Dou02; LZ06]. Blink frequency can vary between gender and age and is influenced by the current activity. For instance, Sforza, Rango, Galante, Bresolin, and Ferrario found that women blink more often than men, and older women more often than younger women. Hall found differences in blink frequency while reading, and Patel, Henderson, Bradley, Galloway, and Hunter found that the frequency of blinks is greatly reduced when looking at a computer screen. In contrast, Dennison, Wisti, and D'Zmura observed an increased blink frequency when wearing an HMD compared to a non-immersive computer screen, and they suggested that an increased blink frequency is correlated with and potentially caused by increased visual stress and fatigue in VR.

Overall, this rich body of literature on blinks shows that there is a high number of naturally occurring blinks in VR as well as the potential to induce additional blinks due to external stimuli if needed. This illustrates the usefulness and potential impact of the techniques introduced in this chapter.

10.2.2 Change Blindness

Change blindness denotes the inability of human observers to notice significant changes to visual scenes [Kev+00], in particular, during brief phases of visual interruptions such as eye blinks or saccades [Ren02; ROC97]. These visual changes can be of various types and magnitudes. Earlier work focused on artificial stimuli, showing that observers often fail to notice the displacement of a prominent line-drawn object on a computer screen if the change occurs during an eye movement [BHV94]. More recent studies showed that these effects are even stronger with naturalistic and complex stimuli usually found in the real world, such as when a conversation partner is replaced by a different person [SL98] or when the walls and doors around us change position [Ste+11; Sum+10; Sum+12b]. This counter-intuitive result is of special interest; most people firmly (and erroneously) believe that they would notice such large changes of their surroundings [Lev+02; Lev+00].

Change blindness is made possible by a general limitation in the human ability to retain and compare visual information from moment to moment. Early experiments by Rensink, Kevin O'Regan, and Clark found a clear impact of the duration of visual interruptions (called *inter-stimulus intervals*) between scene changes on detection rates, showing that rates were significantly higher for durations of 40 ms compared to 80 ms and 160 ms. This effect could be explained by a brief lapse in human short-term high-capacity iconic memory [Col80; Dic74], which includes a fleeting visual representation of the raw sensory input. When the duration of inter-stimulus intervals exceeds the duration for which the scene pertains in iconic memory, the ability to detect differences in successive scenes is reduced [BPA00; PGM12].

Additionally to these theories about visual memory, change detection is influenced by oculomotor and suppression mechanisms during eye blinks and saccades. According to current theories, the human visual system uses a built-in prior assumption that the world is stable during eye movements. For instance, the perception of displacements of the scene during a saccade is suppressed or, more precisely, thresholds for the detection of a displacement of the current retinal image are elevated when this displacement occurs during an eye movement [BHS75; NCT03].

In summary, eye blinks are a common and natural cause of change blindness. The limited durations of eye blinks (100–400 ms [Mos81; Ram08; Rel06]) require exact timing of visual changes to have a significant effect, which can happen in the real world, e. g., causing accidents while driving [Häk+99], but provide much higher potential in VR as eye blinks can be reliably tracked and registered with computer graphics changes. Moreover, the associated suppression mechanisms indicate large potential in VR as the underlying assumptions of human visual perception do not have to be true in computer graphics virtual worlds.

10.2.3 Orthogonal Approach to RDW

Instead of inducing continuous rotations or translations as in traditional RDW implementations, an orthogonal approach is to introduce discrete manipulations by leveraging change blindness as described above. Early work by Wallis and Bulthoff has indicated that change blindness does not only pertain to changes of objects in the surroundings but can also apply to the observer's own position, orientation, and movement, which suggests applications in RDW. Steinicke, Bruder, Hinrichs, and Willemsen introduced change blindness techniques for stereoscopic VR systems such as projection systems and HMDs [Ste+11] with a focus on changing the position and appearance of individual objects in the scene, whereas camera motions were not considered. Bruder, Pusch, and Steinicke have shown that change blindness can significantly change speed perception in VEs if inter-stimulus intervals are induced by blanking the view for 100 ms. Moreover, Bolte and Lappe found that saccadic eye movements can mask changes in orientation and position. They investigated the sensitivity to rotations in the transverse plane and forward/backward translations during saccades. They found detection thresholds for rotations of ± 5 degrees around the up axis and translations of ± 50 cm along the forward axis. Recent work by Sun, Patney, Wei, Shapira, Lu, Asente, Zhu, McGuire, Luebke, and Kaufman leveraged saccadic eye movements to improve RDW with GPU-based path planning algorithms. However, manipulations during saccades impose very high demands on eye trackers with ultra-high performance eye tracking, rendering and display: it is necessary to detect the saccade onset, predict its length, render a new image, display this image, and hope that the saccade has not ended earlier, which requires low-latency gaze data at circa 2000 Hz refresh rate or more. Bolte and Lappe had to build a research prototype of an electrooculogram to fulfill some of these requirements.

A first attempt to using eye blinks for RDW was done by Ivleva. Eye blinks are much easier to track than saccades (even with commercial off-the-shelf eye trackers integrated in HMDs), less dependent on refresh rate due to the longer blink durations, less fallible to misclassification of blinks, and useful due to both voluntary and involuntary blinks. In this chapter, we document that blink-induced suppression is a useful and versatile method for RDW.

10.3 Psychophysical Experiments

This section describes the experiments we performed to analyze human sensitivity to subtle translations and rotations induced during eye blinks. Both experiments shared a common procedure and a similar setup but they were conducted with different participants.

10.3.1 Experimental Setup

Hardware and Software

We instructed the participants to wear an HTC Vive HMD (see Figure 10.2), which provides a resolution of 1080×1200 pixels per eye with an approximately 110° diagonal field of view and a refresh rate of 90 Hz. Positional and rotational tracking was done by a Lighthouse tracking system that is delivered with the HTC Vive. The participants received task instructions on slides presented on the HMD. An HTC Vive controller served as an input device via which the participants provided responses during the experiment.

The VE was rendered using the Unity3D engine 5.5 and showed an architectural visualization of a living room to the participants of the experiment (see Figure 10.2).

We used an integration of the Pupil Labs eye-tracking device inside the HMD, which includes two 120 Hz infrared cameras and infrared illuminators (see Figure 10.2). The eye-tracking device was connected to the graphics rendering computer via a USB cable and configured using *Pupil Capture* v0.9.12, the software provided by Pupil Labs. During the experiment, eye and gaze data

(a)

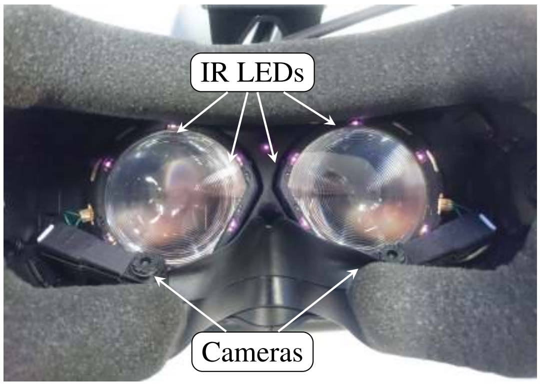

(b)

Figure 10.2: A participant of the experiment wearing the HTC Vive HMD and a hand-controller (inset) and the virtual environment of the experiment, which is an architectural visualization of a living room (a). Inside the HMD, the Pupil Labs eye tracking device was integrated (b). It consists of several infrared LEDs to illuminate the eyes and two cameras to enable stereoscopic tracking.

was sent from Pupil Capture to the Unity3D application permanently via UDP using the Pupil Remote plugin and the Unity3D plugin provided on Github.[1]

Blink Detection

The detection of blinks was implemented in the Unity3D application. In each frame, Pupil Capture provides data about eye and gaze direction, and also a confidence value between 0 and 1 that indicates how likely it is that the eyes were correctly detected. Pupil Labs recommends a confidence value of greater than 0.6.[2] We exploited this confidence interval to detect eye blinks. Based on a pre-test, we identified that if the confidence level was below 0.01 for more than 300ms (see Figure 10.1), chances were very high that this data was caused by an eye blink. For these values we evaluated the performance of the blink detection and measured 120 blinks from 3 different persons (ages $24-36$, $M=30$, 2 male, 1 female). Participants of this test were instructed to blink consciously. When a blink was detected, a note sign appeared in the VE to inform the participants that this blink was detected. Each time a participant blinked consciously but no sign appeared, the participant reported this and it was counted as a false negative. Each time a sign appeared but the participant did not blink consciously, the participant reported this and it was counted as a false positive. The results show a success rate of 83.3% (100 out of 120) blinks that were correctly detected, which means that 16.7% (20 out of 120) blinks were false negatives. Furthermore, participants reported 8.3% (10 out of 120) false positives.

Hence, the above mentioned values appear to be a good estimate to identify eye blinks and we used those in our experiments to trigger the corresponding action, i. e., manipulation of the scene using translation and rotation. During the experiment, a false positive blink could be reported by pressing a button on the controller. Then, their current trial was repeated later and they continued with the next one. A false negative blink did not disturb the experiment since the participants were instructed to blink again until they get the detection notification.

10.3.2 Procedure

When participants arrived, they gave their informed consent and were provided with detailed instructions on how to perform the experimental task. The IPD of the participants was measured

[1] https://github.com/pupil-labs/hmd-eyes
[2] https://docs.pupil-labs.com

and they filled out a questionnaire about vision disorders and experience with VR, games, and stereoscopic imagery, as well as the SSQ [Ken+93].

During the experiment, participants completed several trials one by one (see Sections 10.3.3 and 10.3.4). In each trial, they stood still in the VE and were instructed to blink consciously. When the participants were ready for the next trial (indicated by a button press), the next detected eye blink was used to induce the manipulation. After the detection of a blink the participants' viewpoint in the VE was rotated or translated on one of the three axes (or 3 anatomical planes of the human body): the forward axis (which indicates the viewing direction), the right axis (which is from the left to the right of the participant), and the up axis (which is the inverse gravitation direction).Participants were notified that the blink was detected by a note sign that appeared in the VE in front of them. After two seconds the scene went black and we asked the participants via a slide to indicate in which direction their viewpoint was rotated/translated[3] using a 2AFC task with two possible answers such as "left" or "right", "forward" or "backward", or "up" or "down" depending on the experiment. The two answer options could be chosen by using the touchpad of the controller. Afterwards, the next trial was started.

For each trial, participants saw the VE from a different perspective. Orientations varied between 0 and 350 degrees on the up axis and were chosen by steps of 10 degrees. The position varied between 0 and 10 cm in both directions of the forward or right axis in the transverse plane around a fixed point in the center of the virtual room.

The SSQ was filled out again immediately after the experiment, further the SUS presence questionnaire [Uso+99b], and a demographics questionnaire. Moreover, we asked the participants if they had used any cognitive strategy to fulfill the task. The total time per participant, including pre-questionnaires, instructions, experiment, breaks, post-questionnaires, and debriefing, was $30-45$ minutes. Participants wore the HMD for approximately 25 minutes.

10.3.3 Experiment 1: Reorientation during Eye Blinks

This section describes the first experiment, which we performed to analyze how much rotation of the user's view in VR can be applied during an eye blink without users noticing.

Participants

16 participants (3 female and 13 male, ages 20–35, $M = 27.06$) completed the experiment. The participants were students or professionals at the local department of computer science, who obtained a monetary compensation for their participation. All of our participants had normal or corrected-to-normal vision. One participant wore glasses during the experiment and two wore contact lenses. None of our participants reported a disorder of equilibrium. No other vision disorders have been reported by our participants. 13 participants had some experience with HMDs before. The experience of the participants with 3D stereoscopic displays (cinema, games etc.) in a range of 1 (no experience) to 5 (much experience) was $M = 2.37$ ($SD = 1.63$). Most of them had some experience with 3D computer games ($M = 2.31$, $SD = 1.58$, in a range of 1 = no experience to 5 = much experience) and they usually played 3.1 hours per week on average ($SD = 3.58$). The body height of the participants varied between 1.55–1.83 m ($M = 1.74$ m, $SD = 0.08$ m). The IPD of the participants varied between 5.9–6.9 cm ($M = 6.23$ cm, $SD = 0.25$ cm).

Materials and Methods

We used a 3×11 full-factorial within-subjects experimental design. We had 3 different blocks where we tested rotations on all 3 axes (see Figure 10.3) and with 11 different offsets $\in \{0, \pm 3, \pm 6, \pm 9, \pm 12, \pm 15\}$ degrees. The order of the blocks was counter-balanced. Each condition was repeated 6 times. All trials were randomized. In total, the participants completed $3 \times 11 \times 6 = 198$

[3]This question is equivalent to asking for the direction of the camera manipulation, but pre-tests revealed that it was easier for the participants to judge the manipulation from their egocentric perspective.

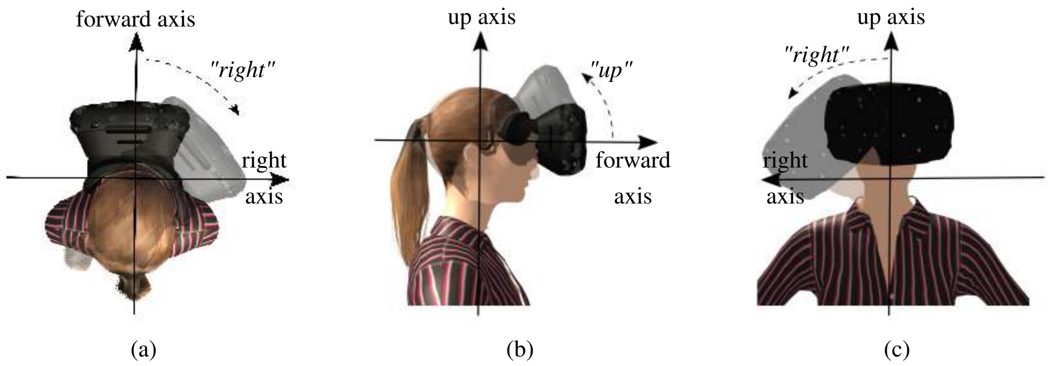

Figure 10.3: Rotations that were caried out during blinking: Around the up axis (also known as *yaw*) (a), the right axis (also known as *pitch*) (b), and the forward axis (also known as *roll*) (c). Only rotations with a positive gain (i. e., $\in \{3, 6, 9, 12, 15\}$ degrees) are shown here. Rotations with a negative gain (i. e., $\in \{-3, -6, -9, -12, -15\}$ degrees) are just in the opposite direction. The view direction before blinking is always straight ahead according to the forward axis. Of course, the view direction in the real world stays the same (the user is not moving physically); this figure just clarifies how the view in the virtual world changes.

trials. Participants completed 6 training trials before each block. They were allowed to abort the experiment at any time and to take breaks at any time between blocks.

We decided on these offsets after initial tests. It turned out that 15 degrees is such a value that could be detected easily by all of the three subjects of this initial test. Hence, we chose it as the greatest offset. Furthermore, the thresholds Bolte et al. found for saccadic suppression [BL15] are in the middle of our range which supports our choice, too.

For rendering, system control, and logging we used a computer with Intel Xeon 2.4 GHz processor and 16 cores, 32 GB of main memory and two Nvidia Geforce GTX 980 Ti graphics cards.

Results

Figure 10.4 shows the pooled results over all participants seperated by block: around the up axis (a), the right axis (b), and the forward axis (c).

In each plot, the x-axes show the applied offset in degrees. The y-axes show the probability of the participants' statement that their view was rotated right or up, respectively. For each offset, the mean and standard error bars are displayed. Each plot was fitted with a sigmoidal psychometric function, which determines the PSE and DTs.

The PSE in Figure 10.4(a) is 0.495, the lower detection threshold is at -4.763 and the upper detection threshold is at 5.780. The PSE in Figure 10.4(b) is -0.245, the lower detection threshold is at -2.358 and the upper detection threshold is at 1.898. The PSE in Figure 10.4(c) is -0.243, the lower detection threshold is at -3.703 and the upper detection threshold is at 3.248.

From the psychometric functions a slight bias for all PSEs was determined. In order to compare the found bias to the offset of 0.0, we performed a one sample t-test per PSE, which did not show any significant differences (Plot 10.4(a): $t = 1.32$, $df = 15$, $p = .21$, Plot 10.4(b): $t = -1.16$, $df = 15$, $p = .26$, Plot 10.4(c): $t = -1.28$, $df = 15$, $p = .22$).

We measured a mean SSQ-score of 11.45 ($SD = 9.41$) before the experiment, and a mean SSQ-score of 32.49 ($SD = 27.98$) after the experiment, which indicates a typical increase in VR sickness symptoms for using an HMD for this duration. The mean SUS score for the sense of feeling present in the VE was 4.66 ($SD = 0.3$) on a seven-point Likert scale, which indicates a mid-high sense of presence.

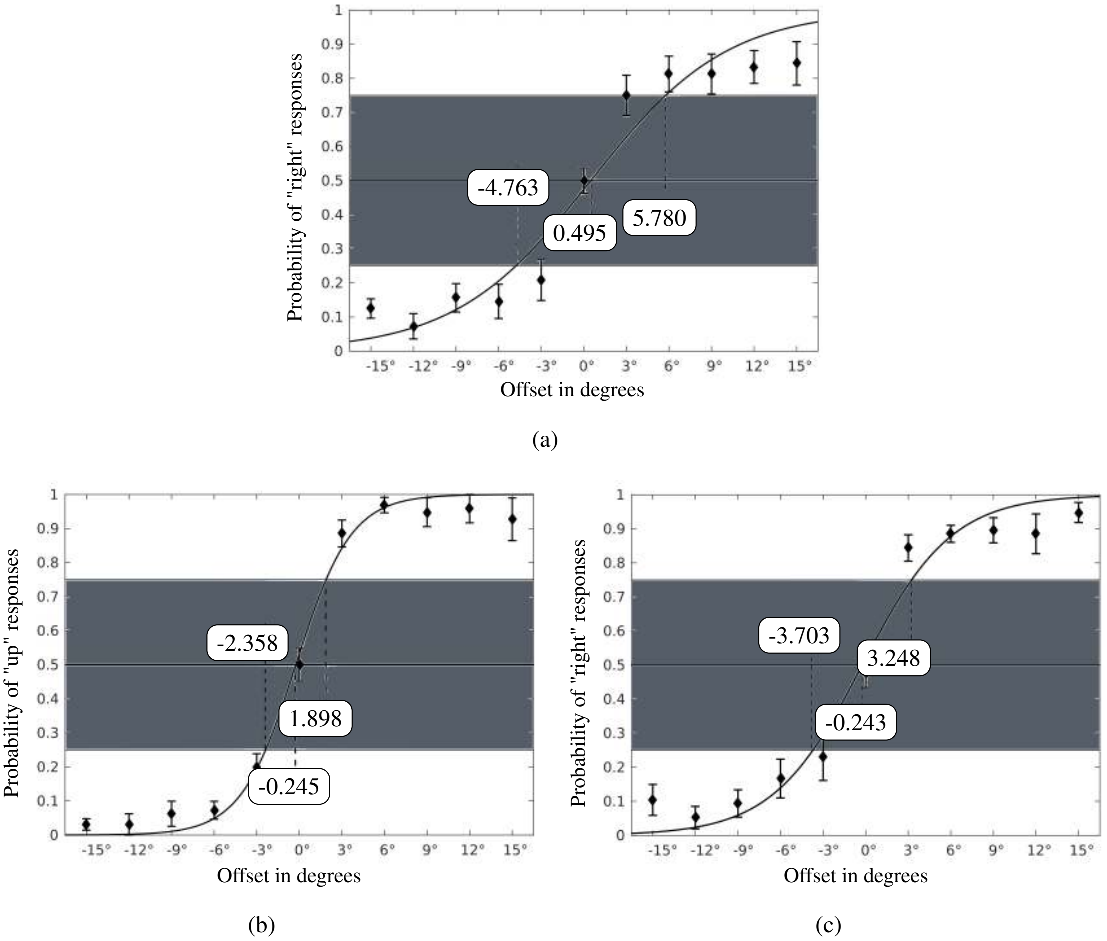

Figure 10.4: The results of the detection thresholds experiment for reorientation during blinking. We plotted one function per block: rotations around the up axis (yaw) (a), rotations around the right axis (pitch) (b), and rotations around the forward axis (roll) (c). The PSEs as well as the lower and upper detection thresholds are highlighted in each plot.

Most of the participants stated that they tried to focus on a certain point or feature in the VE to compare their position before and after blinking.

Discussion

For rotations, our results show detection thresholds of approximately 2–5 degrees. Furthermore, there are differences between the three axes. It appears that rotations around the right axis (pitch) are easier to detect (approximately 2.1 degrees deviation from the PSE) than rotations around the forward axis (roll) (approximately 3.5 degrees deviation from the PSE), and rotations around the up axis (yaw) (approximately 5.3 degrees deviation from the PSE). Rotations around the up axis (yaw) might be more difficult to detect because this is a more natural movement that people are used to do in the real world whereas the other two rotation axes are used less often. Rotations around the up axis are also the most relevant for RDW techniques such as curvature gains.

10.3.4 Experiment 2: Repositioning during Eye Blinks

This section describes the experiment we performed to determine how much unnoticeable translation of the user's view in VR is possible during an eye blink.

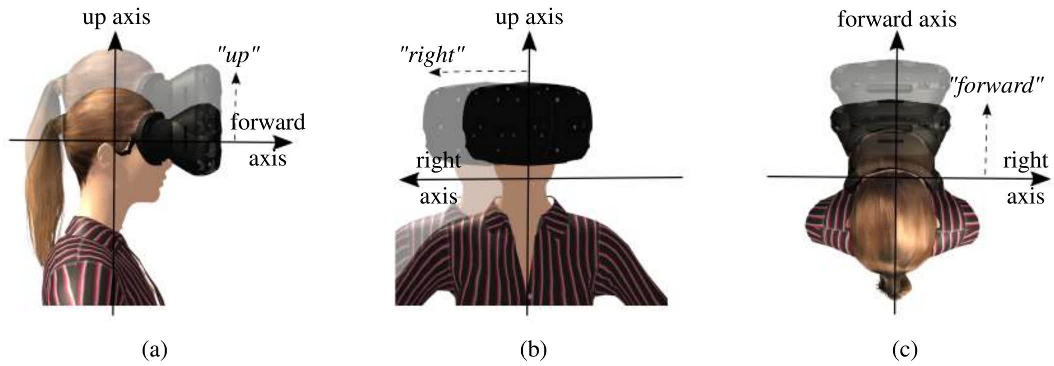

Figure 10.5: Translations that were caried out during blinking: On the up axis (a), the right axis (b), and the forward axis (c). Only translations with a positive gain (i. e., $\in \{3, 6, 9, 12, 15\}$ cm) are shown here. Translations with a negative gain (i. e., $\in \{-3, -6, -9, -12, -15\}$ cm) are just to the opposite direction. The view direction before blinking is always straight ahead according to the forward axis. Of course, the view direction in the real world stays the same (the user is not moving physically); this figure just clarifies how the view in the virtual world changes.

Participants

16 participants (2 female and 14 male, ages 21–38, $M = 28.25$) completed the experiment. The participants were students, who obtained class credits, or professionals at the local department of computer science. All of our participants had normal or corrected-to-normal vision. None of our participants reported a disorder of equilibrium. One of our participants reported an astigmatism (corrected via glasses). No other vision disorders have been reported by our participants. All participants had experienced HMDs before. The experience of the participants with 3D stereoscopic displays (cinema, games etc.) in a range of 1 (no experience) to 5 (much experience) was $M = 3.5$ ($SD = 0.63$). Most of them had experience with 3D computer games ($M = 3.68$, $SD = 0.6$, in a range of 1 = no experience to 5 = much experience) and they usually played 8.6 hours per week on average ($SD = 8.36$). The body height of the participants varied between 1.60–1.85 m ($M = 1.77$ m, $SD = 0.07$ m). The IPD of the participants varied between 5.9–7.6 cm ($M = 6.39$ cm, $SD = 0.43$ cm).

Materials and Methods

We used a 3×11 full-factorial within-subjects experimental design. We had 3 different blocks where we tested translations on all 3 axes (see Figure 10.5) and with 11 different offsets $\in \{0, \pm 3, \pm 6, \pm 9, \pm 12, \pm 15\}$ cm. The order of the blocks was counter-balanced. Each condition was repeated 6 times. All trials were randomized. In total, the participants completed $3 \times 11 \times 6 = 198$ trials. Participants completed 6 training trials before each block. They were allowed to abort the experiment at any time and to take breaks at any time between blocks.

We decided on these offsets after initial tests. The lowest value that could be detected easily by all of the three subjects of this initial test was 15 cm. Hence, we chose it as the greatest offset.

For rendering, system control, and logging we used an Intel computer with 3.5 GHz Core i7 processor, 32 GB of main memory and two Nvidia Geforce GTX 980 graphics cards.

Results

Figure 10.6 shows the pooled results over all participants seperated by block: on the up axis (a), the right axis (b), and the forward axis (c).

In each plot, the x-axes show the applied offset in cm. The y-axes show the probability of the participants' statement that their view was translated right, up, or forward, respectively. For

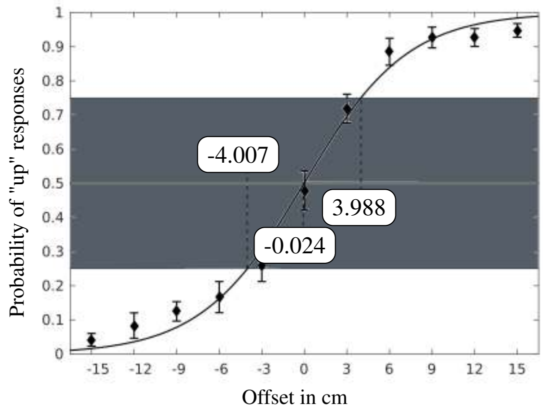

(a)

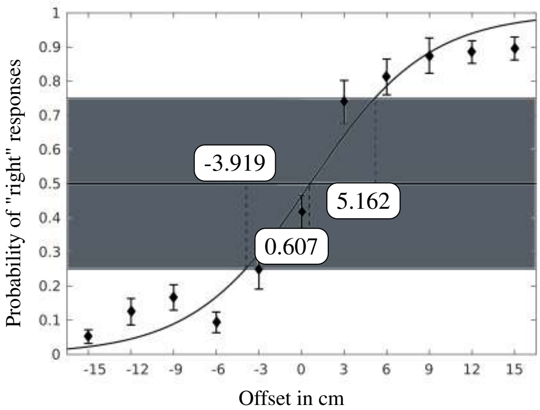

(b)

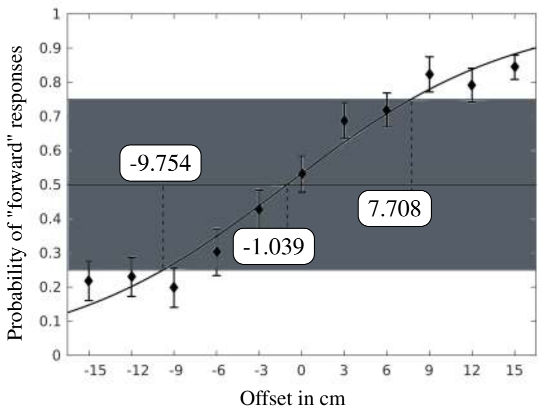

(c)

Figure 10.6: The results of the detection thresholds experiment for repositioning during blinking. We plotted one function per block: translations on the up axis (a), translations on the right axis (b), and translations on the forward axis (c). The PSE as well as the lower and upper detection thresholds are highlighted in each plot.

each offset, the mean and standard error bars are displayed. Each plot was fitted with a sigmoidal psychometric function.

The PSE in Figure 10.6(a) is -0.024 cm, the lower detection threshold is at -4.007 cm and the upper detection threshold is at 3.988 cm. The PSE in Figure 10.6(b) is 0.607 cm, the lower detection threshold is at -3.919 cm and the upper detection threshold is at 5.162 cm. The PSE in Figure 10.6(c) is -1.039 cm, the lower detection threshold is at -9.754 cm and the upper detection threshold is at 7.708 cm.

From the psychometric functions a slight bias for all PSEs was determined. In order to compare the found bias to the offset of 0.0, we performed a one sample t-test per PSE, which did not show any significant differences (Plot 10.6(a): $t = -0.2$, $df = 15$, $p = .84$, Plot 10.6(b): $t = 1.16$, $df = 15$, $p = .26$, Plot 10.6(c): $t = -1.63$, $df = 15$, $p = .12$).

We measured a mean SSQ-score of 7.01 ($SD = 7.34$) before the experiment, and a mean SSQ-score of 23.38 ($SD = 16.36$) after the experiment, which indicates a similar increase in VR sickness symptoms as in the first experiment. The mean SUS score for the sense of feeling present in the VE was 4.85 ($SD = 0.1$) on a seven-point Likert scale, which indicates a similar sense of presence as in the first experiment.

Discussion

For translations, the results revealed detection thresholds of approximately 4–9 cm. Furthermore, there are differences between the three axes. It appears that translations on the up axis (approximately 4 cm deviation from the PSE) and translations on the right axis (approximately 4.5 cm deviation from the PSE) are easier to detect than translations on the forward axis (approximately 8.7 cm deviation from the PSE). The reason for this might be that we are used to walking forward in viewing direction but a movement to the left or right or up or down is less often carried out. This result does not match exactly the results of Bolte et al., who found a detection threshold of 50 cm for translations on the forward axis during saccades [BL15]. This is likely due to the difference between saccades and blinks and could also be affected by the different hardware, especially the HMD, that was used in the experiments. Furthermore, the VE might have an effect. In our experiment, the number of objects in the VE is greater and the distance from the user to some of these objects is smaller. This leads to stronger cues from the environment and more change in the retinal image. However, we also found the trend that translations on the forward axis are less obvious than on the other axes.

10.4 Supplement for Redirection Gains

Translations and rotations during unconscious eye blinks could be used to supplement translation, rotation, curvature or bending gains. The idea is that due to these gains additional unnoticeable redirection can be applied, and thus, redirection has potential to become more effective.

10.4.1 Translation Gain

Steinicke et al. found that a 5m virtual distance can be mapped unnoticeably to a physical distance between 3.96 and 5.81 m [Ste+10b]. If we assume an average walking velocity of a user with an HMD of approximately 1.2 m/s [Moh+07a], we get a total duration of the walk of 3.3 to 4.8 seconds. Again, with one blink every 4 seconds, it appears reasonable to assume that within a 5 m virtual distance, at least one eye blink will occur. This blink can trigger an additional translation of around 0.087 m, which cannot be detected reliably by the user (see Section 10.3). Hence, we can map a 5 m virtual distance to a physical distance between 3.873 m (i. e., $3.96 - 0.087$ m) and 5.897 m (i. e., $5.81 + 0.087$ m), which corresponds to an increase of the range of applicable translations by approximately 10 %.

10.4.2 Rotation Gain

Steinicke et al. found that users can be turned physically about 49% more or 20% less than a perceived virtual 90 degrees rotation without noticing the difference. Hence, a 90 degrees virtual rotation can be mapped unnoticeably to a physical rotation between 134 and 72 degrees [Ste+10b]. If we assume 15 blinks per minute, we get approximately one blink every 4 seconds (see Section 10.1), which might be too low for a rapid head movement. However, it has been shown that saccadic eye movements and rapid head movements tend to be accompanied by blinks [Evi+84]. Therefore, it appears reasonable to assume that if users either slowly or rapidly rotate their head by 90 degrees, chances are high that they will probably perform 1 blink [Evi+84].

This blink can be exploited to trigger another rotation of around 5 degrees, which cannot be detected reliably by the user (see Section 10.3). Hence, we could map a 90 degrees virtual rotation to a physical rotation between 139 and 67 degrees, which corresponds to an increase of the range of applicable rotations by more than 16%.

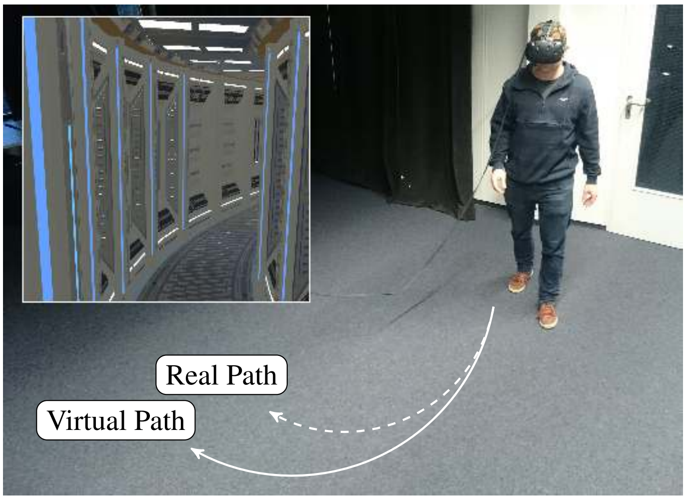

Figure 10.7: A user during the confirmatory study: The bending of the virtual corridor (inset) corresponds to the path marked as *virtual path* while the user actually walks a path in the real world that is bent even more.

10.4.3 Curvature Gain

Steinicke et al. found that a virtual straight path of 5 m can be mapped unnoticeably to a physical circular path of 5 m with a radius of 22 m [Ste+10b]. If we assume an average walking velocity of a user with an HMD of approximately 1.2 m/s [Moh+07a], a user would need about 4.16 s to walk a distance of 5 m on the curved radius. Hence, it is reasonable to assume that the user will at least blink once along the 5 m virtual path. Walking 5 m on a circle with a radius of 22 m corresponds to a rotation of 10.43 degrees. The results of our experiment described in Section 10.3 revealed that a blink can trigger another rotation of around 5 degrees. Such a manipulation would result in a total rotation of approximately 15 degrees after 5 m walking a circular arc, which corresponds to an increase in degrees of more than 43 %, which can be applied without users noticing.

10.5 Confirmatory Study

Section 10.4 describes how the blink-induced translational and rotational redirection can be used to increase the range of unnoticeable gains. However, so far it is still an open question whether or not those additional manipulations can be combined with the traditional RDW techniques. In a confirmatory study, we explored the question if traditional RDW techniques such as the prominent bending gains, can be improved by additional blink-induced rotations as described in Section 10.4.

10.5.1 Materials and Methods

For this confirmatory study, we used bending gains (see Chapter 8) and added our technique of yaw rotations during blinking. We used the setup illustrated in Figure 10.7. A total of 5 participants (2 female and 3 male, ages 27–38, $M = 30$, experienced VR users from our lab) with normal or corrected-to-normal vision participated in the confirmatory study. The participants were equipped with an HTC Vive HMD and an integrated Pupil Labs eye tracker. The participants were wearing Bose Quiet Comfort 25 headphones. The VE, which was rendered using Unity3D 2017.2, showed a virtual corridor as illustrated in Figure 10.7 (inset). The participants' task was to walk down the corridor 10 times in a clockwise direction.

We applied a bending gain of 2 to a real-world curve with a radius of 2.5 m. The walking path covered a 4 m distance in total. We used again a typical 2-AFCT method in this confirmatory study. Therefore, we asked the participants to perform a blink while walking when they heard a "beep" sound, which was displayed on their headphones. During the 4 m distance, we displayed this sound twice. When an eye blink was successfully detected afterwards, we randomly applied a yaw rotation of 5 degrees either during the first or second blink, whereas there was no manipulation during the other eye blink. The task of the participants was to identify the blink at which the scene rotation has been performed, i. e., the first or the second blink.

10.5.2 Results

The results show that participants indicated the blink correctly in half of the trials ($M = 5$, $SD = 2,34$). In total, 25 out of 50 answers indicated the blink that hid the rotation. Since we used a 2-AFCT paradigm, this means that the participants were not able to reliably detect the blink at which we added the rotation, and could only guess, resulting in a 50-50 distribution at the chance level. These results confirm that additional blink-induced rotations can be used successfully in concert with traditional RDW techniques such as bending gains, thus validating our approach.

10.6 General Discussion

In this section, we discuss our approach, the experimental findings, and their application for RDW and other scenarios.

Our psychophysical experiments (see Section 10.3) revealed that imperceptible rotations of 2–5 degrees and translations of 4–9 cm of the user's viewpoint are possible during a blink without users noticing. In these experiments, the participants had to blink consciously while wearing an HMD and standing in a VE. Detection thresholds for conscious blinking might be different from natural unconscious blinking. However, during a conscious blink, the participants were more focussed on detecting the changes. Hence, our results provide conservative estimates that might even be relaxed by unconscious blinking, in which the user's attention is on different tasks such as navigation or wayfinding.

Moreover, our results show that translations and rotations during eye blinks are able to support RDW in general due to an orthogonal approach from common techniques in the literature. While the benefits for rotation and translation gains are moderate in the range of 10–20 % (see Section 10.4), major improvements can be gained for curvature gains for which rotations can be increased around 5 degrees, which corresponds to an improvement of approximately 50 % (see Section 10.4). Our confirmatory study validated that participants could not reliably detect in which of two blinks their viewpoint was manipulated while walking a curved path. This result provides again a conservative estimate since blink-induced redirection is independent from walking. Hence, it could be used at lower locomotor speeds, too, when a continuous gain is rather ineffective and a rotation of 2–5 degrees might have much more impact. However, the task during the confirmatory study, i. e., participants blink when they hear a beep, is not really a natural use case scenario. This might limit the results and a revised test in an application scenario might be appropriate.

Of course, our blink-induced masking technique might also be applied for other use cases than RDW. One promising scenario is a novel viewer guidance approach for storytelling in VR, e. g., in immersive games or interactive 360-degree movies, which is a challenging domain since users can freely decide on their own perspective in these environments in contrast to typical movies in which directors define their view [Nie+16; RHA17]. For these new paradigms of narratives, it is necessary to find novel ways of guiding the user's attention to specific regions or objects. Here, a subtle rotation of the virtual camera during a blink could attract the user's attention towards an object of interest in the story.

However, all of the examples presented so far relied on unconscious natural blinking, but redirections during blinking might also be carried out consciously. Intentionally triggering repositioning or reorientation using a hands-free method such as an eye blink can be used in a small physical space, without bulky hardware and has potential to avoid VR sickness symptoms due to blink-masked optic flow [LaV00]. Since users can consciously blink numerous times per minute without effort, eye blinks provide great potential to be used as intential trigger. Because conscious blinking is required for this kind of repositioning and reorientation anyway, the detection thresholds could be neglected and even greater distances could be covered, which is refered to as *teleportation*.

10.7 Conclusion

Our novel approach of imperceptible repositioning and reorientation in immersive computer-mediated environments during blink-induced visual suppression promises to improve perceptually-inspired locomotion techniques such as RDW significantly. Our psychophysical experiments revealed that users failed to reliably detect translations of approximately 4–9 cm and rotations of approximately 2–5 degrees that are carried out during blinking, which indicates a conservative estimate that might even be relaxed by unconscious natural blinking. Differences in the amount of redirection concern the three different axes. The application of these thresholds in the context of RDW showed an improvement of around 50 %.

IV

LOCOMOTION TECHNIQUES

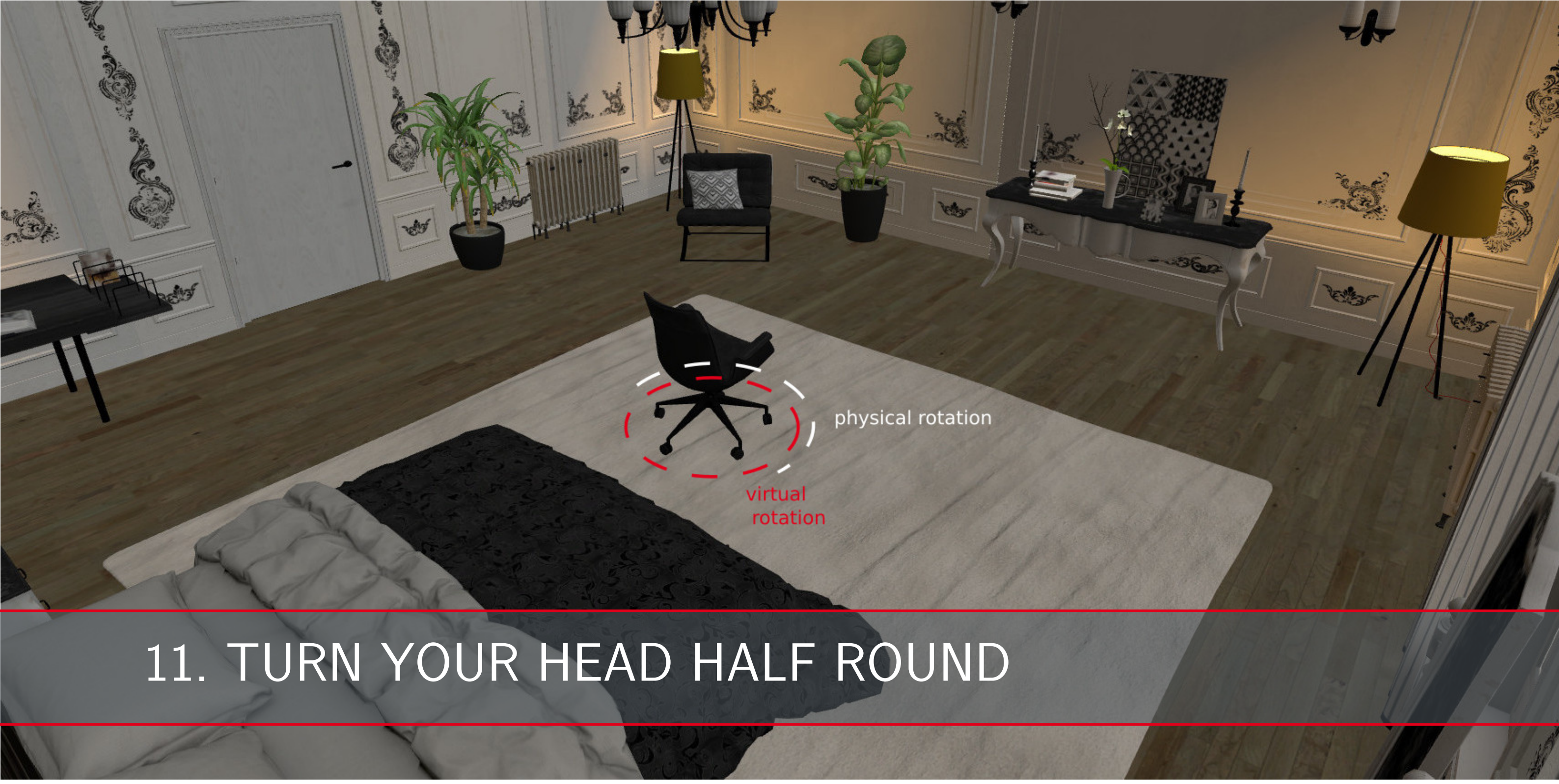

11. TURN YOUR HEAD HALF ROUND

11.1 Motivation

VR technology is becoming more widespread and accessible. In addition to diverse application domains, usage contexts such as location or time of day are also diversifying. VR applications are used at home, at the workplace, or in public. This entails certain challenges. For instance, there are situations where the user's turning angle is physically limited and therefore looking around freely in a 360° environment is not possible. This could happen, for example, when HMDs are used in a bus or airplane (see Figure 11.1). Moreover, some users, e. g., people with disabilities, might not even be capable of turning their head 360° physically due to motor issues [Nor+19].

This motivates the need to develop interaction techniques which facilitate turning 360° in the virtual world to explore the VE completely, even in situations when a 360° physical rotation is not possible. Such techniques need to decouple the one-to-one mapping between physical and virtual rotation.

A standard method to do that is *rotation gains* (see Chapter 3.4). This technique, however, has implications on spatial orientation or VR sickness [KCT08]. Moreover, rotation gains below the detection thresholds do not suffice for turning around 360°. Hence, alternative solutions are necessary that cover the entire 360°. Solutions that are characterized by high usability, low VR sickness symptoms, and no impairment of spatial orientation.

In this chapter, we introduce two rotation techniques for these situations: *Dynamic rotation gains* and *scrolling*. We compare these techniques with traditional static rotation gains and actual physical rotations in an experiment to assess VR sickness, spatial orientation, and usability. We furthermore conducted a confirmatory study to prove the applicability of dynamic rotation gains, the technique that showed the most potential in the experiment.

The remainder of this chapter is structured as follows. Section 11.2 presents the different rotation techniques in detail and Section 11.3 describes the experiment we conducted to compare those techniques. Section 11.4 discusses our findings and section 11.5 presents the confirmatory study. Section 11.6 concludes the chapter.

Figure 11.1: A VR user is sitting in a bus and wears an HMD. In this situation, it is not possible to turn around 360° physically but at the most 180°.

11.2 Rotation Techniques

All of the proposed techniques are designed to enable 360° virtual rotation with a physical rotation range of only 180°. We decided for this physical range motivated by situations in public transport (see Figure 11.1). Of course, different situations might provide smaller or larger physical rotation ranges. Hence, the described techniques have to be adapted to those situations accordingly.

11.2.1 Static Gains

A common possibility to amplify a physical head rotation is to use a static rotation gain. This method multiplies the physical rotation with a factor which remains constant throughout the rotation and is independent of the head direction.

With the aim of investigating which technique is most suitable for reaching targets that are directly behind the user, we need to rotate 180° virtually. While seated, a physical head rotation of approximately 90° is possible. This means we need to double this physical rotation to achieve the targeted 180° virtual rotation. Therefore, we chose a gain $g_R = 2$ for the experiment (see Figure 11.2).

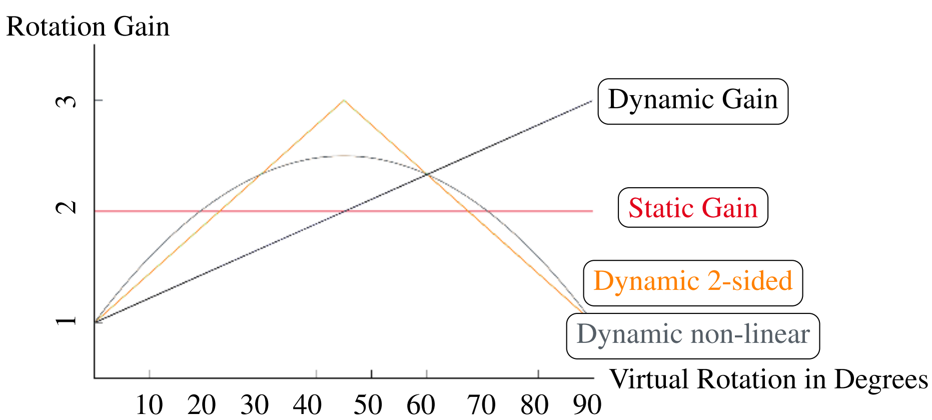

Figure 11.2: Applied rotation gains during a 90° virtual rotation. In all implementations, except static gains, the gain changes depending on the current head direction.

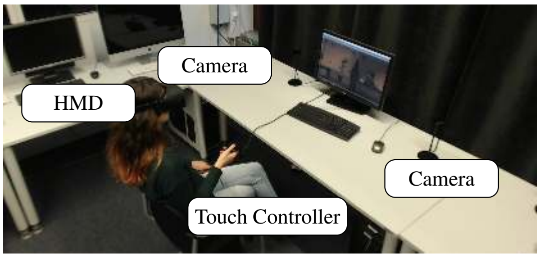

(a)

(b)

Figure 11.3: A participant is wearing the Oculus Rift HMD and a touch controller for input while she sits on a chair (a). The virtual bedroom that was used in the experiment (b).

11.2.2 Dynamic Gains

A high static gain, i. e., a high control/display (C/D) ratio, comes at a cost of accuracy [RT18; YTM17]. The user has to stay calm and move carefully towards the target point.

Hence, rather than using a static rotation gain, it might be advantageous to use a dynamic rotation gain. In contrast to the static gain, a dynamic gain is not constant but changes during rotation. Specifically, it would be possible to increase the gain up to a certain point during turning and, then, decrease it again when the user gets close to the target. This way, rotation would have an ease-in and ease-out phase similar to techniques to enhance animation. A similar approach has been used for hand interactions in VR [FKK07].

There are several possibilities to implement a dynamic gain. For example, the gain control could be speed-based as in the work of Frees et al. [FKK07]. The shortcoming of this method is that the final rotation can be different for every user since different users rotate with different velocities. Therefore, it would not be guaranteed that the user can reach their desired rotation target given this dynamic gain. Because of this, we decided to couple the gain to the head direction of the user instead of the rotation velocity.

In a first naive implementation, we just increased the gain starting at 1 until the user directly looked at the target. This enabled a smoother entry into the amplification, targeting a positive effect for VR sickness. To achieve the same effect as with the static gain, the dynamic gain has to be 3 at the end of the rotation (see Figure 11.2). The gain can be calculated using the formula 11.1:

$$g_R = g_{min} * (1 - \frac{R_{virtual}}{R_{target}}) + g_{max} * \frac{R_{virtual}}{R_{target}} \tag{11.1}$$

g_{min} is the minimum gain of 1, g_{max} is the maximum gain of 3, $R_{virtual}$ is the virtual rotation and R_{target} the target rotation angle. Because the gain is very high when the user approaches the target, we have a similar problem as with a high static gain: The C/D ratio is very large and accuracy decreases.

In the second implementation, we decreased the gain again linearly half-way to the target rotation (see Figure 11.2). This way, the start of the turn trajectory as well as the end is smooth and hitting the target is made easier. The gain can be calculated using formula 11.2:

$$g_R = g_{min} * |\frac{R_{virtual} - R_{half}}{R_{half}}| + g_{max} * (1 - |\frac{R_{virtual} - R_{half}}{R_{half}}|) \tag{11.2}$$

R_{half} is half of the target rotation angle. The maximum gain is weighted more, when the user gets closer to this threshold.

These first two implementations have a common disadvantage: The maximum gain in the first as well as in the second implementation is 3. Since the probability of motion sickness increases with a high gain, the goal of our third implementation was to decrease the maximum gain while the total amplification should stay the same. Therefore, the increase of the gain must not be linear. Instead, we used a parabola (see Figure 11.2). In the beginning of the rotation the gain is $g_R(0) = 1$ and in the end of the rotation it is $g_R(R_{target}) = 1$. At half of the target rotation angle the gain has to be $g_R(R_{half}) = g_{max}$. Using these three points we can put up quadratic equations for all targets to calculate the gains. To achieve the same total amplification as with the first two approaches the maximum gain of this implementation has to be $g_{max} = 2.5$. This is 0.5 less than the other approaches. Hence, using this final implementation, the beginning as well as the ending is smooth, focusing the target is made easier, and the maximum gain is lower. Furthermore, we conducted an informal pilot study with 6 participants. They had one minute per technique (dynamic-linear vs dynamic-non-linear) for free exploration of a VE. All participants preferred the dynamic-non-linear approach.

So, we decided to use this approach in the main experiment (see Section 11.3).

11.2.3 Scrolling

In addition to static and dynamic gains, we implemented *Scrolling* which is a gain-independent rotation technique. The user turns around as usual without an amplification of the rotation. And after a certain threshold angle has passed, the virtual rotation will be continued automatically until the target is reached.

For example, if the user wants to look at an object that is behind her at 180°, she starts turning around towards the target. When the threshold angle is reached, she can stop turning and the virtual camera is continuing the rotation. As long as the user's head is positioned behind the threshold angle, the virtual rotation is carried out. The virtual rotation stops as soon as the user is turning back her head below the threshold angle.

Hence, a threshold angle of 90° means that the user can turn freely without amplification in the range from $-90°$ to 90°. The virtual rotation would start automatically when the user turns her head more than 90° or less than $-90°$ and stop when she turns back into the range from $-90°$ to 90°. If the user continues to physically rotate after the virtual rotation started, it has no effect on the angular velocity.

We performed some initial tests with a threshold of 90° but discarded that value since it can be very uncomfortable to hold a head rotation of 90° for some time. Instead, we chose a threshold angle of 60° which is more suitable in the long run.

11.3 Experiment

In this experiment, we compared the three rotation techniques static gains, dynamic gains, scrolling and a baseline condition; the goal was to assess VR sickness, spatial orientation, and usability.

11.3.1 Participants

32 participants (12 female and 20 male, age on average $M = 26$ years, $SD = 8.87$) completed the experiment. The participants were students, who obtained class credits, or professionals at the local department of computer science. One participant was left handed and the rest were right handed. All of our participants had normal or corrected-to-normal vision. 24 participants had used HMDs before. Their average experience with HMDs was $M = 2.97$ ($SD = 1.43$, in a range of 1 = no experience to 5 = much experience). Most of them had some experience with 3D computer games and they usually played 4.75 hours per week on average.

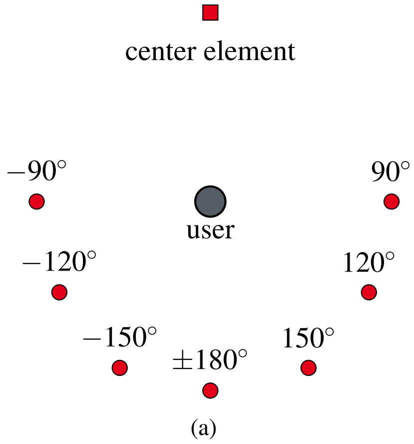

Figure 11.4: The arrangement of the seven targets and the center element around the participant.

11.3.2 Materials

The experiment took place in a 10m × 6m laboratory room. We instructed the participants to wear an Oculus Rift HMD (see Figure 11.3 (a)), which has a resolution of 1080 × 1200 pixels per eye with an approximately 110° diagonal field of view and a refresh rate of 90 hz. Positional tracking was performed by the Oculus Rift cameras. Participants were seated on a swivel chair or stationary chair (depending on the condition) in the center of the tracking area. A touch controller served as an input device via which the participants provided responses during the experiment. For rendering, system control, and logging we used an Intel computer with 3.4 GHz Core i7 processor, 16 GB of main memory and two Nvidia Geforce GTX 780 Ti graphics cards. The virtual environment was rendered using the Unity3D engine 2017.2 and showed an architectural visualization of a square bedroom (see Figure 11.3 (b)).

The participants were seated on a chair in the center of this virtual room so that they look at the wall opposite the bed. In the center of the participant's view is a small circle which served as pointer and input method. To interact with an object, the participant just had to fixate their HMD forward vector towards the object for two seconds during which the circle fills up. There are two types of objects the participant could interact with: the *center element* and the targets. The center element was a pink cube that was located in the center of the user's field of view when a trial was started. The targets were 7 pink spheres which were located around the participant at angles of 90°, 120°, 150°, 180° as well as −90°, −120°, and −150° (see Figure 11.4). Interacting with the center element started and finished a trial.

11.3.3 Methods

We tested the 4 conditions shown in table 11.1 in a within-subject design. The order of the conditions was balanced using the latin square method. For each condition, each of the 7 targets was repeated 4 times. This means there were $7 \times 4 = 28$ trials per condition which were randomized and $28 \times 4 = 112$ trials in total per participant. Participants completed 3 training trials before each condition.

In the baseline condition, the participants were seated on a swivel chair and the physical rotation was not amplified. The other conditions are described in section 11.2. During those conditions, the participants were seated on a stationary chair, so that they could only move their head but not the whole body.

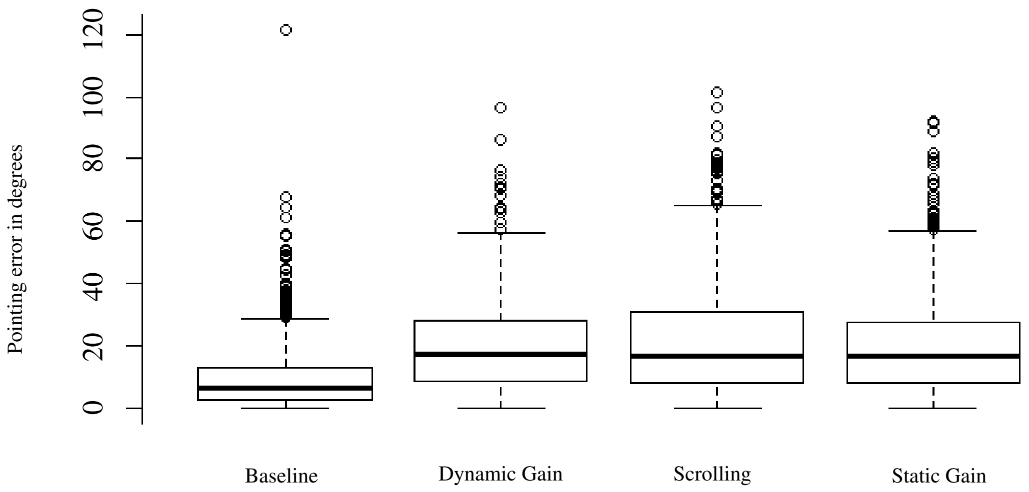

Figure 11.5: Results of the pointing task: The absolute error in degrees (y-axis) is shown for all four conditions (x axis). Overshoot and undershoot errors are merged.

Interaction Task

At the start of one trial a target was positioned somewhere behind the participant. Moreover, an arrow was shown above the center element that indicated the direction at which the target could be found (see Figure 11.4). Participants were asked to turn in the specified direction until the target was in their field of view. This turn was manipulated depending on the condition. Participants did not turn their body but only the head (except in the baseline condition). After reaching the target, participants had to hover their cursor on it for two seconds. Upon completion of the trial, the scene changed to a grey environment and the participants had to perform a pointing task, which was also used in similar studies to investigate spatial orientation [PM94]. In this new environment, the amplification of the rotation was disabled. This means, that movements of the participant were transferred one-to-one to the virtual world. Participants had to return and point to the virtual position of the starting/center element, i. e., to the position where the trial was started, using the touch controller with a ray extending from the controller. The yaw difference between the pointing direction and the actual position of the center element was saved. If the turn of the participant is estimated greater than it should be, this is called an *overshoot* and, if it is estimated smaller, an *undershoot*. Because rotation modifications were disabled when the scene changed, it is not possible to hit the center element by simply pointing physically forwards. Therefore, it is not

Condition 1:	Baseline condition
Condition 2:	Dynamic gain
Condition 3:	Scrolling
Condition 4:	Static gain

Table 11.1: The four conditions of the experiment.

Technique	Undershoots	Overshoots
Baseline	**350**	**546**
Dynamic Gain	**596**	**300**
Scrolling	439	457
Static Gain	**519**	**377**

Table 11.2: Number of over- and undershoots separated by rotation technique (significant differences are marked as bold).

sufficient to remember only the executed physical rotation but the participant has to perceive the VE during the amplified rotation to become aware of their spatial orientation. After participants confirmed the pointing direction, the virtual bedroom was displayed again rotated around a random value to avoid a habituation to the orientation of the room.

Experiment Procedure

Before the experiment, all participants filled out an informed consent form and received detailed instructions on how to perform the experimental task. Furthermore, they filled out a demographic questionnaire. The Oculus Rift was calibrated individually according to the needs of the participant. After each condition, the participants had to rate the deterioration of their well-being on an eleven point likert-scale (0: as before the condition, 10: much worse). It was made clear that this question targets only on the pure deterioration that occurred during the last condition. This means that a participant had to answer "0" (no change) when she does not feel worse than before the condition even if she felt sick already. A similar approach was used in another experiment successfully [FF16]. We used this method to measure VR sickness instead of the Simulator Sickness Questionnaire (SSQ) [Ken+93] since the participants would not have enough time between the conditions to recover their sickness level to its prior level. Furthermore, the participants filled out the System Usability Scale (SUS) questionnaire after each condition.

At the end of the experiment, participants were asked to give a subjective estimation about their preferred technique. The four techniques had to be ranked from bad to good.

11.3.4 Results

Spatial Orientation

Figure 11.5 shows the overall results of the pointing task. A Shapiro-Wilk test revealed that the data is not normally distributed. Hence, we analyzed the results with a Friedman test at the 5% significance level. We found a significant effect of the rotation technique on the total pointing error ($p < .0001$). A post-hoc Wilcoxon signed-rank test found out that the pointing error was significantly lower in the baseline condition than in the other conditions ($p < .0001$). The pointing error in the other conditions did not differ significantly.

We then analyzed the pointing error in each condition separately for overshoots and undershoots using Wilcoxon-Mann-Whitney tests. Table 11.2 shows the number of under- and overshoots for each technique. In the baseline condition, overshoots occurred significantly more often than undershoots ($p < .0001$). On the other hand, undershoots occurred significantly more often than overshoots when dynamic or static gains were used ($p < .0001$). Figure 11.6 shows the average undershoot and overshoot errors for each technique. We found that the overshoot error was significantly larger than the undershoot error in the baseline condition ($p < .0001$) and for the scrolling technique ($p = .005$). For the dynamic gain, the undershoot error was significantly larger than the overshoot error ($p < .0001$).

To compare over- and undershoots between the different techniques, we analyzed the data with a Kruskal-Wallis test at the 5% significance level. We found a significant effect of the rotation technique on the overshoot error ($p < .0001$). A post-hoc test using Mann-Whitney tests showed

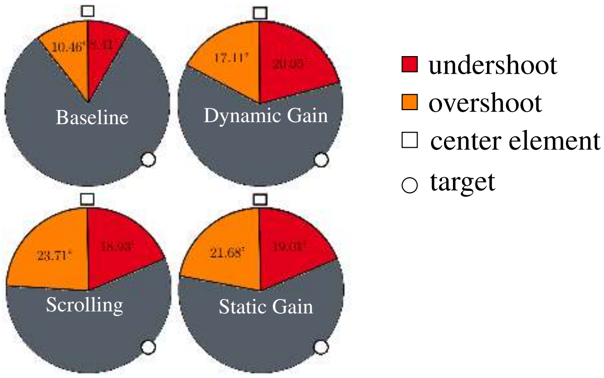

Figure 11.6: Average overshoot and undershoot errors per condition. The participant is located in the center of the circle and looks at the target (white circle) while she is pointing to the center element (white square). Undershoot is marked in red and overshoot is marked in orange. For better clarity, all parts are scaled up.

significant differences between the baseline condition and all other conditions ($p < .0001$). It also showed that the overshoot error for dynamic gains is significantly lower than for scrolling ($p < .0001$) and static gains ($p = .001$). We could not found any significant differences between scrolling and static gains.

Furthermore, we found a significant effect of the rotation technique on the undershoot error ($p = .012$). The undershoot error in the baseline condition is significantly lower than in all other conditions ($p < .0001$). For dynamic gains, we found a significantly larger undershoot error than for scrolling ($p = .004$) and static gains ($p = .009$). We could not found any significant differences between scrolling static gains.

VR Sickness

We analyzed the results of the question about the participants' well-being. A Shapiro-Wilk test revealed that the data is not normally distributed. Hence, we analyzed the results with a Friedman test at the 5% significance level. We found a significant effect of the rotation technique on the well-being ($p = .0005$). A post-hoc Wilcoxon signed-rank test found that the worsening in the baseline condition is significantly lower than for scrolling ($p = .001$) and static gains ($p = .006$). Also, the deterioration for dynamic gains is significantly lower than for scrolling ($p = .0008$) and static gains ($p = .004$). We could not find any significant differences between the baseline condition and dynamic gains ($p = .387$) as well as between scrolling and static gains ($p = .134$).

Usability

Figure 11.7 shows the results of the SUS questionnaire. Scrolling got the lowest rating with an average score of 69.7 ($SD = 16.12$). Static gains received an average score of 77.3 ($SD = 14.92$). The baseline condition and the dynamic gains achieved the highest scores with an average of 83.2 ($SD = 14.37$) and 85.2 ($SD = 13.28$), respectively. A Shapiro-Wilk test revealed that the data is not normally distributed. Hence, we analyzed the results with a Friedman test at the 5% significance level. We found a significant effect of the rotation technique on usability ($p < .0001$). A post-hoc Wilcoxon signed-rank test found that the scores of the baseline condition are significantly higher than for scrolling ($p = .007$) and the scores for dynamic gains are significantly higher than for scrolling ($p = .0001$) and for static gains ($p = .016$). We could not find a significant difference between scrolling and static gains ($p = .657$) as well as between the baseline condition and dynamic gains ($p = .657$)

When asked for sorting the techniques according to their preferences, participants showed preference towards dynamic gains (17 votes), followed by the baseline condition (9 votes), scrolling (4 votes), and static gains (2 votes).

11.4 Discussion

In the pointing task, none of the techniques could compete with the baseline condition. However, in the results, we observed some interesting aspects regarding spatial orientation using dynamic gains. For dynamic gains, the undershoot error was larger and occured more often than the overshoot error. Furthermore, the overshoot error for dynamic gains was smaller than with static gains or scrolling while the undershoot error was larger for dynamic gains than with static gains or scrolling. This means, participants tended to estimate the rotation smaller than it was, which is an indicator that the amplification of the physical rotation was quite subtle. This was not the case for static gains and scrolling.

Regarding VR sickness, scrolling turned out to be the worst technique while dynamic gains performed as good as the baseline condition.

Analyzing the SUS usability questionnaire, dynamic gains and the baseline condition resulted in the best usability. Dynamic gains were even preferred over the baseline technique which appears to be surprising but might be attributed to the nature of the question: Participants judged the best experience, and dynamic gains have some advantages over the baseline technique like reduced turning effort.

In summary, dynamic gains scored in most of the criteria and, therefore, might be a good alternative to natural physical rotation. A limitation of this technique that has to be stated is that the target of the rotation has to be known beforehand. This might not be the case for all situations. However, in the future, prediction algorithms might be used to approximate this.

11.5 Confirmatory Study

To verify the applicability of the approach that performed best, i. e., the dynamic gains, we performed a brief confirmatory study and gathered qualitative feedback in a narrative VR experience.

11.5.1 Materials and Methods

The same setup as described in Section 11.3 was used. We also used the same VE as in the experiment but instead of the seven targets virtual humans were placed in the room around the user. These virtual humans told the fairy tale *The Princess and the Pea*. They did this alternately: Each human spoke some sentences and then another one continued until the complete tale was told. The spoken sentences were generated beforehand using an online text-to-speech tool. During playback in the VR experience the lips of the virtual humans were synchronized with the spoken words using the Oculus Lipsync plugin. The sound source was set to the position of the currently speaking human to create a spatial impression.

The task was to listen to the tale and to face always the human who is currently speaking. Hence, participants had to turn around when the speaker changed, according to the origin of the sound. During these turns, dynamic rotation gains were applied. This way, we could enable the user to turn around in a 360° virtual environment during the whole experience while the user only had to use a 180° range in the physical world. The participants did not know about the rotation gains before and during the study.

After the tale was told the participants had to fill out some questionnaires including the SSQ, the Slater-Usoh-Steed presence questionnaire [SU93; SUS94], a demographic questionnaire and a custom questionnaire.

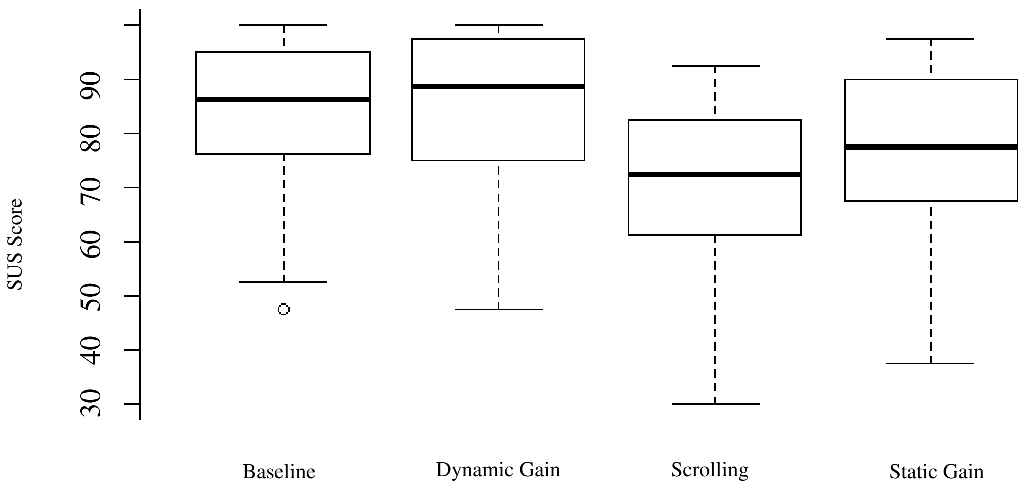

Figure 11.7: SUS scores of the different rotation techniques.

11.5.2 Participants

In total, 14 participants (5 female and 9 male, ages $18-26$, $M = 21.5$) completed the confirmatory study. The participants were students or members of the local department of informatics. All participants had normal or corrected-to-normal vision. Four participants wore glasses during the experiment. No participant reported a disorder of equilibrium. No vision disorders have been reported by the participants. Nine participants had participated in an experiment involving HMDs before. The experience of the participants with 3D stereoscopic displays (cinema, games etc.) in a range of 1 (no experience) to 5 (much experience) was $M = 3.64$ ($SD = 0.93$). Most of them had experiences with 3D computer games ($M = 3.36$, $SD = 1.65$, in a range of 1 = no experience to 5 = much experience) and they usually played 6.8 hours per week on average ($SD = 13.19$). The body height of the participants varied between $1.57-1.97$m ($M = 1.77$m, $SD = .09$m). The total time per participant, including pre-questionnaires, instructions, study, post-questionnaires, and debriefing, was 20 minutes. Participants wore the HMD for approximately 10 minutes.

11.5.3 Results

After the tale, we asked the participants if they noticed that there was an acceleration during the rotation. Only four participants noticed this. However, when asked if this acceleration disturbed them, all participants responded negatively. Only one participant stated that this acceleration distracted him from listening to the speakers and that he was briefly confused. After we explained the used rotation technique to the participants, eleven participants said that they did not notice anything and that it felt very smooth to them. For example, one participant said: "It worked so well, it felt like naturally turning your head in real life". On the other hand, one participant stated that he felt sick because of the fast rotations while another one said that it was comfortable after a short acclimation.

These results suggest that most of the participants did not notice the rotation gain, and most of them were actually surprised that the rotations were manipulated.

We measured a mean SSQ-score of 13.62 ($SD = 19.71$) before the experiment, and a mean SSQ-score of 16.83 ($SD = 25.69$) after the experiment. The mean score for the sense of feeling present in the VE was 2.14 ($SD = 1.46$) on a five-point likert scale.

11.6 Conclusion

We introduced a new technique based on dynamic rotation gains for rotating around in a VE when in a situation where only a limited physical turning angle is available. Results suggest that this technique performs similar to natural rotation when it comes to spatial orientation, usability, and VR sickness, and better than other techniques like static gains or scrolling. This was evaluated in an experiment with 32 participants. Additionally, we demonstrated in a confirmatory study that the technique is appropriate for use in actual VR experiences.

12. LEANING-AMPLIFIED-SPEED WALKING-IN-PLACE

12.1 Motivation

WIP locomotion techniques have in common that they analyze the gait of users while stepping in-place to initiate virtual movements, but they can differ largely in terms of which gait characteristics their algorithms extract. When stepping in-place the feet show large vertical movements and very limited horizontal displacements, which means that it is not possible to perform a biomechanically veridical one-to-one mapping of physical to virtual walking steps. In particular, this means that it becomes difficult to estimate the step width that a physical foot movement should correspond to in the VE, which controls the speed and thus the distance a user covers while walking. One of the major remaining challenges of WIP techniques is the ability to naturally control the virtual walking speed.

Different approximations have been presented such as based on the stepping frequency [WWB10] or amplitude of vertical foot movements [BPJ13] to scale step distances and thus walking speed. However, as far as we know, no previous work evaluated interaction effects between the forward or backward leaning angle of the user's upper body and perceived self-motion speed with WIP techniques. Since slight or heavy forward leaning of the upper body against the horizontal movement direction is a characteristic of runners and sprinters, we hypothesize that a positive correlation exists with increased virtual walking speeds. Additionally, based on the same arguments we hypothesize that using leaning to scale self-motion speed has the potential to provide an intuitive addition to improve the usability of WIP.

Different locomotion techniques have been proposed that initiate virtual self-motion based on the leaning anlge of the user's torso in the real world when wearing a HMD or in CAVEs [Guy+15; MPL11]. Such techniques are motivated by movements in the real world, which often show people leaning forward when running or driving faster to assume a stable body position in the presence of increased horizontal force during movements in addition to gravitational force. Such static and dynamic leaning poses have been found to affect self-motion sensations during traveling in IVEs [Kru+15]. Notable here is also the SilverSurfer virtual surfboard locomotion technique [WL11].

While previous locomotion techniques used leaning alone to initiate virtual movements, we are not aware of any related work that uses leaning in combination with WIP techniques to scale the virtual locomotion speed. Therefore, we propose a novel extension of WIP techniques by incorporating leaning angles to scale virtual locomotion speed and show in an experiment that the extension provides a viable locomotion experience.

This chapter is structured as follows. Section 12.2 describes our novel WIP technique called Leaning-Amplified-Speed Walking-in-Place (LAS-WIP). In Section 12.3, we present the experiment that we conducted to evaluate the WIP technique. Section 12.4 concludes the chapter.

12.2 Locomotion Technique

The LAS-WIP locomotion technique is based on an omnidirectional tracking system [Eic14] which consists of four Microsoft Kinect v2 sensors that are mounted on tripods and placed around the tracking area (see Figure 12.1). The data of the four Kinects is combined using a sensor fusion algorithm in order to obtain a 360 degree skeleton of the user [Eic14]. With this setup the user is standing in the center of the tracking space with an upright posture and wearing an HMD that is connected to a laptop in the backpack of the user (see Figure 12.1). Hence, no wires disturb the user's sense of presence in the VE [Sla09]. In previous versions of our locomotion setup we used a wireless transmission system to provide real-time audiovisual data to the user wearing an HMD, but due to the recent changes in display resolution of HMDs such as the Oculus Rift DK2 it becomes increasingly difficult to find compatible wifi transmission systems.

For our locomotion technique, we expect that accurate tracking data is provided independently of the orientation the user is facing in the laboratory setup. Hence, in our WIP design it is not necessary to introduce an artificial interaction technique to enable the user to rotate in the VE, but instead the user can accomplish rotations just by turning around in the real world. Additionally, this means that the user's hands are not required for locomotion, and thus may be used for orthogonal tasks such as selection or manipulation in the VE. Although the torso and head orientations are provided by our omnidirectional tracking system, we found that the sensors of HMDs such as an Oculus Rift DK2 provide more precise tracking of the user's head. Hence, we use this headtracking data instead of that of our omnidirectional tracking system to provide the user with feedback to head movements.

12.2.1 Step Detection

We follow the main literature on implementations of WIP techniques in that we detect when the user performs a step in the real world and map it to a forward translation in the VE. Therefore, we had to choose between using the torso or head as reference for forward movements, and we decided on using the head orientation, which is similar to the choice between torso-directed and view-directed steering methods [Bow+01]. Our choice is based mainly on the lower latency and higher accuracy of the headtracking data, but informal tests also suggested that it becomes easier to steer around more difficult paths when using the head instead of having to turn the torso.

With our technique the user is instructed to step in-place to move forward in the VE. Our step detection algorithm uses the ankle joints of the fused skeleton model to allow as natural as possible locomotion and an accurate detection. A step is detected when the distance of the joints to the floor plane is higher than a threshold. We assume normal step speed and alternating foot movement to filter out false positive detections.

Depending on how rapidly the user raises and lowers the feet during in-place stepping, this results in a change of virtual self-motion speed. Caused by the tracking latency and algorithm we observed a temporal offset between when the user initiates a step and the moment the step generates visual feedback. Overall, our visual feedback is roughly half a step behind the user's movements, which is similar to other WIP implementations with low-cost consumer hardware [Wil+11].

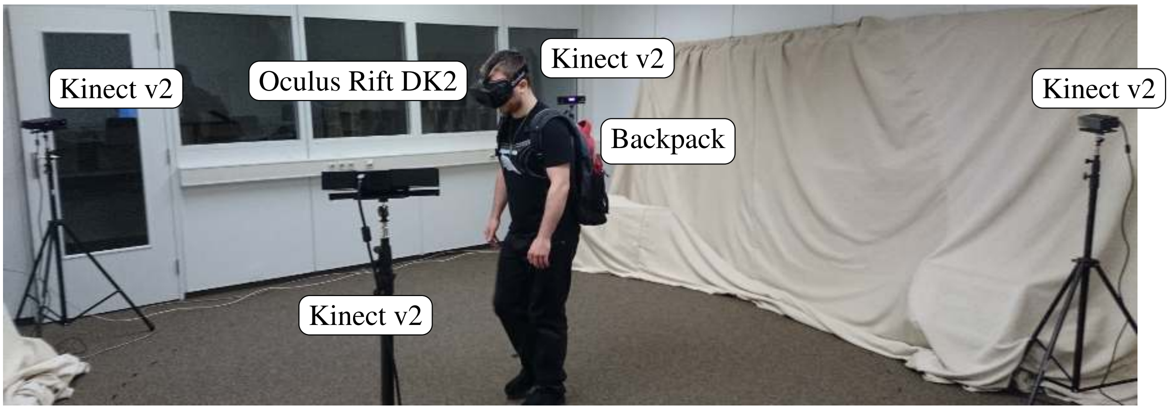

Figure 12.1: Illustration of the LAS-WIP system: user wearing an Oculus Rift DK2 HMD and a rendering laptop in a backpack, while he is tracked by four Kinect v2 sensors.

In our system, we defined a parameter for the step width in the VE when a user performs an in-place step in the real world. While we designed the technique in such a way that this parameter could be estimated before a user starts using the WIP system by measuring the typical step width, we observed that an average walking speed of 2m/s already results in acceptable impressions of self-motion. We provide visual feedback to a step by triggering a forward translation based on a velocity profile. The LAS-WIP technique supports different velocity curves with parameters for ease-in and ease-out velocities during virtual walking, which might be used to fine-tune the feedback for a particular user, if required.

12.2.2 Torso Leaning Angle

The main novel part of the LAS-WIP technique is the ability to change virtual walking speeds by changing the torso leaning angle. Therefore, we calculate the leaning angle by computing the difference of the *"spine_shoulder"* and *"spine_base"* joints in the Kinect's skeleton model. We currently do not distinguish between forward or backward leaning, since initial tests suggested that even backward leaning can be interpreted as increased speed, e. g., when being pressed into the seat when driving fast with a car. Depending on the intended maximum virtual walking speed when leaning, we observed that it is advantageous to define a limit for the leaning angle, or users might start to assume very uncomfortable body poses in order to move faster in the VE. We decided to switch to maximum speed if a leaning angle of θ_{max} degrees or higher is reached to ensure that the body pose remains comfortable; we found a value of θ_{max}=35 degrees to work fine in initial tests. Also, we observed that it is advantageous to define a minimum angle, e. g., θ_{min}=5. Below this angle we do not manipulate the walking speed, which leads to a more stable walking experience on standard walking speed.

12.3 Experiment

In this section, we present the evaluation of the LAS-WIP locomotion technique. We compared the leaning angle extension with a traditional WIP implementation, in which the virtual speed is only dependent on the stepping frequency and not additionally on the leaning angle.

12.3.1 Participants

We recruited 14 participants for our evaluation, 11 male and 3 female (ages from 21 to 36, M=27.9). The participants were students or professionals of human-computer interaction, computer science or engineering. All of our participants had normal or corrected-to-normal vision. 9 wore glasses and 1 participant wore contact lenses during the experiment. None of our participants reported a disorder of equilibrium or binocular vision disorders. 12 participants had experienced HMDs before. The total time per participant, including pre-questionnaires, instructions, experiment, breaks, post-questionnaires, and debriefing, was 30 minutes. Participants wore the HMD for approximately 20 minutes. They were allowed to take breaks at any time.

12.3.2 Materials and Methods

We used a within-subjects design, in which we compared two WIP techniques: LAS-WIP and traditional WIP implementation without leaning. The order of these tests was randomized and counterbalanced. As dependent variables we measured VR sickness using the SSQ [Ken+93], presence using the SUS questionnaire [Uso+99b], as well as subjective estimates of preference and experience in a custom questionnaire.

We performed the experiment in an 8m×5m laboratory room. As illustrated in Figure 12.1, we used a wireless setup. Participants wore an Oculus Rift DK2 HMD for the stimulus presentation and a rendering laptop in a backpack. We used a graphics laptop with an Intel i7 CPU, Nvidia GeForce GTX 970M and 16GB RAM for rendering the VE. The omnidirectional body tracking system was running with four Kinect v2 sensors, each connected to a graphics workstation with Intel i7 CPU, Nvidia GeForce GTX 970 and 16GB RAM. The workstations were connected via GBit Ethernet. The rendering laptop received tracking data via wifi.

In the experiment we generated virtual step feedback based on a linear velocity function, which consisted of an ease-in and ease-out phase. Each phase lasted 0.5 seconds; the overall duration of a step was 1 second, which corresponds to a walking speed of 2m/s if a mean step frequency of one step per second is assumed. When another step is received during this time, the first step is discarded and the speed is increased from the current level up to the maximum speed. Hence, stepping at the expected frequency results in a uniform movement velocity. We used a velocity scaling factor of 5 for maximum leaning angles, with constraints θ_{min}=5 and θ_{max}=35 (see Section 12.2).

The virtual world was rendered using the the Unreal Engine 4. The participants had to walk a periodic path in the VE, which was indicated by a gravel road. The virtual path had a length of ca. 1000m. The path consisted of multiple curvatures so the participants had to turn around and utilize the full 360 degrees tracking range (see Figure 12.2). The VE was a 3D model of the medieval *Hammaburg*, a castle and adjacent village of the 9th century in Hamburg, Germany. The castle is of significant importance for archaeology, tourism and city marketing. In cooperation with the local archaeological museum we are currently considering different possibilities to create interactive experiences for museum visitors. LAS-WIP with our omnidirectional tracking setup provides one possibility to explore this virtual medieval world.

12.3.3 Results and Discussion

We measured VR sickness symptoms before and after each of the two WIP conditions, and we computed the change in VR sickness.

For the traditional WIP technique we measured an average increase in SSQ scores of 17.63 ($SD = 28.23$) and for LAS-WIP an average increase of 9.88 ($SD = 16.83$), which both are in the range of usual increases in symptoms with an Oculus Rift DK2 HMD over the time of the experiment. We analyzed the questionnaire data with Wilcoxon signed rank tests. We found no significant difference in VR sickness symptoms between the LAS-WIP technique and the traditional technique ($Z = 1.22$, $p = .22$). The apparent trend can be interpreted in light of the shorter time participants spent in the VE for LAS-WIP (ca. 7min) compared to the traditional technique (ca. 14min), since the LAS-WIP technique allowed participants to complete the path in the VE at an increased speed.

We measured the participants' sense of presence with the SUS questionnaire, which revealed

Figure 12.2: Visual stimulus used in the experiment: 3D model of the Hammaburg, a local medieval castle of the 9th century. Participants had to follow the virtual path in (randomized) clockwise or counterclockwise direction.

an SUS mean score of 3.95 ($SD = 1.52$) for the traditional technique and 3.83 ($SD = 1.53$) for LAS-WIP, which both indicate high presence in the VE. We found no significant difference in SUS scores between the two techniques ($Z = 1.30$, $p = .20$). Informal responses, however, suggest that the apparently slightly lower presence with LAS-WIP might stem from an increased concentration of the participants on locomotion in the VE. As one participant remarked, *"Walking slowly gives you more time to look around. With the other technique [LAS-WIP], I was more focused on moving fast along the path and had less time to appreciate the world and smell the virtual roses."*

Questioned about which of the two techniques the participants preferred, 12 stated that they would use LAS-WIP, whereas 2 preferred the traditional approach. We additionally collected informal responses, which mainly support the notion that participants prefer to be able to walk faster in the VE than their normal walking speed in the real world, in particular, if it comes at less energy cost than having to step faster. However, they expressed appreciation for the ability to easily reduce speed with LAS-WIP when they had to perform sharp turns in the VE in order to prevent collisions. One participant noted that LAS-WIP did not work well for her due to an occurrence of back strain that she experienced when trying to use that feature, which has to be considered for future applications.

Participants judged their fear to collide with physical obstacles during WIP on a 5-point scale (0 no fear, 4 high fear) for the traditional technique on average as 1.0 ($SD = 1.2$) and for LAS-WIP as 0.7 ($SD = 1.1$), $Z = 1.63$, $p = .10$. Questioned about their impression of self-motion with their body in the VE (0 very low, 4 very high) they responded for the traditional technique on average with 1.6 ($SD = 1.3$) and for LAS-WIP with 2.0 ($SD = 1.0$), $Z = 1.73$, $p = .08$. Moreover, they felt that their posture affected their self-motion sensation (0 no, 4 yes) for the traditional technique significantly less with an average of 1.6 ($SD = 1.5$) compared to LAS-WIP with 2.9 ($SD = 1.4$), $Z = 2.57$, $p = .10$. They judged the comfort of their pose during walking (0 uncomfortable, 4 comfortable) for the traditional technique on average as 1.5 ($SD = 1.3$) and for LAS-WIP as 1.4 ($SD = 1.3$), $Z = .51$, $p = .61$. The subjective estimates suggest that LAS-WIP may increase impressions of self-motion, although the estimates are still far from real walking, which is in line with previous research [Uso+99a]. The comfort of LAS-WIP seems slightly reduced over traditional WIP, even though both approaches are not judged as particularly comfortable.

12.4 Conclusion

In this chapter, we presented and evaluated a novel solution to WIP locomotion techniques. Using an omnidirectional tracking setup based on multiple Kinects and a sensor fusion approach that combines the available skeleton data, we detailed our novel leaning extension for WIP, called LAS-WIP, and presented an experiment, which indicates that the leaning extension can improve the usability of WIP and also has the potential to improve subjective self-motion estimation.

13. SCALE & WALK

13.1 Motivation

Based on the results of our experiments on dominant scale perception (see Chapter 6), we wanted to develop scale-based locomotion techniques. The idea is to scale the virtual size of the user. Then, she can increase her size to cover larger virtual distances while walking naturally in a confined space in the real world. And she can decrease her size to explore a certain spot in detail with a one-to-one mapping. Hence, the user still gains vestibular and proprioceptive feedback during walking, but is able to explore virtual worlds larger than the real world tracking space.

In this chapter, we present an experiment, which compares two different scale-based locomotion techniques and a baseline condition. The remainder of this chapter is structured as follows. Section 13.2 describes the used techniques. Section 13.3 presents the experiment. Section 13.4 discusses the results and Section 13.5 concludes the chapter.

13.2 Locomotion Techniques

We implemented two different scale-based locomotion techniques: (i) manual scaling and (ii) automatic scaling. Manual scaling provides the possibility to change the user's virtual size by using an input device. This provides control to the user and decouples locomotion and scaling. Automatic scaling changes the user's virtual size automatically during walking. First, size is increased, and after half of the way, size is decreased. If the target is known, the change per meter can be calculated using a mathematical function. The goal is that the user is at regular size again when she reaches the target. The advantage of this technique is that the user does not have to be actively concentrated on navigation but can carry out different tasks while walking. However, the target needs to be known beforehand. This could be solved by using a selection technique, similar as in teleportation techniques.

The baseline condition in the experiment is walking with a translation gain applied such as implemented by Interrante et al. [IRA07]. We decided for this technique because it is based on natural walking, just like the scale-based technique, and it required a similar amount of space in the real world.

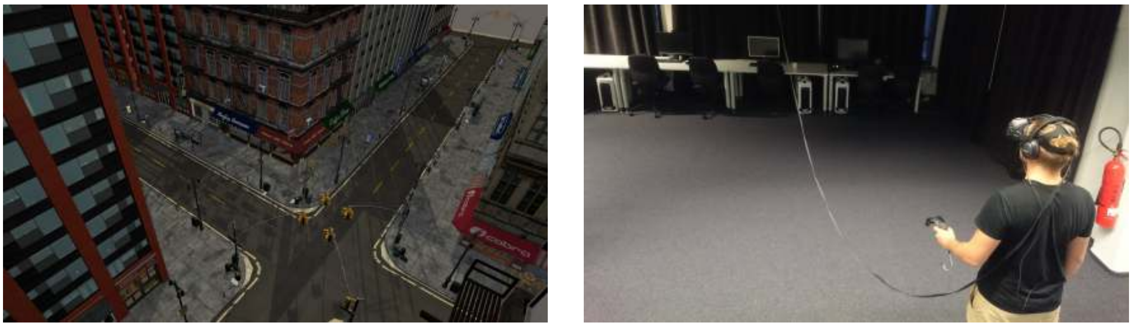

(a) (b)

Figure 13.1: The virtual environment (a) and the real world tracking space (b) of the experiment.

In a pilot study, we tested several scaling functions for manual and automatic scaling. Scaling functions describe how much the size increases or decreases in dependence of time or walked distance. For each scale-based technique, the best function was determined regarding criteria such as comfort, presence, and usability. For manual scaling, an asymmetric interval-based sigmoid function was selected. For automatic scaling, the parabolic function $f(x) = max(a*x^2 + b*x + c, c)$ offered best results. In this function, c denotes the virtual start size, a denotes the virtual distance, and b denotes the real distance to the boundary of the tracking space.

13.3 Experiment

In this experiment, we evaluated these three techniques regarding presence, usability, VR sickness, and spatial knowledge. We defined the following hypotheses:

H_1 Spatial knowledge is increased for manual and automatic scaling compared to baseline.
H_2 VR sickness is decreased for manual scaling compared to the other techniques.
H_3 Usability is higher for manual and automatic scaling than for baseline.

13.3.1 Participants

In total, 27 participants (11 female and 16 male, ages $16-49$, $M = 23.15$) completed the experiment. The participants were students, who received credits for participation, or members of the local department of informatics. All participants had normal or corrected-to-normal vision. Eight participants wore glasses during the experiment. Two participants wore contact lenses. 22 participants had experience with VR HMDs before.

Most of them had experiences with 3D computer games: 12 participants play games at least one time per week and 8 participants never play games. The total time per participant, including pre-questionnaires, instructions, experiment, post-questionnaires, and debriefing, was 60 minutes. Participants wore the HMD for approximately 40 minutes.

13.3.2 Materials

We instructed the participants to wear an HTC Vive HMD, which provides a resolution of 1080×1200 pixels per eye with an approximately 110° diagonal field of view and a refresh rate of 90 hz. Positional tracking was done by a lighthouse tracking system that is delivered with the HTC Vive. The lighthouse system was calibrated so that there was an available walking space of 4m $\times$ 4m (see Figure 13.1 (b)). A HTC Vive controller served as an input device via which the participants provided responses during the experiment. The urban city scene (see Figure 13.1 (a)) was rendered using the Unity3D engine 2017.2. And for interactions, the VRTK was used.

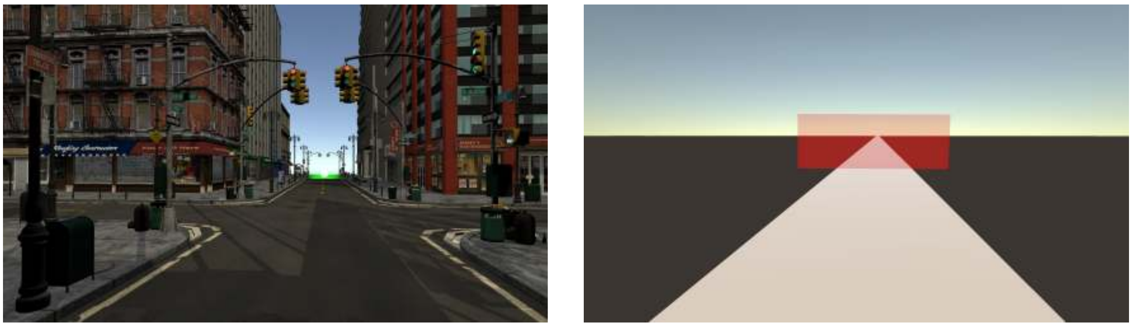

(a) (b)

Figure 13.2: During the experiment, the current target was marked green (a). After reaching the target, participants had to estimate the walked distance in the VE by moving a red semi-transparent wall in depth using the controller (b).

13.3.3 Methods

We used a within-subjects experimental design with one block per technique. The order of the blocks was counter-balanced. All participants filled out the Kennedy-Lane simulator sickness questionnaire [Ken+93] immediately before and after the first block. Since VR sickness might not be gone completely after the first block, we did not use the SSQ after the second and third block. Hence, regarding VR sickness, the experiment appeared to have a between-subject design.

In the first phase of each block, the participants started on a crossing in the center of the city model. On the street, a target was presented at one of five distances (see Figure 13.2 (a)). For automatic scaling and baseline condition, the participants just had to walk to this target. For manual scaling, participants had to increase their size first. Then, they could walk to the target and decrease their size again. After reaching the target, the scene was faded out (see Figure 13.2 (b)). Using the controller, the participants had to estimate the walked distance in the VE by moving a red semi-transparent wall in depth. This estimation was used as a measurement for spatial knowledge. After this, the city scene was faded in again and the next target was visible. In each block, we had 2×5 different distances. Participants completed 3 training trials before each block. After the trials, participants were asked to rate the decrease of their well-being on a scale from 0 to 6.

In the second phase of each block, participants could freely explore the city for 2 minutes. During this time, we collected qualitative feedback using the think-aloud method. After this phase, participants filled out the system usability scale questionnaire [Bro96] and the SUS presence questionnaire [Uso+99b].

When all three blocks were done, the participants filled out a final demographic questionnaire.

13.3.4 Results

Table 13.1 shows the means and standard deviations for the SUS presence questionnaire [Uso+99b]. A Shapiro-Wilk test did not indicate that the assumption of normality had been violated. We analyzed the results with an ANOVA at the 5% significance level. We found no significant effect of the locomotion technique on presence ($F = 3.365$, $p = .0703$).

Table 13.2 shows the means and standard deviations for the system usability scale questionnaire [Bro96]. A Shapiro-Wilk test reveals that the data is not normally distributed. Hence, we analyzed the results with a Friedman test at the 5% significance level. We found a significant effect of the locomotion technique on usability ($df = 2$, $\chi^2 = 14.06$, $p < .0009$). A post-hoc test using Wilcoxon tests showed that automatic scaling has a significantly lower usability score than baseline condition ($p < .004$) and manual scaling ($p < .0003$). We did not find a significant difference

	automatic	manual	baseline
M	4.31	5.14	4.64
SD	1.07	1.04	0.77

Table 13.1: Means and standard deviations for SUS presence scores.

	automatic	manual	baseline
M	67.59	78.61	76.85
SD	15.65	13.14	17.47

Table 13.2: Means and standard deviations for system usability scale questionnaire.

between baseline and manual scaling ($p = .2092$).

Figure 13.3 shows the normalized estimated walking distances. A Shapiro-Wilk test reveals that the data is not normally distributed. Hence, we analyzed the results with a Friedman test at the 5% significance level. We did not find a significant effect of the locomotion technique on distance estimation ($\chi^2 = 2.7857$, $df = 2$, $p = .2484$). Means and standard deviations suggest that distances were underestimated mostly.

Table 13.3 shows the means and standard deviations for the SSQ [Ken+93]. A Shapiro-Wilk test did not indicate that the assumption of normality had been violated. We analyzed the results with an ANOVA at the 5% significance level. We found no significant effect of the locomotion technique on VR sickness ($p = .519$).

Furthermore, we evaluated the worsening of the well-being after each block. A Shapiro-Wilk test reveals that the data is not normally distributed. Hence, we analyzed the results with a Friedman test at the 5% significance level. We found a significant effect ($\chi^2 = 9.6562$, $df = 2$, $p < .009$). A post-hoc test using Wilcoxon tests showed that there is no significant difference between manual und automatic scaling ($V = 121$, $p = .05869$) as well as between manual scaling and baseline ($V = 23.5$, $p = .8234$). Worsening of well-being is significantly greater for automatic scaling than for the baseline condition ($V = 121$, $p < .003$).

When asked for their preferred technique, 78.6% of the participants chose manual scaling and 21.4% of the participants chose the basline condition. Automatic scaling was not chosen by anyone.

The evaluation of the think-aloud phase revealed that a lot of participants found manual scaling pleasant because they had much more control. Automatic scaling was rated uncomfortable because of the lack of control. Furthermore, decreasing the size was associated with a feeling of freefall, especially in the last phase of scaling. In general, changing the size often induced malaise. The high acceleration in the baseline condition was also described as unfamiliar.

	automatic	manual	baseline
M	8.727	5.818	10.804
SD	8.569	7.735	26.143

Table 13.3: Means and standard deviations for SSQ.

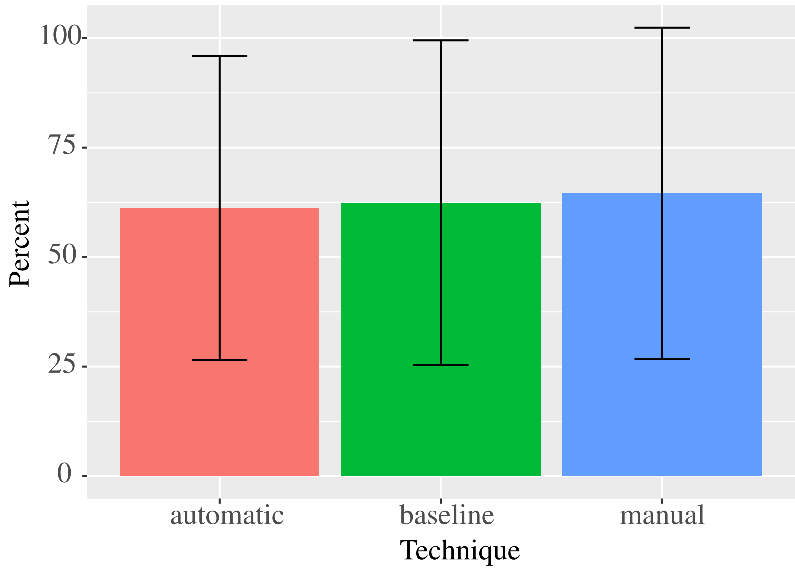

Figure 13.3: Estimated walked distances in percent.

13.4 Discussion

We could not find any significant results for presence. Further investigation is necessary to draw a conclusion.

Automatic scaling was significantly worse regarding usability. Hence, hypothesis H_3 can not be confirmed. The low usability score might be caused by the unfamiliar and uncomfortable feeling of not being in control. The other techniques allowed more control by the user and were rated higher.

It is known that there is a distance underestimation in VR in many situations [Bru+15]. Our results are in line with that. However, we did not find a significant difference between the techniques. So, hypothesis H_1 can not be confirmed. Maybe, a different, more precise, method for distance estimation might result in different values.

We could not find any significant differences between techniques regarding VR sickness. Hypothesis H_2 can not be confirmed. This might be due to the low number of data since the SSQ was only raised during the first block of the experiment.

The well-being decreased significantly more during automatic scaling than during the baseline condition. Again, this might be because of the lack of control during automatic scaling.

Qualitative feedback revealed that manual scaling is preferred by most of the participants. This result can not be confirmed by the quantitative data. Especially, when using manual scaling, the participants liked the possibility to explore the city in detail and to get an overview. The malaise in the last phase of decreasing size might be reduced with an adjusted scaling function. Though the baseline condition was described as unfamiliar, it was preferred and accepted as more natural since it could be compared to driving a car.

Because of the previous discussion, we assume that lack of control and scaling are effects, which affect the well-being negatively. For automatic scaling, both effects interact with each other. This could explain the worsening of well-being. For the other techniques, only one of these effects occur. On the other hand, automatic scaling could have a training effect that reduces negative consequences.

13.5 Conclusion

In this chapter, we presented an experiment, in which two scale-based locomotion techniques and a baseline condition were compared. The techniques were evaluated regarding usability, presence, VR sickness, and spatial knowledge. We did not find any significant differences between the techniques regarding spatial knowledge. Automatic scaling induced significantly more VR sickness to the participants than the baseline condition. Moreover, automatic scaling got significant worse ratings for usability than manual scaling and the baseline condition. In summary, manual scaling appears to be an equivalent alternative to the baseline condition, but automatic scaling needs to be further improved. A habituation phase or different mathematical functions for scaling might produce better results.

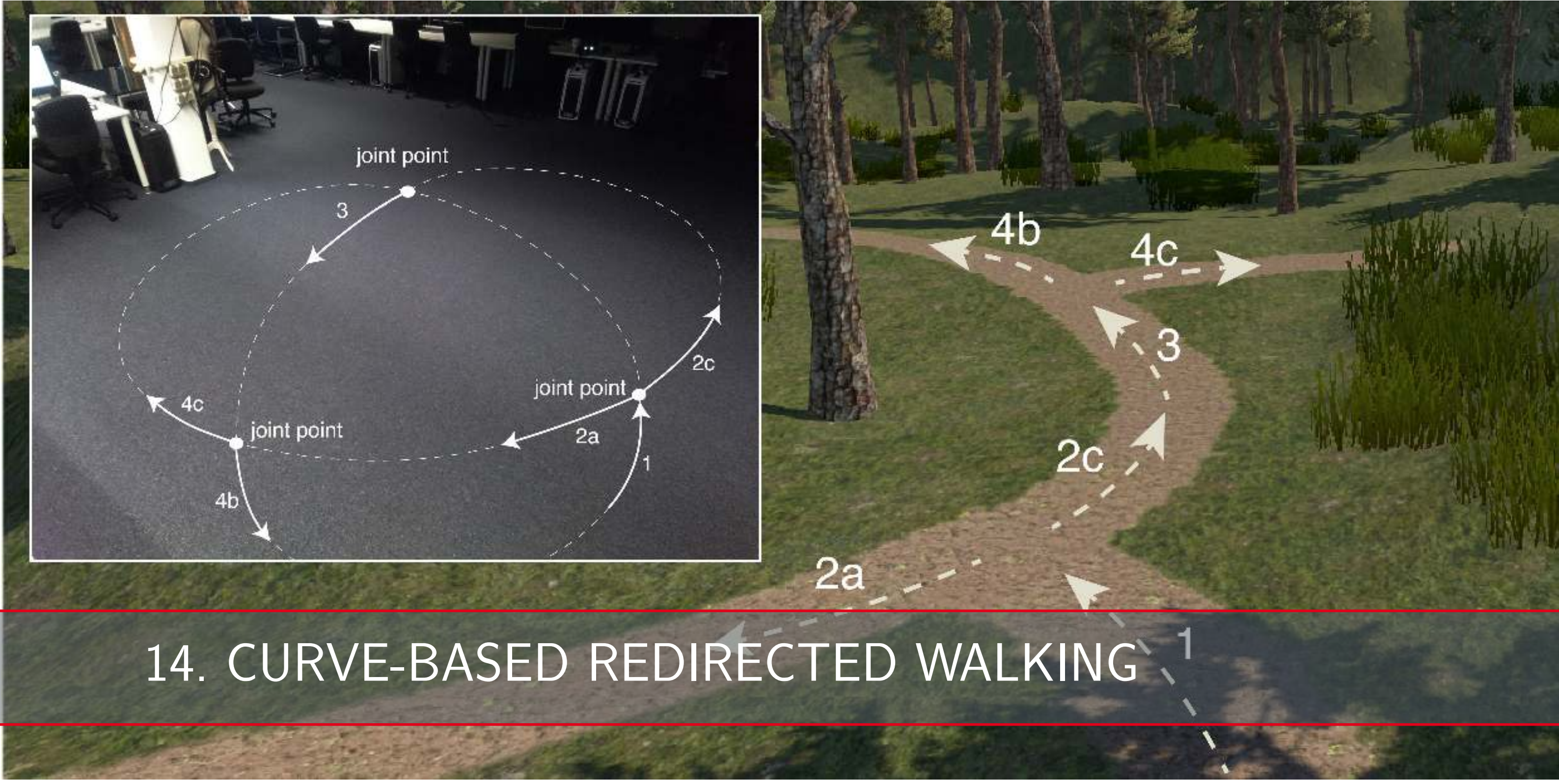

14. CURVE-BASED REDIRECTED WALKING

14.1 Motivation

Considering the broader detection thresholds for bending gains that we observed in the psychophysical experiment in Chapter 8, it becomes reasonable to leverage such curved walking for much smaller physical workspaces compared to those suggested in previous work [Ste+10b].

In this chapter, we present a novel RDW locomotion technique based on a mathematical approach to fit generalized curved paths into a room-scale VR workspace, and we discuss the range of virtual paths that can be simulated by manipulating curvatures. In order to allow near-natural omnidirectional walking, our approach is based on the idea to use several curved paths with intersections between them. At each intersection, the user may continue her walk either on the curve or change the direction by walking on a different curve. Figure 14.2 (a) shows such a situation in the VE with several curves and intersections between them. We conducted a user study to confirm the validity and usability of our approach. Furthermore, we sketch three possibilities to create VEs with such virtual path layouts: (i) manually building the virtual world as well as the virtual paths using a specialised tool, (ii) procedurally generating the virtual world according to pre-defined virtual paths, or (iii) procedurally generating a virtual path layout according to a pre-defined virtual world.

The remainder of this chapter is structured as follows. Section 14.2 presents two different walking configurations for the real-world tracking space. Section 14.3 describes the concept of mapping virtual paths to those real-world walking configurations and introduces three creation methods. Section 14.4 reports the confirmatory study. Section 14.5 discusses our approach and its limitations and Section 14.6 concludes the chapter.

14.2 Real-World Walking Configuration

In contrast to previous work on RDW, the main idea of our approach is to provide users with virtual curved paths on which they can walk. In this section, we describe how we construct a real-world walking configuration with several curved paths in such a way that users can walk on them while remaining within a room-scale VR setup without hitting the boundaries of the space, i. e., without

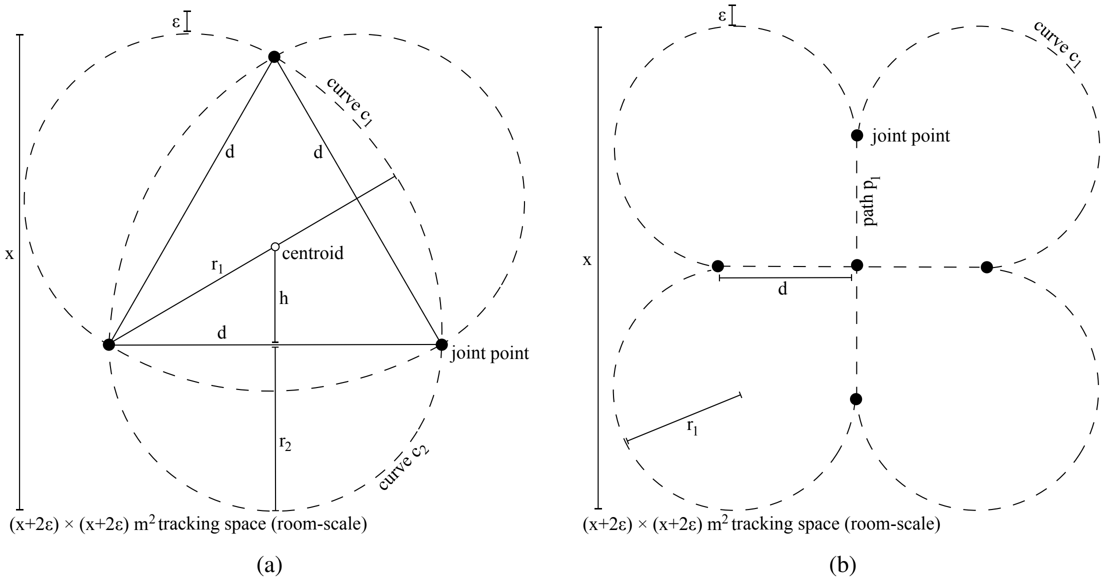

Figure 14.1: Illustration of two physical walking configurations consisting of curves, which fulfill the constraints: three overlapping circles and a Reuleaux triangle with resulting curves 1 and curves 2 and three identical joint points (a), and four adjacent curves and two straight paths resulting in two different joint points (b). Please note, that the joint points in configuration illustrated in (a) provide intersections with four physical directions, whereas the configuration in (b) provides four intersection with three and one intersection with four physical directions.

the need for resetting phases. In theory, numerous configuration could be composed of an infinite number of arbitrary curves. However, in order to allow ecologically realistic as well as smooth walking paths, we define the following constraints for the curves:

- **Constraint 1**: It must be possible that a user can walk infinitely on a curved path with the same curvature direction.
- **Constraint 2**: The curves must provide intersections at *joint points* at which users can change their direction. At the joint points, the curves must satisfy G^0 geometric continuity, i. e., the curves touch in the joint point.
- **Constraint 3**: Two curves at each joint point must satisfy G^1 geometric continuity, i. e., curves share a common tangent direction at the joint points.
- **Constraint 4**: The curves should provide a minimal bending, and therefore use the maximal possible radius approximating a straight path in the room-scale VR setup.

Figure 14.1 shows two different constructions of physical curves, which follow the constraints described above. Figure 14.1 (a) shows a configuration, which consists of an equilateral Reuleaux triangle and three overlapping circles. The Reuleaux triangle is formed by connecting up the vertices of an equilateral triangle with arcs, where the arc between any two vertices has its center at the third vertex. Hence, the Reuleaux triangle with a side length of d leads to the radius of the arcs $r_1 = d$, which is the diameter of the triangle. Next, the three overlapping circles result in three half circles each providing a radius of r_2.

This configuration fulfills all above mentioned constraints:

- *Constraint 1*: At each joint point the user can continue walking in the same direction, i. e., either to the left or to the right. Hence, it is possible to walk infinitely in the same direction; indeed, the amount of curvature slightly change at joint points or might lead to a circle.
- *Constraint 2*: There are three joint points. At each of these joint points, the user can continue walking along four possible directions.

- *Constraint 3*: At each joint point, there are two curves that share a common tangent direction, e. g., curve c_1 and curve c_2.
- *Constraint 4*: The curves of the Reuleaux triangle feature a large radius, but the curves of the three overlapping circles have only a smaller one due to the other constraints, i. e., providing intersections at joint points.

In order to calculate the radii of the different curves, we need to ensure that all three circles plus a safety area fit into the tracking space. Therefore, let all three line segments ranging from the centroid, i. e., geometric mean position of all the points in the Reuleaux triangle, towards the extremes of the circles plus a safety distance ε, fit inside the tracking space with a length of $(x+2\varepsilon)$.

From the construction of the room-scale walking configuration with $d = 2 \cdot r_2$, it follows that

$$r_2 = \frac{x}{2} - h, \tag{14.1}$$

where h is the in-radius of the equilateral triangle given by $r_2/\sqrt{3}$. For these values, we can calculate r_2 and r_1 by

$$r_2 = \frac{\sqrt{3}}{\sqrt{3}+1} \cdot \frac{x}{2} \approx 0.32 \cdot x \tag{14.2}$$

$$r_1 = 2 \cdot r_2 \tag{14.3}$$

Let us consider one example: Valve's HTC Vive setup typically results in a room-scale VR setup with $x \approx 4$ and $\varepsilon \approx 0.2$. According to equation (5) and equation (6), such a room-scale VR setup results in $r_1 \approx 2.5$ and $r_2 \approx 1.25$. These are the radii that we tested in the experiment described in Chapter 8.

Figure 14.1 (b) shows an alternative physical walking configuration, which consist of four adjacent curve segments and two straight paths resulting in five joint points.

Again, this configuration fulfills the above mentioned constraints as well:

- *Constraint 1*: At each joint point the user can go further in the same direction. Exception might occur in situations in which the user moves from path p_1 to curve c_1. At this joint point, she could also choose the other possible and continue walking in the same direction.
- *Constraint 2*: The four outer joint points offer three possible directions, whereas the center joint point offers four directions.
- *Constraint 3*: At each joint point, there are two curves/paths that share a common tangent direction, e.g., path p_1, except the situation described at bullet point 1.
- *Constraint 4*: The radius of the curves is smaller than in the first configuration, but it still exploits the whole available space.

In a similar way as described above the radii of the curve segments can be calculated as follows: Assuming that $d = r_1$, it follows that

$$r_1 = d = \frac{x}{4} \tag{14.4}$$

According to equation (7), the above described room-scale setup with $x \approx 4$ and $\varepsilon \approx 0.2$ results in $r_1 = 1$.

Please note that the first configuration provides larger radii, whereas the second configuration allows straight paths, which might be beneficial for certain situations.

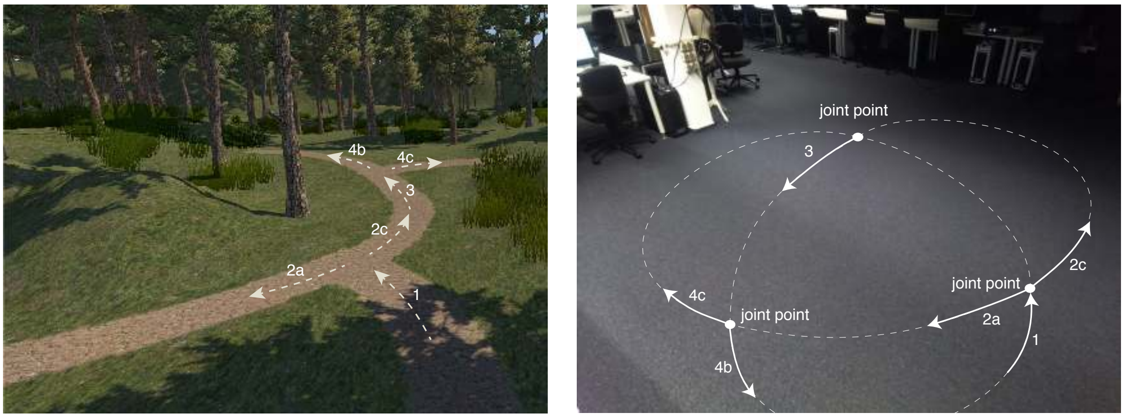

(a) (b)

Figure 14.2: Illustration of our approach in a VR-based outdoor application: a virtual pathway in the VE constructed of several curves and intersections (a) with the corresponding real-world walking configuration consisting of several curve segments in the laboratory (b). The presented application requires approximately a tracked real-word space of about 4m $\times$ 4m, whereas the VE presents approximately a 25m $\times$ 25m large model. The virtual pathways have been generated according to the detection thresholds identified in Chapter 8.

14.3 Virtual Path Layout

Assume a given walking configuration with curves as described above on which a user can walk in the real world. According to the detection thresholds identified in Chapter 8, the virtual curves can provide much larger radii without users being able to identify the discrepancy.

Figure 14.2 shows an example of some virtual paths with a corresponding real-world walking configuration. The layout of the virtual paths as illustrated in Figure 14.2 (a) was constructed by using detection thresholds $2 \leq g_B \leq 4.35$. The arrows and numbers at each path show how virtual and real curves are connected. Starting with path number 1, the user can decide if she wants to go left (2a) or right (2c) at the first joint point. The real-world walking configuration (Figure 14.2 (b)) also offers the possibility to continue straight ahead. However, there is no corresponding virtual path (2b) in the VE since the designer of the VE has not implemented this path. Hence, users should not walk in this direction (see Figure 14.2 (a)). In a similar way, when the user walks along path number 2c there is only one directional option at the next joint point as she has to follow path number 3. According to *constraint 3*, the paths 2c and 3 are directly connected and no turning is required at the joint point. Although, paths 2c and 3 have different radii in the real-world configuration, the virtual paths can be adjusted by different bending gains to seamlessly fit together. Hence, we have to apply a different gain at each joint point depending on the direction the user chose.

Though, we used a visual appearance of the virtual paths, which is similar to those used in the experiments, the visual representation of the curves in the VE is not limited to trail-like paths. The described concept can be applied to curved corridors, hallways, streets, or footprints on the floor (see Figure 14.3). In general, two approaches are possible:

- The VE includes a virtual path layout that consists of curves, which fits one of the predefined walking configurations. As illustrated in Figure 14.2 (a), users have to walk on these predefined paths. The paths could be created manually by hand, by complete procedural generation, or by using a semi-automatic approach (the system suggests paths and the VE designer adjusts them and fine-tunes).
- The VE uses a virtual guidance system like a sequence of footprints, which procedurally

(a) (b)

Figure 14.3: Examples of different implementations of virtual path layouts: footprints in an architectural visualization (a) and curved corridors in a virtual spacecraft game-like scenario (b).

appear during runtime with respect to the user's current position on the walking configuration and the appearance of the virtual world.

In both approaches, users might leave the predefined paths at certain points, e. g., to explore a special location without redirection. One has to ensure that this happens in "safe" areas, such as the inside of the Reuleaux triangle in Figure 14.1 (a) at which no redirection is required.

For the first approach, we implemented three different ways to create virtual worlds with such path layouts which are described in the following subsections.

Manually Building

We developed a tool as a plugin for the Unity3D engine (see Figure 14.5) that helps the designer of the virtual environment to manually build path layouts [1]. First, she has to enter the size of the tracking space. Then, the tool calculates a real-world walking configuration similar to the one in Figure 14.1 that fits the entered size of the tracking space. After this, she can pick a starting joint and create a path, which corresponds to one of the curves of the configuration. For this, the gain needs to be set, which is used to calculate the bending of the virtual path.

This procedure can be repeated several times until the environment consists of many paths. Afterwards, the actual virtual world will be created manually around this path layout using the tools of the engine (see Figure 14.4). When starting the VR application, the tool automatically chooses the correct redirection gain depending on the position of the user. If she crosses an intersection, the redirection is turned off until she enters the next path. Hence, a smooth transition is ensured.

[1] Published as open source software: `https://github.com/klngbhn/RDW_CurvedPathConfigurator`

(a) (b) (c)

Figure 14.4: After the path layout was created, the virtual world can be built around it.

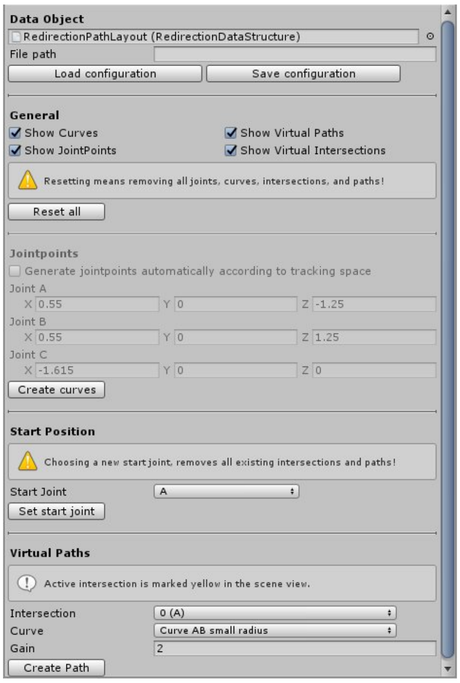

Figure 14.5: The tool for manually creating virtual path layouts was developed as a plugin for the Unity3D engine.

Procedurally Generating Virtual Worlds

Instead of creating the virtual world around the path layout manually, it can also be procedurally generated. We developed an algorithm [Fun18], which generates a terrain randomly but sets trails where a path is supposed to be (see Figure 14.6). This facilitates the creation of the world and relieves the designer.

Procedurally Generating Virtual Paths

In a lot of cases, we have a different situation: The virtual environment is already given and we want to explore it using RDW. Therefore, we have to generate a path layout in such a way that it fits into the given environment. That is, the paths must not collide with obstacles in the world.

For this, we implemented a brute-force algorithm [Win18], which tries to find virtual paths with the smallest possible gain that do not collide with any objects on the terrain (see Figure 14.7).

14.4 Confirmatory Study

To verify the usability of our approach, we performed a brief confirmatory study and gathered qualitative feedback in an application similar to the one illustrated in Figure 14.2.

14.4.1 Materials and Methods

The tracked real-world space had boundaries of 4m $\times$ 4m. The distance between each two vertices of the triangle (see Figure 14.1 (a)) was $d = 2.5$m. Hence, the radii were $r_1 = 2.5$m and $r_2 = 1.25$m.

We used the VE from Figure 14.2 (a), but the virtual paths were arranged differently. At each joint point, several paths branched and a sign showed into one of the four possible directions. The participants were told to follow the signs. Furthermore, there was one letter on each sign. To distract the participants from the redirection, they were told to memorize the letters in correct order. In total, they walked on four path segments with an overall distance of 14.38m. The participants

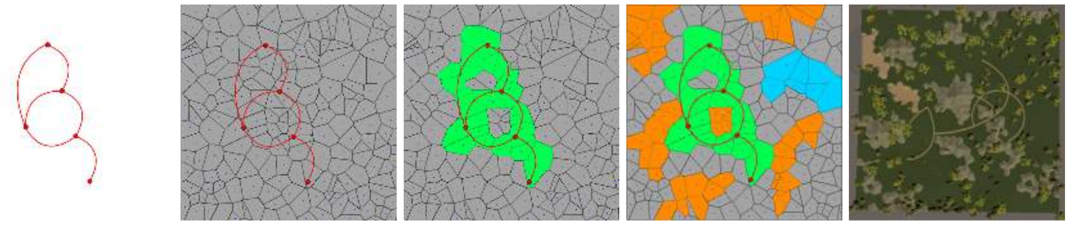

(a) (b) (c) (d) (e)

Figure 14.6: The virtual world is procedurally generated around the path layout (images from [Fun18]).

started at path (1) (see Figure 14.2 (b)). Then, they took the path straight ahead which would be number (2b). At the next joint point, they went to the right (2c) and then to the left (1). Finally, the participants stood on the same real-world position, where they started. However, due to the redirection they were on a completely different position in the virtual world. We applied a bending gain of $g_B = 3$ to all curved paths.

14.4.2 Participants

In total, 10 participants (1 female and 9 male, ages $26-38$, $M = 31.7$) completed the confirmatory study. The participants were students or members of the local department of informatics. All participants had normal or corrected-to-normal vision. Three participants wore glasses during the experiment. One participant reported a disorder of equilibrium. One participant reported a strong eye dominance and one reported a color blindness. No other vision disorders have been reported by the remaining particpants. All participants had participated in an experiment involving head-mounted displays (HMDs) before. The experience of the participants with 3D stereoscopic displays (cinema, games etc.) in a range of 1 (no experience) to 5 (much experience) was $M = 3.7$ ($SD = 1.42$). Most of them had experiences with 3D computer games ($M = 4.2$, $SD = 1.13$, in a range of 1 = no experience to 5 = much experience) and they usually played 5.5 hours per week on average ($SD = 5.78$). The body height of the participants varied between $1.60-1.85$m ($M = 1.76$m, $SD = .07$m). The total time per participant, including pre-questionnaires, instructions, study, post-questionnaires, and debriefing, was 15 minutes. Participants wore the HMD for approximately 5 minutes.

14.4.3 Results

When standing on the last joint point, we asked the participants to point at the real-world start position. Only one participant recognized that he was on the position where he started. The others pointed somewhere near the virtual-world start position ($M = 55.8$, $SD = 24.9$, in degrees), which was orientated 46 degrees from the virtual end position indicating that they could not reliably detect the redirection. After the experiment, the participants were asked to sketch the path that they walked in the VE on a piece of paper. All of them could roughly reproduce the outlines of the VE. They were asked for the total distance of the walked paths as well. On average, they estimated the total distance of the travelled path to be 10.5m ($SD = 5.6$), which corresponds to an underestimation of approximatly 25%. However, distance underestimation of this magnitude is often observed in IVEs [Bru+15].

These result indicate that most of the participants did not notice the redirection, and most of them were actually surprised that they did not walk on the same path as in the VE.

Furthermore, the participants were asked to recall the letters in correct order. Eight of them could successfully reproduce all letters in correct order, whereas two forgot only one letter. We

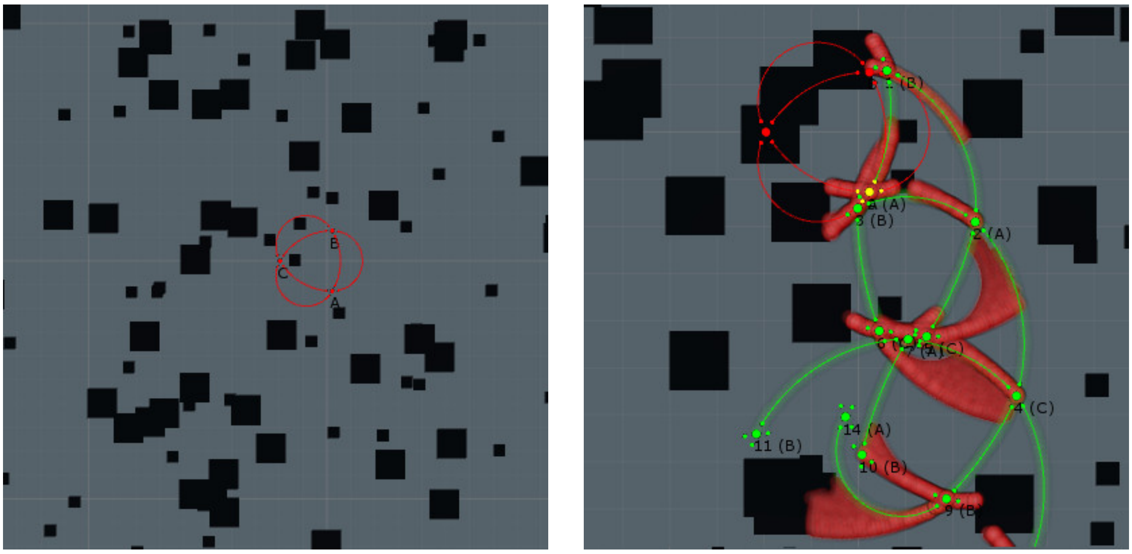

(a) (b)

Figure 14.7: After the real world walking configuration is set (a), the paths are generated (b) and it is tested if they collide with obstacles (black rectangles) in the virtual world. The red parts are tested paths that collided with obstacles and were discarded (images from [Win18]).

measured a mean SSQ-score of 3.97 ($SD = 4.82$) before the experiment, and a mean SSQ-score of 4.91 ($SD = 4.87$) after the experiment. The mean SUS score for the sense of feeling present in the VE was 3.38 ($SD = 0.23$) on a five-point likert scale. Most of them stated, that it did not feel uncomfortable. In the interviews, we asked the participants to estimate whether or not as well as which of the path segments was manipulated. Six participants stated that the third path segment had an identifiable redirection. This is interesting since the gain applied to this path was identical to the one applied to the first and fourth path. Maybe the third segment was perceived differently because to walk on this path the participants had to perform a sharp turn to the right first.

14.5 Discussion

The described approach of leveraging near-natural walking in IVEs to room-scale VR has some limitations. First, it relies on pre-defined paths in the VE. The user is not free to walk in any direction at any time, but she has to stay on the paths most of the time. Probably, there are solutions to this problem, like turning off the redirection at specific locations in the virtual world. Then, the user can utilize a regular one-to-one mapping of real to virtual movements. However, we have not tested such approaches for the bending gains so far.

Furthermore, the paths in the VE are limited to curved paths, at least when the configuration of Figure 14.1 (a) is used. The configuration in Figure 14.1 (b) allows straight paths as well. However, in a lot of situations curved paths are even more appropriate than straight paths. So, this might be neglected for practical use.

Another limitation is the fact that the distances of all paths in the VE have to match the distance of the corresponding paths in the real-world walking configuration. However, it is possible to extend virtual paths by concatenating several real paths without intersections. Unfortunately, this approach will not work the other way around: The distance between two intersections has to be at least the distance of a path in the real-world walking configuration as long as the user walks on the curves defined by the layout.

14.6 Conclusion

In this chapter, we introduced a novel RDW locomotion technique, which is based on guiding users to walk on curved paths. For this purpose, we used bending gains on virtual paths that are mapped to a walking configuration in a room-scale VR setup. As we have shown it is possible to construct a walking configuration in a reasonably small tracking space in such a way that users are able to walk infinitely on a curved path with the same curvature direction or change their direction at defined intersections. As a proof of concept, we derived two different layouts, which fulfill these constraints. The confirmatory study showed that the approach allows to use RDW in room-scale VR without using interruptions or overt resetting phases. Indeed, the approach induces some limitations to the design of a VE as we outlined.

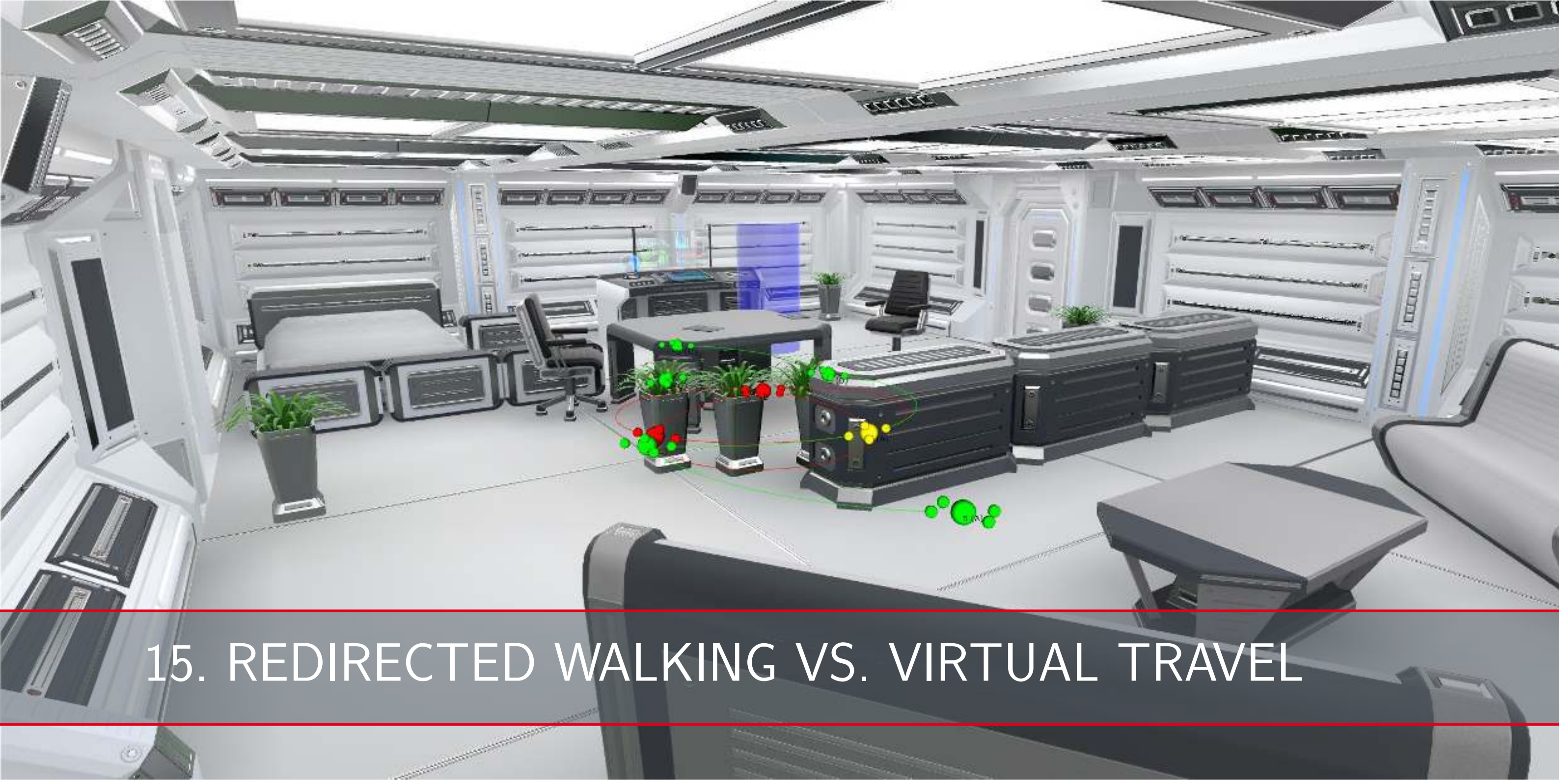

15. REDIRECTED WALKING VS. VIRTUAL TRAVEL

15.1 Motivation

When the users main task is to explore a VE, it is essential that they get a reasonable spatial knowledge of the VE. In this context, the task to acquiring spatial knowledge is called cognitive map building [Bow+04]. To own such a cognitive map is essential for many tasks such as training, architecture, or real estate. Therefore, an important question is if and how a locomotion technique might influence the cognitive map building of the user.

Nowadays, a lot of VR applications make use of some kind of teleportation (TP) technique. With TP techniques, a user can travel over large distances by specifying the travel destination, for example, using an input device such as a wand. After the TP has been initiated, for instance, with a button press, the user's viewpoint is transferred to the corresponding target position either in a discrete jump or using a smooth viewpoint animation. Varying qualities of multimodal feedback provided by different locomotion techniques may evoke or provide different levels of VR sickness, sense of presence, usability as well as spatial knowledge, which in turn might affect task performance, effectiveness, and efficiency. TP does not offer the same quality of multimodal feedback as a walking-based locomotion technique such as RDW. Therefore, an interesting question is how TP performs comparing to RDW.

There is a vast body of literature comparing the performance of different locomotion techniques in VR (see Chapter 3). For instance, it is known that TP causes spatial disorientation [Bow+99], which could be reduced by continuous joystick-based movements, which in turn often lead to VR sickness [LaV00]. And it is known that RDW improves cognitive map building [PFW11]. However, RDW and TP have not been directly compared in typical room-scale VR setups for exploring indoor VEs with a focus on cognitive map building. For these reasons, in this chapter, we present an experiment that compares three different locomotion techniques, mainly with a focus on cognitive map building. In addition, other aspects such as VR sickness, presence, effectiveness, and user preferences are also considered. These techniques are:

1. **JS**: joystick-based,
2. **TP**: teleportation, and
3. **RDW**: redirected walking.

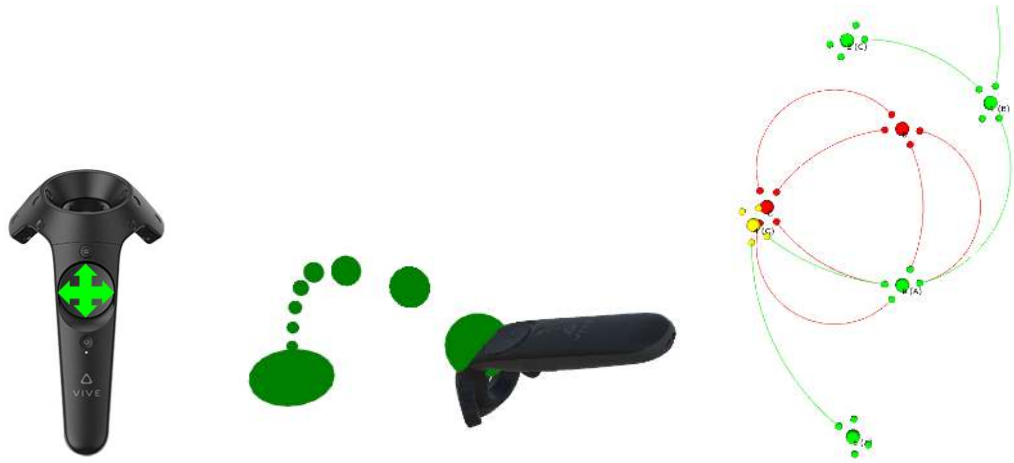

(a) (b) (c)

Figure 15.1: Illustration of the three compared locomotion techniques: Joystick-based navigation (a), Teleportation (b), and curve-based RDW (c): virtual paths (green) are mapped to paths in the real world (red).

Furthermore, recent implementations of these techniques in novel consumer hardware might also affect the performance of these techniques, since several parameters have significantly improved in recent years, such as latency, field of view, resolution etc. Hence, this work also evaluates if a replication of previous results is possible on current hardware.

The remainder of this chapter is structured as follows. Section 15.2 describes in detail the three considered locomotion techniques of the experiment. Section 15.3 explains the experiment. Section 15.4 discusses the results and Section 15.5 concludes the chapter.

15.2 Techniques

The three chosen techniques (JS, TP, and RDW) are locomotion techniques that can be implemented with commodity VR setups without additional bulky or experimental hardware. Furthermore, they provide different qualities of multimodal feedback. RDW offers visual as well as proprioceptive and vestibular feedback. JS offers only visual feedback during transitional movements, whereas the user herself is not moving. However, for rotational movements the user perceives vestibular and proprioceptive cues as well. Instant TP does not provide visual, proprioceptive or vestibular feedback during the teleportation. There is only visual feedback before and after the teleportation. Even though, these techniques provide different feedback about the user's self-motion, each of them can be used to implement locomotion in a restricted tracking space of 4m $\times$ 4m. In particular, we are interested in analyzing the effects on cognitive map building for locomotion techniques that can be applied in current VR applications. Furthermore, the focus of this work is on traveling near and medium distances usually required to explore indoor VEs such as an office building or real estate. The three described techniques JS, TP and RDW are suitable for this.

The joystick-based navigation JS (see Figure 15.1 (a)) was implemented using a touchpad. Using this feature, the user is able to walk forwards, backwards, to the left, and to the right by moving her thumb on the touchpad. Rotations are only possible by actual head rotations.

The teleportation technique TP (see Figure 15.1 (b)) consists of two phases: a pointing phase in which the user chooses a target location and the actual teleportation phase, which is instantly carried out when pressing a button on the controller. During the pointing phase, the user can see a

Figure 15.2: Illustration of the experimental setup: A user (inset) navigates through the VE.

dotted arc that points at the ground of the currently chosen target location.

For RDW (see Figure 15.1 (c)), we used our curve-based RDW approach (see Chapter 14) because it enables walking in room-scale VR without the need for interrupting resetting phases. Indeed, this technique has the limitation that the user must walk on pre-defined paths. In this experiment, the paths are not shown directly to the participants, but are provided by the arrangement of furniture and objects of the VE.

15.3 Experiment

In this experiment, we analyze the effects of locomotion techniques on cognitive map building in VR, and furthermore consider other essential aspects of VEs such as VR sickness, sense of presence, and effectiveness of the locomotion technique. Based on the previous work, we define the following hypotheses:

- H1 RDW will provide better spatial knowledge than JS and TP (based on [Bow+99; PFW11]).
- H2 JS will induce higher VR sickness symptoms than RDW and TP (based on [LaV00]).
- H3 RDW will provide higher sense of presence than JS and TP (based on [Uso+99a]).

15.3.1 Participants

33 participants (9 female, 23 male, and 1 other, ages $21-38$, $M = 25.2$) completed the experiment, i. e., 11 participants per group. The participants were students, who obtained class credit for their participation, or members of the local department of computer science. All of our participants had normal or corrected-to-normal vision. 13 participants wore glasses during the experiment and 1 wore contact lenses. None of our participants reported a disorder of equilibrium. None of our participants reported a strong eye dominance. 1 of our participants reported an astigmatism. No other vision disorders have been reported by our participants. 27 participants had experiences with HMDs before. The most frequent response, i. e., the mode, when asked for the experience with 3D stereoscopic displays (cinema, games etc.) in a range of 1 (no experience) to 5 (much experience) was 4.Most of them had a lot of experience with 3D computer games (mode = 5 in a range of 1 = no experience to 5 = much experience) and they usually played 7.09 hours per week on average ($SD = 8.01$). The body height of the participants varied between $1.57-1.88$m ($M = 1.77$m, $SD = 0.09$m). The total time per participant, including pre-questionnaires, instructions, experiment, post-questionnaires, and debriefing, was 30-40 minutes. Participants wore the HMD

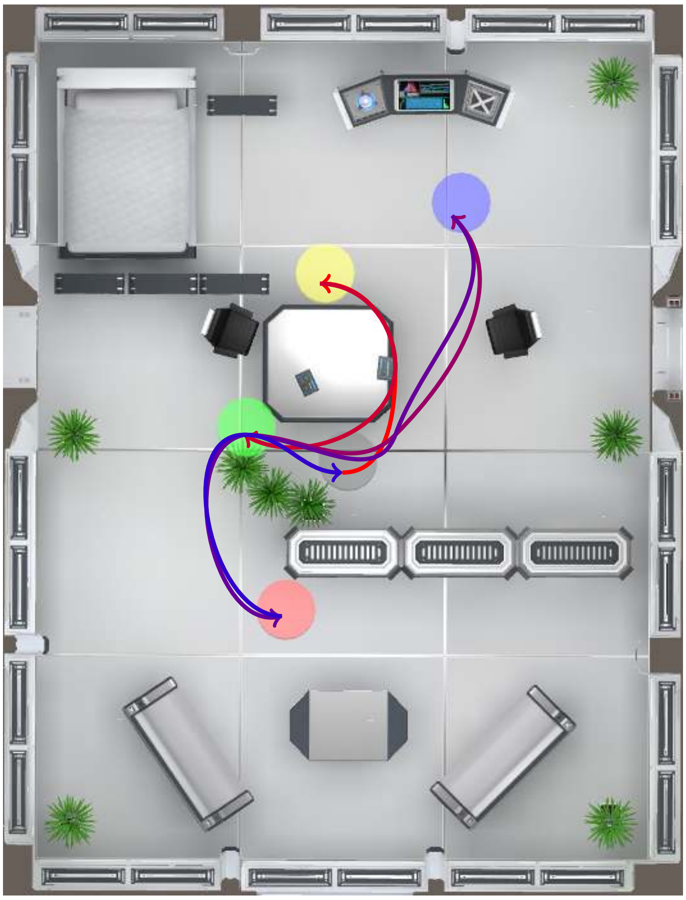

Figure 15.3: The VE as top-down view. Participants started and ended at the grey target. The target order was yellow, green, blue, red.

for approximately 15 minutes. They were allowed to abort the experiment at any time. Before the experiment, all participants received informed consent and detailed instructions on how to perform the experimental task. All participants were naive to the purpose of the experiment. They filled out a demographic questionnaire after the experiment and a questionnaire about their experiences with games, VR, and 3D stereoscopic displays before the experiment.

15.3.2 Materials

The experiment took place in a 6m $\times$ 10m laboratory room. We instructed the participants to wear an HTC Vive HMD (see Figure 15.2), which provides a resolution of 1080 $\times$ 1200 pixels per eye with an approximately 110° diagonal field of view and a refresh rate of 90 hz. Positional and rotational tracking was implemented by a lighthouse tracking system that is delivered with the HTC Vive. The lighthouse system was calibrated so that there was an available walking space of 4m $\times$ 4m. The participants received instructions on slides presented on the HMD. An HTC Vive controller served as an input device via which the participants provided responses during the experiment. For rendering, system control and logging we used an Intel computer with 3.5 GHz Core i7 processor, 32GB of main memory and two Nvidia Geforce GTX 980 graphics card. The VE was rendered using the Unity3D engine 5.6 and showed a room in a science-fiction inspired space station to the participants of the experiment (see Figure 15.2). The room had a size of 13.9m $\times$ 10.4m. For the interior of the VE, we used objects known from the real world that are easy to identify for the participants like chairs, tables, a bed, and plants.

For the RDW technique, we used our own implementation from Chapter 14. We applied bending gains between 1.5 and 3, which are below the detection thresholds identified by the experiment in Chapter 8. For TP and JS, we used the implementations integrated in the VRTK Unity-Plugin[1] without modfying them.

15.3.3 Methods

We used a between-subjects experimental design with 3 groups. Each group used one of the described locomotion techniques resulting in a JS group, a TP group, and a RDW group (see Figure 15.1).

In the experiment, the participants had to navigate to several targets, which were visualized as colored semi-transparent pillars (see Figure 15.2 and Figure 15.3). Only one target was visible at a time. When participants reached the current target, it disappeared and the next target appeared. In total, there were five targets as illustrated in Figure 15.3, which were identical for all three groups. The participants were not allowed to walk through virtual objects. Hence, they walked paths as marked in the figure, for instance.

In order to analyze the effects of the different locomotion techniques on cognitive map building, the participants had to fulfill a pointing task as well as a spatial arrangement task. Finally, they had to sketch the layout of the room. These methods were successfully used in previous experiments [BW95; Cli+09; PFW11; Zan+05].

After reaching the last target, the participants were asked to point to the position of the targets in the order of appearance. During this task, they were able to see the virtual indoor room, but the targets were not displayed anymore. For each target, we saved the angle error between the direction vector to the actual target position and the pointed direction. Using this metric, an angle error of 0° corresponds to a perfect estimation, whereas 180° corresponds to the maximum error resulting from pointing in the opposite direction. Directly after the pointing task, the screen turned black and the participants were asked to verbally estimate the length and width of the room size in meters. After donning off the HMD, the participants had to draw a 2D map of the VE on a piece of paper. Afterwards, the participants were provided with a piece of paper with the outlines of the virtual room as well as a set of all furnitures and objects of the room (see Figure 15.7). The room was scaled down to an extent of 17.5cm $\times$ 23.3cm to fit a DIN A4 format. Of course, all objects were scaled down accordingly as well. The participant's task was to arrange all objects on the 2D ground plan in such a way they remembered them from the VE exposure (see Figure 15.3). If they could not remember the position and orientation of an object, they were told to guess.

We were interested in how far the different locomotion techniques affect cognitive map building while participants were using the techniques. Hence, during the VR exposure participants were not aware that they had to complete the spatial arrangement task and the drawing task, but they were told before to remember the position of the targets. In addition, we measured VR sickness, sense of presence, and user preferences using questionnaires. The participants filled out the SSQ [Ken+93] before and after the experiment. In addition, the participants filled out the SUS presence questionnaire [Uso+99b] after the experiment. The participants were asked how much they liked the used locomotion technique on a five-point Likert scale. Finally, we measured the time, which was required to complete the task.

All participants completed a training trial with two targets, which were not considered in the analysis. They were allowed to stay as long as they wanted in the training environment in order to get familiar with the locomotion techniques.

[1] $https://www.assetstore.unity3d.com/en/\#!/content/64131$

15.3.4 Results

Figure 15.4 shows the results of the pointing task and Table 15.1 shows the average angle errors and standard deviations. A Shapiro-Wilk test did not indicate that the assumption of normality had been violated for target 1. We analyzed the results with an ANOVA at the 5% significance level. We found no significant effect of the locomotion technique on the angle error for target 1; $F(1,31) = .329, p = .571$. A Shapiro-Wilk test reveals that the data is not normally distributed for target 2. Hence, we analyzed the results with a Kruskal-Wallis test at the 5% significance level. We found a significant effect of the locomotion technique on the angle error for target 2 ($p = .00853$). A post-hoc test using Mann-Whitney tests with Bonferroni correction showed significant differences between RDW and TP ($p = .017$) and between JS and TP ($p = .045$). A Shapiro-Wilk test reveals that the data is not normally distributed for target 3. Hence, we analyzed the results with a Kruskal-Wallis test at the 5% significance level. We found no significant effect of the locomotion technique on the angle error for target 3 ($p = .9153$). A Shapiro-Wilk test reveals that the data is not normally distributed for target 4. Hence, we analyzed the results with a Kruskal-Wallis test at the 5% significance level. We found no significant effect of the locomotion technique on the angle error for target 4 ($p = .154$).

We analyzed the estimations for width as well as length of the virtual room. A Shapiro-Wilk test showed that this data is not normally distributed. Therefore, we analyzed the results with a Kruskal-Wallis test at the 5% significance level. We found no significant effect of the locomotion technique on size estimation for length ($p = .54$) and for width ($p = .95$). In general, participants underestimated the size of the room ($M_{length} = 8.62$m, $SD_{length} = 4.21$m and $M_{width} = 7.54$m, $SD_{length} = 4.31$m, while it was actually 13.9m $\times$ 10.4m).

The drawings of the VE (see Figure 15.7) were judged by an uninvolved person on a scale from 1 (totally wrong) to 10 (perfect). This judge was neither a participant nor a supervisor of the experiment. The task for the judge was to compare the drawings to a 2d presentation of the virtual environment. Figure 15.5 shows the results. A Shapiro-Wilk test did not indicate that the assumption of normality had been violated We analyzed the data with an ANOVA at the 5% significance level. We found no significant main effect of the locomotion technique on the drawing score; $F(2,30) = .45, p = .642$.

For the analysis of the arrangement task, we had to exclude 3 participants (one from each group), who did not place all objects. For the remaining 30 participants, we measured the distances between the arranged positions of all objects and their actual positions in the virtual room. Figure 15.5 (c) shows the results of these measurements. A Shapiro-Wilk test showed that this data is not normally distributed. We analyzed the data with a Kruskal-Wallis test at the 5% significance level. We found a significant main effect of the locomotion technique on position judgements ($p = .002$). Tukey post-hoc tests showed significant differences at the 5% significance level between judgements

Target	1st	2nd	3rd	4th
JS	63.55°	51.25°	43.14°	40.24°
	($SD = 52.68$)	($SD = 53.59$)	($SD = 52.57$)	($SD = 29.53$)
TP	45.88°	16.93°	46.86°	17.4°
	($SD = 42.88$)	($SD = 31.71$)	($SD = 50.21$)	($SD = 22.52$)
RDW	75.81°	71.33°	35.67°	29.54°
	($SD = 52.58$)	($SD = 65.48$)	($SD = 48.87$)	($SD = 22.83$)

Table 15.1: Average angle error and standard deviation of the pointing task for JS, TP, and RDW.

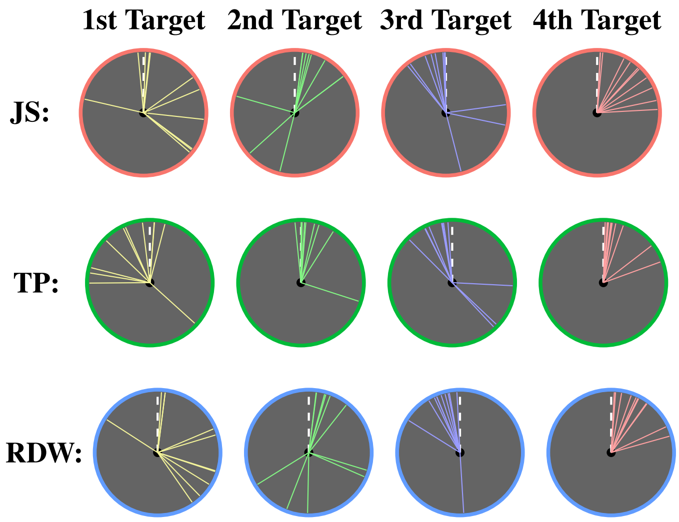

Figure 15.4: Results of the pointing task for JS (top), TP (middle), and RDW (bottom). The center point of the circle is the position of the participant and the dotted white line is the direction to the actual target position. A colored line is the response of one participant. This is shown for the first (yellow), second (green), third (blue), and fourth (red) target.

in conditions for RDW and TP ($p = .0037$) and for RDW and JS ($p = .0151$), but not for TP and JS ($p = .8977$). Hence, users in the RDW group performed significantly better in the spatial arrangement task compared to users from the TP and JS groups.

Additionally, two uninvolved persons judged all arrangements on a scale from 1 (completely wrong) to 10 (perfect). These judges were neither participants nor supervisors of the experiment. The task for the judges was to compare the arrangements to a 2d presentation of the virtual environment. Figure 15.5 shows the results. A Shapiro-Wilk test showed that this data is not normally distributed. We analyzed the data with a Kruskal-Wallis test at the 5% significance level. We found no significant main effect of the locomotion technique on the arrangement score ($p = .1849$).

Table 15.2 shows the mean SSQ-scores (M) and standard deviations (SD). A Shapiro-Wilk test showed that the data is not normally distributed. Hence, we analyzed the results with a Wilcoxon test at the 5% significance level. We found no significant effect of a change of VR sickness for

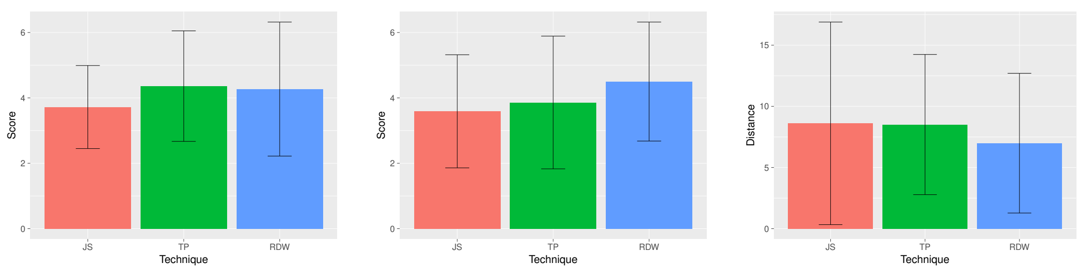

(a) (b) (c)

Figure 15.5: The ratings for the drawing task (a) and the arrangement task (b) as well as the results of the arrangement task (c). The y-axis shows the scores or distances, respectively, and the x-axis the different locomotion techniques.

RDW ($p = .5068$) and TP ($p = .1173$). However, the analysis revealed a significant effect of the increase of VR sickness for the JS group ($p = .03545$).

	JS*	**TP**	**RDW**
M	6.07	12.15	5.61
SD	6.67	10.26	6.96
M	14.73	7.01	6.78
SD	13.62	6.38	6.58

Table 15.2: Mean SSQ-scores before (top) and after (bottom) the experiment for JS, TP, and RDW. The increase for the JS group is statistically significant.

The SUS questionnaire for the sense of feeling present in the VE consists of six questions and five-point Likert scales [Uso+99b]. The SUS-score is taken as the number of $'4'$ and $'5'$ responses. Table 15.3 shows the mean SUS-scores (M) and standard deviations (SD). A Shapiro-Wilk test did not indicate that the assumption of normality had been violated. Therefore, we analyzed the results with an ANOVA at the 5% significance level. We found no significant effect of the locomotion technique on SUS-score; $F(1,31) = 2.065, p = .161$.

	JS	**TP**	**RDW**
M	2.82	3.09	3.82
SD	1.94	1.81	1.08

Table 15.3: Mean SUS-scores for JS, TP, and RDW. No significant effects.

We measured the time participants needed to complete the task from the start position to the last target. Table 15.4 shows the mean travel time (M) and standard deviations (SD). A Shapiro-Wilk test did not indicate that the assumption of normality had been violated. Hence, we analyzed the results with an ANOVA at the 5% significance level. We could not find any significant effect of the locomotion technique on task completation time; $F(1,31) = .115, p = .737$.

	JS	**TP**	**RDW**
M	66.19	54.89	63.49
SD	21.01	21.44	10.22

Table 15.4: Mean travel time in seconds for JS, TP, and RDW. No significant effects.

We asked the participants how much they liked the technique on a five-point Likert scale (see Figure 15.6). A Shapiro-Wilk test showed that this data is not normally distributed. We analyzed the data with a Kruskal-Wallis test at the 5% significance level. We found a significant main effect of the locomotion technique on preference ($p = .0009$). Post-hoc tests using pairwise comparisons with a Mann-Whitney test with Bonferroni correction showed significant differences between preferences in conditions for JS and TP ($p = .0077$) and for JS and RDW ($p = .0031$), but not for TP and RDW ($p = 1.0$). Hence, RDW and TP techniques were preferred significantly over JS.

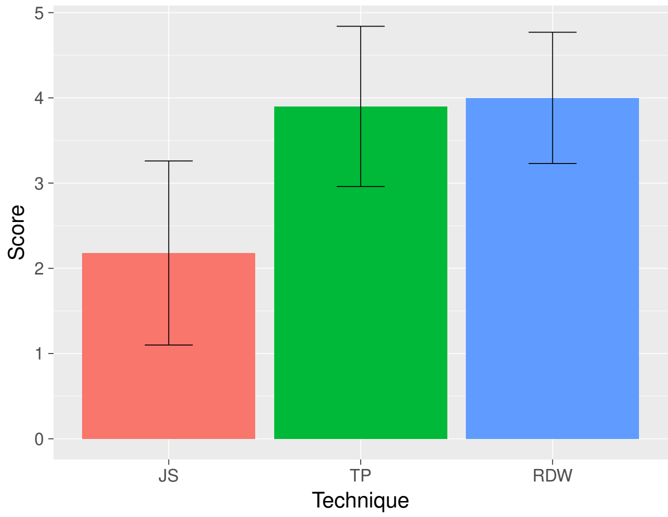

Figure 15.6: The preferences of the participants. The y-axis shows the score and the x-axis the different locomotion techniques.

15.4 Discussion

The results revealed some significant effects of the locomotion techniques. Indeed, regarding the pointing task, we could only find significant differences between the three groups for one of the four targets. This suggest that the choice between the three locomotion techniques does not affect the spatial orientation, especially, when the participants knew that they were supposed to remember the position of the targets. However, participants from the RDW group performed significantly better in recalling the interior of the indoor VE according to the arrangement task measured distances. This means that RDW improves the cognitive map building, especially, for those objects on which the user is not consciously focused. Moreover, the results also show a significant difference between RDW and JS; the group who used RDW locomotion technique performed significantly better compared to participants from the JS group. This finding suggests that visual self-motion feedback alone is not sufficient to provide reliable cognitive map building, but it is important that inner body cues such as the vestibular and proprioceptive sense are stimulated as well. However, the ratings of the drawing task and the arrangement task did not show significant differences between the locomotion techniques. Hence, hypothesis H1 can be partially accepted since we found significant differences only in some of the tasks that were related to spatial knowledge. This might be due to the design of the VE as well as the task in the VE. It might produce more significant results when using a more interleaved environment that involves a search task.

The results show that VR sickness significantly increased for participants from the JS group, which confirms hypothesis H2. These results can be explained by the larger discrepancy between visual and vestibular as well as proprioceptive cues, which occur when users are physically stationary while they navigate and move with a joystick only. But this might also be related to our specific implementation of this technique since speed and FOV affect VR sickness significantly [FF16; NLW17]. We could not find any significant increase of VR sickness for RDW and TP. In the TP group, VR sickness even tends to be decreased after the experiment. This might be because the user is neither moving virtually nor physically and is able to recover during the task.

Regarding the subjective feeling of presence, our findings show that the mean SUS-score for RDW was higher than for the TP group and for the JS group. However, a significant effect could not be found, which could be due to the small effect size. Hence, hypothesis H3 cannot be confirmed.

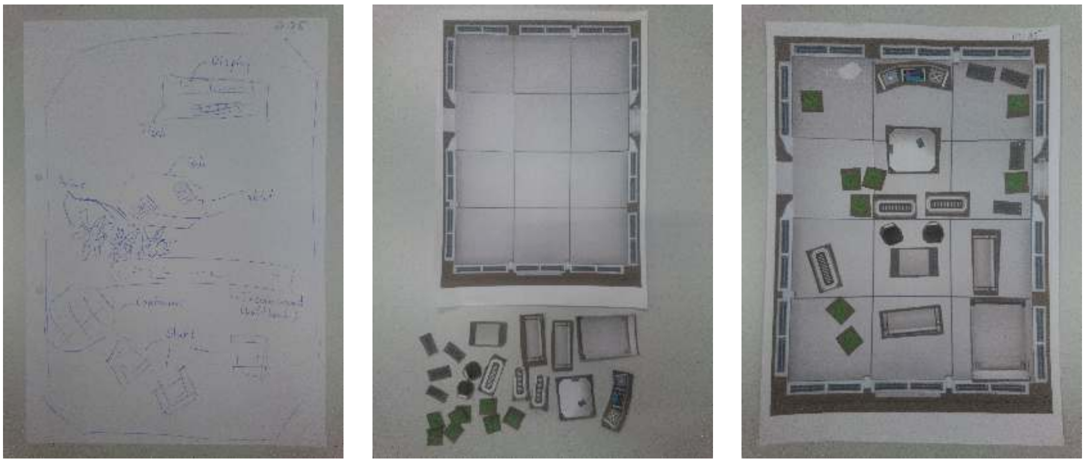

(a) (b) (c)

Figure 15.7: Illustration of the spatial sketching and arrangement tasks: drawing of the virtual room as sketched by one of the participants (a), an empty piece of paper with the outlines of the virtual room and a set of all objects of the room (b), and a finished arrangement of the objects in the virtual room as completed by one of the participants (c).

Our results suggest that the effect is either small and that the time that the users spent in the VE was too short to reveal such an effect.

We could not find any significant differences regarding the task completion time. Of course, the actual travel time, i. e. jumping from one point to another, is lower with TP than with RDW or JS. However, it turned out that the participants actually required some time for rebuilding their spatial orientation before they could aim and activate the next teleport. Furthermore, the arrangement of the objects in the VE (as illustrated in Figure 15.3) required several successive teleportations before users could reach the next target.

We found that participants underestimated the size of the virtual room. Such underestimation effects are often observed in VEs [Bru+15]. At least, our results could not reveal any significant differences in this effect for the different locomotion techniques.

Finally, in the subjective ratings participants significantly preferred RDW and TP techniques over JS. For instance, participants commented that JS did not feel like being in the VE since it was not a presence-enhancing locomotion technique. Another participant stated that he felt a little bit dizzy when using JS. Actually, one participant of the RDW group reported that he was aware of the redirection sometimes but that he did not get sick.

In summary, it can be stated that there are different locomotion techniques for different purposes. In most of the criteria we tested, RDW and TP are superior to JS. But there might be application domains where some of these criteria (e. g. presence) are not important. Hence, the designer of a VR application should choose the locomotion technique that fits best for their context.

15.5 Conclusion

In this chapter, we presented an experiment to evaluate the effects of three different locomotion techniques with a focus on cognitive map building, but we also considered VR sickness, sense of presence, effectiveness and user preferences. Parts of the results show that curve-based RDW allows users to acquire significantly better spatial knowledge compared to the virtual travel techniques. Furthermore, RDW and TP were preferred by most of the participants. Finally, the JS technique lead to a significant increase of VR sickness compared to the other locomotion techniques. However, we could not find any significant effects of the locomotion technique on the user's sense of presence or the effectiveness regarding the required completion time. Summarized, our results suggest that RDW and TP are techniques with different benefits and drawbacks and should be preferred over JS.

16. COLLISION AVOIDANCE WITH SHADOW AVATARS

16.1 Motivation

In a typical living room scenario, it might not only be possible but also necessary to leverage the same physical space for several users. Tracking systems, e. g., the lighthouse stations from HTC Vive, already allow the independent tracking of multiple HMDs. However, since VR users are fully immersed they do not perceive the other co-located users in the physical world. Hence, to avoid collisions and prevent accidents, i. e., to make the VR experience safe for everyone, the physically co-located users have to be displayed in the VE in some situations. An obvious solution for this might be the use of avatars, which is unsuitable in most situations since an avatar usually suggests that there is another user that is part of this VE.

In general, two cases have to be differentiated: (i) the physically co-located VR users collaborate in the same VE, or (ii) the physically co-located VR users do not collaborate in the same VE.

In the latter case, the co-located users are not part of the VE of the other users, and would usually not be visible to each other. In the first case, we have to distinguish between the *physical spatial relations*, i. e., distances and orientations between users in the physical world, and *virtual spatial relations*, i. e., distances and orientations between them in the VE. In several situations, the physical and virtual spatial relations between users do not match, for example, their actual physical distances are different from distances between their avatars in the VE (see Figure 16.1). Such situations can happen due to several reasons, but most often it is caused by the difference between physical and virtual travel. For instance, virtual travel techniques, such as teleportation [Boz+16], move the user's virtual viewpoint while the user itself stays at the same position and orientation in the physical space. Furthermore, redirection techniques are also based on a discrepancy between physical and virtual movements. When applying a curvature gain, the user is virtually moving forward but physically on a curve. Hence, virtual and physical positions do not match; even after small movements.

Therefore, in the VE there should be a distinction between the avatar, i. e., the user's virtual representation, which is displayed at the position in the VE, where the user has virtually navigated to, and the visualization of their physical location that is used only for collision avoidance. This collision avoidance method should warn the user in an effective way if required, but not disturb

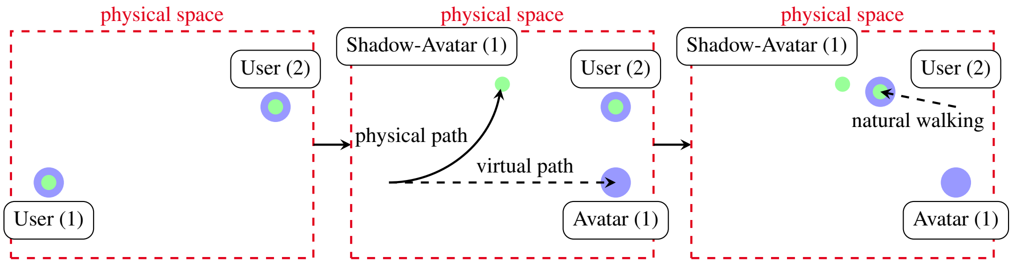

Figure 16.1: Illustration of the basic problem: Two users share the same physical space and collaborate in the same VE. The purple dots mark the users' virtual position and the green dots represent their physical position. In the beginning, both positions match. Then, user 1 walks and is redirected in the physical world. User 2 would only see the representation of the virtual position of user 1 (avatar) and could collide with her physically when he walks around naturally in the physical space. Therefore, the shadow-avatar is needed.

her or break her sense of presence. Indeed, as long as no collision is imminent, the position and orientation of other physically co-located VR users is not important. In general, collision avoidance might be implemented visually as well as through audio or even haptic displays.

In this chapter, we introduce shadow-avatars, which provide a visualization to prevent collisions between users by showing semi-transparent silhouettes of virtual humans representing them at their physical position. We tested two types of these shadow-avatars and evaluated them regarding presence, usability, and number of collisions.

The remainder of this chapter is structured as follows. Section 16.2 presents background work about collision avoidance in social VR. Section 16.3 describes the experiment and discusses the results. Section 16.4 concludes the work.

16.2 Background

Collaborative or Social VR is a topic in VR research since decades [Agr+97; Ben+01]. But there is almost no literature on collision avoidance of physically co-located VR users [Hol12]. Simeone presented a solution to track and visualize non-participants that are not part of the VR experience but in the same room [Sim16]. RDW methods for two users that share a physical space were evaluated regarding their number of collisions [AGR17]. Scavarelli et al. first introduced different collision avoidance techniques for physically co-located VR users [ST17]. They compared avatars, bounding boxes, and camera overlays in a user study. It turned out that each technique has different advantages and disadvantages. The camera overlay produced more collisions but was prefered by most participants. The bounding box had fewest collisions and the avatar offered quicker movement [ST17].

In their study, no collaborators were present in the VE. Therefore, participants stated that it may break presence to see an avatar when the user is actually not part of the VR experience [ST17].

Because of that, we propose shadow avatars in this chapter. Shadow avatars might not be perceived as regular VR users because of their semi-transparent visualization.

16.3 Experiment

In our experiment, we evaluated two different types of shadow-avatars regarding their suitability as method for collision avoidance visualization. Therefore, we considered presence, usability, and

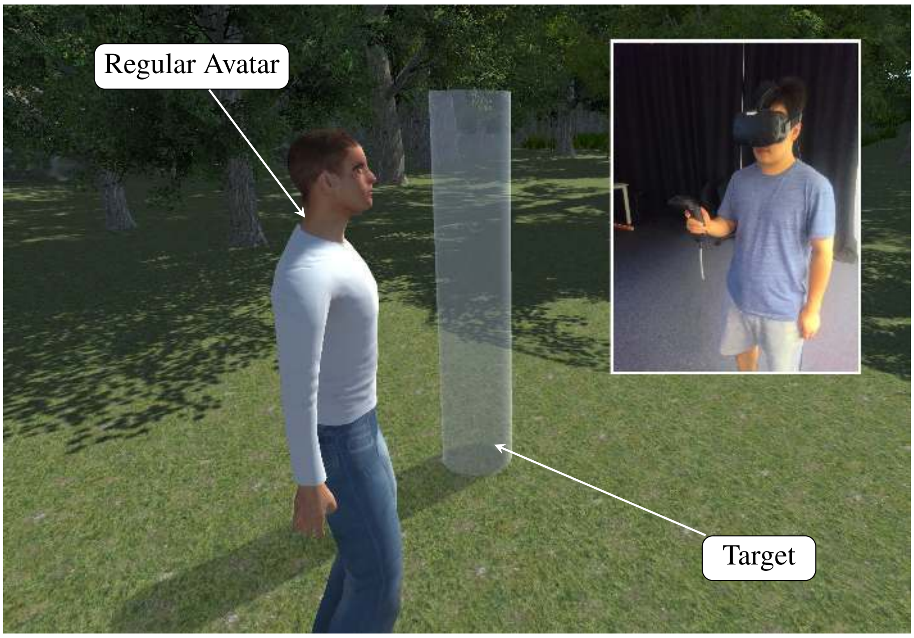

Figure 16.2: A scene from the VE of the experiment: the semi-transparent pillar in the center visualizes a target and the avatar on the left just crosses the walking path of the participant. The inset shows a participant of the experiment wearing an HTC Vive HMD.

number of collisions. In the experiment, for the safety of the participants, the shadow-avatars were just simulated, so that no actual collisions with another physical user could occur.

16.3.1 Participants

22 participants (8 female, 14 male, ages $18-31$, $M=23.9$) completed the experiment. The participants were students, who obtained class credit for their participation, or members of the local department of computer science. The most frequent response, i. e., the mode, when asked for the experience with VR in a range of 1 (no experience) to 5 (much experience) was 4 ($M=3.05$, $SD=1.29$). The experience with 3D computer games was individually different. When asked for played hours per week participants answered 9×0 hours, $6\times 1-5$ hours, $2\times 6-10$ hours, $4\times 11-15$ hours, and $1\times > 15$ hours. The total time per participant, including pre-questionnaires, instructions, experiment, post-questionnaires, and debriefing, was around 30 minutes. Participants wore the HMD for approximately 15 minutes. They were allowed to abort the experiment at any time. Before the experiment, all participants provided informed consent and received detailed instructions on how to perform the experimental task. They filled out a demographic questionnaire and a questionnaire about their experiences with games and VR after the experiment.

16.3.2 Materials

The experiment took place in a 6×10 m laboratory room. We instructed the participants to wear an HTC Vive HMD (see Figure 16.2 inset), which provides a resolution of 1080×1200 pixels per eye with an approximately $110°$ diagonal field of view and a refresh rate of 90 hz. Positional and rotational tracking was implemented by a lighthouse tracking system that is delivered with the HTC Vive. The lighthouse system was calibrated so that there was an available walking space of 4×4 m. An HTC Vive controller served as an input device via which the participants provided responses during the experiment. For rendering, system control and logging we used an Intel computer with

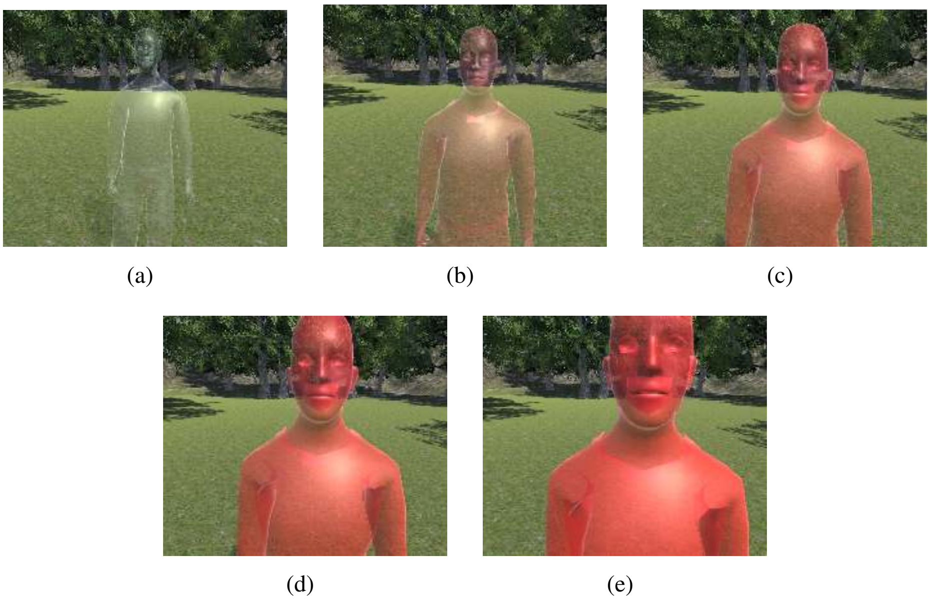

Figure 16.3: The shadow-avatars that were used in the experiment: condition C1 used the avatar from (a) that was continuously visible throughout the condition, and condition C2 used a shadow-avatar that was only visible in a range of 1.25 m around the participant (a) and dynamically changed its appearance depending on the distance to the participant. The closer the participant came, the redder the avatar became (b-e).

3.2 GHz Core i7 processor, 16GB of main memory and two Nvidia Geforce GTX 1080 graphics cards. The VE was rendered using the Unity3D engine 2017.1 and showed a natural outdoor scene including trees and grass to the participants of the experiment (see Figure 16.2).

16.3.3 Methods

We used a within-subjects experimental design. Each participant experienced three different conditions:

- C0: baseline condition without any avatar,
- C1: condition with avatar in combination with a continuously visible shadow-avatar, and
- C2: condition with avatar in combination with a dynamically visible shadow-avatar.

The baseline condition was the first condition for all participants while the order of the other two conditions was counter-balanced. In each condition, the participants had to navigate to several targets by natural walking. The targets were visualized as semi-transparent pillars (see Figure 16.2). Only one target was visible at a time. When participants reached the current target, it lit up green and the participants had to press a button on the controller. Then, it disappeared and the next target appeared. The distance between two targets was 3.5 m. In total, participants completed 16 walks per condition, i. e., walking 16 times the distance of 3.5 m.

In conditions C1 and C2, two avatars crossed the walking path of the participant: One regular avatar and one shadow-avatar (see Figure 16.3). In condition C1, the shadow-avatar was continuously visible and did not change its appearance. In condition C2, the shadow-avatar became only visible within a range of 1.25 m around the participant and dynamically changed its appearance depending on the distance to the participant: the closer the participant came, the redder the avatar became. We decided to use two avatars in each condition, the regular avatar and the shadow-avatar, because we wanted to simulate the mentioned scenario where physically co-located users share the

Condition	Regular Avatar	Shadow-Avatar
C1 (continuous):	M = 1.81	M = 1.95
	($SD = 1.4$)	($SD = 1.86$)
C2 (dynamic):	**M = 1.68**	**M = 2.45**
	($SD = 1.98$)	($SD = 1.68$)

Table 16.1: Mean number of collisions with regular and shadow-avatars in conditions C1 and C2. Significant differences are marked in bold text.

same VE, and thus, two types of visualizations are necessary (see Section 16.1). In each walk, one of both avatars in the scene crossed the walking path of the participant. Which avatar crossed the scene was randomized, but both avatars occured equally frequent. The exact crossing position and its point of time were randomized. We mentioned that the avatars might cross the walking path of the participants but we did not instruct them how they should behave in case of a collision. We assumed that they would unconsciously avoid collisions with avatars when the visualization of the avatars induces social presence to the participants. This way, a lower number of collisions indicates a more suitable avatar visualization.

The number of collisions with both avatars, the regular and the shadow-avatar, was measured. A collision was counted when the distance between participant and avatar was less than 0.5m. Furthermore, we measured the time per walk. The baseline condition, which did not include any avatars, was just used to measure time and walking paths in a regular VR setup. We measured VR sickness, sense of presence, usability and user preferences using questionnaires. The participants filled out the Kennedy-Lane simulator sickness questionnaire (SSQ) [Ken+93] before and after the experiment. In addition, the participants filled out the igroup presence questionnaire (IPQ) [SFR99] after each condition and the system usability scale (SUS) questionnaire [Bro96] after condition C1 and condition C2. Furthermore, they were asked to give qualitative feedback.

16.3.4 Results

Figure 16.4 (a) shows the results of the user preferences. 17 participants preferred the continuously visible shadow-avatar and 5 participants preferred the dynamically visible shadow-avatar.

Table 16.1 shows the mean number of collisions with regular and shadow-avatars in the different conditions. A Shapiro-Wilk test showed that the data is not normally distributed. We analyzed the results with several Wilcoxon tests at the 5% significance level. We found no significant effect of the type of avatar (regular vs. shadow) on number of collisions in condition C1 ($p = .726$) but in condition C2 ($p = .018$). This means, participants collided significantly more often with the dynamically visible shadow-avatar than with the regular avatar. We found no significant difference between continuously and dynamically visible shadow-avatars ($p = .119$).

Table 16.2 shows the mean walking times in the different conditions. A Shapiro-Wilk test showed that the data is not normally distributed. We analyzed the results with several Wilcoxon tests at the 5% significance level. We found no significant effect of the type of avatar (regular vs. shadow) on walking times in condition C1 ($p = .592$) but in condition C2 ($p = .02$). This means, participants needed significantly longer when the dynamically visible shadow-avatar crossed their path than when the regular avatar crossed their path. Furthermore, we found a significant difference between continuously and dynamically visible shadow-avatars regarding walking times ($p = .01$)

Figure 16.4 (b) shows the results of the SUS questionnaire. We measured a mean SUS-score of 84.43 ($SD = 11.47$) for the continuously visible shadow-avatar and a mean SUS-score of 76.36

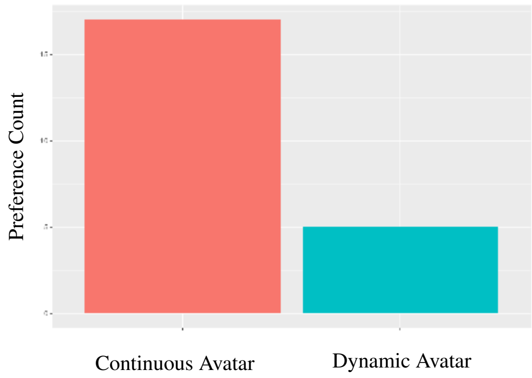

(a)

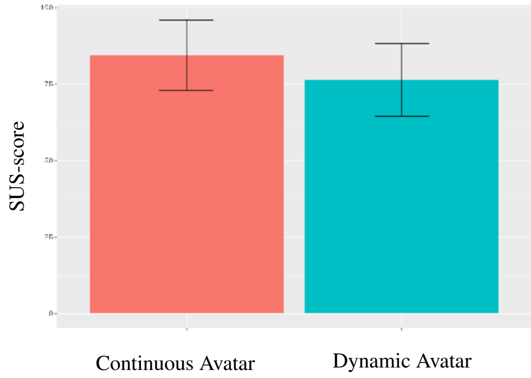

(b)

Figure 16.4: The continuously visible shadow-avatar was clearly prefered by the participants (a). We found a significant effect of the type of shadow-avatar on usability (b).

($SD = 11.89$) for the dynamically visible shadow-avatar. A Shapiro-Wilk test showed that the data is not normally distributed. We analyzed the results with a Wilcoxon test at the 5% significance level. We found a significant effect of the type of shadow-avatar on usability ($p = .001$).

The mean IPQ-score for the sense of feeling present in the VE was 4.35 ($SD = 0.48$) for the baseline condition, 4.27 ($SD = 0.66$) for the continuously visible shadow-avatar and 4.26 ($SD = 0.59$) for the dynamically visible shadow-avatar. A Shapiro-Wilk test did not indicate that the assumption of normality had been violated. We analyzed the results with an ANOVA at the 5% significance level. We found no significant effect of the type of shadow-avatar on presence; $F(2,63) = .164, p = .849$.

We measured a mean SSQ-score of 11.56 ($SD = 20.08$) before the experiment, and a mean SSQ-score of 12.58 ($SD = 17.86$) after the experiment A Shapiro-Wilk test showed that the data is not normally distributed. Hence, we analyzed the results with a Wilcoxon test at the 5% significance level. We found no significant difference of the SSQ-score ($p = .526$).

16.3.5 Discussion

The results suggest that it might be advantageous to use continuously visible shadow-avatars. They were preferred by most participants and showed a significantly higher usability. Moreover, continuously visible shadow-avatars produced significantly less collisions than regular avatars and needed less walking times. Although, we did not find a significant difference between continuously

Condition	Regular Avatar	Shadow-Avatar
C1 (continuous):	M = 6.18	**M = 6.08**
	($SD = 1.0$)	($SD = 0.96$)
C2 (dynamic):	**M = 6.28**	**M = 6.67**
	($SD = 1.27$)	($SD = 1.45$)

Table 16.2: Mean walking times in seconds in conditions C1 and C2 and seperated by walks that were crossed by the regular avatar or by the shadow-avatar. Significant differences are marked in bold text.

and dynamically visible shadow-avatars, we could not observe an effect between dynamically visible shadow-avatars and regular avatars as well. The better performance of continuously visible shadow-avatars might be due to the better predictability. The participants could see the shadow-avatar all the time and did not have to fear a spontaneously appearing obstacle. This might also be the reason why they walked slower in the condition with dynamically visible shadow-avatars.

However, we did not find any significant difference between the conditions regarding the sense of presence. Hence, it seems as if the continuously visible shadow-avatar did not disturb the participants' feeling of being in a virtual environment.

During the qualitative feedback session after the experiment, multiple participants stated that they liked the color adjustments of the dynamically visible shadow-avatar. But they just felt more safe when they could see the potential obstacle the whole time. Probably, a combination of these two types of shadow-avatars might be an appropriate approach: The shadow-avatar should be continuously but faintly visible and increase its intensity when a user comes closer.

16.4 Conclusion

In this chapter, we introduced shadow-avatars as visualization method for avoiding human collisions when physically co-located VR users are redirected in the same VE. Two different types of shadow-avatars were compared in a user study and results suggest that these shadow-avatars should be continuously visible to the VR users.

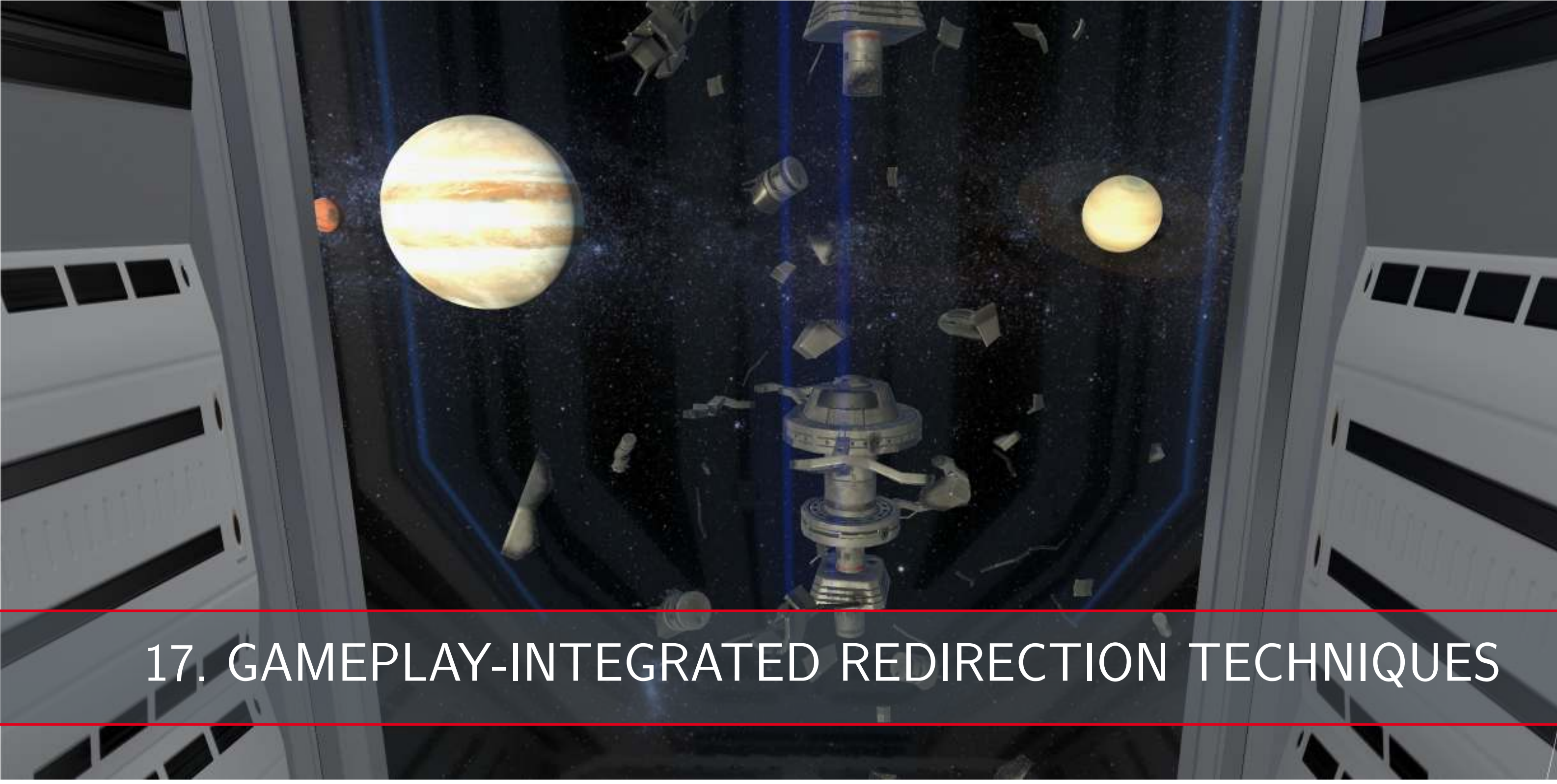

17. GAMEPLAY-INTEGRATED REDIRECTION TECHNIQUES

17.1 Motivation

Previous approaches to RDW often focused on finding generalized solutions for unlimited walking in VR which can be used in any IVE - with only limited success. For instance, algorithms like steer-to-center or steer-to-orbit try to keep the user inside the walkable space [Raz05], but they work only for large tracking spaces and even cannot guarantee that the user does not hit the boundaries. Hence, such issues especially occur in small, i.e., room-scale, VR setups [Azm+15]. Therefore, reorientation phases are necessary, which turn the user back to the walkable area (see Chapter 3.4.2). Often, these phases are not subtle and induce a break of presence in the user. The high sense of presence, which is supposed to be correlated with natural walking in IVEs, is impaired.

However, RDW via gains is not the only locomotion technique that enables near-natural walking in virtual worlds. Another approach to implement real walking in VR is to use impossible or flexible spaces [Vas+13], i. e., self-overlapping or changing architectural layouts. Instead of the user's viewpoint, in these spaces, the VE itself is manipulated with the goal to enlarge the explorable virtual space (see Chapter 3.4.4).

In this chapter, we present a new approach that couples the redirection techniques directly to the IVE, without using generalizing algorithms, and integrates them with other interactions, gameplay, and narration.

Furthermore, we show how RDW techniques and impossible spaces can be combined in order to achieve a novel user experience that enables a user to explore even larger VEs than when using just a single approach. Therefore, we created two playful VR experiences in a science-fiction inspired spacestation which make use of such combined redirection techniques. Gameplay and narration were directly integrated with the redirection techniques. Our approach was evaluated in a confirmatory study regarding usability and validity.

The remainder of this chapter is structured as follows. Section 17.2 describes the VR experience called *Redirected Spaces* and Section 17.3 the one called *Space Walk*. Section 17.4 presents the confirmatory study and Section 17.5 concludes the chapter.

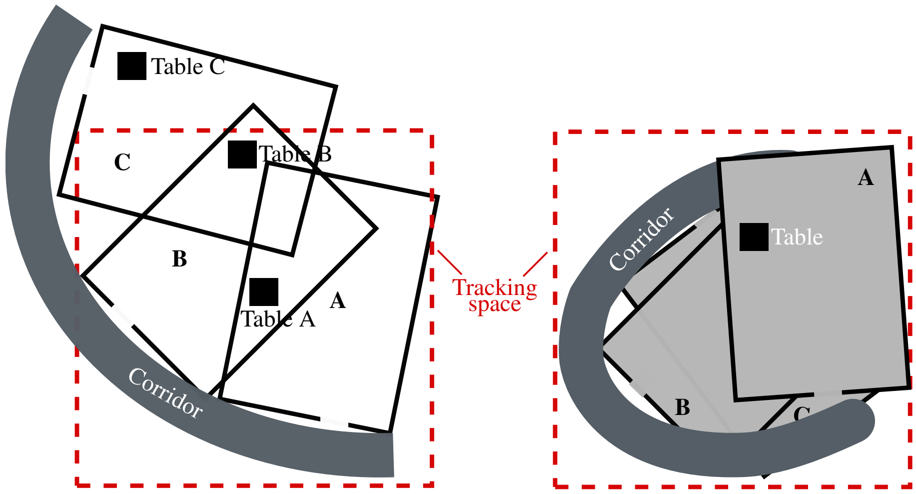

Figure 17.1: An illustration of the combination of redirected walking and impossible spaces. The corridor and the rooms are larger than the available tracking space although the rooms overlap already (left). When applying a redirection gain at the corridor the VE is compressed even more and the whole setup fits into the tracking space (right). There, the virtual tables are merged into one physical table.

17.2 Experience 1: Redirected Spaces

The VR experience combines two techniques to enable natural walking in a restricted tracking space:

- **Redirected Walking** using bending gains when users walk on virtually curved paths, and
- **Impossible Spaces** with subtle overlapping rooms.

This is done by using a curved corridor that connects three virtual rooms A, B and C (see Figure 17.1). The virtual rooms overlap by approximately 50%. As soon as the user opens the door to one of the three rooms, all other rooms are hidden, so she can not directly see the actual overlap of the different rooms. When walking through the corridor a subtle redirection gain is applied that forces the user to walk on an even more curved path in the physical world. The redirection is turned off when the user enters a room. Hence, she can explore the room with a one-to-one mapping. When the user leaves a room the bending gain is turned on again, and she can continue walking down the corridor until she enters the next room.

Using a curved corridor supports the illusion of the VR experience in two ways:

- (i) Applying bending gains to an already curved path is less obvious compared to curvature gains applied to a straight path (see Chapter 8).
- (ii) The detection of overlapping spaces is more difficult if a curved corridor connects these spaces [VK17b].

The redirection and the bending of the corridor is designed in such a way that these rooms always fit into the tracking space. This way, the user benefits from a good use of the available space. The entire virtual environment can be explored by real walking within a tracking space of $4m \times 4m$. The design of our curve-based RDW approach (see Chapter 14) allows it to connect several curved corridors to further extend the size of the VE.

Additionally, there are virtual tables in the rooms which are related to a physical table in the real world to provide passive haptic feedback [Ste+08c] Due to the redirection and the overlapping it is possible to use just one physical table that serves as a proxy object for several virtual tables.

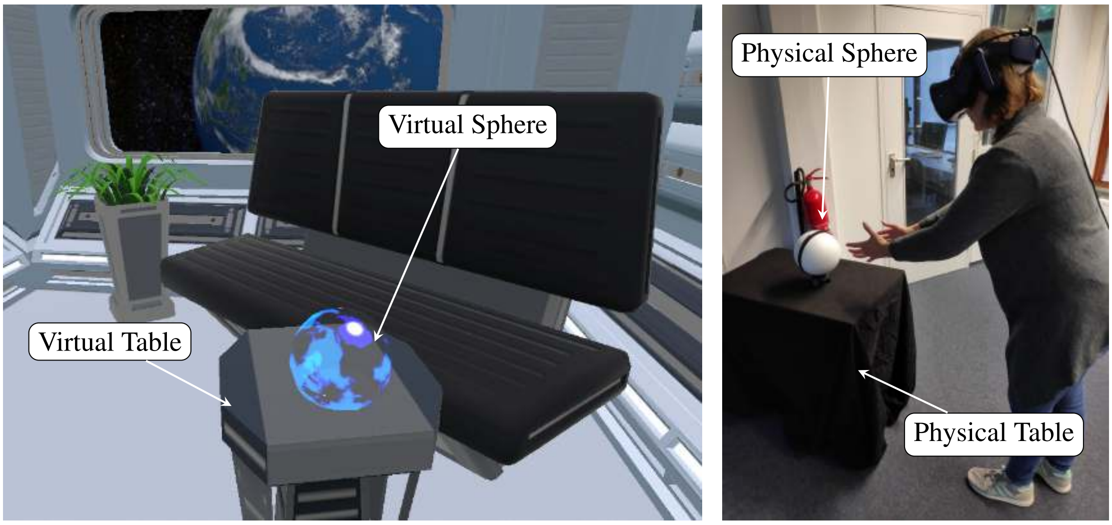

(a) (b)

Figure 17.2: One room of the VR experience containing a virtual table and a virtual sphere (a). The task of the user is to take the sphere and bring it to the next room. Physically, there is only one table in the real world (b).

The visual appearance of the experience is a virtual space station inspired by science-fiction literature or cinematography that could be used, for instance, in a VR game context.

The user has the task to enter the first room and take a sphere, which was placed on the table (see Figure 17.2). There is a physical sphere on the table in the real room that is tracked as well. Then, the user has to leave the room and walk to the next room while she is carrying the sphere in her hands. There, she can put it back on the table. In the real world, she is guided back to the same phyiscal table where she picked up the sphere. However, in the virtual world, she is in a completely different room.

17.3 Experience 2: Space Walk

The VR experience presents a combination of three different redirection techniques which are subtly integrated with the gameplay and narration to perfectly fit the given environment. These techniques are (i) bending gains (see Chapter 8), (ii) rotation gains [Ste+10b], and (iii) impossible spaces [Sum+12b]. Hence, in addition to the techniques from Experience 1, rotation gains were added. The redirection techniques allow users to explore a virtual space station of $45m^2$ in a room-scale setup of $4m \times 4m$ by natural walking only. A strength of our approach is that this area can easily be extended by just integrating more instances of redirection techniques into the virtual environment.

These techniques are applied at specific locations and moments in the IVE (see Figure 17.3). The complete VR experience has a connecting narrative that blends together the science fiction setting and the interactions. When the user dons on the HMD and starts the experience, she is transported as astronaut into an abandoned space station. Her mission is to explore the station, which includes simple puzzles and tasks. The above mentioned redirection techniques are subtly integrated with those tasks. For instance, during the experience, a laser barrier is in the middle of a corridor and blocks the user's way (see Figure 17.4). Hence, the user needs to unmount the laser beams and attach them to the other side of the corridor. This task requires turning back and forth

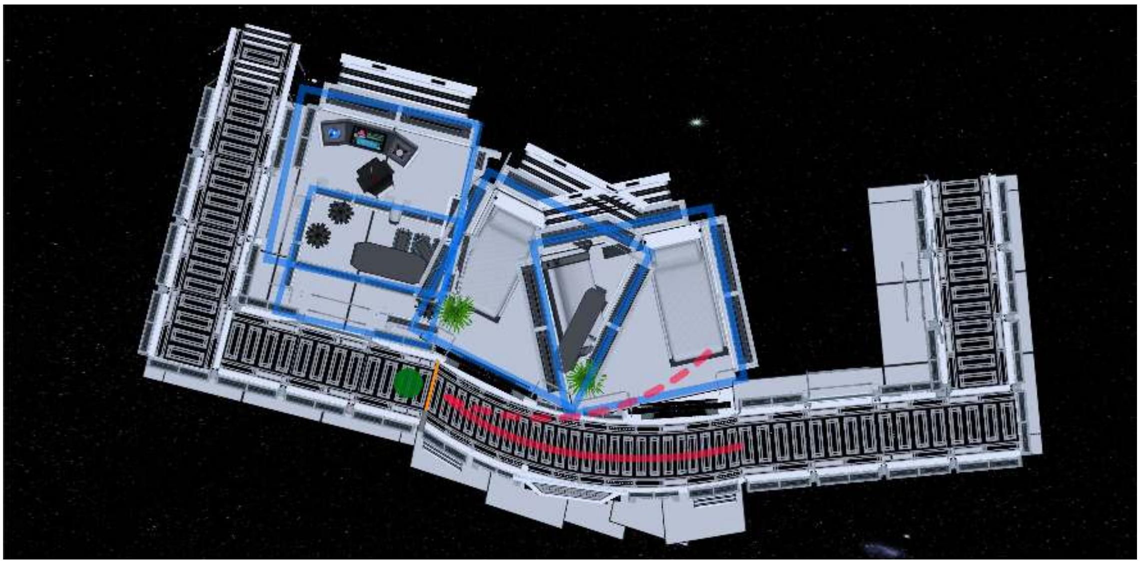

Figure 17.3: An overview of the environment and its integrated redirection techniques: impossible spaces (blue rectangles), bending gains (red lines), and rotation gains (green point).

several times. At this point, we apply rotation gains which allows us to rotate the user virtually more than physically. After all laser beams have been moved to the other side, the whole IVE is rotated around the user and spaces that were not in the walkable area before can be explored now (see Figure 17.4 insets).

Furthermore, in order to present the RDW walking techniques also for bystanders, we include a novel way of presenting the redirection techniques by projecting a top-down view of the IVE to the ground under the VR user (see Figure 17.5).

17.4 Confirmatory Study

We conducted a confirmatory study for Experience 1 *Redirected Spaces* to evaluate usability and gather informal qualitative feedback for our approach.

17.4.1 Materials and Methods

The experiment took place in a 12m $\times$ 6m laboratory room. We instructed the participants to wear an HTC Vive HMD, which provides a resolution of 1080×1200 pixels per eye with an approximately 110° diagonal field of view and a refresh rate of 90 hz. Positional tracking was done by a lighthouse tracking system that is delivered with the HTC Vive. The lighthouse system was calibrated so that there was an available walking space of 4m $\times$ 4m. For rendering, system control and logging we used an Intel computer with 3.5GHz Core i7 processor, 32GB of main memory and two Nvidia Geforce GTX 980 graphics card. The virtual environment was rendered using the Unity3D engine 2017.

The participants were not told about the redirection techniques. They were instructed to follow the instructions of a robotic guide in the virtual world. The guide explained the different tasks, such as *"Please, go to the first room", "Take the sphere"* etc. After the participants placed the sphere on the table in the second room, the scene faded out and they could remove the HMD.

17.4.2 Participants

19 participants (7 female and 12 male, ages $21-34$, $M = 24.63$) completed the experiment. The participants were students or members of the local department of informatics, who obtained class

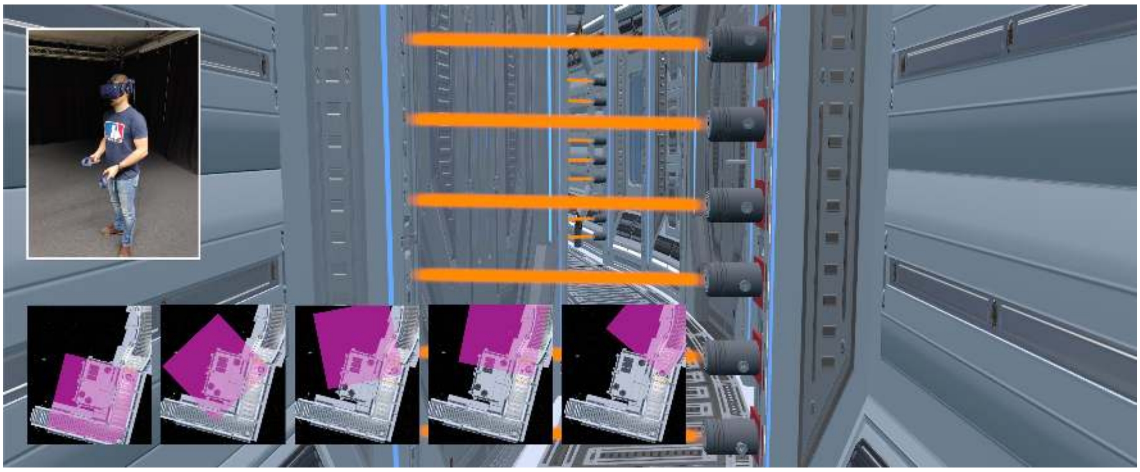

Figure 17.4: Illustration of an interaction task which is integrated within a rotation gain: The user (top left inset) has to move each laser beam (background image) from one wall to another while the virtual environment is turned around him (bottom). The pink area marks the real world tracking space.

credit for their participation. All of our participants had normal or corrected-to-normal vision. Ten participants wore glasses and one wore contact lenses during the experiment. None of our participants reported a disorder of equilibrium. None of our participants reported a strong eye dominance. No other vision disorders have been reported by our participants. 12 participants had participated in an experiment involving HMDs before. The experience of the participants with 3D stereoscopic displays (cinema, games etc.) in a range of 1 (no experience) to 5 (much experience) was $M = 3.47$ ($SD = .9$). Most of them had experiences with 3D computer games ($M = 3.74$, $SD = 1.41$, in a range of 1 = no experience to 5 = much experience) and they usually played 6.74 hours per week on average ($SD = 8.44$). The body height of the participants varied between $1.65 - 1.9$m ($M = 1.76$m, $SD = .08$m). The total time per participant, including pre-questionnaires, instructions, experiment, breaks, post-questionnaires, and debriefing, was 20 minutes. Participants wore the HMD for approximately $5 - 10$ minutes.

17.4.3 Results

We measured a mean SSQ-score of 7.25 ($SD = 7.54$) before the experiment, and a mean SSQ-score of 3.51 ($SD = 5.71$) after the experiment. The mean SUS score for the sense of feeling present in the VE was 3.77 ($SD = 0.34$) on a five-point Likert scale.

Furthermore, the participants were asked if they noticed something special or strange during the experience. 6 participants explicitly answered that they did not notice anything. 2 participants stated that they felt a redirection and 1 noticed that the table was in the same spot both times. The rest reported different issues of the experience that are not related to redirection.

We also asked for each redirection technique individually if the participants detected it. 5 participants noticed that there was a slight rotation when walking through the corridor. No participant noticed that the two rooms virtually overlapped. 7 participants noticed that the second virtual table was at the same position in the real world as the first one. In case they detected some redirection, participants were asked how and why they noticed. 6 participants said that they saw only one physical table in the room before they donned on the HMD. Hence, they concluded from it that it had to be the same table. 2 participants said that they already had experience with RDW and, therefore, were aware of it. 2 other participants stated that they noticed discrepancies between virtual and real movements.

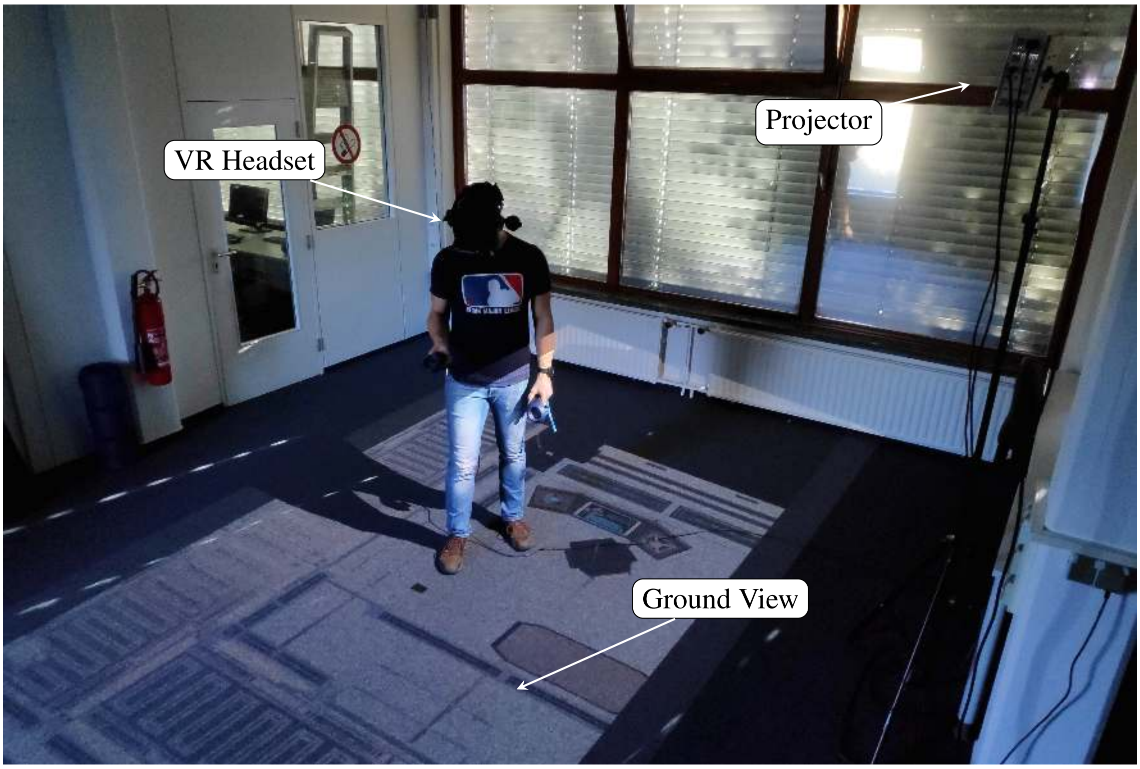

Figure 17.5: The observer view: An orthogonal top-down view of the virtual environment is projected to the ground.

In the end, we asked for general feedback and got a lot of positive answers. The participants described the experience as funny, interesting, realistic, nice and beautiful. One participant was surprised that he could actually touch the sphere. Another participant stated: *"I felt like I was moving in a really large space without any boundaries"*.

17.5 Conclusion

This chapter introduced a novel approach to RDW, which combines several redirection techniques to enable unconstrained walking in room-scale VR. Instead of developing RDW algorithms that want to fit all kind of environments but fail for room-scale VR, our approach fits perfectly for one environment without disrupting the flow of the VR experience.

Qualitative feedback that we collected during a confirmatory study suggests that the overlapping of the rooms could not be detected. Most of the participants did not even recognize that the physical table was the same in both virtual rooms.

A limitation of our approach is that the environment has to be created dedicatedly to the integrated redirection techniques and, therefore, the approach is not suitable for every purpose. Thus, VR creators may already think about RDW integration when designing levels, gameplay, story, and interactions. However, this approach might be interesting especially for location-based experiences, such as VR arcades, VR escape rooms, VR theme park rides, virtual museums, or training applications.

V

CONCLUSION

18. SUMMARY

Natural walking in VR offers a lot of advantages compared to virtual locomotion techniques such as steering with joysticks or gamepads. It reduces VR sickness, supports wayfinding as well as spatial knowledge, and induces a high sense of presence. However, natural walking in VR is limited by the available tracking space.

In this dissertation, perceptually-inspired locomotion techniques were investigated, developed, and evaluated. These techniques aim to leverage the benefits of real walking by exploiting illusions and limitations of the human perceptual system.

In Part I, fundamentals of perception and locomotion in VR were presented. For this, the human perceptual system, immersion, presence, and spatial perception were covered. Furthermore, virtual travel techniques, walking-in-place, redirected walking, and comparisons of different techniques were discussed.

In Part II, we evaluated spatial perception, including distance, speed, and size estimation, and its effects on locomotion. We found that the results for distance and speed estimation with and without additional artificial visual blur were very similar. Therefore, perceptual discrepancies between real and virtual worlds might mainly originate in technical constraints like FOV and resolution, which have larger effects on distance and speed perception than blurring peripheral vision. Moreover, the fixed distance from eyes to screen in common HMDs leading to accommodation-convergence conflict is also known to cause distance misperception. Since its influence was clearly negligible, we did not consider visual blur in the following parts of this work. Instead, we used the gained knowledge about visual perception and eye tracking for detecting blinks (see Part III). Moreover, we found interesting results concerning the estimation of dominant scale. The visibility of the user's virtual body, the type of the VE, as well as the presence of a group of avatars have an effect on scale estimation. This is important knowledge for designing scale-based locomotion techniques, which was used in Part IV.

In Part III, perceptual detection thresholds for redirected walking in various situations were estimated. We showed that the type of environment has a greater influence on thresholds than the visual self-representation of the feet. In the next step, we introduced bending gains as a special type of curvature gains for situations when users walk on already curved paths in the VE and estimated thresholds for these gains. These bending gains were used in Part IV to develop a novel approach to RDW that is based on curved path layouts. Bending gains were also used when we investigated how thresholds change when transcranial direct-current stimulation is applied to the brain of the user. Interestingly, it did only show an effect for the highest tested gain. However, VR sickness could be reduced significantly. As an orthogonal concept to previous RDW approaches such as bending gains, we presented reorientation and repositioning techniques that are executed during eye blinks. These techniques showed a potential to improve RDW for around 50%.

In Part IV, we developed perceptually-inspired locomotion techniques for seated, standing, and room-scale VR, which are based on the results of the previous two parts. These new techniques have been evaluated in several user studies. Dynamic rotation gains were compared with static gains and scrolling in a seated VR experience and achieved better results for usability, VR sickness, and spatial knowledge. Scale-based walking techniques were evaluated regarding usability, presence, VR sickness, and spatial knowledge, and manual scaling was superior for most of the criteria. Furthermore, we presented a curve-based approach to RDW that relies on previously introduced bending gains. Several configurations were discussed and one configuration was implemented as an informative example. A tool for easily integrating these configurations with the VR engine was developed including algorithms for procedural generation. In a user study, this RDW approach was compared to joystick-based locomotion and teleportation. We found that it performed significantly better regarding cognitive map building. Furthermore, the curve-based RDW approach as well as teleportation were preferred by most participants. There were no effects on presence and effectiveness. Then, a main problem was discussed which may occur when applying RDW techniques in a multi-user scenario: Users can collide physically since virtual and real position do not match necessarily. In order to address this issue, we introduced shadow avatars as a solution und evaluated different types of these avatars in a user study. Finally, it was demonstrated how different redirection techniques, such as rotation gains, bending gains, and impossible spaces, can be combined and integrated with gameplay and narration of a VR experience.

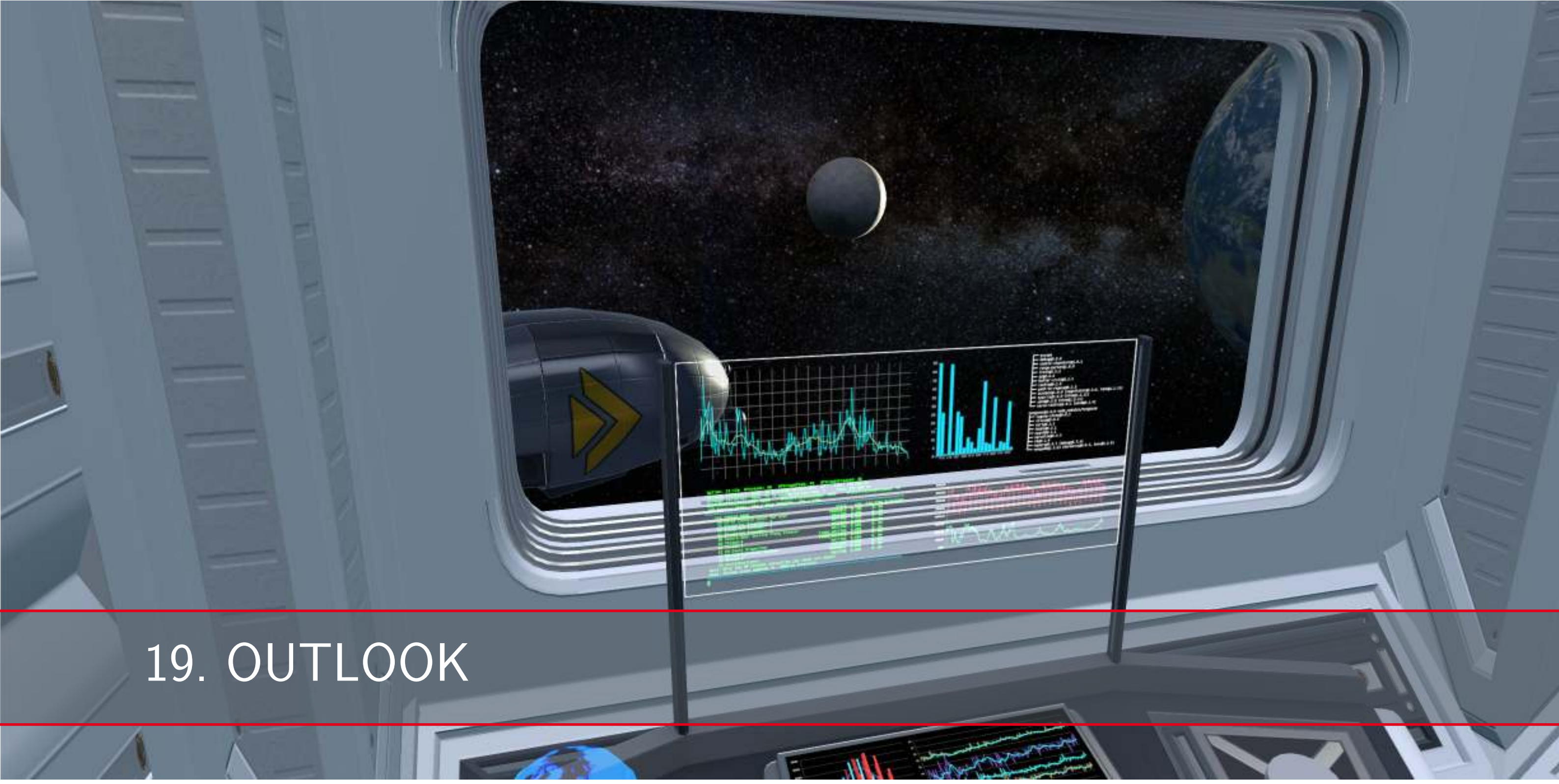

19. OUTLOOK

Although, we presented a large number of locomotion techniques for different situations, this thesis might stimulate further research in this direction. Specific applications require individualized techniques to perfectly fit the user's tasks. Hence, the techniques introduced in this dissertation might be used as examples to further integrate with VR experiences. Some of the most interesting application domains for perceptually-inspired locomotion techniques are:

- **Robotics and Telepresence:** Remote control of distant autonomous systems such as robots and drones is a fascinating use case for VR [Kru+16]. To enable natural walking for the VR user, RDW might be deployed. Hence, the VR user is able to walk in a confined tracking space while the remote robot or drone explores a much larger environment. In this context, we already presented a first approach [Zha+18a; Zha+18b], but much more research has to be considered in the future.
- **Rehabilitation and Therapy:** RDW can be used to trigger a certain walking behavior. This may be exploited for developing therapies for people with walking restrictions [KDF17]. For instance, we conducted first experiments with Parkinson patients and elderly people and showed that RDW can be used to affect walking velocity and step size [Jan+17a; Jan+17b].
- **Entertainment:** Natural walking is, especially, interesting for location-based VR experiences, that offer a larger tracking space than a typical living room. This includes, for example, VR arcades, VR theme park rides, and VR escape games.

The focus of this work was on designing and developing techniques for specific situations and evaluating them in perceptual and psychophysical experiments. However, the overall goal of locomotion research has to be the utopia of a general solution to enable unconstrained natural walking in infinite virtual worlds. This means, a smart algorithm needs to predict the way that the user wants to walk, and process the most suitable gain or technique for this. Current steering algorithms can only partly support this without drawbacks (see Section 3.4). The following approaches could provide some more advancements:

- **Beyond Perceptual Thresholds:** So far, all RDW techniques are limited by the human perceptual detection thresholds. Recently, we showed that much wider thresholds are accepted by VR users [Rie+18]. This means that it is possible to even use perceivable gains, at least for some amount of time.
- **Eye Tracking:** In this work, we showed how tracking of eye blinks can improve RDW techniques (see Chapter 10). This work was extended by Nguyen and Kunz [NK18]. In combination with redirections during saccades, it might even be more powerful. Moreover, eye tracking might also be very interesting to gain information about the environment and predict walking paths. This could open up completely new possibilities for redirection.
- **Brain Stimulation:** BCIs are a promising approach for future interactions with a computer system. In this work, we conducted first experiments with tDCS applied during natural walking. This method might be extended to improve the overall user experience as well as perceptually-inspired locomotion techniques.

ACKNOWLEDGMENTS

First of all, I would like to thank my supervisor Prof. Dr. Frank Steinicke and my former colleague and advisor Prof. Dr. Gerd Bruder for introducing me to the world of Virtual Reality. I have learned a lot from them since I joined the Human-Computer Interaction group as a student co-worker in 2014 and I am very grateful for this. It was a great chance to have two advisors who are internationally renowned experts in the field of redirected walking. Franks support and guidance was very helpful during the work on this dissertation. His input stimulated my thoughts and enriched my research. Gerd always had time for my many questions, especially in the beginning, and encouraged me to continue when I did not know how. I would also like to thank Prof. Dr. Greg Welch for welcoming me at the Synthetic Reality Lab and teaching me how to write a SIGGRAPH paper. I had a great time in Florida, and not just because of disney world.

Furthermore, I would like to thank the researchers who agreed to review this thesis! Special thanks go to all my co-authors, without whom this work would not have been possible. Especially, I would like to thank my collaborators in the DFG project "interactive Locomotion User Interfaces (iLUI)", Prof. Dr. Markus Lappe and Benjamin Bolte, and all the people in our HCI research group for providing valuable feedback and a nice company. There was always a pleasant atmosphere in our lab. I appreciate the voluntary participation in the many experiments conducted throughout the work on this dissertation. Thanks go to all the students that worked with me on projects or their theses. And I am thankful to everyone who took the time to proofread this dissertation.

Moreover, I thank my friends and family for helping and supporting me, especially, my parents Karsten and Erika as well as my sister Lisa and my brother Holger. They have been a great support in the last 32 years.

Finally, I am very pleased to thank my wife Silja and our son Bela for being there and I am very much looking forward to the birth of our daughter. Silja always supported me with my work and helped to keep my patience, especially in stressful times. I will never forget the evenings when we tinkered materials for my experiments. Bela reminded me which things in life are really important.

BIBLIOGRAPHY

[Abt+19] P. Abtahi, M. Gonzalez-Franco, E. Ofek, and A. Steed. “I’m a Giant: Walking in Large Virtual Environments at High Speed Gains”. In: *ACM Conference on Human Factors in Computing Systems (CHI)*. 2019, page 522.

[AGE04] W. J. Adams, E. W. Graf, and M. O. Ernst. “Experience can Change the ’light-from-above’ Prior”. In: *Nature Neuroscience* 7.10 (2004), page 1057.

[Agr+97] M. Agrawala, A. C. Beers, I. McDowall, B. Fröhlich, M. Bolas, and P. Hanrahan. “The Two-User Responsive Workbench: Support for Collaboration Through Individual Views of a Shared Space”. In: *Computer Graphics and Interactive Techniques*. ACM Press/Addison-Wesley Publishing Co. 1997, pages 327–332.

[Ahm+10] F. Ahmed, J. D. Cohen, K. S. Binder, and C. L. Fennema. “Influence of Tactile Feedback and Presence on Egocentric Distance Perception in Virtual Environments”. In: *IEEE Virtual Reality (VR)*. 2010, pages 195–202.

[Aki+03] H. Akiduki, S. Nishiike, H. Watanabe, K. Matsuoka, T. Kubo, and N. Takeda. “Visual-Vestibular Conflict Induced by Virtual Reality in Humans”. In: *Neuroscience Letters* 340.3 (2003), pages 197–200.

[Ant+12] A. Antal, G. Kovacs, L. Chaieb, C. Cziraki, W. Paulus, and M. W. Greenlee. “Cathodal Stimulation of Human MT+ Leads to Elevated fMRI Signal: A tDCS-fMRI Study”. In: *Restorative Neurology and Neuroscience* 30.3 (2012), pages 255–263.

[APS19] J. Auda, M. Pascher, and S. Schneegass. “Around the (Virtual) World: Infinite Walking in Virtual Reality Using Electrical Muscle Stimulation”. In: *ACM Conference on Human Factors in Computing Systems (CHI)*. 2019, page 431.

[Azm+16a] M. Azmandian, T. Grechkin, M. Bolas, and E. Suma. “The Redirected Walking Toolkit: A Unified Development and Deployment Platform for Exploring Large Virtual Environments”. In: *Everyday VR Workshop, IEEE VR*. 2016.

[Azm+15] M. Azmandian, T. Grechkin, M. Bolas, and E. Suma. “Physical Space Requirements for Redirected Walking: How Size and Shape Affect Performance”. In: *Proceedings of International Conference on Artificial Reality and Telexistence and Eurographics Symposium on Virtual Environments (ICAT-EGVE)*. 2015, pages 93–100.

[Azm+16b] M. Azmandian, T. Grechkin, M. Bolas, and E. Suma. “Automated Path Prediction for Redirected Walking Using Navigation Meshes”. In: *IEEE Symposium on 3D User Interfaces (3DUI)*. 2016, pages 63–66.

[AGR17] M. Azmandian, T. Grechkin, and E. S. Rosenberg. “An Evaluation of Strategies for Two-User Redirected Walking in Shared Physical Spaces”. In: *IEEE Virtual Reality (VR)*. 2017, pages 91–98.

[Bac+19] E. R. Bachmann, E. Hodgson, C. Hoffbauer, and J. Messinger. “Multi-User Redirected Walking and Resetting Using Artificial Potential Fields”. In: *IEEE Transactions on Visualization and Computer Graphics (TVCG)* (2019).

[BPW03] N. H. Bakker, P. O. Passenier, and P. J. Werkhoven. “Effects of Head-Slaved Navigation and the Use of Teleports on Spatial Orientation in Virtual Environments”. In: *Human factors* 45.1 (2003), pages 160–169.

[Ban+05] T. Banton, J. Stefanucci, F. Durgin, A. Fass, and D. Proffitt. “The Perception of Walking Speed in a Virtual Environment”. In: *Presence: Teleoperators & Virtual Environments* 14.4 (2005), pages 394–406.

[BB00] J. D. Bayliss and D. H. Ballard. “A Virtual Reality Testbed for Brain-Computer Interface Research”. In: *IEEE Transactions on Rehabilitation Engineering* 8.2 (2000), pages 188–190.

[BM98] B. Becker and G. Mark. “Social Conventions in Collaborative Virtual Environments”. In: *ACM International Conference on Collaborative Virtual Environments (CVE)*. 1998, pages 17–19.

[BPA00] M. W. Becker, H. Pashler, and S. M. Anstis. “The Role of Iconic Memory in Change-Detection Tasks”. In: *Perception* 29.3 (2000), pages 273–286.

[BH94] B. B. Bederson and J. D. Hollan. “Pad++: A Zooming Graphical Interface for Exploring Alternate Interface Physics”. In: *ACM Symposium on User Interface Software and Technology (UIST)*. ACM. 1994, pages 17–26.

[Ben+01] S. Benford, C. Greenhalgh, T. Rodden, and J. Pycock. “Collaborative Virtual Environments”. In: *Communications of the ACM* 44.7 (2001), pages 79–85.

[BK11] M. Berniker and K. Kording. “Bayesian Approaches to Sensory Integration for Motor Control”. In: *Wiley Interdisciplinary Reviews: Cognitive Science* 2.4 (2011), pages 419–428.

[Ber00] A. Berthoz. *The Brain’s Sense of Movement*. Cambridge, Massachusetts: Harvard University Press, 2000.

[BIL00] R. J. Bertin, I. Israël, and M. Lappe. “Perception of two-dimensional, simulated ego-motion trajectories from optic flow”. In: *Vision Research* 40.21 (2000), pages 2951–2971.

[BS16] G. Bertolini and D. Straumann. “Moving in a Moving World: A Review on Vestibular Motion Sickness”. In: *Frontiers in Neurology* 7 (2016), page 14.

[BW95] M. Billinghurst and S. Weghorst. “The Use of Sketch Maps to Measure Cognitive Maps of Virtual Environments”. In: *IEEE Virtual Reality Annual International Symposium*. 1995.

[Bla+16] P. A. Blankenship, S. L. Stuebing, S. S. Winter, J. L. Cheatwood, J. D. Benson, I. Q. Whishaw, and D. G. Wallace. “The Medial Frontal Cortex Contributes to but does not Organize Rat Exploratory Behavior”. In: *Neuroscience* 336 (2016), pages 1–11.

[Bog+06] R. Bogacz, E. Brown, J. Moehlis, P. Holmes, and J. D. Cohen. “The Physics of Optimal Decision Making: A Formal Analysis of Models of Performance in Two-Alternative Forced-Choice Tasks.” In: *Psychological review* 113.4 (2006), page 700.

[Bol17] C. Boletsis. “The New Era of Virtual Reality Locomotion: A Systematic Literature Review of Techniques and a Proposed Typology”. In: *Multimodal Technologies and Interaction* 1.4 (2017), page 24.

[Böl+19] L. Bölling, N. Stein, F. Steinicke, and M. Lappe. “Shrinking Circles: Adaptation to Increased Curvature Gain in Redirected Walking”. In: *IEEE Transactions on Visualization and Computer Graphics (TVCG)* (2019).

[BL15] B. Bolte and M. Lappe. “Subliminal Reorientation and Repositioning in Immersive Virtual Environments using Saccadic Suppression”. In: *IEEE Transactions on Visualization and Computer Graphics (TVCG)* 21.4 (2015), pages 545–552.

[BSB11] B. Bolte, F. Steinicke, and G. Bruder. “The Jumper Metaphor: an Effective Navigation Technique for Immersive Display Setups”. In: *Proceedings of Virtual Reality International Conference (VRIC)*. 2011.

[BS02] L. Bouguila and M. Sato. “Virtual Locomotion System for Large-Scale Virtual Environment”. In: *Proceedings of IEEE Virtual Reality (VR)*. 2002, pages 291–292.

[Bou+02] L. Bouguila, M. Sato, S. Hasegawa, H. Naoki, N. Matsumoto, A. Toyama, J. Ezzine, and D. Maghrebi. “A New Step-in-Place Locomotion Interface for Virtual Environment with Large Display System”. In: *Proceedings of ACM SIGGRAPH*. 2002, pages 197–207.

[Bow+01] D. A. Bowman, E. Kruijff, J. J. LaViola, and I. Poupyrev. “An Introduction to 3-D User Interface Design”. In: *Presence: Teleoperators & Virtual Environments* 10.1 (2001), pages 96–108.

[BKH97] D. Bowman, D. Koller, and L. Hodges. “Travel in Immersive Virtual Environments: An Evaluation of Viewpoint Motion Control Techniques”. In: *Proceedings of IEEE Virtual Reality Annual International Symposium (VRAIS)*. Volume 7. IEEE, 1997, pages 45–52.

[Bow+04] D. Bowman, E. Kruijff, J. LaViola, Jr., and I. Poupyrev. *3D User Interfaces: Theory and Practice*. Addison-Wesley Professional, 2004.

[Bow+99] D. A. Bowman, E. T. Davis, L. F. Hodges, and A. N. Badre. “Maintaining Spatial Orientation During Travel in an Immersive Virtual Environment”. In: *Presence: Teleoperators and Virtual Environments* 8.6 (1999), pages 618–631.

[Bow+98] D. A. Bowman, J. Wineman, L. F. Hodges, and D. Allison. “Designing Animal Habitats within an Immersive VE”. In: *IEEE Computer Graphics and Applications* 18.5 (1998), pages 9–13.

[Boy+18] Y. Boysen, M. Husung, T. Mantei, L. Müller, J. Schimmelpfennig, L. Uzolas, and **E. Langbehn**[1]. “Scale & Walk: Evaluation von skalierungsbasierten Interaktionstechniken zur natürlichen Fortbewegung in VR”. In: *Mensch und Computer*. 2018, (12 pages).

[Boz+16] E. Bozgeyikli, A. Raij, S. Katkoori, and R. Dubey. “Point & Teleport Locomotion Technique for Virtual Reality”. In: *Proceedings of ACM Symposium on Computer-Human Interaction in Play (CHI Play)*. 2016, pages 205–216.

[BHV94] B. Bridgeman, A. H. C. van der Heijden, and B. M. Velichkovsky. “A Theory of Visual Stability Across Saccadic Eye Movements”. In: *Behav. Brain Sci.* 17 (1994), pages 247–292.

[BHS75] B. Bridgeman, D. Hendry, and L. Stark. “Failure to Detect Displacement of the Visual World During Saccadic Eye Movements”. In: *Vision Research* 15.6 (1975), pages 719–722.

[Bri+05] D. Bristow, J.-D. Haynes, R. Sylvester, C. D. Frith, and G. Rees. “Blinking Suppresses the Neural Response to Unchanging Retinal Stimulation”. In: *Current Biology* 15.14 (2005), pages 1296–1300.

[Bro96] J. Brooke. “SUS-A Quick and Dirty Usability Scale”. In: *Usability Evaluation in Industry* 189.194 (1996), pages 4–7.

[Bro10] F. Brooks. *TVCG Technical Achievement Award Talk*. 2010.

[Bro02] L. E. Brown. “Limb Position Drift and its Implications for Movement and Position Control”. PhD thesis. Pennsylvania State University, 2002.

[Bru+09] G. Bruder, F. Steinicke, K. Hinrichs, and M. Lappe. “Reorientation During Body Turns”. In: *Joint Virtual Reality Eurographics Conference on Virtual Environments*. Eurographics Association. 2009, pages 145–152.

[BSH09] G. Bruder, F. Steinicke, and K. Hinrichs. “Arch-Explore: A Natural User Interface for Immersive Architectural Walkthroughs”. In: *Proceedings of IEEE Symposium on 3D User Interfaces (3DUI)*. 2009, pages 75–82.

[BE17] G. Bruder and **E. Langbehn**. “Subliminal Rotations During Eye Blinks for Redirected Walking”. In: *Journal of Vision (Talk)* 17.10 (2017), pages 1266–1266.

[Bru+12] G. Bruder, V. Interrante, L. Phillips, and F. Steinicke. “Redirecting Walking and Driving for Natural Navigation in Immersive Virtual Environments”. In: *IEEE Transactions on Visualization and Computer Graphics (TVCG)* 18.4 (2012), pages 538–545.

[BLS15] G. Bruder, P. Lubos, and F. Steinicke. “Cognitive Resource Demands of Redirected Walking”. In: *IEEE Transactions on Visualization and Computer Graphics (TVCG)* 21.4 (2015), pages 539–544.

[1]This publication is based on a bachelor project. The students implemented and ran the experiment under my supervision. I designed the experiment and wrote the paper.

[BPS12] G. Bruder, A. Pusch, and F. Steinicke. “Analyzing Effects of Geometric Rendering Parameters on Size and Distance Estimation in On-Axis Stereographics”. In: *Proceedings of ACM Symposium on Applied Perception (SAP)*. ACM, 2012, pages 111–118.

[Bru+15] G. Bruder, F. A. Sanz, A.-H. Olivier, and A. Lécuyer. “Distance Estimation in Large Immersive Projection Systems, Revisited”. In: *IEEE Virtual Reality (VR)*. 2015, pages 27–32.

[Bru+13] G. Bruder, F. Steinicke, B. Bolte, P. Wieland, H. Frenz, and M. Lappe. “Exploiting Perceptual Limitations and Illusions to Support Walking Through Virtual Environments in Confined Physical Spaces”. In: *Displays* 34.2 (2013), pages 132–141.

[BPJ13] L. Bruno, J. Pereira, and J. Jorge. “A New Approach to Walking in Place”. In: *INTERACT*. 2013, pages 370–387.

[BYB18] L. E. Buck, M. K. Young, and B. Bodenheimer. “A Comparison of Distance Estimation in HMD-based Virtual Environments With Different HMD-based Conditions”. In: *ACM Transactions on Applied Perception (TAP)* 15.3 (2018), page 21.

[Bur+05] E. Burns, S. Razzaque, A. Panter, M. Whitton, M. McCallus, and F. Brooks. “The Hand is Slower than the Eye: A quantitative exploration of visual dominance over proprioception”. In: *IEEE Proceedings of the Virtual Reality (VR)*. IEEE, 2005, pages 3–10.

[BR02] D. C. Burr and J. Ross. “Direct Evidence that Influence Motion Mechanisms”. In: *The Journal of Neuroscience* 22.19 (2002), pages 8661–8664.

[BBB07] P. Byrne, S. Becker, and N. Burgess. “Remembering the Past and Imagining the Future: A Neural Model of Spatial Memory and Imagery”. In: *Psychological Review* 114.2 (2007), page 340.

[CMN83] S. Card, T. Moran, and A. Newell. *The Psychology of Human-Computer Interaction*. Edited by N. Hillsdale. Lawrence Erlbaum Associates, 1983.

[CR15] K. Carnegie and T. Rhee. “Reducing Visual Discomfort with HMDs Using Dynamic Depth of Field”. In: *IEEE Computer Graphics and Applications* 35.5 (2015), pages 34–41.

[CH02] Y. S. Chee and C. M. Hooi. “C-VISions: Socialized Learning Through Collaborative, Virtual, Interactive Simulations”. In: *Proceedings of the Conference on Computer Support for Collaborative Learning: Foundations for a CSCL Community*. CSCL ’02. Boulder, Colorado: International Society of the Learning Sciences, 2002, pages 687–696. URL: `http://dl.acm.org/citation.cfm?id=1658616.1658789`.

[Che06] Y. Chen. “Olfactory Display: Development and Application in Virtual Reality Therapy”. In: *IEEE International Conference on Artificial Reality and Telexistence (ICAT)*. 2006, pages 580–584.

[CP16] Cherry Pop Games and Perilous Orbit. SportsBar VR. Game [HTC Vive]. Cherry Pop Games and Perilous Orbit. Played December 2016. June 2016.

[Che+19] M. Chessa, G. Maiello, A. Borsari, and P. J. Bex. “The Perceptual Quality of the Oculus Rift for Immersive Virtual Reality”. In: *Human–Computer Interaction* 34.1 (2019), pages 51–82.

[Cid+16] M. A. Cidota, R. M. Clifford, S. G. Lukosch, and M. Billinghurst. “Using Visual Effects to Facilitate Depth Perception for Spatial Tasks in Virtual and Augmented Reality”. In: *IEEE International Symposium on Mixed and Augmented Reality (ISMAR)*. 2016, pages 172–177.

[Cli+09] D. Cliburn, S. Rilea, D. Parsons, P. Surya, and J. Semler. “The Effects of Teleportation on Recollection of the Structure of a Virtual World”. In: *Proceedings of Joint Virtual Reality Eurographics Conference on Virtual Environments (JVRC)*. 2009, pages 117–120.

[Col+89] M. Collins, R. Seeto, L. Campbell, and M. Ross. “Blinking and Corneal Sensitivity”. In: *Acta ophthalmologica* 67.5 (1989), pages 525–531.

[Col+17] D. Colombo, S. Serino, C. Tuena, E. Pedroli, A. Dakanalis, P. Cipresso, and G. Riva. “Egocentric and Allocentric Spatial Reference Frames in Aging: A Systematic Review”. In: *Neuroscience & Biobehavioral Reviews* 80 (2017), pages 605–621.

[Col80] M. Coltheart. “Iconic Memory and Visible Persistence”. In: *Perception & Psychophysics* 27.3 (1980), pages 183–228.

[Cor62] T. N. Cornsweet. “The Staircase-Method in Psychophysics”. In: *The American Journal of Psychology* 75.3 (1962), pages 485–491.

[Cor17] N. Corporation. Budget Cuts. Game [HTC Vive]. Neat Corporation. Played -. 2017.

[Cre+05] S. H. Creem-Regehr, P. Willemsen, A. A. Gooch, and W. B. Thompson. “The Influcences of Restricted Viewing Conditions on Egocentric Perception: Implications for Real and Virtual Environments”. In: *Perception* 34.2 (2005), pages 191–204.

[Cre+15] S. H. Creem-Regehr, J. K. Stefanucci, W. B. Thompson, N. Nash, and M. McCardell. “Egocentric Distance Perception in the Oculus Rift (DK2)”. In: *ACM SIGGRAPH Symposium on Applied Perception (SAP)*. 2015, pages 47–50.

[Cro+98] J. A. Crowell, M. S. Banks, K. V. Shenoy, and R. A. Andersen. “Visual Self-Motion Perception During Head Turns”. In: *Nature Neuroscience* 1.8 (1998), page 732.

[Cru95] C. Cruz-Neira. “Virtual Reality based on Multiple Projection Screens: The CAVE and Its Applications to Computational Science and Engineering”. PhD thesis. University of Illinois at Chicago, 1995, pages 89–96.

[Cry16] Crytek. Robinson: The Journey. Game [PSVR]. Crytek. Played November 2016. Nov. 2016.

[CV95] J. E. Cutting and P. M. Vishton. “Perceiving Layout and Knowing Distances: The Integration, Relative Potency, and Contextual Use of Different Information About Depth”. In: *Perception of Space and Motion*. Elsevier, 1995, pages 69–117.

[DAA98] R. P. Darken, T. Allard, and L. B. Achille. “Spatial Orientation and Wayfinding in Large-scale Virtual Spaces: An Introduction”. In: *Presence* 7.2 (1998), pages 101–107.

[DC99] R. P. Darken and H. Cevik. “Map Usage in Virtual Environments: Orientation Issues”. In: *IEEE Virtual Reality (VR)*. 1999, pages 133–140.

[DWD16] M. S. Dennison, A. Z. Wisti, and M. D’Zmura. “Use of Physiological Signals to Predict Cybersickness”. In: *Displays* 44 (2016), pages 42–52.

[DB78] J. Dichgans and T. Brandt. “Visual Vestibular Interaction: Effects on Self-Motion Perception and Postural Control”. In: *Perception. Handbook of Sensory Physiology*. Edited by R. Held, H. Leibowitz, and H. Teuber. Volume 8. Berlin, Heidelberg, New York: Springer, 1978, pages 755–804.

[Dic74] A. Dick. “Iconic Memory and its Relation to Perceptual Processing and Other Memory Mechanisms”. In: *Attention, Perception, & Psychophysics* 16.3 (1974), pages 575–596.

[Don19] I.-K. L. Dong-Yong Lee Yong-Hun Cho. “Real-time Optimal Planning for Redirected Walking Using Deep Q-Learning”. In: *IEEE Virtual Reality (VR)*. 2019.

[Don+17] Z.-C. Dong, X.-M. Fu, C. Zhang, K. Wu, and L. Liu. “Smooth Assembled Mappings for Large-Scale Real Walking”. In: *ACM Transactions on Graphics (TOG)* 36.6 (2017), page 211.

[Dou02] M. J. Doughty. “Further Assessment of Gender-and Blink Pattern-related Differences in the Spontaneous Eyeblink Activity in Primary Gaze in Young Adult Humans”. In: *Optometry & Vision Science* 79.7 (2002), pages 439–447.

[Dup+97] P. Dupont, B. De Bruyn, R. Vandenberghe, A.-M. Rosier, J. Michiels, G. Marchal, L. Mortelmans, and G. Orban. “The Kinetic Occipital Region in Human Visual Cortex”. In: *Cerebral Cortex (New York, NY: 1991)* 7.3 (1997), pages 283–292.

[E L16] **E. Langbehn**. “Development and Evaluation of Interactive Locomotion User Interfaces”. In: *IEEE Virtual Reality (VR) (Doctoral Consortium)*. 2016.

[E L19] **E. Langbehn**. “Fortbewegung im virtuellen Raum”. In: *Mit weit geschlossenen Augen. Virtuelle Realitäten entwerfen*. Edited by P. Reinfeld and C. Höfler. (Architektur der Medien - Medien der Architektur, ed. by K. Nakas and Ph. Reinfeld, Vol. 1.) Wilhelm Fink Verlag, 2019.

[E L+16] **E. Langbehn**, B. Bolte, T. Raupp, G. Bruder, M. Lappe, and F. Steinicke. “Visual Blur in Immersive Virtual Environments: Does Depth of Field or Motion Blur Affect Distance and Speed Estimation?” In: *ACM Symposium on Virtual Reality Software and Technology (VRST)*. 2016, pages 241–250.

[EBS15] **E. Langbehn**, G. Bruder, and F. Steinicke. “Moving Towards Natural Interaction Between Multiscale Avatars in Multi-User Virtual Environments[2]”. In: *International Conference on Artificial Reality and Telexistence, Eurographics Symposium on Virtual Environments (ICAT-EGVE) (Poster)*. 2015.

[EBS16a] **E. Langbehn**, G. Bruder, and F. Steinicke. “Scale Matters! Analysis of Dominant Scale Estimation in the Presence of Conflicting Cues in Multi-Scale Collaborative Virtual Environments”. In: *IEEE Symposium on 3D User Interfaces (3DUI)*. 2016, pages 211–220.

[EBS16b] **E. Langbehn**, G. Bruder, and F. Steinicke. “Subliminal Reorientation and Repositioning in Virtual Reality During Eye Blinks[3]”. In: *ACM Symposium on Spatial User Interaction (SUI) (Poster)*. 2016, pages 213–213.

[E L+15] **E. Langbehn**, T. Eichler, S. Ghose, K. von Luck, G. Bruder, and F. Steinicke. “Evaluation of an Omnidirectional Walking-in-Place User Interface with Virtual Locomotion Speed Scaled by Forward Leaning Angle”. In: *GI Workshop on Virtual and Augmented Reality (GI VR/AR)*. 2015, pages 149–160.

[EHS18] **E. Langbehn**, E. Harting, and F. Steinicke. “Shadow-Avatars: A Visualization Method to Avoid Collisions of Physically Co-Located Users in Room-Scale VR”. In: *IEEE Virtual Reality (VR) Workshop on Everyday Virtual Reality (WEVR)*. 2018, (4 pages).

[E L+17a] **E. Langbehn**, P. Lubos, G. Bruder, and F. Steinicke. “Application of Redirected Walking in Room-Scale VR”. In: *IEEE Virtual Reality (VR) (Demo)*. 2017.

[E L+17b] **E. Langbehn**, P. Lubos, G. Bruder, and F. Steinicke. “Bending the Curve: Sensitivity to Bending of Curved Paths and Application in Room-Scale VR”. In: *IEEE Transactions on Visualization and Computer Graphics (TVCG)* 23.4 (2017), pages 1389–1398.

[ELS18a] **E. Langbehn**, P. Lubos, and F. Steinicke. “Evaluation of Locomotion Techniques for Room-Scale VR: Joystick, Teleportation, and Redirected Walking”. In: *ACM Virtual Reality International Conference (VRIC)*. 2018, (9 pages).

[ELS18b] **E. Langbehn**, P. Lubos, and F. Steinicke. “Redirected Spaces: Going Beyond Borders”. In: *IEEE Virtual Reality (VR) (Demo)*. 2018.

[ES18] **E. Langbehn** and F. Steinicke. “Redirected Walking in Virtual Reality”. In: *Encyclopedia of Computer Graphics and Games*. Edited by N. C. Nilsson. Springer International Publishing, 2018.

[2]This publication received the *Best Poster Award* and the *Best Poster Audience Award*.

[3]This publication received the *Honorable Mention for Best Poster*.

[ES19] **E. Langbehn** and F. Steinicke. “Space Walk: A Combination of Subtle Redirected Walking Techniques Integrated with Gameplay and Narration”. In: *ACM SIGGRAPH Emerging Technologies*. 2019.

[E L+19a] **E. Langbehn**, F. Steinicke, P. Koo-Poeggel, L. Marshall, and G. Bruder. “Stimulating the Brain in VR: Effects of Transcranial Direct-Current Stimulation on Redirected Walking”. In: *ACM Symposium on Applied Perception (SAP) (under review)*. 2019, (8 pages).

[E L+18] **E. Langbehn**, F. Steinicke, M. Lappe, G. F. Welch, and G. Bruder. “In the Blink of an Eye - Leveraging Blink-Induced Suppression for Imperceptible Position and Orientation Redirection in Virtual Reality”. In: *ACM Transactions on Graphics (TOG), Special Issue on ACM SIGGRAPH* 37.4 (2018), 66 (11 pages).

[E L+19b] **E. Langbehn**, J. Wittig, N. Katzakis, and F. Steinicke. “Turn Your Head Half Round: VR Rotation Techniques for Situations With Physically Limited Turning Angle”. In: *Mensch und Computer (accepted)*. 2019, (9 pages).

[EHP05] H. H. Ehrsson, N. P. Holmes, and R. E. Passingham. “Touching a Rubber Hand: Feeling of Body Ownership is Associated with Activity in Multisensory Brain Areas”. In: *Journal of Neuroscience* 25.45 (2005), pages 10564–10573.

[Ehr+05] H. H. Ehrsson, T. Kito, N. Sadato, R. E. Passingham, and E. Naito. “Neural Substrate of Body Size: Illusory Feeling of Shrinking of the Waist”. In: *PLoS biology* 3.12 (2005), page 2200.

[ESP04] H. H. Ehrsson, C. Spence, and R. E. Passingham. “That’s my Hand! Activity in Premotor Cortex Reflects Feeling of Ownership of a Limb”. In: *Science* 305.5685 (2004), pages 875–877.

[Eic14] T. Eichler. *Master Thesis: Agent-based Middleware for Supporting Developers in a Smart Home Laboratory*. 2014.

[Eng+08] D. Engel, C. Curio, L. Tcheang, B. Mohler, and H. Bülthoff. “A Psychophysically Calibrated Controller for Navigating Through Large Environments in a Limited Free-Walking Space”. In: *ACM Symposium on Virtual Reality Software and Technology (VRST)*. 2008, pages 157–164.

[Eps08] R. A. Epstein. “Parahippocampal and Retrosplenial Contributions to Human Spatial Navigation”. In: *Trends in Cognitive Sciences* 12.10 (2008), pages 388–396.

[Ern06] M. Ernst. “A Bayesian View on Multimodal Cue Integration”. In: *Human Body Perception From The Inside Out*. Edited by G. Knoblich, I. Thornton, M. Grosjean, and M. Shiffrar. Oxford University Press, 2006, pages 105–131.

[EB02] M. O. Ernst and M. S. Banks. “Humans Iintegrate Visual and Haptic Information in a Statistically Optimal Fashion”. In: *Nature* 415.6870 (2002), page 429.

[EB04] M. O. Ernst and H. H. Bülthoff. “Merging the Senses into a Robust Percept”. In: *Trends in Cognitive Sciences* 8.4 (2004), pages 162–169.

[EB05] M. O. Ernst and H. H. Bülthoff. “Multisensorische Wahrnehmung des Menschen”. In: *Jahrbuch der Max-Planck-Gesellschaft* 2005 (2005), page 127.

[ETP04] Á. Esteban, A. Traba, and J. Prieto. “Eyelid Movements in Health and Disease. The Supranuclear Impairment of the Palpebral Motility”. In: *Neurophysiologie Clinique/Clinical Neurophysiology* 34.1 (2004), pages 3–15.

[Evi+94] C. Evinger, K. A. Manning, J. J. Pellegrini, M. A. Basso, A. S. Powers, and P. A. Sibony. “Not Looking While Leaping: The Linkage of Blinking and Saccadic Gaze Shifts”. In: *Experimental Brain Research* 100.2 (1994), pages 337–344.

[Evi+84] C. Evinger, M. Shaw, C. Peck, K. Manning, and R. Baker. “Blinking and Associated Eye Movements in Humans, Guinea Pigs, and Rabbits”. In: *Journal of Neurophysiology* 52.2 (1984), pages 323–339.

[FWW08] J. Feasel, M. Whitton, and J. Wendt. “LLCM-WIP: Low-Latency, Continuous-Motion Walking-in-Place”. In: *Proceedings of IEEE Symposium on 3D User Interfaces*. IEEE, 2008, pages 97–104.

[Fec60] G. Fechner. *Elemente der Psychophysik*. Holt, Rinehart & Winston, New York, 1860.

[FF16] A. S. Fernandes and S. K. Feiner. “Combating VR Sickness Through Subtle Dynamic Field-of-View Modification”. In: *IEEE Symposium on 3D User Interfaces (3DUI)*. 2016.

[Fer08] J. Ferwerda. “Psychophysics 101: How to run perception experiments in computer graphics”. In: *Proceedings of ACM SIGGRAPH*. 87. ACM, 2008.

[FV04] T. Field and P. Vamplew. “Generalised Algorithms for Redirected Walking in Virtual Environments”. In: (2004).

[Fit15] J. Fitzakerley. *Eyelid Movements*. `http://www.d.umn.edu/~jfitzake/Lectures/DMED/Vision/Optics/Blinking.html`. [Online; accessed 28-Feb-2017]. 2015.

[Fon61] A. M. Fonarev. “A Vestibulo-Palpebral Reflex”. In: *Bulletin of Experimental Biology and Medicine* 50.6 (June 1961), pages 1249–1251. ISSN: 1573-8221. DOI: `10.1007/BF00785378`. URL: `https://doi.org/10.1007/BF00785378`.

[FK01] G. Francis and H. Kim. “Perceived Motion in Orientational Afterimages: Direction and Speed”. In: *Vision research* 41.2 (2001), pages 161–172.

[FKK07] S. Frees, G. D. Kessler, and E. Kay. “PRISM Interaction for Enhancing Control in Immersive Virtual Environments”. In: *ACM Transactions on Computer-Human Interaction (TOCHI)* 14.1 (2007), page 2.

[FRK14] S. Freitag, D. Rausch, and T. Kuhlen. “Reorientation in Virtual Environments Using Interactive Portals”. In: *IEEE Symposium on 3D User Interfaces (3DUI)*. 2014, pages 119–122.

[FWK16a] S. Freitag, B. Weyers, and T. W. Kuhlen. “Automatic Speed Adjustment for Travel Through Immersive Virtual Environments Based on Viewpoint Quality”. In: *IEEE Symposium on 3D User Interfaces (3DUI)*. 2016, pages 67–70.

[FWK16b] S. Freitag, B. Weyers, and T. W. Kuhlen. “Examining Rotation Gain in CAVE-like Virtual Environments”. In: *IEEE Transactions on Visualization and Computer Graphics (TVCG)* 22.4 (2016), pages 1462–1471.

[FWK17] S. Freitag, B. Weyers, and T. W. Kuhlen. “Efficient Approximate Computation of Scene Visibility Based on Navigation Meshes and Applications for Navigation and Scene Analysis”. In: *IEEE Symposium on 3D User Interfaces (3DUI)*. 2017, pages 134–143.

[FWK18] S. Freitag, B. Weyers, and T. W. Kuhlen. “Interactive Exploration Assistance for Immersive Virtual Environments Based on Object Visibility and Viewpoint Quality”. In: *IEEE Virtual Reality and 3D User Interfaces (VR)*. 2018, pages 355–362.

[FSW17] J. Frommel, S. Sonntag, and M. Weber. “Effects of Controller-based Locomotion on Player Experience in a Virtual Reality Exploration Game”. In: *ACM Foundations of Digital Games*. 2017, page 30.

[Fun18] S. Funck. *Bachelor Thesis: Prozedurale Level Generierung mit vordefinierten Pfaden*. 2018.

[FB95] G. W. Furnas and B. B. Bederson. “Space-Scale Diagrams: Understanding Multiscale Interfaces”. In: *ACM Conference on Human Factors in Computing Systems (CHI)*. 1995, pages 234–241.

[Gam16] S. Games. Until Dawn: Rush of Blood. Game [PSVR]. SIEE. Played December 2016. Oct. 2016.

[Gib79] J. Gibson. “The Ecological Approach to Visual Perception”. PhD thesis. Boston, Houghton Mifflin, 1979.

[GK11] M. Glueck and A. Khan. “Considering Multiscale Scenes to Elucidate Problems Encumbering Three-Dimensional Intellection and Navigation”. In: *Artificial Intelligence for Engineering Design, Analysis and Manufacturing* 25.04 (2011), pages 393–407.

[Gol12] J. Goldfeather. “Adaptive Redirected Walking in a Virtual World”. In: *IEEE VR Workshop on Perceptual Illusions in Virtual Environments (PIVE)*. 2012, pages 17–20.

[Gol09] E. Goldstein. *Sensation and Perception*. Cengage Learning, 2009.

[Gra99] M. S. Graziano. “Where is my Arm? The Relative Role of Vision and Proprioception in the Neuronal Representation of Limb Position”. In: *Proceedings of the National Academy of Sciences* 96.18 (1999), pages 10418–10421.

[Gre+16] T. Grechkin, J. Thomas, M. Azmandian, M. Bolas, and E. Suma. “Revisiting Detection Thresholds for Redirected Walking: Combining Translation and Curvature Gains”. In: *Proceedings of ACM Symposium on Applied Perception (SAP)*. 2016, pages 113–120.

[Gro+05] H. Groenda, F. Nowak, P. Rößler, and U. Hanebeck. “Telepresence Techniques for Controlling Avatar Motion in First Person Games”. In: *Intelligent Technologies for Interactive Entertainment (INTETAIN 2005)*. 2005, pages 44–53.

[Guy+15] E. Guy, P. Punpongsanon, D. Iwai, K. Sato, and T. Boubekeur. “LazyNav: 3D Ground Navigation with Non-Critical Body Parts”. In: *IEEE Symposium on 3D User Interfaces (3DUI)*. 2015, pages 1–8.

[Häk+99] H. Häkkänen, H. Summala, M. Partinen, M. Tiihonen, and J. Silvo. “Blink Duration as an Indicator of Driver Sleepiness in Professional Bus Drivers”. In: *Sleep* 22.6 (1999), pages 798–802.

[Hal45] A. Hall. “The Origin and Purposes of Blinking”. In: *The British Journal of Ophthalmology* 29.9 (1945), page 445.

[Hal66] E. T. Hall. *The Hidden Dimension*. Volume 609. Garden City, NY: Doubleday, 1966.

[HBH14] B. M. Hampstead, G. S. Brown, and J. F. Hartley. “Transcranial Direct Current Stimulation Modulates Activation and Effective Connectivity During Spatial Navigation”. In: *Brain Stimulation* 7.2 (2014), pages 314–324.

[Hay+19] D. Hayashi, K. Fujita, K. Takashima, R. W. Lindeman, and Y. Kitamura. “Redirected Jumping: Imperceptibly Manipulating Jump Motions in Virtual Reality”. In: *IEEE Virtual Reality (VR)*. 2019.

[Hee92] C. Heeter. “Being There: The Subjective Experience of Presence”. In: *Presence: Teleoperators & Virtual Environments* 1.2 (1992), pages 262–271.

[HES17] P. Heidicker, **E. Langbehn**, and F. Steinicke. “Influence of Avatar Appearance on Presence in Social VR”. In: *IEEE Symposium on 3D User Interfaces (3DUI) (Poster)*. 2017, pages 233–234.

[Hel+10] R. T. Held, E. A. Cooper, J. F. O’Brien, and M. S. Banks. “Using Blur to Affect Perceived Distance and Size”. In: *ACM Transactions on Graphics (TOG)* 29.2 (2010).

[Hil+07] S. Hillaire, A. Lécuyer, R. Cozot, and G. Casiez. “Depth-of-Field Blur Effects for First-Person Navigation in Virtual Environments”. In: *ACM Symposium on Virtual Reality Software and Technology (VRST)*. ACM. 2007, pages 203–206.

[HB13] E. Hodgson and E. Bachmann. “Comparing four approaches to generalized redirected walking: Simulation and live user data”. In: *IEEE transactions on visualization and computer graphics (TVCG)* 19.4 (2013), pages 634–643.

[HBT14] E. Hodgson, E. Bachmann, and T. Thrash. “Performance of Redirected Walking Algorithms in a Constrained Virtual World”. In: *IEEE transactions on visualization and computer graphics (TVCG)* 20.4 (2014), pages 579–587.

[HBW11] E. Hodgson, E. Bachmann, and D. Waller. “Redirected walking to explore virtual environments: Assessing the potential for spatial interference”. In: *ACM Transactions on Applied Perception (TAP)* 8.4 (2011), page 22.

[Hof+08] D. M. Hoffman, A. R. Girshick, K. Akeley, and M. S. Banks. “Vergence–Accommodation Conflicts Hinder Visual Performance and Cause Visual Fatigue”. In: *Journal of vision* 8.3 (2008), pages 33–33.

[Hol12] J. E. Holm. “Collision Prediction and Prevention in a Simultaneous Multi-User Immersive Virtual Environment”. PhD thesis. Miami University, 2012.

[How02] I. P. Howard. *Seeing in Depth, Vol. 1: Basic Mechanisms.* University of Toronto Press, 2002.

[HLW15] F.-C. Huang, D. P. Luebke, and G. Wetzstein. “The Light Field Stereoscope”. In: *ACM SIGGRAPH Emerging Technologies*. 2015, pages 24–1.

[Hut+18] C. Hutton, S. Ziccardi, J. Medina, and E. S. Rosenberg. “Individualized Calibration of Rotation Gain Thresholds for Redirected Walking”. In: *ICAT-EGVE*. The Eurographics Association, 2018.

[Ill16] I-Illusions. Space Pirate Trainer. Game [HTC Vive]. I-Illusions. Played December 2016. Apr. 2016.

[Int18] Intel. *VR Content Developer Guide*. `https://software.intel.com/en-us/articles/vr-content-developer-guide`. [Online; accessed 19-December-2018]. 2018.

[Int+07] V. Interrante, B. Ries, J. Lindquist, and L. Anderson. “Elucidating the Factors that can Facilitate Veridical Spatial Perception in Immersive Virtual Environments”. In: *IEEE Virtual Reality (VR)*. IEEE, 2007, pages 11–18.

[IRA07] V. Interrante, B. Riesand, and L. Anderson. “Seven League Boots: A New Metaphor for Augmented Locomotion through Moderately Large Scale Immersive Virtual Environments”. In: *Proceedings of IEEE Symposium on 3D User Interfaces*. IEEE, 2007, pages 167–170.

[Ito+15] H. T. Ito, S.-J. Zhang, M. P. Witter, E. I. Moser, and M.-B. Moser. “A Prefrontal–Thalamo–Hippocampal Circuit for Goal-directed Spatial Navigation”. In: *Nature* 522.7554 (2015), page 50.

[Iva+97] Y. Ivanenko, R. Grasso, I. Israël, and A. Berthoz. “The Contribution of Otoliths and Semicircular Canals to the Perception of Two-Dimensional Passive Whole-Body Motion in Humans”. In: *The Journal of Physiology* 502.1 (1997), pages 223–233.

[Ivl16] V. Ivleva. “Redirected Walking in Virtual Reality during Eye Blinking”. Master’s thesis. University of Bremen, 2016.

[Iwa99] H. Iwata. “The Torus Treadmill: Realizing Locomotion in VEs”. In: *IEEE Computer Graphics and Applications* 19.6 (1999), pages 30–35.

[IHT06] H. Iwata, Y. Hiroaki, and H. Tomioka. “Powered Shoes”. In: *International Conference on Computer Graphics and Interactive Techniques*. 28. ACM, 2006.

[Iwa+05] H. Iwata, H. Yano, H. Fukushima, and H. Noma. “CirculaFloor”. In: *IEEE Computer Graphics and Applications* 25.1 (2005), pages 64–67.

[Jan+17a] O. Janeh, **E. Langbehn**, F. Steinicke, G. Bruder, A. Gulberti, and M. Poetter-Nerger. “Biomechanical Analysis of (Non-)Isometric Virtual Walking of Older Adults”. In: *IEEE Virtual Reality (VR) (Poster)*. 2017, pages 217–218.

[Jan+17b] O. Janeh, **E. Langbehn**, F. Steinicke, G. Bruder, A. Gulberti, and M. Poetter-Nerger. “Walking in Virtual Reality: Effects of Manipulated Visual Self-Motion on Walking Biomechanics”. In: *ACM Transactions on Applied Perception (TAP)* 14.2 (2017), 12 (15 pages).

[Jer+08] J. Jerald, T. Peck, F. Steinicke, and M. Whitton. “Sensitivity to Scene Motion for Phases of Head Yaws”. In: *Proceedings of Applied Perception in Graphics and Visualization*. ACM, 2008, pages 155–162.

[Jer15] J. Jerald. *The VR Book: Human-Centered Design for Virtual Reality*. Morgan & Claypool, 2015.

[Joh+09] M. Johns, K. Crowley, R. Chapman, A. Tucker, and C. Hocking. “The Effect of Blinks and Saccadic Eye Movements on Visual Reaction Times”. In: *Attention, Perception, & Psychophysics* 71.4 (2009), pages 783–788.

[Joh+99] A. Johnson, T. Moher, S. Ohlsson, and M. Gillingham. “The Round Earth Project-Collaborative VR for Conceptual Learning”. In: *IEEE Computer Graphics and Applications* 19.6 (1999), pages 60–69.

[JSB13] J. Jones, J. E. Swan II, and M. Bolas. “Peripheral Stimulation and its Effect on Perceived Spatial Scale in Virtual Environments”. In: *IEEE Transactions on Visualization and Computer Graphics (TVCG)* 19.4 (2013), pages 701–710.

[Jun+18] S. Jung, G. Bruder, P. J. Wisniewski, C. Sandor, and C. E. Hughes. “Over My Hand: Using a Personalized Hand in VR to Improve Object Size Estimation, Body Ownership, and Presence”. In: *ACM Symposium on Spatial User Interaction (SUI)*. 2018, pages 60–68.

[Jus19] E. R. B. Justin Messinger Eric Hodgson. “Effects of Tracking Area Shape and Size on Artificial Potential Field Redirected Walking”. In: *IEEE Virtual Reality (VR)*. 2019.

[Kee+11] D. Keeser, T. Meindl, J. Bor, U. Palm, O. Pogarell, C. Mulert, J. Brunelin, H.-J. Möller, M. Reiser, and F. Padberg. “Prefrontal Transcranial Direct Current Stimulation Changes Connectivity of Resting-State Networks During fMRI”. In: *Journal of Neuroscience* 31.43 (2011), pages 15284–15293.

[KCS17] J. W. Kelly, L. A. Cherep, and Z. D. Siegel. “Perceived Space in the HTC Vive”. In: *ACM Transactions on Applied Perception (TAP)* 15.1 (2017), page 2.

[Ken+93] R. S. Kennedy, N. E. Lane, K. S. Berbaum, and M. G. Lilienthal. “Simulator Sickness Questionnaire: An Enhanced Method for Quantifying Simulator Sickness”. In: *The International Journal of Aviation Psychology* 3.3 (1993), pages 203–220.

[KCO10] S. Kerns, D. Cliburn, and M. O'Rourke. "Teleporting in Virtual Worlds While Learning Real World Places". In: *International Conference on Artificial Reality and Telexistence (ICAT)*. 2010, pages 126–130.

[Kev+00] J. Kevin O'Regan, H. Deubel, J. J. Clark, and R. A. Rensink. "Picture Changes during Blinks: Looking Without Seeing and Seeing Without Looking". In: *Visual Cognition* 7.1-3 (2000), pages 191–211.

[KDF17] A. Kim, N. Darakjian, and J. M. Finley. "Walking in Fully Immersive Virtual Environments: An Evaluation of Potential Adverse Effects in Older Adults and Individuals with Parkinson's Disease". In: *Journal of Neuroengineering and Rehabilitation* 14.1 (2017), page 16.

[KF98] H. Kim and G. Francis. "A Computational and Perceptual Account of Motion Lines". In: *Perception* 27.7 (1998), pages 785–797.

[Kla+98] R. L. Klatzky, J. M. Loomis, A. C. Beall, S. S. Chance, and R. G. Golledge. "Spatial Updating of Self-position and Orientation During Real, Imagined, and Virtual Locomotion". In: *Psychological science* 9.4 (1998), pages 293–298.

[Kle01] S. Klein. "Measuring, Estimating, and Understanding the Psychometric Function: A Commentary". In: *Perception and Psychophysics* 63.8 (2001), pages 1421–1455.

[Kod15] R. Koduri. *In Pursuit of Presence and True Immersion*. 2015.

[Koh+05] L. Kohli, E. Burns, D. Miller, and H. Fuchs. "Combining Passive Haptics with Redirected Walking". In: *Proceedings of Conference on Augmented Tele-Existence*. Volume 157. ACM, 2005, pages 253–254.

[Kop+06] R. Kopper, T. Ni, D. Bowman, and M. Pinho. "Design and Evaluation of Navigation Techniques for Multiscale Virtual Environments". In: *IEEE Virtual Reality (VR)*. 2006, pages 175–182.

[KSB11] R. Kopper, C. Stinson, and D. Bowman. "Towards an Understanding of the Effects of Amplified Head Rotations". In: *IEEE VR Workshop on Perceptual Illusions in Virtual Environments*. Volume 2. 2011.

[Kru+15] E. Kruijff, B. Riecke, C. Trepkowski, and A. Kitson. "Upper Body Leaning can Affect Forward Self-Motion Perception in Virtual Environments". In: *ACM Symposium on Spatial User Interaction (SUI)*. 2015.

[Kru+16] D. Krupke, L. Einig, **E. Langbehn**, J. Zhang, and F. Steinicke. "Immersive Remote Grasping: Realtime Gripper Control by a Heterogenous Robot Control System". In: *ACM Symposium on Virtual Reality Software and Technology (VRST) (Poster)*. Nov. 2016, pages 337–338.

[KEF18] L. Kruse, **E. Langbehn**, and F. Steinicke[4]. "I Can See on my Feet While Walking: Sensitivity to Translation Gains with Visible Feet". In: *IEEE Virtual Reality (VR)*. 2018, pages 305–312.

[KTC08] S. Kuhl, W. Thompson, and S. Creem-Regehr. "HMD calibration and its effects on distance judgments". In: *Proceedings of Symposium on Applied Perception in Graphics and Visualization (APGV)*. 2008, pages 15–22.

[KCT08] S. A. Kuhl, S. H. Creem-Regehr, and W. B. Thompson. "Recalibration of Rotational Locomotion in Immersive Virtual Environments". In: *ACM Transactions on Applied Perception (TAP)* 5.3 (2008), page 17.

[Lab16] O. Labs. Job Simulator. Game [HTC Vive]. Owlchemy Labs. Played October 2016. Apr. 2016.

[LL13] D. Lanman and D. Luebke. "Near-Eye Light Field Displays". In: *ACM Transactions on Graphics (TOG)* 32.6 (2013), page 220.

[LBv99] M. Lappe, F. Bremmer, and A. V. van den Berg. "Perception of self-motion from visual flow". In: *Trends in Cognitive Sciences* 3.9 (1999), pages 329–336.

[LaV00] J. J. LaViola Jr. "A Discussion of Cybersickness in Virtual Environments". In: *ACM SIGCHI Bulletin* 32.1 (2000), pages 47–56.

[LaV+01] J. J. LaViola Jr., D. A. Feliz, D. F. Keefe, and R. C. Zeleznik. "Hands-Free Multi-Scale Navigation in Virtual Environments". In: *ACM Symposium on Interactive 3D Graphics*. 2001, pages 9–15.

[LaV+17] J. LaViola, E. Kruijff, R. McMahan, D. Bowman, and I. Poupyrev. *3D User Interfaces: Theory and Practice Second Edition*. Usability. Pearson Education, 2017. ISBN: 9780134034461.

[LHM97] R. Lea, Y. Honda, and K. Matsuda. "Virtual Society: Collaboration in 3D Spaces on the Internet". In: *Computer Supported Cooperative Work (CSCW)* 6.2-3 (1997), pages 227–250.

[Léc+08] A. Lécuyer, F. Lotte, R. B. Reilly, R. Leeb, M. Hirose, and M. Slater. "Brain-Computer Interfaces, Virtual Reality, and Videogames". In: *Computer* 41.10 (2008).

[LZ06] R. J. Leigh and D. S. Zee. *The Neurology of Eye Movements, edition 4 (contemporary neurology series)*. 2006.

[Lev+02] D. T. Levin, S. B. Drivdahl, N. Momen, and M. R. Beck. "False Predictions About the Detectability of Visual Changes: The Role of Beliefs About Attention, Memory, and the Continuity of Attended Objects in Causing Change Blindness Blindness". In: *Consciousness and Cognition* 11.4 (2002), pages 507–527.

[Lev+00] D. T. Levin, N. Momen, S. B. Drivdahl IV, and D. J. Simons. "Change Blindness Blindness: The Metacognitive Error of Overestimating Change-Detection Ability". In: *Visual Cognition* 7.1-3 (2000), pages 397–412.

[Lew82] C. Lewis. *Using the 'Thinking-Aloud' Method in Cognitive Interface Design*. Technical report RC-9265. IBM, 1982.

[4]This publication is based on a Bachelor thesis. The student implemented and ran the experiment under my supervision. I designed the experiment and wrote the paper.

[Li+15] B. Li, R. Zhang, A. Nordman, and S. A. Kuhl. "The Effects of Minification and Display Field of View on Distance Judgments in Real and HMD-based Environments". In: *ACM SIGGRAPH Symposium on Applied Perception (SAP)*. 2015, pages 55–58.

[Lin+13] S. A. Linkenauger, M. Leyrer, H. H. Bülthoff, and B. J. Mohler. "Welcome to Wonderland: The Influence of the Size and Shape of a Virtual Hand on the Perceived Size and Shape of Virtual Objects". In: *PloS one* 8.7 (2013), pages 1–16.

[Liu+18] J. Liu, H. Parekh, M. Al-Zayer, and E. Folmer. "Increasing Walking in VR using Redirected Teleportation". In: *ACM Symposium on User Interface Software and Technology (UIST)*. 2018, pages 521–529.

[Llo07] D. M. Lloyd. "Spatial Limits on Referred Touch to an Alien Limb May Reflect Boundaries of Visuo-Tactile Peripersonal Space Surrounding the Hand". In: *Brain and Cognition* 64.1 (2007), pages 104–109.

[LK03] J. Loomis and J. Knapp. "Visual Perception of Egocentric Distance in Real and Virtual Environments". In: *Virtual and Adaptive Environments*. Edited by L. Hettinger and M. Haas. Erlbaum, 2003, pages 21–46.

[Loy18] M. Loyola. "The Influence of the Availability of Visual Cues on the Accurate Perception of Spatial Dimensions in Architectural Virtual Environments". In: *Virtual Reality* 22.3 (2018), pages 235–243.

[LBS14] P. Lubos, G. Bruder, and F. Steinicke. "Safe-&-Round: Bringing Redirected Walking to Small Virtual Reality Laboratories". In: *Proceedings of ACM Symposium on Spatial User Interaction (SUI)*. 2014, pages 154–154.

[MPL11] M. Marchal, J. Pettre, and A. Lécuyer. "Joyman: A human-scale joystick for navigating in virtual worlds". In: *Proceedings of IEEE 3D User Interfaces (3DUI)*. 2011, pages 19–26.

[MS96] C. A. Martin Usoh and M. Slater. *Presence: Experiments in the Psychology of Virtual Environments*. 1996.

[MB18] S. Marwecki and P. Baudisch. "Scenograph: Fitting Real-Walking VR Experiences into Various Tracking Volumes". In: *ACM Symposium on User Interface Software and Technology (UIST)*. 2018, pages 511–520.

[Mar+18] S. Marwecki, M. Brehm, L. Wagner, L.-P. Cheng, F. Mueller, and P. Baudisch. "VirtualSpace - Overloading Physical Space with Multiple Virtual Reality Users". In: *ACM Conference on Human Factors in Computing Systems (CHI)*. 2018, page 241.

[Mas+17] T. Massetti, T. B. Crocetta, T. D. d. Silva, I. L. Trevizan, C. Arab, F. A. Caromano, and C. B. d. M. Monteiro. "Application and Outcomes of Therapy Combining Transcranial Direct Current Stimulation and Virtual Reality: A Systematic Review". In: *Disability and Rehabilitation: Assistive Technology* 12.6 (2017), pages 551–559.

[Mat+16a] K. Matsumoto, Y. Ban, T. Narumi, T. Tanikawa, and M. Hirose. "Curvature Manipulation Techniques in Redirection Using Haptic Cues". In: *IEEE Symposium on 3D User Interfaces (3DUI)*. 2016, pages 105–108.

[Mat+16b] K. Matsumoto, Y. Ban, T. Narumi, Y. Yanase, T. Tanikawa, and M. Hirose. "Unlimited Corridor: Redirected Walking Techniques Using Visuo Haptic Interaction". In: *ACM SIGGRAPH Emerging Technologies*. 2016, page 20.

[McC13] D. McCandless. *The beauty of data visualization*. TED Talk. 2013.

[MNF16] F. Meyer, M. Nogalski, and W. Fohl. "Detection Thresholds In Audio-Visual Redirected Walking". In: *Proceedings of Sound and Music Composition Conference (SMC)*. Volume 16. 1. 2016, pages 17–27.

[MK94] P. Milgram and F. Kishino. "A Taxonomy of Mixed Reality Visual Displays". In: *IEICE Transactions on Information and Systems, Special issue on Networked Reality*. 1994.

[Min95] M. R. Mine. "Virtual Environment Interaction Techniques". In: *UNC Chapel Hill CS Dept* (1995).

[MLY01] R. Mintz, S. Litvak, and Y. Yair. "3D-Virtual Reality in Science Education: An Implication for Astronomy Teaching". In: *Journal of Computers in Mathematics and Science Teaching* 20.3 (2001), pages 293–305.

[MGD09] M. Moehring, A. Gloystein, and R. Doerner. "Issues With Virtual Space Perception Within Reaching Distance: Mitigating Adverse Effects on Applications Using HMDs in the Automotive Industry". In: *IEEE Virtual Reality (VR)*. 2009, pages 223–226.

[Moh+07a] B. J. Mohler, J. L. Campos, M. Weyel, and H. H. Bülthoff. "Gait Parameters While Walking in a Head-Mounted Display Virtual Environment and the Real World". In: *Proceedings of Eurographics Symposium on Virtual Environments*. 2007, pages 85–88.

[Moh+10] B. J. Mohler, S. H. Creem-Regehr, W. B. Thompson, and H. H. Bülthoff. "The Effect of Viewing a Self-Avatar on Distance Judgments in an HMD-based Virtual Environment". In: *Presence: Teleoperators and Virtual Environments* 19.3 (2010), pages 230–242.

[Moh+07b] B. J. Mohler, W. B. Thompson, S. H. Creem-Regehr, H. L. Pick, and W. H. Warren. "Visual Flow Influences Gait Transition Speed and Preferred Walking Speed". In: *Experimental Brain Research* 181.2 (2007), pages 221–228.

[Mos81] R. A. Moses. *Adler's Physiology of the Eye*. Mosby, 1981.

[NB16] M. Nabiyouni and D. A. Bowman. "A Taxonomy for Designing Walking-based Locomotion Techniques for Virtual Reality". In: *ACM Companion on Interactive Surfaces and Spaces (ISS)*. 2016, pages 115–121.

[Nab+15] M. Nabiyouni, A. Saktheeswaran, D. A. Bowman, and A. Karanth. "Comparing the performance of natural, semi-natural, and non-natural locomotion techniques in virtual reality". In: *3D User Interfaces (3DUI), 2015 IEEE Symposium on*. IEEE. 2015, pages 3–10.

[NCH11] A. Naceri, R. Chellali, and T. Hoinville. "Depth Perception Within Peripersonal Space Using Head-Mounted Display". In: *Presence: Teleoperators and Virtual Environments* 20.3 (2011), pages 254–272.

[Nag+17] R. Nagao, K. Matsumoto, T. Narumi, T. Tanikawa, and M. Hirose. “Infinite Stairs: Simulating Stairs in Virtual Reality Based on Visuo-Haptic Interaction”. In: *ACM SIGGRAPH Emerging Technologies*. 2017, page 14.

[NBG17] F. Nemmi, M. Boccia, and C. Guariglia. “Does Aging Affect the Formation of new Topographical Memories? Evidence From an Extensive Spatial Training”. In: *Aging, Neuropsychology, and Cognition* 24.1 (2017), pages 29–44.

[NHK14] T. Nescher, Y.-Y. Huang, and A. Kunz. “Planning Redirection Techniques for Optimal Free Walking Experience Using Model Predictive Control”. In: *IEEE Symposium on 3D User Interfaces (3DUI)*. 2014.

[Net+11] C. T. Neth, J. L. Souman, D. Engel, U. Kloos, H. Bülthoff, and B. J. Mohler. “Velocity-dependent dynamic curvature gain for redirected walking”. In: *Proceedings of IEEE Virtual Reality (VR)*. 2011, pages 151–158.

[Net+12] C. T. Neth, J. L. Souman, D. Engel, U. Kloos, H. H. Bulthoff, and B. J. Mohler. “Velocity-Dependent Dynamic Curvature Gain for Redirected Walking”. In: *IEEE Transactions on Visualization and Computer Graphics (TVCG)* 18.7 (2012), pages 1041–1052.

[Ngo+16] N. T. A. Ngoc, Y. Rothacher, P. Brugger, B. Lenggenhager, and A. Kunz. “Estimation of Individual Redirected Walking Thresholds Using Standard Perception Tests”. In: *Proceedings of ACM Conference on Virtual Reality Software and Technology (VRST)*. 2016, pages 329–330.

[NK18] A. Nguyen and A. Kunz. “Discrete Scene Rotation During Blinks and its Effect on Redirected Walking Algorithms”. In: *ACM Symposium on Virtual Reality Software and Technology (VRST)*. 2018, page 29.

[NLW17] G. Nie, Y. Liu, and Y. Wang. “Prevention of Visually Induced Motion Sickness Based on Dynamic Real-Time Content-Aware Non-salient Area Blurring”. In: *IEEE International Symposium on Mixed and Augmented Reality (ISMAR)*. 2017, pages 75–78.

[NLL17] D. C. Niehorster, L. Li, and M. Lappe. “The Accuracy and Precision of Position and Orientation Tracking in the HTC Vive Virtual Reality System for Scientific Research”. In: *i-Perception* 8.3 (2017), page 2041669517708205.

[Nie+16] L. T. Nielsen, M. B. Møller, S. D. Hartmeyer, T. C. M. Ljung, N. C. Nilsson, R. Nordahl, and S. Serafin. “Missing the Point: An Exploration of How to Guide Users’ Attention During Cinematic Virtual Reality”. In: *Proceedings of ACM Virtual Reality Software and Technology (VRST)*. VRST ’16. Munich, Germany: ACM, 2016, pages 229–232. ISBN: 978-1-4503-4491-3. DOI: `10.1145/2993369.2993405`. URL: `http://doi.acm.org/10.1145/2993369.2993405`.

[NCT03] M. Niemeier, J. Crawford, and D. B. Tweed. “Optimal Transsaccadic Integration Explains Distorted Spatial Perception”. In: *Nature* 422.6927 (2003), pages 76–80.

[NSN14] N. C. Nilsson, S. Serafin, and R. Nordahl. “Establishing the Range of Perceptually Natural Visual Walking Speeds for Virtual Walking-In-Place Locomotion”. In: *IEEE Transactions on Visualization and Computer Graphics (TVCG)* 20.4 (2014), pages 569–578.

[NSN15] N. C. Nilsson, S. Serafin, and R. Nordahl. “The Effect of Head Mounted Display Weight and Locomotion Method on the Perceived Naturalness of Virtual Walking Speeds”. In: *IEEE Virtual Reality (VR)*. 2015, pages 249–250.

[NSN16] N. C. Nilsson, S. Serafin, and R. Nordahl. “Walking in Place Through Virtual Worlds”. In: *International Conference on Human-Computer Interaction*. Springer. 2016, pages 37–48.

[Nil+16] N. C. Nilsson, E. Suma, R. Nordahl, M. Bolas, and S. Serafin. “Estimation of Detection Thresholds for Audiovisual Rotation Gains”. In: *IEEE Virtual Reality (VR)*. 2016, pages 241–242.

[Nil+18] N. Nilsson, T. Peck, G. Bruder, E. Hodgson, S. Serafin, E. Suma, M. Whitton, and F. Steinicke. “15 Years of Research on Redirected Walking in Immersive Virtual Environments”. In: *IEEE Computer Graphics and Applications* PP.99 (2018), pages 1–1.

[NP00] M. A. Nitsche and W. Paulus. “Excitability Changes Induced in the Human Motor Cortex by Weak Transcranial Direct Current Stimulation”. In: *The Journal of Physiology* 527.3 (2000), pages 633–639.

[NHS04] N. Nitzsche, U. Hanebeck, and G. Schmidt. “Motion Compression for Telepresent Walking in Large Target Environments”. In: *Presence*. Volume 13. 1. 2004, pages 44–60.

[NF16] M. Nogalski and W. Fohl. “Acoustic Redirected Walking with Auditory Cues by Means of Wave Field Synthesis”. In: *IEEE Virtual Reality (VR)*. 2016, pages 245–246.

[Nor99] D. Norman. “Affordance, Conventions and Design”. In: *ACM Interactions* 6.3 (1999), pages 38–42.

[Nor+19] N. Norouzi, L. Bölling, G. Bruder, and G. Welch. “Augmented Rotations in Virtual Reality for Users With a Reduced Range of Head Movement”. In: *Journal of Rehabilitation and Assistive Technologies Engineering* 6 (2019), page 2055668319841309.

[Ocu18] Oculus. *Guidelines for VR Performance Optimization*. `https://developer.oculus.com/documentation/pcsdk/latest/concepts/dg-performance-guidelines/`. [Online; accessed 19-December-2018]. 2018.

[OSG00] J. C. Oliveira, X. Shen, and N. D. Georganas. “Collaborative Virtual Environment for Industrial Training and e-Commerce”. In: *IEEE VRTS* 288 (2000).

[Ols+11] J. L. Olson, D. M. Krum, E. A. Suma, and M. Bolas. “A Design for a Smartphone-Based Head Mounted Display”. In: *IEEE Virtual Reality (VR)*. 2011, pages 233–234.

[Pal99] S. Palmer. *Vision Science: Photons to Phenomenology*. A Bradford Book, 1999.

[Pal+16] A. G. Paludan, J. Elbaek, M. Mortensen, M. Zobbe, N. C. Nilsson, R. Nordahl, L. Reng, and S. Serafin. “Disguising Rotational Gain for Redirected Walking in Virtual Reality: Effect of Visual Density”. In: *Proceedings of IEEE Virtual Reality (VR)* (2016).

[Pat+91] S. Patel, R. Henderson, L. Bradley, B. Galloway, and L. Hunter. “Effect of Visual Display Unit Use on Blink Rate and Tear Stability.” In: *Optometry & Vision Science* 68.11 (1991), pages 888–892.

[PFW11] T. Peck, H. Fuchs, and M. Whitton. “An Evaluation of Navigational Ability Comparing Redirected Free Exploration with Distractors to Walking-in-Place and Joystick Locomotion Interfaces”. In: *Proceedings of IEEE Virtual Reality (VR)*. IEEE, 2011, pages 56–62.

[PFW08] T. C. Peck, H. Fuchs, and M. C. Whitton. “Evaluation of Reorientation Techniques for Walking in Large Virtual Environments”. In: *Proceedings of IEEE Virtual Reality (VR)*. IEEE, 2008, pages 121–128.

[PF93] K. Perlin and D. Fox. “Pad: An Alternative Approach to the Computer Interface”. In: *ACM Conference on Computer Graphics and Interactive Techniques (SIGGRAPH)*. 1993, pages 57–64.

[PGM12] M. Persuh, B. Genzer, and R. D. Melara. “Iconic Memory Requires Attention”. In: *Frontiers in Human Neuroscience* 6 (2012).

[Phi+12] L. Phillips, V. Interrante, M. Kaeding, B. Ries, and L. Anderson. “Correlations Between Physiological Response, Gait, Personality, and Presence in Immersive Virtual Environments”. In: *Presence: Teleoperators and Virtual Environments* 21.2 (2012), pages 119–141.

[Phi+09] L. Phillips, B. Ries, V. Interrante, M. Kaeding, and L. Anderson. “Distance Perception in NPR Immersive Virtual Environments, Revisited”. In: *Symposium on Applied Perception in Graphics and Visualization (APGV)*. ACM. 2009, pages 11–14.

[Pix16] T. Pixels. Unseen Diplomacy. Game [HTC Vive]. Triangular Pixels. Played November 2016. Apr. 2016.

[Pix17] T. Pixels. Smash Hit Plunder. Game [GearVR]. Triangular Pixels. Played -. 2017.

[Pol+12] B. Pollock, M. Burton, J. W. Kelly, S. Gilbert, and E. Winer. “The Right View From the Wrong Location: Depth Perception in Stereoscopic Multi-User Virtual Environments”. In: *IEEE Transactions on Visualization and Computer Graphics (TVCG)* 18.4 (2012), pages 581–588.

[PNK76] M. I. Posner, M. J. Nissen, and R. M. Klein. “Visual Dominance: An Information-processing Account of its Origins and Significance”. In: *Psychological Review* 83.2 (1976), page 157.

[PC83] M. Potmesil and I. Chakravarty. “Modeling Motion Blur in Computer-Generated Images”. In: *ACM SIGGRAPH Computer Graphics and Interactive Techniques* 17.3 (1983), pages 389–399.

[PM94] C. C. Presson and D. R. Montello. “Updating After Rotational and Translational Body Movements: Coordinate Structure of Perspective Space”. In: *Perception* 23.12 (1994), pages 1447–1455.

[RT18] A. Ramcharitar and R. J. Teather. “EZCursorVR: 2D Selection with Virtual Reality Head-Mounted Displays”. In: (2018).

[Ram08] D. Ramot. *Average Duration of a Single Eye Blink*. `http://bionumbers.hms.harvard.edu/bionumber.aspx?s=y&id=100706&ver=0`. [Online; accessed 28-Feb-2017]. 2008.

[Raz+02] S. Razzaque, D. Swapp, M. Slater, M. Whitton, A. Steed, and Z. Kohn. “Redirected Walking in Place”. In: *Eurographics Workshop on Virtual Environments (EGVE)*. 2002, pages 123–130.

[Raz05] S. Razzaque. “Redirected Walking”. PhD thesis. University of North Carolina, Chapel Hill, 2005.

[RKW01] S. Razzaque, Z. Kohn, and M. Whitton. “Redirected Walking”. In: *Proceedings of Eurographics*. ACM, 2001, pages 289–294.

[Rel06] U. M. Relations. *Blink and You Miss It!* `http://www.ucl.ac.uk/media/library/blinking`. [Online; accessed 28-Feb-2017]. 2006.

[RVH13] R. S. Renner, B. M. Velichkovsky, and J. R. Helmert. “The Perception of Egocentric Distances in Virtual Environments - a Review”. In: *ACM Computing Surveys (CSUR)* 46.2 (2013), page 23.

[Ren02] R. A. Rensink. “Change Detection”. In: *Annual Review of Psychology* 53 (2002), pages 245–277.

[ROC97] R. A. Rensink, J. O’Regan, and J. J. Clark. “To See or Not to See: The Need for Attention to Perceive Changes in Scenes”. In: *Psychological Science* 8.5 (1997), pages 368–373.

[RKC00] R. A. Rensink, J. Kevin O’Regan, and J. J. Clark. “On the Failure to Detect Changes in Scenes Across Brief Interruptions”. In: *Visual Cognition* 7.1-3 (2000), pages 127–145.

[Rew+19] N. Rewkowski, A. Rungta, M. C. Whitton, and M. C. Lin. “Evaluating the Effectiveness of Redirected Walking with Auditory Distractors for Navigation in Virtual Environments”. In: *IEEE Virtual Reality (VR)*. 2019.

[RW07] A. R. Richardson and D. Waller. “Interaction With an Immersive Virtual Environment Corrects Users’ Distance Estimates”. In: *Human Factors: The Journal of the Human Factors and Ergonomics Society* 49.3 (2007), pages 507–517.

[Rie+90] J. Rieser, D. Ashmead, C. Taylor, and G. Youngquist. “Visual Perception and the Guidance of Locomotion Without Vision to Previously Seen Targets”. In: *Perception* 19.5 (1990), pages 675–689.

[Rie+18] M. Rietzler, J. Gugenheimer, T. Hirzle, M. Deubzer, **E. Langbehn**, and E. Rukzio. “Rethinking Redirected Walking: On the Use of Curvature Gains Beyond Perceptual Limitations and Revisiting Bending Gains”. In: *IEEE International Symposium on Mixed and Augmented Reality (ISMAR)*. 2018, (8 pages).

[RDE16] M. Rohde, L. C. van Dam, and M. O. Ernst. “Statistically Optimal Multisensory Cue Integration: A Practical Tutorial”. In: *Multisensory research* 29.4-5 (2016), pages 279–317.

[RGA95] J. P. Rolland, W. Gibson, and D. Ariely. “Towards Quantifying Depth and Size Perception in Virtual Environments”. In: *Presence: Teleoperators & Virtual Environments* 4.1 (1995), pages 24–49.

[Ros04] J. Ross. “The Perceived Direction and Speed of Global Motion in Glass Pattern Sequences”. In: *Vision research* 44.5 (2004), pages 441–448.

[RHA17] S. Rothe, H. Hussmann, and M. Allary. “Diegetic Cues for Guiding the Viewer in Cinematic Virtual Reality”. In: *Proceedings of ACM Virtual Reality Software and Technology (VRST)*. VRST ’17. Gothenburg, Sweden: ACM, 2017, 54:1–54:2. ISBN: 978-1-4503-5548-3. DOI: 10.1145/3139131.3143421. URL: http://doi.acm.org/10.1145/3139131.3143421.

[Rou+15] T. Rousset, C. Bourdin, C. Goulon, J. Monnoyer, and J.-L. Vercher. “Does Virtual Reality Affect Visual Perception of Egocentric Distance?” In: *IEEE Virtual Reality (VR)*. 2015, pages 277–278.

[RVB10] R. A. Ruddle, E. P. Volkova, and H. H. Bülthoff. “Walking improves your cognitive map in environments that are large-scale and large in extent”. In: *ACM Transactions on Computer-Human Interaction* 18.2 (2010), 10:1–10:22.

[RL09] R. Ruddle and S. Lessels. “The Benefits of Using a Walking Interface to Navigate Virtual Environments”. In: *ACM Transactions on Computer-Human Interaction (TOCHI)* 16.1 (2009), 5:1–5:18.

[RHS05] J. Ryu, N. Hashimoto, and M. Sato. “Influence of Resolution Degradation on Distance Estimation in Virtual Space Displaying Static and Dynamic Image”. In: *Proceedings of CyberWorlds*. 2005, 8–pp.

[Sar+17] B. Sarupuri, S. Hoermann, F. Steinicke, and R. W. Lindeman. “Triggerwalking: A Biomechanically-inspired Locomotion User Interface for Efficient Realistic Virtual Walking”. In: *ACM Symposium on Spatial User Interaction (SUI)*. 2017, pages 138–147.

[ST17] A. Scavarelli and R. J. Teather. “VR Collide! Comparing Collision-Avoidance Methods Between Co-located Virtual Reality Users”. In: *ACM Conference on Human Factors in Computing Systems (CHI) (Extended Abstracts)*. CHI EA ’17. Denver, Colorado, USA: ACM, 2017, pages 2915–2921. ISBN: 978-1-4503-4656-6. DOI: 10.1145/3027063.3053180. URL: http://doi.acm.org/10.1145/3027063.3053180.

[SAH07] O. C. Schrempf, D. Albrecht, and U. D. Hanebeck. “Tractable Probabilistic Models for Intention Recognition Based on Expert Knowledge”. In: *IEEE/RSJ Intelligent Robots and Systems (IROS)*. 2007, pages 1429–1434.

[SFR01] T. Schubert, F. Friedmann, and H. Regenbrecht. *Igroup Presence Questionnaire*. 2001.

[SFR99] T. Schubert, F. Friedmann, and H. Regenbrecht. “Embodied Presence in Virtual Environments”. In: *Visual Representations and Interpretations*. Springer, 1999, pages 269–278.

[STU07] M. Schwaiger, T. Thümmel, and H. Ulbrich. “Cyberwalk: Implementation of a Ball Bearing Platform for Humans”. In: *Proceedings of HCI*. 2007, pages 926–935.

[Ser+13] S. Serafin, N. C. Nilsson, E. Sikstrom, A. De Goetzen, and R. Nordahl. “Estimation of Detection Thresholds for Acoustic Based Redirected Walking Techniques”. In: *IEEE Virtual Reality (VR)*. 2013, pages 161–162.

[Sfo+08] C. Sforza, M. Rango, D. Galante, N. Bresolin, and V. F. Ferrario. “Spontaneous Blinking in Healthy Persons: an Optoelectronic Study of Eyelid Motion”. In: *Ophthalmic and Physiological Optics* 28.4 (2008), pages 345–353.

[SH08] T. Shiratori and J. Hodgins. “Accelerometer-based User Interfaces for the Control of a Physically Simulated Character”. In: *ACM Transactions on Graphics (TOG)* 27.5 (2008), pages 1–9.

[Sim16] A. L. Simeone. “The VR Motion Tracker: Visualising Movement of Non-Participants in Desktop Virtual Reality Experiences”. In: *IEEE Virtual Reality (VR) Workshop on Everyday Virtual Reality (WEVR)*. 2016, pages 1–4.

[SL97] D. J. Simons and D. T. Levin. “Change Blindness”. In: *Trends in Cognitive Sciences* 1.7 (1997), pages 261–267.

[SL98] D. J. Simons and D. T. Levin. “Failure to Detect Changes to People During a Real-World Interaction”. In: *Psychonomic Bulletin and Review* 5 (1998), pages 644–649.

[Sla09] M. Slater. “Place Illusion and Plausibility Can Lead to Realistic Behaviour in Immersive Virtual Environments”. In: *Philosophical Transactions of the Royal Society of London B: Biological Sciences* 364.1535 (2009), pages 3549–3557.

[SU93] M. Slater and M. Usoh. “Presence in Immersive Virtual Environments”. In: *Virtual Reality Annual International Symposium*. IEEE. 1993, pages 90–96.

[SU94] M. Slater and M. Usoh. “Body Centred Interaction in Immersive Virtual Environments”. In: *Artificial Life and Virtual Reality* 1.1994 (1994), pages 125–148.

[SUS94] M. Slater, M. Usoh, and A. Steed. “Depth of Presence in Virtual Environments”. In: *Presence: Teleoperators & Virtual Environments* 3.2 (1994), pages 130–144.

[SUS95] M. Slater, M. Usoh, and A. Steed. “Taking Steps: The Influence of a Walking Technique on Presence in Virtual Reality”. In: *ACM Transactions on Computer-Human Interaction (TOCHI)* 2.3 (1995), pages 201–219.

[SW97] M. Slater and S. Wilbur. “A Framework for Immersive Virtual Environments (FIVE): Speculations on the Role of Presence in Virtual Environments”. In: *Presence: Teleoperators & Virtual Environments* 6.6 (1997), pages 603–616.

[SLH85] J. G. Snodgrass, G. Levy-Berger, and M. Haydon. *Human Experimental Psychology*. Volume 395. Oxford University Press New York, 1985.

[Son+01] D. H. Sonnenwald, R. E. Bergquist, K. L. Maglaughlin, E. Kupstas-Soo, and M. C. Whitton. "Designing to Support Collaborative Scientific Research Across Distances: The nanoManipulator Environment". In: *ACM Collaborative Virtual Environments (CVE)*. Springer. 2001, pages 202–224.

[Sou+11] J. Souman, P. Robuffo Giordano, M. Schwaiger, I. Frissen, T. Thümmel, H. Ulbrich, A. De Luca, H. Bülthoff, and M. Ernst. "CyberWalk: Enabling unconstrained omnidirectional walking through virtual environments". In: *ACM Transactions on Applied Perception (TAP)* 8.4 (2011), pages 1–22.

[Spe08] C. Spearman. "The Method of 'right and wrong cases'('constant stimuli') without Gauss's Formulae". In: *British Journal of Psychology* 2.3 (1908), pages 227–242.

[Spi08] H. J. Spiers. "Keeping the Goal in Mind: Prefrontal Contributions to Spatial Navigation". In: *Neuropsychologia* 46.7 (2008), page 2106.

[SM06] H. J. Spiers and E. A. Maguire. "Thoughts, Behaviour, and Brain Dynamics During Navigation in the Real World". In: *Neuroimage* 31.4 (2006), pages 1826–1840.

[SGM17] M. Sra, S. Garrido-Jurado, and P. Maes. "Oasis: Procedurally Generated Social Virtual Spaces from 3D Scanned Real Spaces". In: *IEEE Transactions on Visualization and Computer Graphics (TVCG)* (2017).

[Sra+16] M. Sra, S. Garrido-Jurado, C. Schmandt, and P. Maes. "Procedurally Generated Virtual Reality from 3D Reconstructed Physical Space". In: *ACM Virtual Reality Software and Technology (VRST)*. 2016, pages 191–200.

[SXM17] M. Sra, X. Xu, and P. Maes. "GalVR: A Novel Collaboration Interface Using GVS". In: *ACM Symposium on Virtual Reality Software and Technology (VRST)*. 2017, page 61.

[Sra+18] M. Sra, X. Xu, A. Mottelson, and P. Maes. "VMotion: Designing a Seamless Walking Experience in VR". In: *ACM Designing Interactive Systems (DIS)*. 2018, pages 59–70.

[SAN18] C. J. Stagg, A. Antal, and M. A. Nitsche. "Physiology of Transcranial Direct Current Stimulation". In: *The Journal of ECT* 34.3 (2018), pages 144–152.

[SK97] K. M. Stanney and R. S. Kennedy. "The Psychometrics of Cybersickness". In: *Communications of the ACM* 40.8 (1997), pages 66–68.

[SKD97] K. M. Stanney, R. S. Kennedy, and J. M. Drexler. "Cybersickness is not Simulator Sickness". In: *Proceedings of the Human Factors and Ergonomics Society Annual Meeting*. Volume 41. 2. SAGE Publications Sage CA: Los Angeles, CA. 1997, pages 1138–1142.

[Ste+09a] F. Steinicke, G. Bruder, K. Hinrichs, J. Jerald, H. Frenz, and M. Lappe. "Real Walking Through Virtual Environments by Redirection Techniques". In: *Journal of Virtual Reality and Broadcasting (JVRB)* 6.2 (2009).

[Ste+08a] F. Steinicke, G. Bruder, J. Jerald, H. Frenz, and M. Lappe. "Analyses of Human Sensitivity to Redirected Walking". In: *15th ACM Symposium on Virtual Reality Software and Technology*. 2008, pages 149–156.

[Ste+08b] F. Steinicke, G. Bruder, T. Ropinski, and K. Hinrichs. "Moving Towards Generally Applicable Redirected Walking". In: *Proceedings of the Virtual Reality International Conference (VRIC)*. IEEE Press, 2008, pages 15–24.

[Ste+09b] F. Steinicke, G. Bruder, K. Hinrichs, and A. Steed. "Presence-enhancing Real Walking User Interface for First-Person Video Games". In: *Proceedings of ACM SIGGRAPH Symposium on Video Games*. 2009, pages 111–118.

[Ste+10a] F. Steinicke, G. Bruder, K. Hinrichs, and P. Willemsen. "Change Blindness Phenomena for Stereoscopic Projection Systems". In: *Proceedings of IEEE Virtual Reality (VR)*. 2010, pages 187–194.

[Ste+11] F. Steinicke, G. Bruder, K. Hinrichs, and P. Willemsen. "Change Blindness Phenomena for Virtual Reality Display Systems". In: *IEEE Transactions on Visualization and Computer Graphics (TVCG)* 17.9 (2011), pages 1223–1233.

[Ste+10b] F. Steinicke, G. Bruder, J. Jerald, H. Fenz, and M. Lappe. "Estimation of Detection Thresholds for Redirected Walking Techniques". In: *IEEE Transactions on Visualization and Computer Graphics (TVCG)* 16.1 (2010), pages 17–27.

[Ste+08c] F. Steinicke, G. Bruder, L. Kohli, J. Jerald, and K. Hinrichs. "Taxonomy and Implementation of Redirection Techniques for Ubiquitous Passive Haptic Feedback". In: *IEEE Cyberworlds*. 2008, pages 217–223.

[Ste+13] F. Steinicke, Y. Visell, J. Campos, and A. Lécuyer. *Human Walking in Virtual Environments: Perception, Technology, and Applications*. Springer Verlag, 2013.

[Ste58] S. S. Stevens. "Problems and Methods of Psychophysics". In: *Psychological Bulletin* 55.4 (1958), page 177.

[SCP95] R. Stoakley, M. J. Conway, and R. Pausch. "Virtual Reality on a WIM: Interactive Worlds in Miniature". In: *ACM Conference on Human Factors in Computing Systems (CHI)*. Volume 95. 1995, pages 265–272.

[Sum+15] E. A. Suma, M. Azmandian, T. Grechkin, T. Phan, and M. Bolas. "Making Small Spaces Feel Large: Infinite Walking in Virtual Reality". In: *ACM SIGGRAPH 2015 Emerging Technologies*. ACM. 2015, page 16.

[Sum+12a] E. A. Suma, G. Bruder, F. Steinicke, D. M. Krum, and M. Bolas. "A Taxonomy for Deploying Redirection Techniques in Immersive Virtual Environments". In: *Proceedings of IEEE Virtual Reality (VR)*. 2012, pages 43–46.

[Sum+10] E. A. Suma, S. Clark, S. L. Finkelstein, and Z. Wartell. "Exploiting Change Blindness to Expand Walkable Space in a Virtual Environment". In: *Proceedings of IEEE Virtual Reality (VR)*. 2010, pages 305–306.

[Sum+12b] E. A. Suma, Z. Lipps, S. Finkelstein, D. M. Krum, and M. Bolas. "Impossible Spaces: Maximizing Natural Walking in Virtual Environments with Self-Overlapping Architecture". In: *IEEE Transactions on Visualization and Computer Graphics (TVCG)* 18.4 (2012), pages 555–564.

[Sun+18] Q. Sun, A. Patney, L.-Y. Wei, O. Shapira, J. Lu, P. Asente, S. Zhu, M. McGuire, D. Luebke, and A. Kaufman. “Towards Virtual Reality Infinite Walking: Dynamic Saccadic Redirection”. In: *ACM Transactions on Graphics (TOG)* 37.4 (2018), page 67.

[SWK16] Q. Sun, L.-Y. Wei, and A. Kaufman. “Mapping Virtual and Physical Reality”. In: *ACM Transactions on Graphics (TOG)* 35.4 (2016), page 64.

[Sut65] I. E. Sutherland. “The Ultimate Display”. In: *Proceedings of IFIP Congress 2*. 1965, pages 506–509.

[Sut68] I. E. Sutherland. “A Head-Mounted Three Dimensional Display”. In: *Proceedings of the AFIPS Fall Joint Computer Conference*. Volume 33. 1968, pages 757–764.

[TKK03] K. Takehara, S. Kawahara, and Y. Kirino. “Time-Dependent Reorganization of the Brain Components Underlying Memory Retention in Trace Eyeblink Conditioning”. In: *Journal of Neuroscience* 23.30 (2003), pages 9897–9905. ISSN: 0270-6474. eprint: `http://www.jneurosci.org/content/23/30/9897.full.pdf`. URL: `http://www.jneurosci.org/content/23/30/9897`.

[Tak+18] N. Takeuchi, T. Mori, Y. Suzukamo, and S.-I. Izumi. “Modulation of Excitability in the Temporoparietal Junction Relieves Virtual Reality Sickness”. In: *Cyberpsychology, Behavior, and Social Networking* (2018).

[TN10] D. Tan and A. Nijholt. “Brain-Computer Interfaces and Human-Computer Interaction”. In: *Brain-Computer Interfaces*. Springer, 2010, pages 3–19.

[TVY13] J. S. Taube, S. Valerio, and R. M. Yoder. “Is Navigation in Virtual Reality with FMRI Really Navigation?” In: *Journal of Cognitive Neuroscience* 25.7 (2013), pages 1008–1019.

[TDS99] J. Templeman, P. Denbrook, and L. Sibert. “Virtual Locomotion: Walking in Place Through Virtual Environments”. In: *Presence*. 1999, pages 598–617.

[Ter+10] L. Terziman, M. Marchal, M. Emily, and F. Multon. “Shake-Your-Head: Revisiting Walking-in-Place for Desktop Virtual Reality”. In: *ACM Virtual Reality Software and Technology (VRST)*. 2010, pages 27–34.

[TR19] J. Thomas and E. S. Rosenberg. “A General Reactive Algorithm for Redirected Walking using Artificial Potential Functions”. In: *IEEE Virtual Reality (VR)*. 2019.

[Tho+04] W. Thompson, P. Willemsen, A. Gooch, S. Creem-Regehr, J. Loomis, and A. Beall. “Does the Quality of the Computer Graphics Matter When Judging Distances in Visually Immersive Environments?” In: *Presence: Teleoperators & Virtual Environments* 13.5 (2004), pages 560–571.

[Tod55] J. Todd. “The Syndrome of Alice in Wonderland”. In: *Canadian Medical Association Journal* 73.9 (1955), pages 701–704.

[Tom+14] M. de Tommaso, S. Invitto, K. Ricci, V. Lucchese, M. Delussi, P. Quattromini, S. Bettocchi, V. Pinto, G. Lancioni, P. Livrea, et al. “Effects of Anodal TDCS Stimulation of Left Parietal Cortex on Visual Spatial Attention Tasks in Men and Women Across Menstrual Cycle”. In: *Neuroscience Letters* 574 (2014), pages 21–25.

[Tom16] Tomura. *Radial Blur PostProcess Effect*. https://www.unrealengine4.de/index.php?thread/ 176-radial-blur-postprocess-effect/ &s=f0b6a81826ce3268b7bc9671804fafd8b82f8a6b. 2016. URL: `https://www.unrealengine4.de/index.php?thread/%20176-radial-blur-postprocess-effect/%20&s=f0b6a81826ce3268b7bc9671%20804fafd8b82f8a6b`.

[Uso+99a] M. Usoh, K. Arthur, M. C. Whitton, R. Bastos, A. Steed, M. Slater, and F. P. Brooks, Jr. “Walking > Walking-in-Place > Flying, in Virtual Environments”. In: *Proceedings of ACM SIGGRAPH*. 1999, pages 359–364.

[Uso+99b] M. Usoh, E. Catena, S. Arman, and M. Slater. “Using Presence Questionaires in Reality”. In: *Presence: Teleoperators & Virtual Environments* 9.5 (1999), pages 497–503.

[VMH16] D. Valkov, J. Martens, and K. Hinrichs. “Evaluation of the Effect of a Virtual Avatar’s Representation on Distance Perception in Immersive Virtual Environments”. In: *IEEE Virtual Reality (VR)*. 2016, pages 305–306.

[Val16] Valve. The Lab. Game [HTC Vive]. Valve. Played July 2016. Apr. 2016.

[VK15] K. Vasylevska and H. Kaufmann. “Influence of path complexity on spatial overlap perception in virtual environments”. In: *Proceedings of the 25th International Conference on Artificial Reality and Telexistence and 20th Eurographics Symposium on Virtual Environments*. Eurographics Association. 2015, pages 159–166.

[VK17a] K. Vasylevska and H. Kaufmann. “Compressing VR: Fitting Large Virtual Environments Within Limited Physical Space”. In: *IEEE Computer Graphics and Applications* 37.5 (2017), pages 85–91.

[VK17b] K. Vasylevska and H. Kaufmann. “Towards Efficient Spatial Compression in Self-Overlapping Virtual Environments”. In: *Symposium on 3D User Interfaces (3DUI)*. 2017.

[Vas+13] K. Vasylevska, H. Kaufmann, M. Bolas, and E. A. Suma. “Flexible spaces: Dynamic layout generation for infinite walking in virtual environments”. In: *3D User Interfaces (3DUI), 2013 IEEE Symposium on*. IEEE. 2013, pages 39–42.

[Vol86] F. C. Volkmann. “Human Visual Suppression”. In: *Vision Research* 26.9 (1986), pages 1401–1416.

[VRM80] F. C. Volkmann, L. A. Riggs, and R. K. Moore. “Eyeblinks and Visual Suppression”. In: *Science* 207.4433 (1980), pages 900–902.

[WB00] G. Wallis and H. Bulthoff. “What’s Scene and not Seen: Influences of Movement and Task Upon What We See”. In: *Visual Cognition* 7.1-3 (2000), pages 175–190.

[WL11] J. Wang and R. Lindeman. "Silver Surfer: A System to Compare Isometric and Elastic Board Interfaces for Locomotion in VR". In: *IEEE Symposium on 3D User Interfaces (3DUI)*. 2011, pages 121–122.

[WI92] J. P. Wann and S. F. Ibrahim. "Does Limb Proprioception Drift?" In: *Experimental Brain Research* 91.1 (1992), pages 162–166.

[WO90] C. Ware and S. Osborne. "Exploration and Virtual Camera Control in Virtual Three Dimensional Environments". In: *ACM SIGGRAPH Computer Graphics*. Volume 24. 2. ACM. 1990, pages 175–183.

[Web17] E. H. Weber. *Anatomia comparata nervi sympathici*. 1817.

[Web+98] K. Weber, W. Fletcher, C. Gordon, G. M. Jones, and E. Block. "Motor learning in the "podokinetic" system and its role in spatial orientation during locomotion". In: *Experimental brain research* 120.3 (1998), pages 377–385.

[Web+14] M. J. Weber, S. B. Messing, H. Rao, J. A. Detre, and S. L. Thompson-Schill. "Prefrontal Transcranial Direct Current Stimulation Alters Activation and Connectivity in Cortical and Subcortical Reward Systems: A tDCS-fMRI Study". In: *Human Brain Mapping* 35.8 (2014), pages 3673–3686.

[WQL14] T. Wei, Y. Qiao, and B. Lee. "Kinect Skeleton Coordinate Calibration for Remote Physical Training". In: *International Conference on Advances in Multimedia (MMEDIA)*. 2014, pages 23–27.

[WWB10] J. D. Wendt, M. Whitton, and F. Brooks. "GUD-WIP: Gait-Understanding-Driven Walking-in-Place". In: *IEEE Virtual Reality (VR)*. 2010, pages 51–58.

[Whi+05] M. Whitton, J. Cohn, P. Feasel, S. Zimmons, S. Razzaque, S. Poulton, and B. M. und F.P. Brooks, Jr. "Comparing VE Locomotion Interfaces". In: *IEEE Proceedings of the Virtual Reality (VR)*. IEEE, 2005, pages 123–130.

[Wil+08] P. Willemsen, A. Gooch, W. Thompson, and S. Creem-Regehr. "Effects of Stereo Viewing Conditions on Distance Perception in Virtual Environments". In: *Presence: Teleoperators & Virtual Environments* 17.1 (2008), pages 91–101.

[Wil+11] B. Williams, S. Bailey, G. Narasimham, M. Li, and B. Bodenheimer. "Evaluation of Walking in Place on a Wii Balance Board to Explore a Virtual Environment". In: *ACM Transactions on Applied Perception (TAP)* 8.19 (2011), pages 1–14.

[Wil+07] B. Williams, G. Narasimham, B. Rump, T. P. McNamara, T. H. Carr, J. Rieser, and B. Bodenheimer. "Exploring Large Virtual Environments with an HMD when Physical Space is Limited". In: *Proceedings of ACM Symposium on Applied Perception in Graphics and Visualization (APGV)*. 2007, pages 41–48.

[WHB06] C. A. Wingrave, Y. Haciahmetoglu, and D. A. Bowman. "Overcoming World in Miniature Limitations by a Scaled and Scrolling WIM". In: *3D User Interfaces (3DUI'06)*. Mar. 2006, pages 11–16. DOI: 10.1109/VR.2006.106.

[Win18] N. Winkemann. *Bachelor Thesis: Automatisierte Pfadgenerierung für virtuelle Umgebungen*. 2018.

[WK98] B. Witmer and P. Kline. "Judging Perceived and Traversed Distance in Virtual Environments". In: *Presence: Teleoperators & Virtual Environments* 7.2 (1998), pages 144–167.

[WS98] B. Witmer and J. Sadowski, Jr. "Nonvisually Guided Locomotion to a Previously Viewed Target in Real and Virtual Environments". In: *Human Factors: The Journal of the Human Factors and Ergonomics Society* 40.3 (1998), pages 489–484.

[Wol+02] J. R. Wolpaw, N. Birbaumer, D. J. McFarland, G. Pfurtscheller, and T. M. Vaughan. "Brain-Computer Interfaces for Communication and Control". In: *Clinical neurophysiology* 113.6 (2002), pages 767–791.

[YTM17] T. S. Young, R. J. Teather, and I. S. MacKenzie. "An Arm-Mounted Inertial Controller for 6DOF Input: Design and Evaluation". In: *IEEE Symposium on 3D User Interfaces (3DUI)*. 2017, pages 26–35.

[Yu+18] R. Yu, Z. Duer, T. Ogle, D. A. Bowman, T. Tucker, D. Hicks, D. Choi, Z. Bush, H. Ngo, P. Nguyen, et al. "Experiencing an Invisible World War I Battlefield Through Narrative-Driven Redirected Walking in Virtual Reality". In: *IEEE Virtual Reality and 3D User Interfaces (VR)*. 2018, pages 313–319.

[Yu+17] R. Yu, W. S. Lages, M. Nabiyouni, B. Ray, N. Kondur, V. Chandrashekar, and D. A. Bowman. "Bookshelf and Bird: Enabling Real Walking in Large VR Spaces". In: *IEEE Symposium on3D User Interfaces (3DUI)*. 2017, pages 116–119.

[Zan+05] C. A. Zanbaka, B. C. Lok, S. V. Babu, A. C. Ulinski, and L. F. Hodges. "Comparison of Path Visualizations and Cognitive Measures Relative to Travel Technique in a Virtual Environment". In: *IEEE Transactions on Visualization and Computer Graphics (TVCG)* 11.6 (2005), pages 694–705.

[ZK15] M. Zank and A. Kunz. "Using Locomotion Models for Estimating Walking Targets in Immersive Virtual Environments". In: *IEEE International Conference on Cyberworlds (CW)*. 2015.

[ZK16] M. Zank and A. Kunz. "Eye Tracking for Locomotion Prediction in Redirected Walking". In: *IEEE Symposium on 3D User Interfaces (3DUI)*. 2016.

[ZK17] M. Zank and A. Kunz. "Optimized Graph Extraction and Locomotion Prediction for Redirected Walking". In: *IEEE Symposium on 3D User Interfaces (3DUI)*. 2017.

[Zel+02] R. C. Zeleznik, J. J. LaViola, D. A. Feliz, and D. F. Keefe. "Pop through button devices for VE navigation and interaction". In: *Virtual Reality, 2002. Proceedings. IEEE*. IEEE. 2002, pages 127–134.

[Zha+18a] J. Zhang, **E. Langbehn**, D. Krupke, N. Katzakis, and F. Steinicke. "A 360 Video-based Robot Platform for Telepresent Redirected Walking". In: *ACM Human-Robot Interaction (HRI) Workshop on Virtual, Augmented and Mixed Reality for Human-Robot Interaction*. 2018, (5 pages).

[Zha+18b] J. Zhang, **E. Langbehn**, D. Krupke, N. Katzakis, and F. Steinicke. “Detection Thresholds for Rotation and Translation Gains in 360 Video-based Telepresence System”. In: *IEEE Transactions on Visualization and Computer Graphics (TVCG)* 24.4 (2018), pages 1671–1680.

[ZK13] R. Zhang and S. A. Kuhl. “Flexible and general redirected walking for head-mounted displays”. In: *IEEE Virtual Reality (VR)*. 2013, pages 127–128.

[ZWK15] R. Zhang, J. Walker, and S. A. Kuhl. “Improving redirection with dynamic reorientations and gains”. In: *ACM SIGGRAPH Symposium on Applied Perception (SAP)*. 2015, pages 136–136.

[ZF02] X. Zhang and G. W. Furnas. “Social Interactions in Multiscale CVEs”. In: *ACM Collaborative Virtual Environments (CVE)*. 2002, pages 31–38.

[Zha08] X. Zhang. “A Multiscale Progressive Model on Virtual Navigation”. In: *International Journal of Human-Computer Studies* 66.4 (2008), pages 243–256.

[Zha09] X. L. Zhang. “Multiscale Traveling: Crossing the Boundary Between Space and Scale”. In: *Virtual Reality* 13.2 (2009), pages 101–115.

[ZF05] X. Zhang and G. W. Furnas. “mCVEs: Using Cross-Scale Collaboration to Support User Interaction with Multiscale Structures”. In: *Presence* 14.1 (2005), pages 31–46.

[Zmu+13] M. A. Zmuda, J. L. Wonser, E. R. Bachmann, and E. Hodgson. “Optimizing constrained-environment redirected walking instructions using search techniques”. In: *IEEE transactions on visualization and computer graphics (TVCG)* 19.11 (2013), pages 1872–1884.

APPENDIX

EXPERIENCE QUESTIONNAIRE

Have you used a head-mounted-display like the Oculus Rift / HTC Vive before?

Please choose **only one** of the following:

- Yes
- No

How much experience do you have with head-mounted displays?

Please choose **only one** of the following:

- 1
- 2
- 3
- 4
- 5

1 = no experience, 5 = much experience

Do you have experience with 3d computer games?

Please choose **only one** of the following:

- 1
- 2
- 3
- 4
- 5

1 = no experience, 5 = much experience

How many hours do you play per week?

Please write your answer here:

Do you have experience with 3D stereoscopic displays (e.g. 3d cinema)?

Please choose **only one** of the following:

- 1
- 2
- 3
- 4
- 5

1 = no experience, 5 = much experience

SIMULATOR SICKNESS QUESTIONNAIRE

	0 (None)	1	2	3 (Severe)
General discomfort // Allg. Unwohlsein				
Fatigue // Erschöpfung				
Headache // Kopfschmerzen				
Eyestrain // Überanstrengung der Augen				
Difficulty focusing // Probleme bei der Fokussierung				
Increased salivation // Erhöhte Speichelbildung				
Sweating // Schweißbildung				
Nausea // Übelkeit				
Difficulty concentrating // Konzentrationsschwierigkeiten				
Fullness of head // Kopf voller Gedanken				
Blurred vision // Unscharfe Sicht				
Dizzy (eyes open) // Schwindelig o. Duselig bei offenen Augen				
Dizzy (eyes closed) // Schwindelig o. Duselig bei geschlossenen Augen				
Vertigo // Gleichgewichtsstörung				
Stomach awareness // Den Bauch wahrnehmen				
Burping // Aufstoßen				

SUS PRESENCE QUESTIONNAIRE

Please rate your sense of being in the virtual environment, on a scale of 1 to 5, where 5 represents your normal experience of being in a place.

I had a sense of "being there"...

Please choose **only one** of the following:

- ○ 1
- ○ 2
- ○ 3
- ○ 4
- ○ 5

1 = not at all, 5 = very much

To what extent were there times during the experience when the virtual environment was the reality for you?

There were times when the virtual environment was the reality for me...

Please choose **only one** of the following:

- ○ 1
- ○ 2
- ○ 3
- ○ 4
- ○ 5

1 = not at all, 5 = almost all the time

When you think back to the experience, do you think of the virtual environment more as images that you saw or more as somewhere that you visited?

The virtual environment seems to me to be more like...

Please choose **only one** of the following:

- ○ 1
- ○ 2
- ○ 3
- ○ 4
- ○ 5

1 = images that I saw, 5 = somewhere that I visited

During the time of the experience, which was the strongest on the whole, your sense of being in the virtual environment or of being elsewhere?

I had a stronger sense of...

Please choose **only one** of the following:

- ○ 1
- ○ 2
- ○ 3
- ○ 4
- ○ 5

1 = being elsewhere, 5 = being in the virtual environment

During the time of your experience, did you often think to yourself that you were actually in the virtual environment?

During the experiment I often thought that I was really standing in the virtual environment...

Please choose **only one** of the following:

- ○ 1
- ○ 2
- ○ 3
- ○ 4
- ○ 5

1 = not very often, 5 = very much so

Consider your memory of being in the virtual environment. How similar in terms of the structure of the memory is this to the structure of the memory of other places you have been today? By 'structure of the memory' consider things like the extent to which you have a visual memory of the virtual environment, whether that memory is in colour, the extent to which the memory seems vivid or realistic, its size, location in your imagination, the extent to which it is panoramic in your imagination, and other such structural elements.

I think of the virtual environment as a place in a way similar to other places that I have been today...

Please choose **only one** of the following:

- ○ 1
- ○ 2
- ○ 3
- ○ 4
- ○ 5

1 = not at all, 5 = very much so

DEMOGRAPHIC QUESTIONNAIRE

Height // Körpergröße

Please write your answer here:

Enter a number in meters in the 1.82 format.

Age

Please write your answer here:

Profession / field of study *(Beruf / Studiengang)*

Please write your answer here:

Gender

Please choose **only one** of the following:

- Female
- Male
- Other

Additional comments

Please write your answer here:

Vision correction

Please choose **only one** of the following:

- ○ None
- ○ Glasses
- ○ Contact Lenses

Do you suffer from a displacement of equilibrium or similar? *(Gleichgewichtsstörung)*

Please choose **only one** of the following:

- ○ Yes
- ○ No

Do you have a known eye disorder?

Please choose **all** that apply:

- ☐ Color blindness
- ☐ Night blindness
- ☐ Dyschromatopsia (red-green color weakness)
- ☐ Strong eye Dominance
- ☐ Other: ______

Note: This does not include disorders such as near-sightedness or far-sightedness that you correct by wearing glasses or contact lenses

Hiermit erkläre ich an Eides statt, dass ich die vorliegende Dissertationsschrift selbst verfasst und keine anderen als die angegebenen Quellen und Hilfsmittel benutzt habe.

Hamburg, November 7, 2019

(Eike Langbehn)